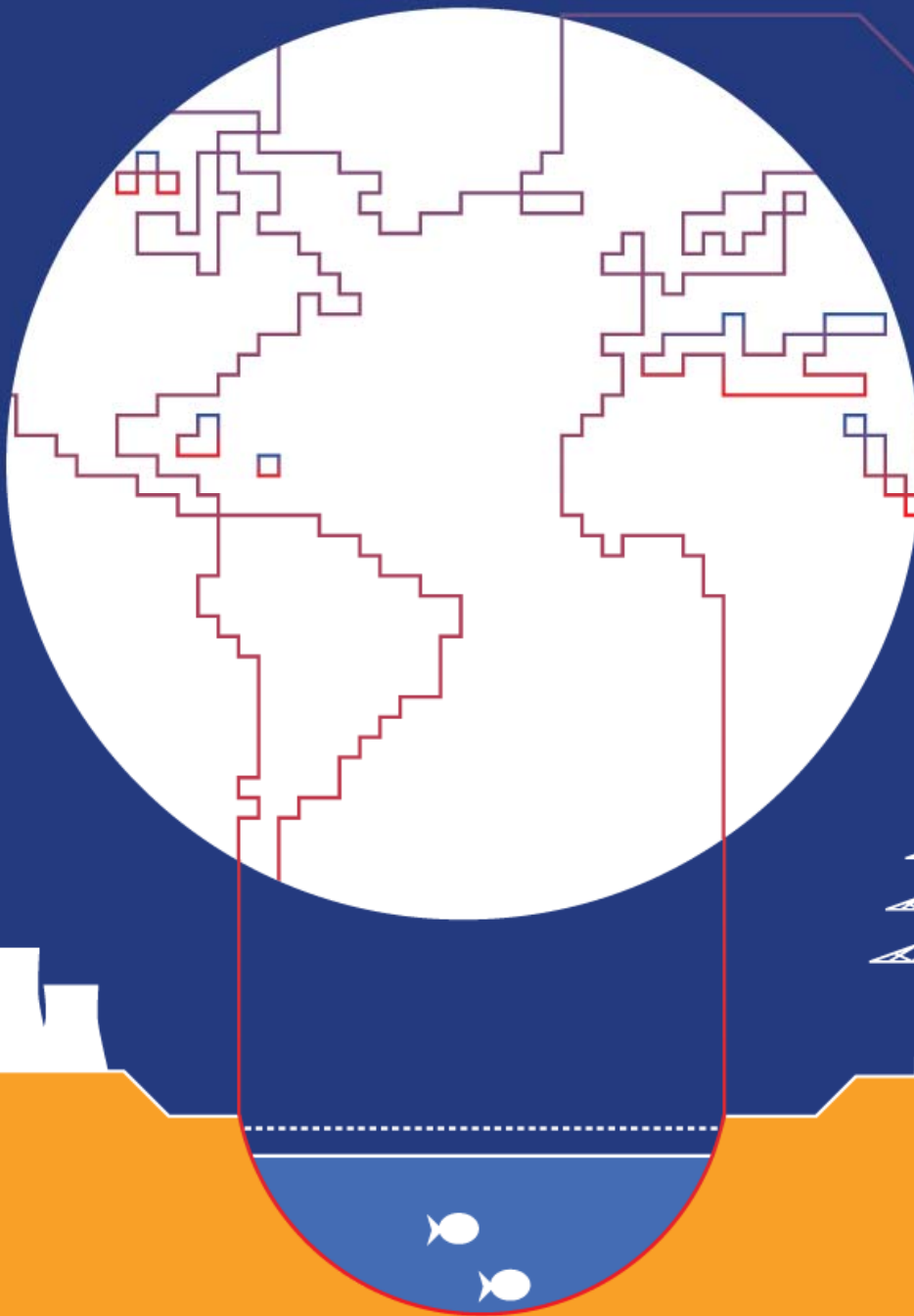


Global Rivers Warming Up: Impacts on Cooling Water Use in the Energy Sector and Freshwater Ecosystems



Michelle T. H. van Vliet

Global Rivers Warming Up:

Impacts on Cooling Water Use in the Energy Sector and Freshwater Ecosystems

Michelle T.H. van Vliet

Thesis committee

Promotor

Prof. dr. P. Kabat

Director/CEO of the International Institute for Applied Systems Analysis (IIASA), Austria

Professor of Earth System Science, Wageningen University

Co-promotor

Dr. F. Ludwig

Research scientist at Earth System Science, Wageningen University

Other members

Prof. dr. E.F. Wood, Princeton University, USA

Dr.-ing. M. Flörke, University of Kassel, Germany

Prof. dr. ir. M.F.P. Bierkens, Utrecht University

Prof. dr. ir. R. Uijlenhoet, Wageningen University

This research was conducted under the auspices of the SENSE research school.

Global Rivers Warming Up:

Impacts on Cooling Water Use in the Energy Sector and Freshwater Ecosystems

Michelle T.H. van Vliet

Thesis

submitted in fulfilment of the requirements for the degree of doctor
at Wageningen University
by the authority of the Rector Magnificus
Prof. dr. M.J. Kropff,
in the presence of the
Thesis Committee appointed by the Academic Board
to be defended in public
on Wednesday 19 December 2012
at 4 p.m. in the Aula.

Michelle T.H. van Vliet
Global Rivers Warming Up:
Impacts on Cooling Water Use in the Energy Sector and Freshwater Ecosystems
196 pages

Thesis, Wageningen University, Wageningen, NL (2012)
With references, with summaries in English and Dutch

ISBN 978-94-6173-424-2

Abstract

This thesis addresses the effects of climate change on global river temperatures and river flows, and the consequences for cooling water use in the energy sector and freshwater ecosystems. The sensitivity of water temperatures to atmospheric warming and changes in river flow is determined with both a statistical and physically-based water temperature modelling approach. A physically-based modelling framework, consisting of the stream temperature River Basin Model (RBM) and the Variable Infiltration Capacity (VIC) macro-scale hydrological model, was further developed for applications to large rivers worldwide. The resulting framework simulated observed conditions realistically. It was then forced with an ensemble of bias-corrected general circulation model output for the 21st century. Strong increases in water temperature and declines in low flows are projected in the south-eastern United States, southern and central Europe, eastern China, and parts of southern Africa and southern Australia. These regions could therefore be potentially affected by increased deterioration of water quality and freshwater habitats, and reduced potentials for human water uses under future climate.

Impacts of projected changes in river flow and water temperature on cooling water use in the energy sector and freshwater ecosystems (i.e. fish habitats) were assessed in more detail. The frequency and magnitude of exceeding maximum temperature tolerance values of several fish species significantly increased. This could, in combination with changes in flow regime, affect the distributions of freshwater species. To maintain and protect current freshwater ecosystems, environmental standards are defined with regard to the volume and temperature of water for cooling water use. In Europe and the U.S., most electricity is produced by thermoelectric power plants depending on cooling water. Projected increases in river temperatures and declines in low summer flow for both regions are expected to increase environmental restrictions on cooling water use, with substantial reductions in power plant capacities for the next 20-50 years. Conflicts between environmental objectives and economic consequences of reduced electricity production are thus expected to increase due to climate change. This study reinforces the need for improved climate adaptation strategies to ensure future water and energy security without compromising environmental objectives.

Contents

1	Introduction	1
1.1	Background and problem outline	1
1.2	Trends in river flow and water temperature during the 20 th century	3
1.3	Hydrological and water temperature modelling	6
1.4	Modelling climate change impacts: emission scenarios, climate models and bias-correction	11
1.5	Research objective and questions	12
1.6	Thesis outline and methodology	14
2	Global river temperatures and sensitivity to atmospheric warming and changes in river flow	17
2.1	Introduction	18
2.2	Data and methods	20
2.3	Performance of nonlinear water temperature regression model	28
2.4	Sensitivity of river temperature to changes in air temperature and river discharge	36
2.5	Discussion and conclusions	39
3	Coupled daily streamflow and water temperature modelling in large river basins	47
3.1	Introduction	48
3.2	Methodology	49
3.3	Results	58
3.4	Discussion and conclusions	68

4	Global river discharge and water temperature under climate change	73
4.1	Introduction	74
4.2	Material and methods	75
4.3	Results	78
4.4	Discussion and conclusions	89
5	Vulnerability of U.S. and European electricity supply to climate change	95
6	Global streamflow and thermal habitats of freshwater fishes under climate change	105
6.1	Introduction	106
6.2	Methods	108
6.3	Results	115
6.4	Discussion and conclusions	125
7	Synthesis	129
7.1	Introduction	129
7.2	Discussion of main results	131
7.3	Scientific contribution	140
7.4	Contribution to water management	141
7.5	Outlook and directions for further research	142
Supplementary information		
A	Global river discharge and water temperature under climate change	145
B	Vulnerability of U.S. and European electricity supply to climate change	151
C	Global streamflow and thermal habitats of freshwater fishes under climate change	165

References	167
Summary	183
Samenvatting	185
In the media ...	188
Acknowledgements	190
Curriculum Vitae	192
Peer-reviewed publications	193
SENSE education certificate	194

Introduction

1.1 Background and problem outline

There is a growing concern that climate change in combination with other anthropogenic changes will negatively affect water for human use and ecosystems. Overall, climate change is expected to contribute to an increasing pressure on water use between different sectors (e.g. agriculture, energy, industry, domestic uses) and ecosystems (Alcamo et al., 2003b). Considering the increasing demand for water with a growing and more prosperous global population (Vörösmarty et al., 2000), sufficient water resources to guarantee human uses and ecosystem health could become one of human's main challenges in the next decades. On a global mean basis, more than 73% of human water uses is currently extracted from fresh surface waters (i.e. rivers and lakes) (WWAP, 2009) (Figure 1.1a). In Europe and North America, largest part of surface water withdrawn is used for the energy and the industrial sector, while in Africa, South America, Oceania and most Asian countries, agriculture (irrigation) is by far the main water user (Figure 1.1b).

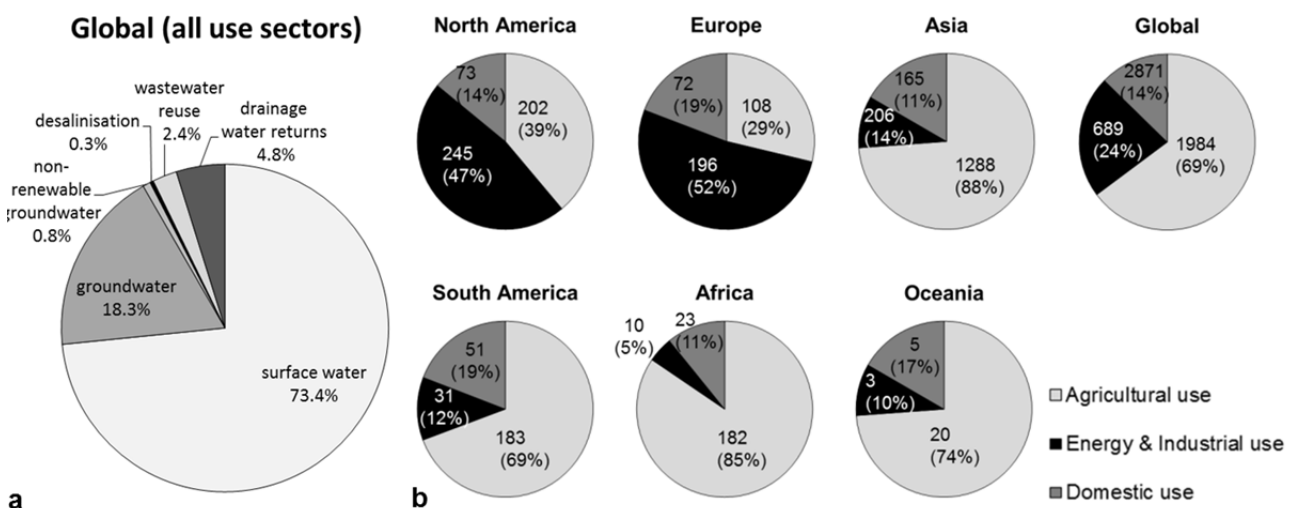


Figure 1.1: Global water withdrawals by supply sources for all sectors (adapted from WWAP (2009)) (a) and mean annual water withdrawal per sector in $10^9 \text{ m}^3 \text{ yr}^{-1}$ (relative contribution to total water withdrawal) for regions globally (created based on data of FAO-AQUASTAT 1998-2002 for all supply sources).

Due to climate change, the global hydrological cycle intensifies with increasing rates of evapotranspiration and precipitation (Del Genio et al., 1991; Durack et al., 2012; Held and Soden, 2006; Huntington, 2006). This results in an overall increase in mean annual river runoff (water availability) on a global mean basis (Oki and Kanae, 2006). However, due to the uneven distribution of water resources over time and space, and projected increases in climate and hydrological extremes, like droughts (e.g. Easterling et al., 2000; Wetherald and Manabe, 1999) risks for water stress (with water demand exceeding water availability) are expected to increase under changing climate (e.g. Arnell, 2004; Palmer et al., 2008).

The increasing awareness that climate change may affect water resources has greatly stimulated the study of the hydrological impacts of a changing climate. While impacts on water quantity have been studied widely on different scales, varying from catchment (e.g. Hamlet and Lettenmaier, 1999; Hurkmans et al., 2010) to continents (e.g. Lehner et al., 2006) and the world (e.g. Arnell, 2003a), considerably less work has been done to assess climate change impacts on water quality. The need to expand hydrological impact assessments to incorporate water quality issues is, however, now strongly recognized (Kundzewicz and Krysanova, 2010; Whitehead et al., 2009). This will result in more realistic estimates of future water resources and water stress under climate change and other anthropogenic changes (e.g. land use changes). Water temperature is directly affected by climate variability and change, and influences on its turn other water quality parameters. Significant rising trends in surface water temperature were observed during the 20th century and were related to increases in air temperature (e.g. Kaushal et al., 2010; Webb and Nobilis, 1994) and climate change induced decreases in summer flow (Pekarova et al., 2008a).

Potential alterations in hydrologic and thermal river regimes due to climate change may affect water quality (Ducharne, 2008; Murdoch et al., 2000), freshwater ecosystems and biodiversity (Carpenter et al., 1992; Rahel et al., 1996), and human water use functions like thermoelectric power production (Manoha et al., 2008), drinking water production (Ramaker et al., 2005; Senhorst and Zwolsman, 2005) and recreation (e.g. swimming water, fisheries (EEA, 2008b)). For most of these water uses, specific threshold values that reflect a deterioration or reduction in water usage potential are defined. For example, for drinking water production, the 25°C water quality standard defined by the World Health Organization (WHO, 2011) is commonly used as a critical water temperature limit for which thermophilic pathogens (e.g. *Legionella Campylobacter* and *Vibrio cholerae*) in surface waters with low residual concentrations of chlorine proliferate. For cooling water use, environmental standards are defined based on regulations to protect the freshwater ecosystems from thermal pollution (European Water Framework Directive and Fish Directive, and U.S. Clean Water Act).

During periods with (extreme) low river flows and high water temperatures, conflicts can arise between enforcing environmental standards and economic damage due to reduced potentials for human water use (Rutten et al., 2008). For example, during recent warm, dry summers in Europe (2003, 2006 and 2009) and the U.S. (2007-2008, 2012), several thermoelectric power plants were forced to reduce production or shut down (Forster and

Lilliestam, 2011; Macknick et al., 2011). Thermoelectric power plants convert thermal energy (heat) into electricity and directly depend on both availability and temperature of water resources to prevent overheating. Limited surface water for cooling and environment restrictions on thermal discharges during periods with low flow and high water temperatures can considerably reduce production capacities. This can have distinct economic impacts with significant rises in electricity prices (Boogert and Dupont, 2005; McDermott and Nilsen, 2011).

Due to climate change, extreme warm and dry periods are expected to occur more frequently and become more intense (e.g. Schar et al., 2004; Wetherald and Manabe, 1999). This could increase the occurrence and severity of large-scale streamflow and soil moisture droughts (e.g. Feyen and Dankers, 2009; Sheffield and Wood, 2008), and high water temperature events. Although climate change impacts on water temperature have been assessed for small catchments and river basins (Ferrari et al., 2007; Morrison et al., 2002), considerably less work has been done at larger regions (or coarser scales). Most previous macro-scale hydrological modelling studies that assessed climate change impacts on river flow focus on monthly or annual mean estimates (e.g. Alcamo et al., 2007; Arnell, 1999b; Oki and Kanae, 2006), while higher temporal resolution (e.g. daily) estimates are required to address impacts on freshwater ecosystems and beneficial uses. Hence, limited knowledge exists regarding the magnitude of both daily water temperature and river flow changes for large regions under future climate. This information is needed to address water management issues and impacts for water users, like the energy sector. Thermoelectric power plants in Europe and the U.S. are connected to continental-scale grids. Large-scale projections of streamflow and water temperature under future climate are therefore needed to anticipate and adapt to changes in cooling water availability.

This thesis focusses on the impacts of climate variability and change on daily streamflow and water temperature of rivers worldwide. Although lake levels, volumes and lake temperatures will also be affected by climate change, the overall focus of this thesis is on river systems, which contribute to a large part of surface water supply for human use. In addition, we address the potential consequences of projected changes in river temperature and flow for freshwater ecosystems and human water uses, with a main focus on thermoelectric power.

1.2 Trends in river flow and water temperature during the 20th century

1.2.1 Trends in river flow

Globally, broadly coherent trends in mean river flow and water availability have been observed during the 20th century (Bates et al., 2008) with an overall increase in annual runoff for high latitude regions and parts of the United States, and decreases for West Africa, southern Europe, southern South America and southern Australia (Dai et al., 2009; Milly et al., 2005). Changes in the amount and timing of precipitation, and whether precipitation falls as snow or rain, mainly affect river runoff changes, along with changes in evapotranspiration.

However, observed trends in river flow are not fully consistent with changes in precipitation and evapotranspiration, because human interventions (e.g. construction of dams and reservoirs, water withdrawals) have also affected flow regimes in many rivers during the 20th century (Bates et al., 2008).

Overall, limited to medium evidence has been found for climate-related large-scale trends in floods and droughts during the 20th century (Hisdal et al., 2001; Kundzewicz et al., 2005; Seneviratne, 2012; Svensson et al., 2005). This is mainly because streamflow gauge records are limited in space and time, and because of confounding effects of human impacts (land use changes, flow regulation) (Seneviratne, 2012). However, some regions, like southern and eastern Europe, have experienced increasing trends toward more intense and longer streamflow droughts (Stahl et al., 2010). In addition, robust trends toward earlier shifts of spring peak flows in snowmelt- and glacier-fed rivers have been detected (Barnett et al., 2005; Hodgkins et al., 2003; Tan et al., 2011).

1.2.2 Trends in river temperature

Studies analysing trends in river temperatures during the 20th century mainly focused on rivers in North America (Bartholow, 2005; Isaak et al., 2012; Morrison et al., 2002), Europe (Moatar and Gailhard, 2006; Pekarova et al., 2008a; Pekarova et al., 2011; Webb and Nobilis, 2007) and Eurasian Arctic rivers (e.g. Lammers et al., 2007; Liu et al., 2005), for which most long-term water temperature series are available. The general trend in water temperature increases in European freshwaters was 0.05-0.8°C decade⁻¹ during the past 30-50 years (EEA, 2008b). For rivers and streams in the United States, an increase in mean water temperature of 0.09-0.77°C decade⁻¹ was observed during the 20th century (Kaushal et al., 2010). Trends in water temperature derived from long-term monitoring records for river stations in Europe and the U.S. in our study are also within this range (see Figure 1.2 for some examples).

Overall, observed changes in water temperature strongly relate to changes in air temperature, which largely reflect changes in the energy budget. However, the fundamental cause of water temperature changes are related to alterations in the individual components of the heat budget. For large rivers, these are mainly changes in radiative heat flux (net radiation reaching the water body), latent heat flux (due to evaporation and condensation) and sensible heat flux (due to differences in water temperature and temperature of the air in contact with river water) (Webb, 1996). In addition, trends in river water temperature are also explained by changes in streamflow, which affect capacities for heat storage (thermal capacity) of the river course and, therefore, the sensitivities to changes in the energy budget (Webb, 1996).

For example, a larger increase in mean annual water temperatures of the Danube was observed for 1975-2005, mainly as a consequence of lower summer flow resulting from an earlier snowmelt (Pekarova et al., 2008a) (see Figure 1.2). Hence, water temperature trends in major rivers over the past century are a function of both climate and hydrological changes

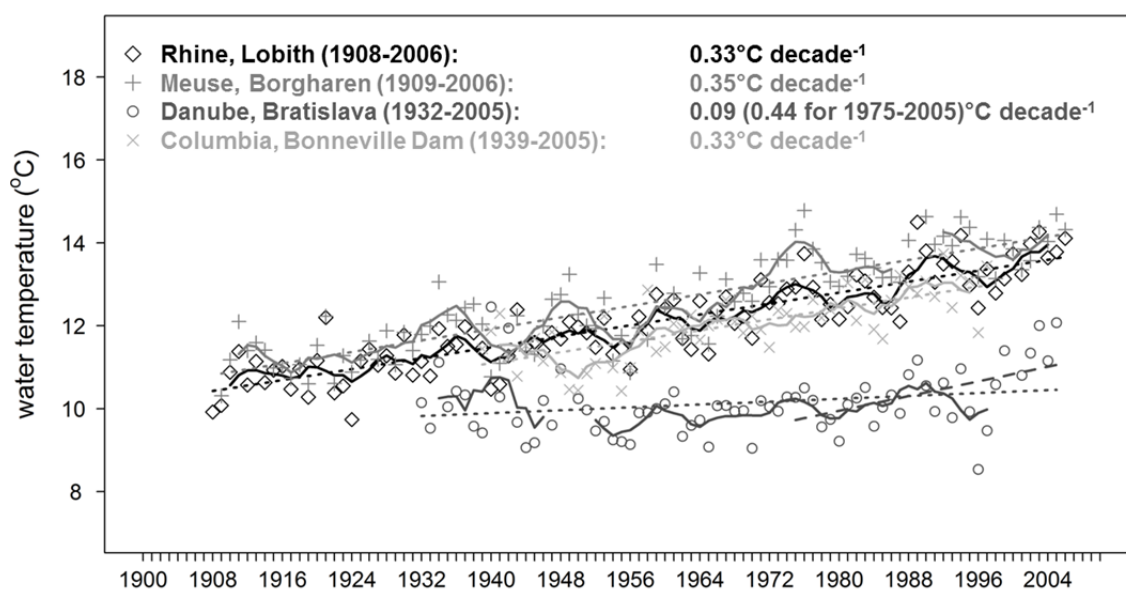


Figure 1.2: Long-term trends in mean annual water temperature for a station in the Rhine, Meuse, Danube (Europe) and Columbia (United States). Solid lines present 5-year moving averages and dotted lines are linear trend lines. Trends were constructed based on annual water temperature data of the Rhine and Meuse (provided by the Ministry of Infrastructure and Environment of The Netherlands), and daily data of the Columbia (Streamnet; <http://www.streamnet.org>) and Danube (Pekarova et al., 2008a).

(Moatar and Gailhard, 2006; Webb and Nobilis, 2007). Limited knowledge, however, exists regarding the contribution of streamflow changes to water temperatures on a large-scale.

Anthropogenic influences also contributed to the observed trends in increasing river water temperature, like thermal effluents of power stations (Edinger et al., 1968a; Webb and Nobilis, 2007), flow regulation and construction of reservoirs (Lowney, 2000; Webb and Walling, 1993), and land use changes, e.g. urbanization (Nelson and Palmer, 2007). Long-term rising trends for stations in the Rhine, Meuse and Danube in Western Europe, are partly due to climate change and due to increased cooling water discharge from thermoelectric power plants (EEA, 2008b). In the Columbia, water temperature trends are locally influenced by construction of dams and reservoirs (Isaak et al., 2012). Although it is recognized that anthropogenic influences (e.g. thermal effluents, regulation of river flow) will also affect future water temperatures, climate change will inevitably affect water temperatures globally, while anthropogenic influences highly vary on a local level, and can be controlled in response to climate change.

The overall focus of this thesis is therefore on the impacts of climate variability and change on global river temperatures and river flows. To improve understanding of changes in thermal regime of rivers, the sensitivities of water temperature to both changes in atmospheric conditions and river flow were studied. In addition, both the impacts of atmospheric warming and climate change induced river flow alterations were included in projections of water temperature under future climate.

1.3 Hydrological and water temperature modelling

Hydrological and water temperature models have been developed for different purposes. They have been used to study processes affecting streamflow and water temperatures or to produce estimates for other time periods or spatial extents than in the measured data. In addition, hydrological and water temperature models have been widely used for scenario analyses, such as climate change impact assessments.

1.3.1 Macro-scale hydrological models

Several macro-scale hydrological models have been developed to improve understanding of the global hydrological cycle and its interaction with land surface and substrate, and to simulate potential effects of climate change on hydrological fluxes globally. In general, macro-scale hydrological models can be classified into two groups. The first group are the land surface models (LSMs), which describe the vertical water and energy balances and which can be linked to atmospheric or climate models. Examples of LSMs, which were part of the global WATCH¹ modelling framework are: H08 (Hanasaki et al., 2008), HTESSEL (Balsamo et al., 2009), JULES (Cox et al., 1999), MATSIRO (Takata et al., 2003), Orchidee (de Rosnay and Polcher, 1998) and VIC (Liang et al., 1994). The second group are the global hydrological models (GHMs), which commonly only solve the water balance and are more focused on lateral water transport and water resources. GHMs are, for example, GWAVA (Meigh et al., 1999), LPJmL (Rost et al., 2008), MacPDM (Arnell, 1999c), MPI-HM (Hagemann and Dumenil, 1998), PCRGLOB-WB (van Beek et al., 2011), WaterGAP (Alcamo et al., 2003a) and WBM (Vörösmarty et al., 1998). A comparison of global water balance estimates for these LSMs and most of these GHMs by Haddeland et al. (2011) showed substantial differences in snow water equivalent between both modelling groups caused by the snow scheme employed. For evapotranspiration and runoff, the processes included and parameterizations used are, however, not distinct to either LSMs or GHMs.

In this PhD study, the Variable Infiltration Capacity (VIC) model (Cherkauer et al., 2003; Liang et al., 1994) (4.1.1 version) was used in the global hydrological - water temperature modelling framework. VIC is a grid-based macro-scale hydrological model that solves both the surface energy and water balance equations. The model represents sub-grid variability in vegetation, elevation, and soils by partitioning each grid cell into multiple land cover (vegetation) and elevation classes and the soil column is commonly divided into three soil layers (Figure 1.3). Evapotranspiration is calculated based on Penman-Monteith equation (Monteith, 1965; Penman, 1948). Snow accumulation and ablation processes are solved on sub-daily time step (regardless if the running time step is daily) via an energy balance approach (Wigmosta et al., 1994). Surface runoff in the upper soil layer is calculated based on the variable infiltration

¹ The Water and Global Change (WATCH) project, which was funded by the European Union (EU) Sixth Framework Programme (FP6), focussed on the global water cycle and related water resources under current and future climate. An important part of WATCH was a model intercomparison project in which both LSMs and GHMs participated.

curve (Zhao et al., 1980), and release of baseflow from the lowest soil layer is simulated according to the non-linear Arno recession curve (Todini, 1996). Surface runoff and baseflow are routed along the stream network to the basin outlet with an offline routing model that uses the unit hydrograph principle within the grid cells and linearized St. Venant's equations to simulate river flow through the stream channel (Lohmann et al., 1998). A reservoir scheme for VIC has been developed by Haddeland et al. (2006), which is combined with the routing scheme of Lohmann et al. (1998).

VIC was mainly selected because of the ability to solve both the surface energy balance and water balance equations, and the capability to simulate streamflow on a daily time step (e.g. Hurkmans et al., 2008; Lobmeyr et al., 1999). Commonly, high temporal resolution (e.g. daily) simulations are used for effective management of water and freshwater ecosystems. Furthermore, VIC has previously been successfully applied for global-scale estimates of streamflow (Nijssen et al., 2001b; Voisin et al., 2008), soil moisture (Sheffield et al., 2009) and water budgets (Pan et al., 2012) under historic conditions. The model has also been used for climate change impact assessments and other scenario studies (Elsner et al., 2010; Hamlet and Lettenmaier, 1999; Hurkmans et al., 2009; Nijssen et al., 2001a). Other advantages of VIC are the flexibility in use of meteorological forcing variables and different spatial resolutions (from 0.0625° to 1.0°) and temporal time steps (from hourly to daily time step) at which this model can be applied (Liang et al., 2004). A description of the model application and flowchart of the hydrological - water temperature modelling framework is given in Chapter 3.

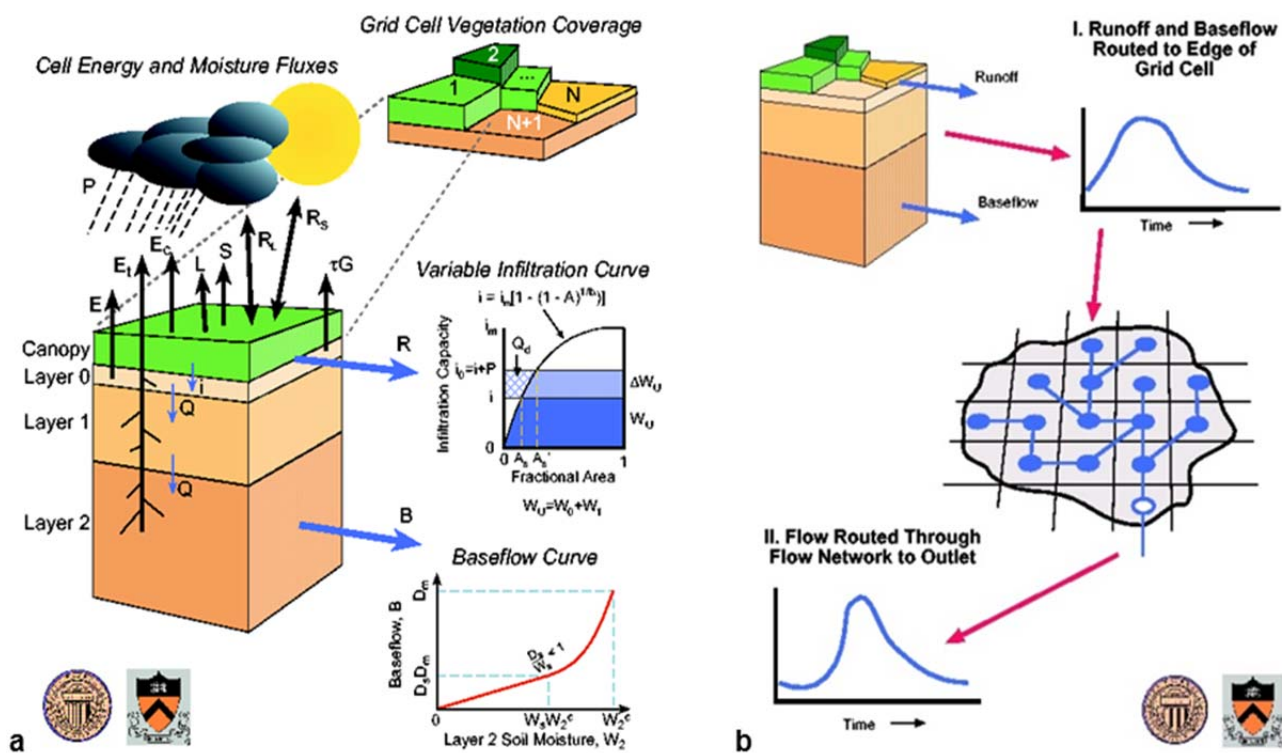


Figure 1.3: Concept of VIC macro-scale hydrological model (a) and routing model (b) (source: website University of Washington, <http://www.hydro.washington.edu/Lettenmaier/Models/VIC/>).

1.3.2 River temperature models

Different modelling approaches, varying in complexity and data input requirements have been developed to predict river temperatures. A distinction can be made between data (statistical) water temperature models, relying on observation records of water temperature, and process (physically-based) water temperature models, which include the physical description of main processes (energy budget) affecting water temperatures.

Data (statistical) water temperature models include regression models (Mohseni et al., 1998; Webb et al., 2008), stochastic models (Ahmadi-Nedushan et al., 2007; Caissie et al., 1998) and artificial neural networks (Chenard and Caissie, 2008; Sahoo et al., 2009) (see Figure 1.4 for a brief explanation and visualisation of the model concepts). These approaches are attractive because of their simplicity and limited requirement for meteorological and hydrological forcing data, while being characterized by high levels of explained variance (Webb and Nobilis, 1997) and small modelling errors (Caissie, 2006). Commonly air temperature is used as predictor variable, reflecting changes in energy budget (Mohseni et al., 1998; Webb et al., 2008). Only a few regression model studies also included river discharge or water level as additional variable to reflect thermal capacity of rivers (Rivers-Moore and Jewitt, 2007; Webb et al., 2003).

Other studies describe the energy budget and include heat transport equations (Haag and Luce, 2008; Sinokrot and Stefan, 1993) or apply the equilibrium temperature concept, that incorporates only net heat transfer processes at the water surface (Bogan et al., 2003; Caissie et al., 2005; Edinger et al., 1968b). Heat transport models include advection and dispersion (Caissie et al., 2005; Haag and Luce, 2008) or only advection terms (Lowney, 2000; Yearsley, 2009). Dispersion dominates only for streams and rivers with low flow velocities and on short length scales (Sinokrot and Stefan, 1993; Toprak and Savci, 2007). Many studies for natural river systems therefore neglect this term and use 1D-heat advection equations (Foreman et al., 2001). Heat exchange between streambed and water interface is generally small on daily basis or longer time steps (Sinokrot and Stefan, 1994) and is therefore often assumed to be negligible (Yearsley, 2012).

Physically-based water temperature models are more complex and require more meteorological and hydrological input data compared to statistical water temperature models. However, physically-based models are generally more useful for scenario studies like climate change impact assessment (e.g. Ferrari et al., 2007; Morrison et al., 2002) than statistical models, which are fitted for a specific historical period and are, therefore, limited in their application to forecasting and scenario studies. In addition, heat transport models are suitable to produce spatially variable estimates of water temperature, while statistical models are commonly fitted for specific point (station) locations.

In this thesis, both a statistical and physically-based water temperature modelling approach were used to assess the sensitivity of river temperatures to atmospheric warming and

	model concept	method	concept	input
DATA MODELS	regression	linear	fit linear Tw-Tair relation	<ul style="list-style-type: none"> • Tw • Tair • (Q)
	nonlinear	fit s-curve Tw-Tair relation		
	multiple	fit Tw-Tair-Q relation		
PROCESS MODELS	stochastic	separate Tw series into an annual (Fourier or sinusoidal function) and short-term component (Box-Jenkins method and/or Markov process)		<ul style="list-style-type: none"> • Tw • Tair
	artificial neural networks (ANN)	fit unknown mathematical functions between Tw, Tair and other parameters		<ul style="list-style-type: none"> • Tw • Tair
	equilibrium temperature concept	use equilibrium temperature (Te) and sum of heat fluxes at air-water interface to predict Tw at point location or stream segment	$Tw = Te - (Htot/K)$ $Htot = HnS + HnL + Hevap + Hcond$	<ul style="list-style-type: none"> • Tw • meteo.
heat transport	use heat advection (dispersion) equations to simulate heat transport	$Htot = HnS + HnL + Hevap + Hcond$	<ul style="list-style-type: none"> • meteo. • Q • geometry 	

Figure 1.4: Overview of water temperature modelling concepts and required input data. Abbreviations are used for water temperature (Tw), air temperature (Tair), river discharge (Q), total heat fluxes at air - water interface (Htot), net shortwave solar radiation (HnS), net longwave atmospheric radiation (HnL), evaporative/latent heat flux (Hevap), conductive/sensible heat flux (Hcond), equilibrium temperature (Te), thermal exchange coefficient (K) and subsurface heat flux (Hsubsurface).

changes in river flow. Although stochastic models and artificial neural networks generally provide good water temperature estimates at daily time steps (Caissie, 2006; Sahoo et al., 2009), a regression modelling approach was used, because this approach is more suitable to explore the sensitivity of water temperatures to changes in input variables (i.e. air temperature and streamflow). A nonlinear water temperature regression model based on air temperature (Mohseni et al., 1998) was modified to include river discharge as independent variable, in addition to air temperature. A nonlinear rather than linear regression model was

used, because it better reflects the physical representation of water temperature regime (Mohseni and Stefan, 1999) (see Chapter 2). In addition, a time lag was incorporated to estimate water temperature on daily basis, because of autocorrelation of water temperature on daily time steps.

In addition to this statistical approach, a heat transport model was coupled to the macro-scale VIC hydrological model. This physically-based modelling approach was used to simulate daily water temperature and river discharge for both the historic and future climate on a global scale. The particle tracking stream temperature River Basin Model (RBM) (Yearsley, 2009) was selected, which solves the time-dependent one-dimensional heat advection equation with a semi-Lagrangian (mixed Eulerian-Lagrangian) numerical scheme. Water temperature is calculated for a specific stream segment based on the upstream water temperature and inflow into the stream segment, the dominant heat exchange at the air - water surface, and the inflow and temperature of water advected from tributaries and, optionally, from subsurface (Figure 1.5). Solutions are obtained by tracking individual water parcels along their flow characteristics and storing the output at discrete points on a fixed grid. This makes the water temperature model computationally efficient and highly scalable in both time and space. RBM was previously tested for subbasins of the Columbia on $1/16^\circ$ (Yearsley, 2009; Yearsley, 2012). In this thesis, modifications were made to RBM for application on global scale and to obtain more realistic water temperature estimates in river basins with anthropogenic impacts (reservoirs and thermal effluents from thermoelectric power plants). The global modelling framework was applied on a $1/2^\circ \times 1/2^\circ$ spatial resolution (which is 55 x 55 km at the equator). The concept of the RBM water temperature model and reverse particle tracking method is shown in Figure 1.5. A more detailed description of the model and flowchart of the hydrological - water temperature modelling framework is given in Chapter 3.

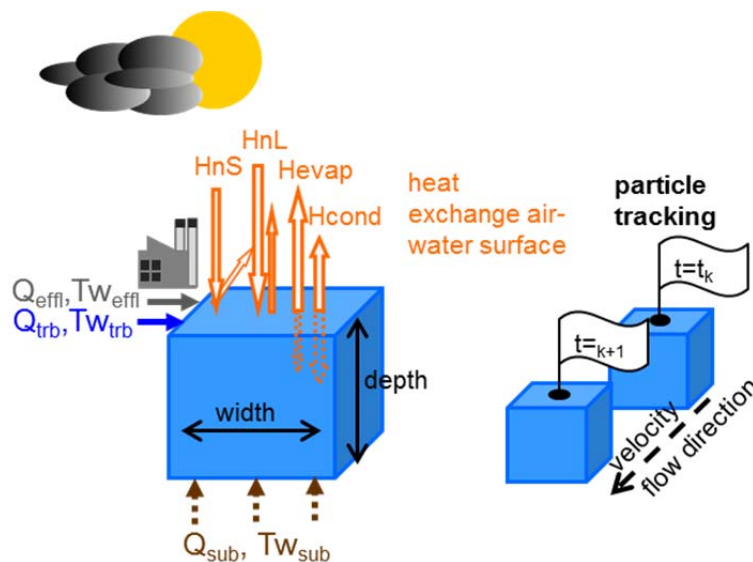


Figure 1.5: Concept of RBM stream temperature model and schematic of reverse particle tracking method. Abbreviations are used for water temperature (T_w) and flow (Q) of tributaries (trb), subsurface (sub) and thermal effluents (effl), net shortwave solar radiation (H_nS), net longwave atmospheric radiation (H_nL), evaporative/latent heat flux (Hevap) and conductive/sensible heat flux (H_{cond}).

1.4 Modelling climate change impacts: emission scenarios, climate models and bias-correction

Climate change impacts are commonly quantified by using climate scenarios as input into impact models (e.g. hydrological models). Climate scenarios are plausible representations of future climate conditions under future greenhouse gas emissions (Moss et al., 2010), and are commonly produced by coupled atmosphere-ocean general circulation models (GCMs). These climate models incorporate the basic physical laws and processes that govern the Earth's atmosphere and oceans circulation, and the interactions with land, ocean and ice surfaces (Ruddiman, 2001). These processes are described by three-dimensional time-dependent equations, which are solved numerically by coarsely discretizing space. Oceans and atmosphere are represented by multiple vertical layers and horizontal resolutions are commonly larger than one degree. As a result, GCMs are limited in the representation of small-scale processes, especially rainfall (Beven, 2011). In addition, uncertainties in climate projections from GCMs are related to feedback mechanisms, for example, cloud feedbacks, snow and ice albedo, and development of ocean circulation (Andrews et al., 2012; Boer and Yu, 2003; Williams et al., 2003).

To produce projections of future climate, GCMs are forced with emission scenarios, describing future emissions of greenhouse gasses and (sulphate) aerosols. The Intergovernmental Panel on Climate Change (IPCC) SRES emissions scenarios (Nakicenovic, 2000) are based on four different storylines. The two main criteria for these four storylines are globalisation (homogenous world) versus regionalisation (heterogeneous world), and economic focus versus environmental focus. The SRES scenarios represent different demographic, social, economic, technological and environmental developments, but do not take into account any current or future measures to reduce greenhouse gas emissions (e.g. the Kyoto protocol).

In line with the growing interest among end users (e.g. policy makers) in climate scenarios that include different approaches to mitigation, a new generation of scenarios for climate research have recently been developed as part of the IPCC's Fifth Assessment Report. The new scenarios include projections of emissions, concentrations and land cover change based on a set of four pathways, the representative concentration pathways (RCPs) (Moss et al., 2010). These four pathways can be achieved by a diverse range of socio-economic and technological development scenarios, and span a range of radiative forcing values for 2100 from 2.6 to 8.5 W/m² (van Vuuren et al., 2011).

In this thesis, GCM experiments based on the SRES emissions scenarios (Nakicenovic, 2000) were used for climate change impact assessment, because the new scenarios based on RCPs (Moss et al., 2010) were not yet available during the start of this study. We used GCM output for the SRES A2 and B1 emissions scenarios to capture a range of uncertainties associated with driving forces and emissions. The A2 scenario considers a primarily regionally oriented world of fragmented and slow technological change, with a continuously increasing global population and economic development. The B1 scenario assumes a world with an emphasis

on global solutions to economic, social, and environmental sustainability with a much more rapid introduction of renewables (Nakicenovic, 2000). Both SRES scenarios were selected in this study, because they represent contrasting storylines and emissions scenarios, which results in the largest range from the IPCC SRES main emissions scenarios. We used output of the three GCMs ECHAM5/MPIOM, CNRM-CM3 and IPSL-CM4 (denoted as ECHAM, CNCM3 and IPSL henceforth) for both SRES scenarios (for details see Hagemann et al. (2011)). These GCMs were selected because of the availability of daily output for both the SRES A2 and B1 scenario. We used GCM output for both SRES emissions scenarios for the 21st century and for a control simulation period.

Because of significant systematic biases in the ability of GCMs for simulations of observed climate (Randall et al., 2007), a bias correction was performed on the GCM output to produce suitable forcings for use in (hydrological) impact models. Several previous studies that assessed the hydrological impacts of climate change used the 'change factor' ('delta') approach (Diaz-Nieto and Wilby, 2005; Hay et al., 2000). This means that projected changes between control and future climate are added to baseline climate observations to represent future climate, which are then used into (hydrological) impact models (Fowler et al., 2007b). Within this approach, the representation of extremes in future climate projections is filtered out in the transfer process, which limits the use for studies of future changes in extreme events (Graham et al., 2007). To obtain more reliable estimates of changes in hydrological variability and extremes, more sophisticated statistical bias correction methods have been developed (e.g. Ines and Hansen, 2006; Li et al., 2010; Piani et al., 2010). Within the WATCH project, a statistical bias correction procedure was performed on daily precipitation, mean, minimum and maximum surface air temperature based on transfer functions that describe the relationship between the daily modelled (corrected) and daily observed time series for each grid cell (Hagemann et al., 2011). These transfer functions are fitted for a historic period and are used to adjust the probability distribution function of intensity for these simulated variables for both historic and future periods (Piani et al., 2010). The modelling chain of the hydrological and water temperature impact assessment of this study is summarized in Figure 1.6.

1.5 Research objective and questions

Climate change will affect thermal and flow regimes of rivers, having a direct impact on freshwater ecosystems and human water uses. Limited knowledge, however, exists regarding the magnitude of water temperature increases and impacts of river flow changes on water temperature, in particular on a large scale. In addition, it is unclear which regions and river basins worldwide will experience the largest increases in water temperature combined with changes in river flow. It is both of scientific and socio-economic importance to understand to what extent river flows and temperatures will change, which regions will be most strongly affected, and whether river temperature rises will simply follow atmospheric warming (reflected by air temperature increase) or are also influenced by changes in flow regime.

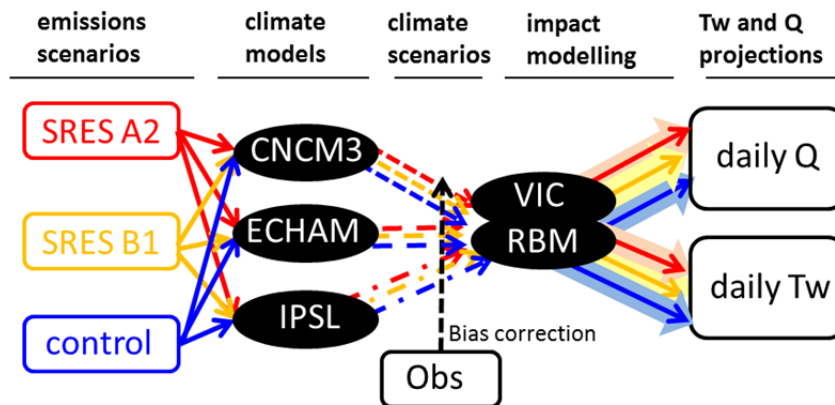


Figure 1.6: Modelling chain of the hydrological - water temperature impact assessment with selected emission scenarios and GCMs, and bias-correction of GCM output with observed meteorological dataset (Obs). These data were used to force the physically-based hydrological - water temperature (VIC-RBM) modelling framework, resulting in daily simulations of river flow (Q) and water temperature (Tw) under control (reference) and future climate.

Recent warm, dry summers showed adverse impacts of high river temperatures and low flows on freshwater ecosystems (Parry et al., 2010) and human water uses, such as thermoelectric power (Forster and Lilliestam, 2011; NETL, 2009) and drinking water production (Ramaker et al., 2005; Senhorst and Zwolsman, 2005). In Europe and the United States, conflicts arose between water use for cooling of power plants and environmental objectives. Due to climate change, situations with high water temperatures and low summer flow might occur more often. A few studies addressed the large-scale impacts of climate change on thermoelectric water use (Flörke et al., 2012; Flörke et al., 2011) and freshwater ecosystems (Döll and Zhang, 2010), but with a focus on hydrological (water quantity) effects. However, streamflow and water temperature both affect the cooling capacity of rivers and are major parameters characterizing the physical conditions of freshwater habitats. In addition, impacts on both cooling water use and electricity production potentials should be quantified to better understand the developments of links between water security and energy security, commonly called the ‘water-energy security nexus’ (Stucki and Sojamo, 2012), under changing climate. This information is also useful for defining river basin management and conservation strategies, and for strategic planning of the electricity sector for the coming decades.

Based on this, the main objective of this thesis is two-fold:

- *To assess climate change impacts on river flows and water temperatures globally; and*
- *To address the potential consequences of changes in river flows and water temperatures for cooling water use in the energy sector and freshwater ecosystems during the 21st century.*

This objective was addressed by using a stepwise methodology. In the first step, hydrological and water temperature models were tested and their performances were evaluated under current climate. Both a statistical and physically-based modelling approach were used to assess the impacts of river flow changes on water temperature. In a second step, projections of both streamflow and water temperature under future climate were produced and analysed

on a global scale. In a third step, the water-energy dependencies under future climate were quantified by using an integrated modelling approach of an electricity production model linked to the physically-based hydrological and water temperature models. In a final step, global projections of streamflow and water temperature under future climate were combined with spatial distributions of freshwater fish species to address the potential consequences for freshwater habitats. Each step in this approach is accompanied by a specific research question:

Q1. What is the performance of a statistical (regression) and physically-based (heat transport) water temperature modelling approach for daily river temperature estimation on macro-hydrological scale, and how sensitive are river temperatures to changes in river flow? (Chapter 2 and 3)

Q2. What are the impacts of climate change on both river flows and water temperatures globally, and which regions show the largest projected changes? (Chapter 4)

Q3. How will cooling water use and electricity production potentials in Europe and the United States be affected by changes in river flow and water temperature under future climate? (Chapter 5)

Q4. What are the potential consequences of climate change induced alterations in river flow and water temperature for freshwater (fish) habitats in different regions worldwide? (Chapter 6)

1.6 Thesis outline and methodology

The objective and research questions are addressed in five scientific papers, which are presented in the chapters two to six. An overview of the research steps and corresponding chapters is shown in Figure 1.7.

To answer the first research question, a nonlinear regression modelling approach was used to explore the sensitivity of daily river temperatures to both atmospheric warming (reflected by air temperature increases) and changes in river flow for a high number of river stations on a global scale (Chapter 2). In addition, the heat transport model RBM, coupled to the VIC macro-scale hydrological model, was further developed for application to river basins on a global scale, including impacts of reservoirs and thermal effluents. The performance of the coupled VIC-RBM modelling framework was evaluated for river basins in different hydro-climatic zones and with different anthropogenic impacts, along with the sensitivities of water temperatures to river flow changes (Chapter 3).

For the second research question, the global VIC-RBM framework was forced with an ensemble of bias-corrected GCM output for both the SRES A2 and B1 scenario to produce global-scale river flow and water temperature series for the 21st century. These projections were combined to get a first impression of regions that could potentially experience an increased deterioration of water quality, freshwater habitats and reduced potentials for

human water uses (e.g. drinking water, thermoelectric power) under future climate (Chapter 4).

For the third research question, the VIC-RBM framework was combined with an electricity production model and forced with the ensemble of bias-corrected GCM output to assess the impacts on cooling water use and thermoelectric power production in Europe and the U.S. over the next 20-50 years (Chapter 5).

For the final research question, global projections of streamflow and water temperature were combined with spatial distributions of several fish species and their thermal tolerances to address the consequences for freshwater (fish) habitats in different regions worldwide (Chapter 6).

Finally in Chapter 7, the main results are discussed in a broader context, along with the contribution to science and water management, and an outlook for further research on this topic.

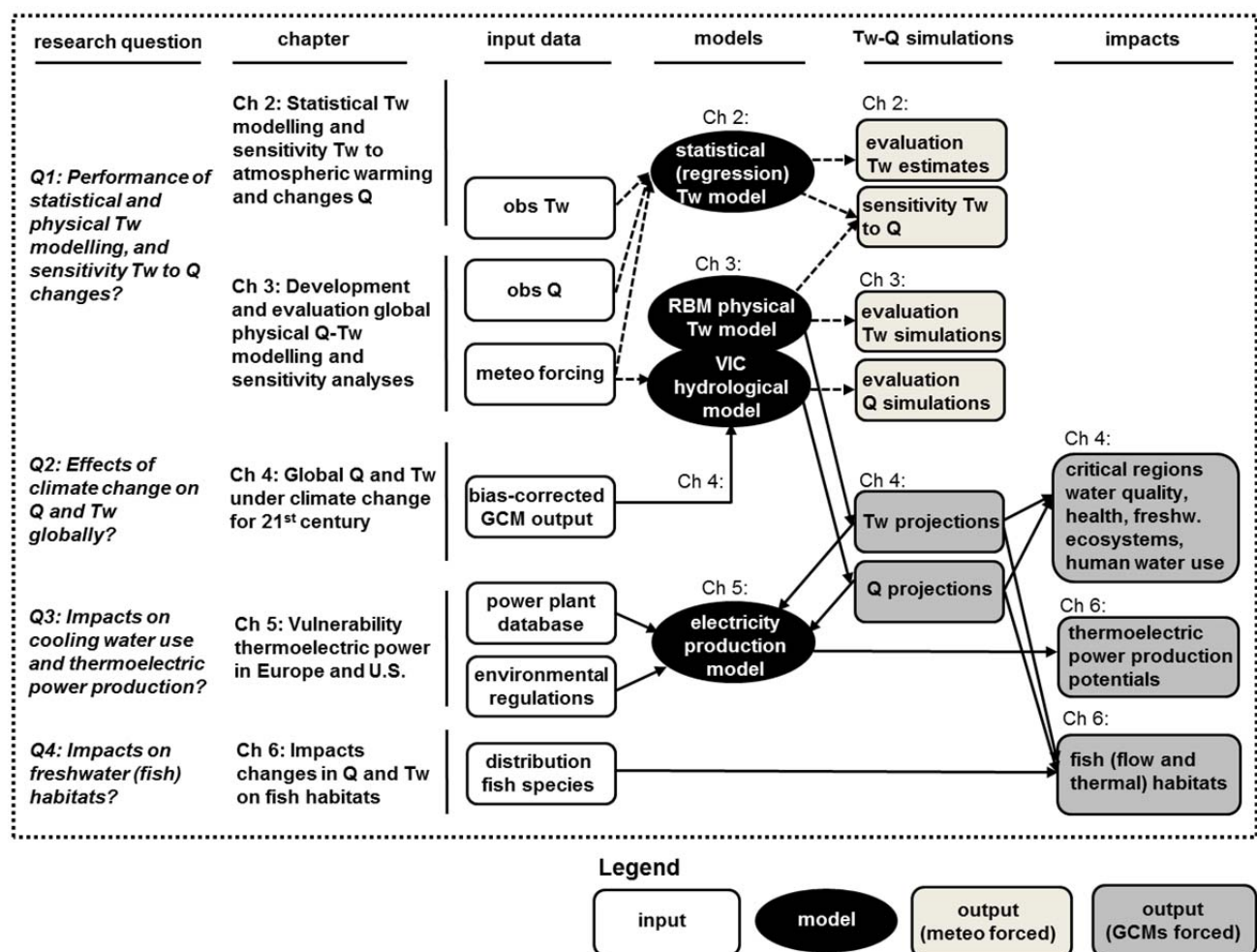


Figure 1.7: Schematic representation of methodological framework with input data, models and output data. Abbreviations are used for water temperature (Tw) and river flow (Q). A distinction is made between output data based on model simulations with a historical meteorological dataset (light grey) and based on simulations with bias-corrected general circulation models (GCMs) output used as forcing (dark grey).

Global River Temperatures and Sensitivity to Atmospheric Warming and Changes in River Flow

Abstract

This study investigates the impact of both air temperature and river discharge changes on daily water temperatures for river stations globally. A nonlinear water temperature regression model was adapted to include discharge as a variable in addition to air temperature, and a time lag was incorporated to apply the model on a daily basis. The performance of the model was tested for a selection of study basin stations and 157 river temperature stations globally using historical series of daily river temperature, air temperature, and river discharge for the 1980–1999 period. For the study basin stations and for 87% of the global river stations, the performance of the model improved by including discharge as an input variable. Greatest improvements were found during heat wave and drought (low flow) conditions, when water temperatures are most sensitive to atmospheric influences and can reach critically high values. A sensitivity analysis showed increases in annual mean river temperatures of +1.3°C, +2.6°C, and +3.8°C under air temperature increases of +2°C, +4°C, and +6°C, respectively. Discharge decreases of 20% and 40% exacerbated water temperature increases by +0.3°C and +0.8°C on average. For several stations, maximum water temperatures on a daily basis were higher under an air temperature increase of +4°C combined with a 40% discharge decrease compared to an air temperature increase of +6°C (without discharge changes). Impacts of river discharge on water temperatures should therefore be incorporated to provide more accurate estimations of river temperatures during historical and future projected dry and warm periods.

This chapter has been published as:

van Vliet, M.T.H., F. Ludwig, J.J.G. Zwolsman, G.P. Weedon, and P. Kabat (2011), Global river temperatures and sensitivity to atmospheric warming and changes in river flow, Water Resources Research, 47, W02544, doi:10.1029/2010WR009198.

2.1 Introduction

Water temperature is an important physical property of rivers, having a direct impact on water quality (e.g. concentrations of dissolved oxygen) (Ozaki et al., 2003), and on the growth rate and distribution of freshwater organisms (Mohseni et al., 2003). Additionally, river temperature is of economic importance in water requirements for industry, electricity and drinking water production, and recreation (EEA, 2008b; Webb et al., 2008). Several studies found a gradual increase in river temperatures during the last century in relation to an increase in air temperatures (e.g. Kaushal et al., 2010; Lammers et al., 2007; Liu et al., 2005; Webb, 1996). In addition, rising water temperatures have also been related to changes in river flow. For example, for the Danube an increase in water temperature was observed as a consequence of lower summer flow, resulting from earlier onset of the snowmelt period and decreased summer precipitation (Pekarova et al., 2008a). Water temperature trends in major rivers over the past century are thus a complex function of both climate and hydrological changes (Moatar and Gailhard, 2006; Webb and Nobilis, 2007). In addition, anthropogenic influences, like thermal effluents from power stations (Edinger et al., 1968a; Webb and Nobilis, 2007), flow regulation and construction of reservoirs (Lowney, 2000; Webb and Walling, 1993), and land use changes (e.g. urbanization (Nelson and Palmer, 2007)) also affect water temperature. These anthropogenic influences vary considerably between catchments and river basins (Caissie, 2006).

To estimate river temperature as a function of climate variables, different model approaches varying in complexity and data input requirements have been developed (Mohseni et al., 1998). The most complex approach uses process (physically-based) water temperature models, including heat advection(-dispersion) transport equations (Haag and Luce, 2008; Sinokrot and Stefan, 1993; Yearsley, 2009). Another group applies the equilibrium temperature concept that incorporates only net heat transfer processes at the water surface (Bogan et al., 2003; Caissie et al., 2005; Edinger et al., 1968b; Mohseni and Stefan, 1999). A recent development is the application of artificial neural networks (ANNs) which use unknown (nonlinear algebraic) functions to predict water temperatures (Chenard and Caissie, 2008; Sahoo et al., 2009). In addition, statistical approaches have been applied, like stochastic models which separate the water temperature time series into an annual component which is represented by a Fourier or sinusoidal function, and a short-term component using Box and Jenkins methods and/or a Markov process (Ahmadi-Nedushan et al., 2007; Caissie, 2006). Finally, water temperature regression models are widely used, calculating stream or river temperature from air temperature, either based on linear or nonlinear regression relations. These models are attractive because of their simplicity and limited requirement of meteorological and hydraulic data, while still being frequently characterized by high levels of explained variance in absence of detailed information on heat fluxes (Webb and Nobilis, 1997).

Air temperature is commonly used as a predictor variable in water temperature regression models, because it is a major component in calculating net changes of heat flux at the water

surface (Webb et al., 2003; Webb et al., 2008). As a result, there is a strong correlation between air and water temperatures. Linear water temperature regression models have been widely applied using weekly and monthly mean values of water temperature (e.g. Webb and Nobilis, 1997; Webb and Walling, 1993). In addition, linear regression analysis has also been successfully applied on two-hour and daily time step by including a time lag in the regression model (Stefan and Preudhomme, 1993).

Several studies have shown that the water - air temperature relationship deviates from linearity when air temperature is below 0°C and above ~ 20°C (e.g. Mohseni and Stefan, 1999; Mohseni et al., 1998). At low temperatures, this departure is due to both the dominant influence of groundwater and the existence of an ice cover that prevents surface heat exchange. At high temperatures, the departure results from extensive evaporative cooling and enhanced back radiation. As a result, the water - air temperature relationship resembles an S-shaped function, rather than a linear function (Mohseni and Stefan, 1999).

Although several studies have demonstrated that water temperature is inversely related to river discharge, reflecting a reduced thermal capacity under decreasing flow volumes (e.g. Hockey et al., 1982; Webb, 1996; Webb et al., 2003), only a few addressed the influence of river flow on the water - air temperature relationship or included river discharge as an additional variable into water temperature regression models (Ozaki et al., 2003; Rivers-Moore and Jewitt, 2007; Webb et al., 2003). A multiple linear regression analysis of Webb et al. (2003) showed that an inverse relation between water temperature and discharge exists for all catchments and timescales, with greater impact at shorter timescales and in larger catchments of the Exe basin (UK). Limited knowledge exists, however, with regard to the influence of discharge on water temperatures for large river basins. In addition, relatively few water temperature studies focused on river temperatures outside Europe and North America, although some examples exist: e.g. for South African rivers (Dallas, 2008; Rivers-Moore and Jewitt, 2007) and for Russian Pan-Arctic rivers (Lammers et al., 2007; Liu et al., 2005).

Considering future perspectives, river temperatures are expected to be affected by warming and modifications in river regime as a result of climate change and other anthropogenic influences (e.g. flow regulation, water withdrawals) (Caissie, 2006). A few studies addressed the impact of climate change on stream temperatures by using air temperature scenarios as input into a water temperature regression model applied on a weekly or monthly basis (Mantua et al., 2010; Mohseni et al., 1999; Mohseni et al., 2003; Webb, 1996). The performance of water temperature regression models and sensitivity of water temperatures have not yet been studied on a daily basis and in particular not on a global scale. However, atmospheric warming and changes in river flow are expected to affect river temperatures globally, with possibly negative consequences for freshwater ecosystems and several usage functions (e.g. industry, thermal power, drinking water and recreation).

Hence, the objectives of our study are as follows: 1) to test the performance of a water temperature regression model that estimates daily river temperatures based on both air

temperature and river discharge data for river temperature stations on a global scale; and 2) to quantify the sensitivity of river temperatures to both atmospheric warming (air temperature increases) and changes in river flow. To address these objectives, a nonlinear water temperature regression model based on air temperature was modified to include river discharge as an additional variable. In addition, a time lag was incorporated to apply the model on a daily basis. This resulted in a daily water temperature regression model with air temperature and discharge as predictor variables without requiring detailed meteorological and hydraulic input data which are scarce for large parts of the world.

The performance of the model was tested for a selection of study basin stations for 1980-1999, and in particular during a heat wave when river temperatures are highest. Subsequently, a global database with water temperature linked to discharge stations was created, and the regression model was applied to 157 river temperature and discharge stations globally. In addition, the sensitivity of river temperatures was assessed under different rates of air temperature increase and changes in river discharge realistic in the context of climate change. Hence, this study is a global assessment of river temperatures and the sensitivity to both atmospheric warming and changes in river flow.

2.2 Data and methods

2.2.1 River temperature and discharge data

Worldwide data of river temperatures are available from the United Nations Environment Programme (UNEP) Global Environment Monitoring System (GEMS/Water; <http://www.gemswater.org/>). Although the availability of river temperature data in this database is very limited during the period 1979-1987, especially for the Southern Hemisphere (Webb, 1996), marked improvements have been made over the last 10 years in both spatial coverage and the amount of data (Lammers et al., 2007). For river discharge, daily mean and monthly mean series for stations on a global scale are available from the Global Runoff Data Centre (GRDC; <http://grdc.bafg.de/>).

In our study, river temperature and discharge data series have been used from 157 stations globally, for which both water temperature data from GEMS/Water and discharge data from GRDC were available over the 1980-1999 period. In addition to the GEMS/Water data, we used high-temporal resolution water temperature series for 14 stations in a selection of study river basins, which were provided by different data sources listed in Table 2.1. The number of measurements during the 1980-1999 period is highest for the Rhine (Lobith) with 7283 (99.7% of record) and lowest for the Orange (Oranjedraai) with 246 measurements (3.4%). For the Lena (Kusur), Ob (Salekhard) and Yenisey (Igarka), water temperature data could only be provided as mean values for every 10 days. The coverage of the records by water temperature measurements for these Arctic rivers is less than 50%, as the rivers are covered with ice during a large part of the year. For all study basin stations, daily instantaneous

Table 2.1: Overview of data sources of water temperature measurements for 1980-1999 period, and study basin characteristics (geographic region, number of measurements, time resolution, mean river discharge (Q), upstream drainage area, and impacts of reservoirs, thermal effluents and melt water). Abbreviations are used for instantaneous measurements (instant.) Links to online databases are: StreamNet (<http://www.streamnet.org>), USGS (<http://waterdata.usgs.gov/>), Waterbase (<http://live.waterbase.nl/>), Murray-Darling Basin Commission (MDBC; <http://www.mdbc.gov.au/>).

river (station)	region	data sources	n meas. (%)	time res.	mean Q (m ³ /s)	area (*10 ³ km ²)	reservoirs	thermal effl.	melt-water
Columbia (The Dalles)	North-America	StreamNet	3584 (49.1)	daily instant.	5250	614	++	+-	+
Mississippi (Clinton)	North-America	USGS	3418 (46.8)	daily instant.	1610	222	+	+	+
Missouri (Omaha)	North-America	USGS	1190 (46.8)	daily instant.	1074	846	+	+-	+
Potomac (Washington D.C.)	North-America	USGS	3687 (50.5)	daily mean	365	30	+-	+	+
San Joaquin (Vernalis)	North-America	USGS	6560 (89.8)	daily mean	157	35	+-	+	+-
Danube (Bratislava)	Europe	Dataset (Pekarova et al., 2008a)	7243 (99.2)	daily instant.	2055	131	+	+	+
Danube (Budapest*)	Europe	Dataset via Zsolt Kozma	3287 (45.0)	daily mean	2284	184	+-	+	+
Meuse (Eijsden)	Europe	Waterbase	6560 (89.8)	daily instant.	269	27	-+	++	+-
Rhine (Lobith)	Europe	Waterbase	7283 (99.7)	daily instant.	2361	161	-	++	+-
Orange (Oranjedraai**)	Africa	Departm. of Water Affairs and Forestry (DWAFF)	246 (3.4)	daily instant.	186	851	+-	-	-
Darling (Burtundy)	Australia	Murray-Darling Basin Commission (MDBC)	1998 (27.4)	daily instant.	40	647	-+	+-	-
Lena (Kusur)	Asia (Arctic)	ART-Russia dataset (Lammers et al., 2007)	215 (29.9)	10-day mean	17140	2430	+-	-	++
Ob (Salekhard)	Asia (Arctic)	ART-Russia dataset	290 (40.3)	10-day mean	12774	2950	+-	+-	++
Yenisey (Igarka)	Asia (Arctic)	ART-Russia dataset	289 (40.1)	10-day mean	18949	2440	++	-	++

* For discharge, data of station Nagymaros have been used as discharge data (from GRDC) were not available for station Budapest; ** For discharge, data of station Violsdreef have been used as discharge data (from GRDC) were not available for station Oranjedraai.

measurements with one observation per day at a fixed time were available except for the rivers Potomac (Washington D.C.), San Joaquin (Vernalis) and Danube (Budapest) for which daily (24h) mean values were provided.

Water temperatures of the selected stations in the Columbia, Mississippi, Missouri, and Yenisey rivers are considerably affected by reservoir operations, while several stations in the European rivers (Danube, Meuse and Rhine) are mainly impacted by thermal effluents of power plants and industries (Table 2.1). River temperatures at the stations of the Lena, Ob, Yenisey and Columbia are highly influenced by melt water. Water temperatures of the Orange and Darling are not affected by melt water, and experience only minor influences of upstream dams or weirs and thermal effluents.

Global river stations involved in our analysis were selected based on different criteria. First, both water temperature data of GEMS/Water and daily discharge data of GRDC during the period 1980-1999 had to be available. In addition, we selected stations with river temperature observations at a depth between 0 and 1 m below surface level, and a minimum amount of 40 measurements. Water temperatures of the selected GEMS/Water stations were measured instantaneously (on average around 11:30 a.m. local time, with a standard deviation of two hours) using a mercury thermometer, battery thermometer or a conductivity-temperature (battery) meter with a precision of 0.1°C. The location of the selected GEMS/Water stations and number of water temperature measurements is shown in Figure 2.1, along with the location of the study basin stations. About 37% of the stations have 40-100 water temperature measurements, the largest group (45%) has 100-200 water temperature measurements, and 13% and 5% of the stations have 200-500 and more than 500 measurements, respectively, during the 1980-1999 period. The amount of stations and number of measurements is highest in Europe, while the availability of water temperature stations for Africa and South America is limited (Table 2.2). A high percentage of the GEMS/Water stations in Oceania (70%) have a small upstream basin area (< 6,000 km²), while a relatively high number of stations in Africa, North America, South America and Asia are characterized by large upstream basin areas (> 75,000 km²).

Table 2.2: Availability of water temperature data of GEMS/Water stations per region. Overview of the total number of GEMS/Water stations, percentage of stations with a small (< 6,000 km²), moderate (6,000 – 75,000 km²) and large (> 75,000 km²) upstream basin area, and mean number of water temperature measurements (n) of the selected GEMS/Water stations per region and globally.

region	n GEMS/Water stations	percentage stations with upstream basin area			mean n per station
		< 6,000 km ²	6,000 – 75,000 km ²	> 75,000 km ²	
North America	28	21%	36%	43%	135
South America	4	0%	50%	50%	111
Europe	74	27%	39%	34%	227
Africa	3	0%	33%	67%	66
Asia	25	24%	32%	44%	101
Oceania	23	70%	22%	9%	138
globally	157	31%	35%	34%	171

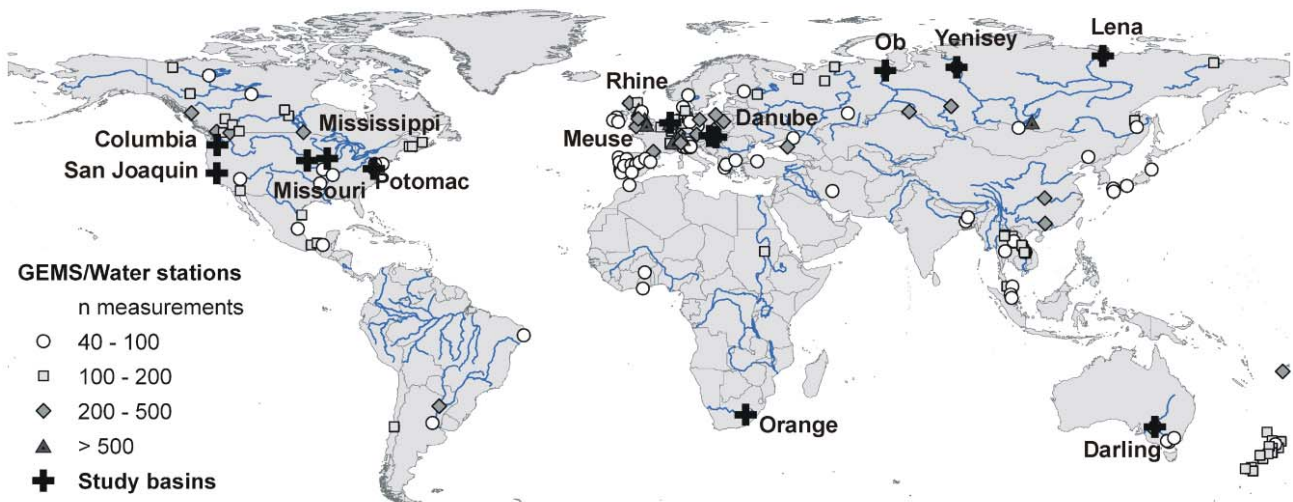


Figure 2.1: Number of measurements for selected GEMS/Water stations for the 1980-1999 period, and location of study basin stations.

In general, daily mean discharge series for all study basin stations and selected global GEMS/Water stations were used. However, for 31 out of 157 GEMS/Water stations, discharge data of GRDC was only available on a monthly basis and therefore monthly discharge data series were used for these stations. For the period 2000-2005 (Section 2.2.4), daily mean discharge series of the Rhine (Lobith) and Meuse (Eijsden) were provided by the water monitoring programme of the Netherlands (<http://live.waterbase.nl/>) and daily discharge series of the Danube (Bratislava) were supplied by the Slovak hydrometeorological Institute (Pekarova et al., 2008b), as discharge data were not available at GRDC during this period.

2.2.2 Air temperature data

For surface air temperature, we used the global gridded half-degree meteorological data set developed within the EU FP6 Water and Global Change (WATCH) project (Weedon et al., 2010). This dataset for 1958-2001 originates from ERA40 analysis (<http://www.ecmwf.int/research/era/do/get/era-40>). Air temperature (at 2m above surface) and other forcing variables were corrected for elevation differences between ERA40 one-degree elevations and CRU (http://www.cru.uea.ac.uk/~timm/grid/CRU_TS_2_1.html) half-degree elevations and have been monthly bias-corrected using CRU-TS2.1 observations. Daily (24 hour) mean air temperature for the 1980-1999 period was extracted from the half-degree grid cells where the study basin and global GEMS/Water stations are located. In addition, daily mean air temperature from the meteorological stations Twente and Maastricht provided by KNMI (<http://www.knmi.nl/klimatologie/daggegevens/>), and Vienna (<http://eca.knmi.nl/>) (Klein Tank et al., 2002) were used for the period 2000-2005 (Section 2.2.4).

2.2.3 The nonlinear water temperature regression model

The regression model in our study is based on the approach of Mohseni et al. (1998), who developed a nonlinear regression model representing the S-shaped function between air temperature and water temperature to calculate mean weekly stream temperature for monitoring stations in the United States. Modifications to the regression model have been made to include discharge as a variable in addition to air temperature, and to apply the model on a daily time step. Although it is recognized that water temperatures and air temperatures are better correlated at weekly and monthly timescales than at hourly or daily scales (Erickson et al., 2000; Pilgrim et al., 1998), we decided to apply the regression model on a daily basis by introducing a time lag between water temperature and air temperature. A practical reason for this daily time step is the need for high temporal resolution estimates of water temperature by river basin managers, in particular with regard to freshwater habitat conditions and usage functions such as cooling (industry and thermal power plants), drinking water production and recreation (Stefan and Preudhomme, 1993). In addition, river temperature measurements of GEMS/Water stations were available at an irregular time interval, and calculation of weekly (or monthly) mean water temperatures based on a highly variable number of measurements would thus result in less representative values (Preudhomme and Stefan, 1992; Webb et al., 2008). We therefore decided to test the robustness of the regression model on a daily time step, and thus water temperature measurements were related to daily mean air temperatures and discharges for that specific date.

River discharge was added as a variable to the nonlinear regression model to include the effects of changes in river flow conditions on water temperature. Although water temperatures depend on water depth and flow velocity, river discharge was selected as the additional predictor variable because it strongly relates to both river depth (thermal capacity) and flow velocity (travel times), and is well-measured on a global scale. An inverse relation between discharge and water temperature was added to the regression model, reflecting higher warming rates under lower discharges as demonstrated in previous studies (e.g. Rivers-Moore and Jewitt, 2007; van Vliet and Zwolsman, 2008). An inverse relation instead of a negative linear relation with discharge (e.g. Ozaki et al., 2003; Webb and Nobilis, 1994) was included, because it reflects both a reduction in the thermal capacity and reduced dilution capacity for anthropogenic heat sources (e.g. wastewater or cooling water discharges) under low river flows. Hence, the modified nonlinear regression model used in our study is:

$$T_w = \mu + \frac{\alpha - \mu}{(1 + e^{\gamma(\beta - T_{air})})} + \frac{\eta}{Q} + \varepsilon \quad (2.1)$$

$$\text{with: } \gamma = \frac{4 \tan \theta}{\alpha - \mu}$$

Where: μ = lower bound of water temperature [°C]; α = upper bound of water temperature [°C]; γ = measure of the slope at inflection point (steepest slope) of the S-shaped relation

[$^{\circ}\text{C}^{-1}$]; β = air temperature at inflection point [$^{\circ}\text{C}$]; η = fitting parameter [$^{\circ}\text{C m}^3\text{s}^{-1}$]; T_w = water temperature [$^{\circ}\text{C}$]; T_{air} = air temperature [$^{\circ}\text{C}$]; Q = river discharge [m^3s^{-1}]; ε = error term [$^{\circ}\text{C}$]; $\tan \theta$ = slope at inflection point [-].

In addition, a function was included to relate the measure of slope (γ) at the inflection point to the discharge variability compared to the variability in water temperature.

$$\gamma_Q = \gamma \left(\tau \frac{\sigma_Q}{\sigma_{T_w}} \right) \quad (2.2)$$

Where: γ_Q = measure of slope for discharge term [$^{\circ}\text{C}^{-1}$]; σ_Q = standard deviation of discharge [m^3s^{-1}]; σ_{T_w} = standard deviation of water temperature [$^{\circ}\text{C}$]; τ = fitting parameter [$^{\circ}\text{C m}^3\text{s}^{-1}$].

A comparable function was previously applied by Webb et al. (2003) to calculate the beta coefficient of the discharge term. In our study, the improvement in model performance was higher when this function was applied on the gamma component, resulting in an increase in the measure of slope for rivers with a high discharge variability compared to water temperature variability, and vice versa. The function generally increases the explained variance and sensitivity to air temperature and discharge changes, especially for monitoring stations with a relatively high discharge variability.

To apply the model on a daily basis, a lag effect was incorporated into the regression analyses, because water temperature variations tend to lag behind air temperature fluctuations at short timescales (on an hourly or daily basis) (Erickson et al., 2000; Jeppesen and Iversen, 1987; Webb et al., 2003). In addition, water temperature has a lower variability than air temperature because of the high thermal inertia of water. Stefan and Preudhomme (1993) concluded, for streams in the central USA, that measured water temperatures follow air temperature closely with a time lag ranging from hours to days, which increases with stream depth. Because water depth information was not available for the majority of river stations, the optimal time lag was estimated by calculating correlation coefficients between water temperature, air temperature and discharge. The optimal time lag was calculated for each station individually using a time lag between 0 to 20 days. The time lag with the highest correlation coefficient was assumed to be the optimal time lag for that river station and was thus selected.

2.2.4 Model application and validation

For the study basin stations and GEMS/Water stations, we generally used daily instantaneous measurements of water temperature and daily mean measurements of air temperature and discharge during the 1980-1999 period to fit the regression relations. For air temperature, daily mean rather than daily maximum values were used, because slightly higher correlations between water temperature measurements and daily mean values of air temperatures were obtained. For discharge, daily mean values were provided and therefore used to fit the regression model. However, for the 31 GEMS/Water stations with discharge only available as

monthly averages, we calculated monthly mean water temperatures and related these to monthly mean air temperature and discharge (without a time lag). For the study basin stations of the Yenisey, Ob and Lena, mean water temperatures were available for every 10 days (Section 2.2.1). Therefore, 10-day averages of air temperature and discharge were calculated to fit the regression model. The least squares method was used to estimate the five parameters α , β , γ , μ and η , minimizing the sum of squared errors between the observed and fitted values of water temperatures. The parameters were estimated numerically using the Gauss-Newton algorithm. To obtain physically reliable estimates of the lower bound of water temperature for rivers with freezing periods, zero was assigned as the lower limit of μ (Mohseni et al., 1998). Although some studies demonstrated better estimations of the upper bound of water temperature (α) by using the standard deviate method (Bogan et al., 2006; Mohseni et al., 2002), only moderate improvements were observed in our study, and therefore α was estimated according to the least squares method.

Hysteresis occurs for river sites affected by seasonal snow- and ice-melt runoff and reservoir operations, which involves a lag in stream temperature response to air temperature (Webb and Nobilis, 1994). This is mainly because of the inflow of cold snowmelt or deep reservoir water during spring and summer, resulting in cooler water temperatures despite the warming in air temperatures. In this case, two regression relations were applied to the water temperature measurements for the rising and falling limb separately, by splitting the dataset for the period January till June and for July till December. As only one α and μ physically exist at each monitoring station, we used the lower μ , upper α , and an average of the two γ , β and η values, which ultimately resulted in one fitted model for each monitoring station (Mantua et al., 2010; Mohseni et al., 1998).

To test the improvement of the regression model by the introduction of discharge as an additional variable, both the original regression model (Mohseni et al., 1998) applied on a daily basis with time lag included (NONLIN) and modified regression model including discharge and time lag (NONLIN_Q) were fitted. The model performance (goodness of fit) was determined for both regression models by calculating the Nash-Sutcliffe coefficient (*NSC*) (Nash and Sutcliffe, 1970) (equation 2.3), which is the coefficient of determination showing the efficiency of the fit. The quality of the fit was calculated by using the root mean squared error (*RMSE*) (Janssen and Heuberger, 1995) (equation 2.4).

$$NSC = 1 - \frac{\sum_{i=1}^n (Tw_{sim i} - Tw_{obs i})^2}{\sum_{i=1}^n (Tw_{obs i} - \bar{Tw}_{obs})^2} \quad (2.3)$$

$$RMSE = \sqrt{\frac{\sum_{i=1}^n (Tw_{sim i} - Tw_{obs i})^2}{n}} \quad (2.4)$$

Where: $T_{w_{sim}i}$ = predicted daily water temperature at time step i [°C]; $T_{w_{obs}i}$ = observed daily water temperature at time step i [°C]; $\bar{T}_{w_{obs}}$ = average of daily observed water temperature [°C]; n = number of data pairs to be compared.

For each station the NSC was calculated for the fitted regression model for the rising and falling limb separately and for a single fitted model. When the average NSC from the fitted regression model for the rising and falling limb was higher than calculated for a single fitted model, river stations were assumed to exhibit hysteresis (Mantua et al., 2010).

In order to test the performance of the regression model and the degree of validity of the parameter estimates for another time period and during a heat wave specifically, the regression model fitted for 1980-1999 for the European study basin stations Rhine (Lobith), Danube (Bratislava) and Meuse (Eijsden) was applied for the time slice 2000-2005 including the heat wave and drought of 2003. These study basin stations were selected, because they were well measured during the period of 2000-2005 and the summer of 2003 specifically, and are characterized by different river regime characteristics and snowmelt influences. The fitted regression model was applied by using daily mean discharge series from the same monitoring station and daily mean air temperature data for 2000-2005 of the nearest meteorological stations, as the global gridded air temperature dataset for the 1958-2001 period does not include data for this validation period (Section 2.2.2). The performance of the regression models was tested by comparing the calculated water temperatures with daily instantaneous water temperature observations for the Rhine (Lobith), Danube (Bratislava) and Meuse (Eijsden) for 2000-2005. These water temperature series came from the same data sources as for the fitting period (1980-1999) (see Table 2.1).

2.2.5 Sensitivity to increases in air temperature and changes in river discharge

To explore the sensitivity of river temperatures to atmospheric warming and changes in river flow on a global scale, we applied the adapted nonlinear regression model including discharge (NONLIN_Q) with the five parameters α , μ , γ , β and η fitted for the period of 1980-1999 with perturbed air temperature and discharge series. The parameter values of the regression model thus were kept similar for this sensitivity analysis, implying that the physical setting of the river (groundwater input, river geometry, influence of melt water, upstream reservoirs, thermal effluents) remains the same (Mohseni et al., 1999). The original historical daily air temperature series for 1980-1999 were augmented incrementally with air temperature increases of +2°C, +4°C and +6°C. Additionally, the sensitivity of water temperatures to changes in river flow was assessed by calculating river temperatures under an air temperature increase of +4°C in combination with a change in river discharge of +20%, -20% and -40%. The selected increments in air temperature include the likely range of the projected global average surface air temperature increase of 1.1 - 6.4°C for 2090-2099 relative to 1980-1999 (IPCC, 2007). The changes in river discharge cover the range of projected changes in global runoff of -40% to +40% according to Milly et al. (2005) for 2041-

2060 compared to 1900-1970 under the SRES A1B emissions scenario. The selected rates of warming and changes in river discharge are thus plausible in the context of climate change.

2.3 Performance of nonlinear water temperature regression model

2.3.1 Model performance for study basins stations

For all selected study basin stations, the mean annual cycle of calculated daily water temperatures with the modified regression model including discharge (NONLIN_Q) represents the observed water temperature regime more realistically than those calculated without discharge (NONLIN) (Figure 2.2). Furthermore, the underestimation of water temperatures during summer and overestimation during winter is generally less for NONLIN_Q compared to NONLIN. This is probably because of higher values of γ (measure of slope) found for NONLIN_Q as compared to NONLIN for all study basin stations except for the Yenisey (Igarka) (Table 2.3). These higher values are obtained by the incorporation of the function relating the measure of slope at the inflection point to the discharge variability compared to the variability in water temperature (equation 2.2). The fitted values of μ , α and β for NONLIN_Q were lower for the majority of study basin stations, except for the stations of the Missouri, Orange, Darling, Lena and Ob, which were slightly higher or remained the same value. This might be explained by differences in the flow regime when compared to the thermal regime for these rivers. The majority of river stations are characterized by high flow conditions during winter when river temperatures are low, and low flow conditions during summer when river temperatures are high, resulting in distinct inverse relations between water temperature and discharge. However, for the selected stations of the Missouri, Orange,

Table 2.3: Fitted parameters of the original regression model with time lag included (NONLIN) and for the adapted regression model including time lag and discharge (NONLIN_Q) for study basin stations.

river	station	μ (°C)	μ_Q (°C)	α (°C)	α_Q (°C)	γ (°C ⁻¹)	γ_Q (°C ⁻¹)	β (°C)	β_Q (°C)	lag (days)
Columbia	The Dalles	4.6	0.5	20.3	15.2	0.26	0.33	9.2	9.0	10
Mississippi	Clinton	0.0	0.0	28.9	28.6	0.17	0.20	13.5	13.4	9
Missouri	Omaha	0.0	3.0	30.0	31.0	0.15	0.18	13.2	13.8	7
Potomac	Washington D.C.	0.0	0.0	35.3	33.3	0.12	0.15	17.1	16.9	6
San Joaquin	Vernalis	6.3	4.5	26.8	25.8	0.19	0.20	15.8	15.0	3
Danube	Bratislava	0.2	0.0	20.6	19.7	0.18	0.21	10.3	10.1	9
Danube	Budapest	0.0	0.0	24.0	22.8	0.16	0.19	11.2	10.9	9
Meuse	Eijsden	5.3	5.1	25.0	24.6	0.23	0.28	11.0	10.9	8
Rhine	Lobith	4.2	2.0	24.1	22.1	0.24	0.27	11.0	11.0	9
Orange	Oranjedraai	11.2	11.6	22.6	23.0	0.48	0.55	17.7	17.6	5
Darling	Burtundy	6.2	7.3	26.9	27.1	0.22	0.26	14.9	15.1	8
Lena	Kusur*	0.0	0.6	11.9	12.0	0.21	0.25	7.2	7.7	20
Ob	Salekhard *	0.0	0.1	16.4	16.4	0.29	0.35	7.4	7.4	10
Yenisey	Igarka *	0.0	0.0	17.6	16.5	0.29	0.28	7.1	6.0	10

* Stations fitted on 10-day mean basis instead of daily basis.

Darling, Lena and Ob, the peak in discharge is in summer and coincides with the peak in water temperature. Therefore, no distinct inverse relation between water temperature and discharge was found for these river stations. The fitted optimal time lag ranges from 3 to 10 days. High time lags were obtained for stations characterized by high annual discharges, which generally correspond with higher depths and thermal inertia (Stefan and Preudhomme, 1993). In contrast, moderate or low values of time lag were generally calculated for stations with a lower annual discharge (except for the Darling and Meuse) (Table 2.3). For the three Arctic river stations fitted on a 10 day mean basis (Section 2.2.1) a time lag of 10 days was found for the Ob and Yenisey and a time lag of 20 days was obtained for the Lena. These long time lags correspond with the relatively high values of annual mean river discharge (Table 2.1) and related water depth, resulting in high thermal inertia.

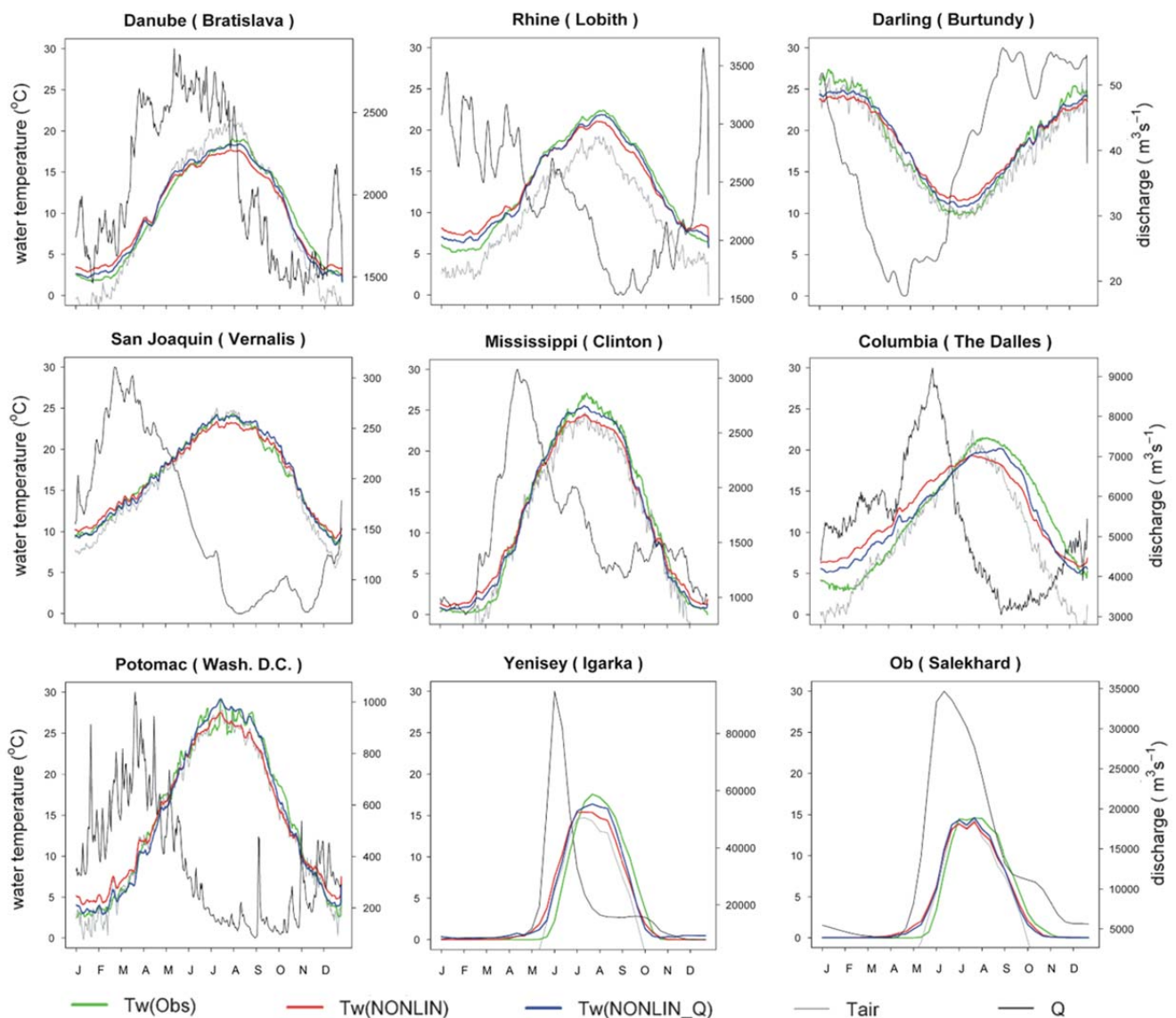


Figure 2.2: Mean annual cycles of observed daily water temperatures ($T_w(\text{Obs})$) and simulated daily water temperatures for the original regression model with time lag included ($T_w(\text{NONLIN})$) and for the adapted regression model including time lag and discharge ($T_w(\text{NONLIN}_Q)$) for a selection of study basin stations averaged over the fitting period 1980-1999.

Although hysteresis due to upstream reservoir operations and melt water was taken into account, the modelled water temperatures for the stations of Columbia, Lena, Ob and Yenisey are still overestimated during spring and underestimated during summer and autumn (Figure 2.2). However, including discharge into the regression model improved the model performance, especially for the Columbia (The Dalles). This was reflected by a higher NSC (0.83 versus 0.73) and lower RMSE (2.4°C versus 3.1°C) (Table 2.4). For the majority of study basin stations, the NSC was slightly higher for NONLIN_Q compared to NONLIN. For the Danube (Bratislava and Budapest), Missouri (Omaha) and San Joaquin (Vernalis) rivers, the values remained the same and were already high (NSC \geq 0.90) without including discharge. The RMSE values also reflected an improvement of the performance and decreased for all study basins stations except for the Lena and Ob, for which values remained the same. Despite this improvement in model performance for the majority of study basin stations, the RMSE is still quite high ($>3.0^\circ\text{C}$) and NSC relatively low (<0.75) for the Orange, Lena and Ob stations. For the Orange, this can be explained by the limited data availability and by the use of discharge series of a different station (Table 2.1). For the Lena and Ob, the limited performance of NONLIN and NONLIN_Q is mainly due to the dominant influence of the snowmelt peak during the period with the highest water temperatures, resulting in a less strong relation between water temperature and air temperature and river discharge. The snowmelt peak for the Yenisey (Igarka) is earlier (and shorter) compared to the Lena and Ob. As a result, the performance for this study basin station and improvement by the introduction of discharge is much better. Despite the limited performance for the Orange, Lena and Ob, the overall median NSC and RMSE for stations of the Mississippi, San Joaquin, Danube, Meuse, Rhine and Darling are 0.92 and 1.76°C, respectively. This indicates the usefulness of this regression model on a daily basis.

Table 2.4: Nash-Sutcliffe coefficient (NSC) and root mean squared error (RMSE) for the original regression model with time lag included (NONLIN) and for the adapted regression model including time lag and discharge (NONLIN_Q) for study basin stations. Values in bold indicate a higher performance for NONLIN_Q compared to NONLIN.

river	station	NSC	NSC_Q	RMSE (°C)	RMSE_Q (°C)
Columbia	The Dalles	0.73	0.83	3.1	2.4
Mississippi	Clinton	0.95	0.96	2.1	1.9
Missouri	Omaha	0.94	0.94	2.2	2.1
Potomac	Washington D.C.	0.87	0.88	3.4	3.3
San Joaquin	Vernalis	0.90	0.90	1.7	1.6
Danube	Bratislava	0.92	0.92	1.8	1.7
Danube	Budapest	0.92	0.92	2.0	1.9
Meuse	Eijsden	0.90	0.91	2.0	1.8
Rhine	Lobith	0.89	0.92	2.0	1.7
Orange	Oranjedraai	0.61	0.62	3.5	3.4
Darling	Burtundy	0.91	0.93	1.7	1.5
Lena	Kusur*	0.55	0.56	3.2	3.2
Ob	Salekhard *	0.74	0.75	3.1	3.1
Yenisey	Igarka *	0.86	0.89	2.3	2.1

* Stations fitted on 10-day mean basis instead of daily basis

2.3.2 Performance during the heat wave and summer drought of 2003 in Europe

Time series of observed and calculated water temperatures for the Rhine (Lobith), Danube (Bratislava) and Meuse (Eijsden) for the period 2000-2005 (Figure 2.3) show that both regression models slightly overestimate low and underestimate high river temperatures. This is the result of the fixed values of upper bound (α) and lower bound (μ) of water temperature calculated from the data series of 1980-1999, which tend to be slightly underestimated and overestimated, respectively. However, the water temperature regression model including the impact of river flow (NONLIN_Q) shows better results during the whole period. This is also reflected by slightly higher values of NSC and lower values of RMSE for NONLIN_Q (mean of 0.90 and 1.9°C) compared to NONLIN (mean of 0.87 and 2.1°C). Comparing the performance

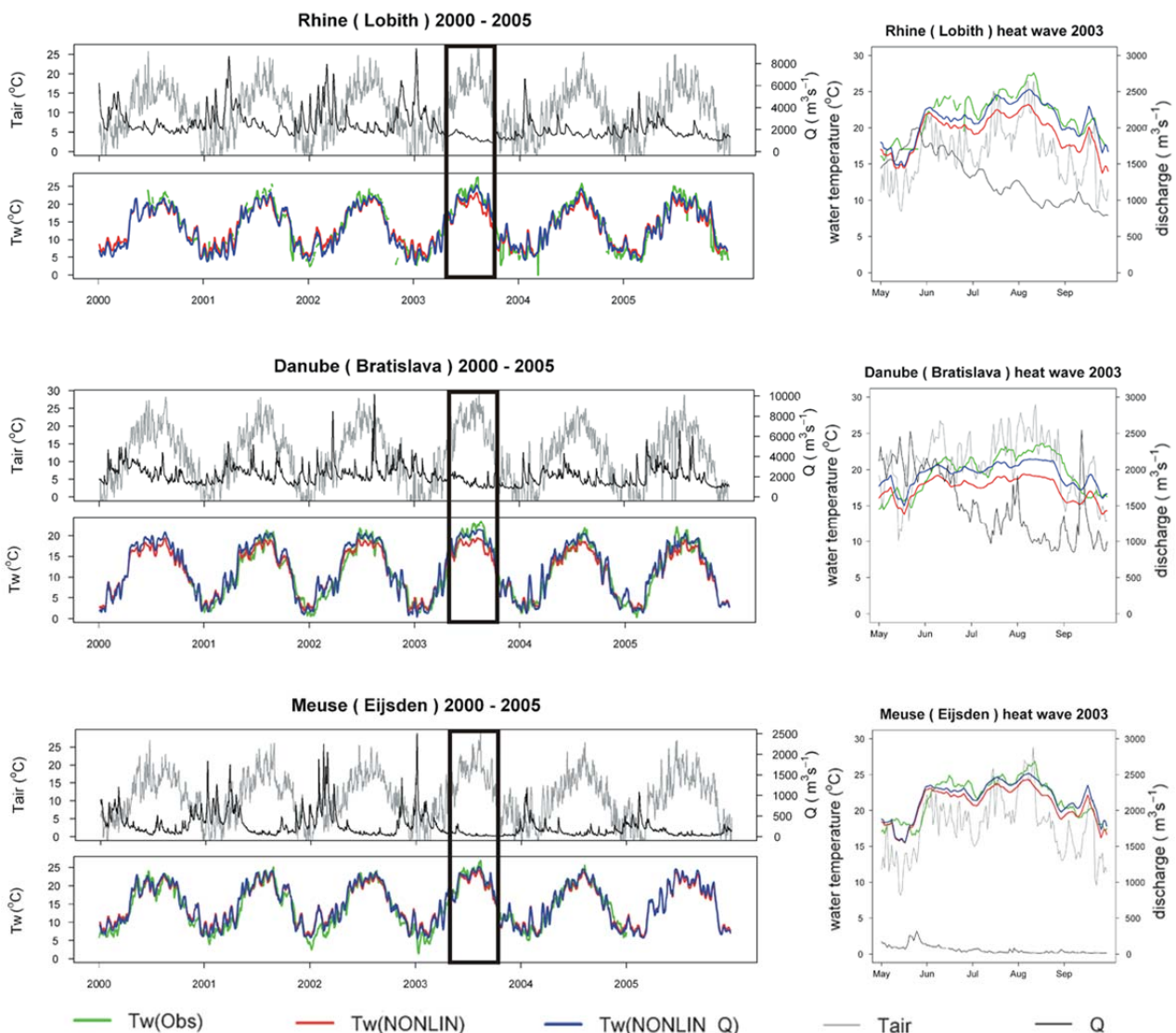


Figure 2.3: Observed daily water temperatures (Tw(Obs)) and simulated daily water temperatures for the original regression model with time lag included (Tw(NONLIN)) and for the adapted regression model including time lag and discharge (Tw(NONLIN_Q)) for the Rhine (Lobith), Danube (Bratislava) and Meuse (Eijsden) during the validation period 2000-2005, and during the heat wave and summer drought of the 2003. The outlined boxes denote the heat wave and summer drought of 2003. The figures at the right side present the results in more detail during this heat wave and drought.

coefficients of NONLIN_Q during 2000-2005 with the values during the fitting period 1980-1999, the NSC is slightly lower (mean of 0.90 versus 0.91) and RMSE is slightly higher (mean of 1.9°C versus 1.8°C), although the differences are small.

The validity of the regression models and parameter estimates for the European rivers was also tested specifically for the heat wave and drought of July and August 2003 (Figure 2.3). Both regression models showed an underestimation of river temperatures, especially during the period when water temperatures are highest (end of July and first two weeks of August). This is because of an underestimation of the defined upper bound of water temperature (α) of the nonlinear regression model of Mohseni et al. (1998), which has also been discussed by Bogan et al. (2006) and Mohseni et al. (1999). However, introduction of discharge into the regression model resulted in a strong decrease in the underestimation of the modelled water temperatures during this warm, dry period. The mean underestimation by NONLIN_Q compared to NONLIN during July-August is 0.9°C versus 3.0°C for the Rhine, 1.3°C versus 3.4°C for the Danube and 0.4°C versus 1.4°C for the Meuse. In addition, a distinct improvement in model performance was reflected by large decreases in RMSE of 1.9°C, 2.0°C and 0.7°C for the Rhine, Danube and Meuse, respectively.

2.3.3 Model performance for global GEMS/Water stations

Although the number of measurements for the selected GEMS/Water stations was generally less than for the study basin stations, the nonlinear regression models NONLIN and NONLIN_Q were successfully applied to the GEMS/Water stations globally. For 126 stations with daily discharge data, the regression models were fitted and the performance was tested on a daily basis, according to the same procedure as for the study basin stations. For 31 GEMS/Water stations with only monthly mean discharge series available, the models were fitted and the performance was tested on a monthly basis (see Section 2.2.4).

Non-parametric Wilcoxon Rank Sum tests were performed on the calculated NSC and RMSE values to test whether the difference between the performance of NONLIN and NONLIN_Q was significant. Results showed that incorporation of discharge led to a statistically significant ($p < 0.01$) improvement of the performance of the water temperature regression model. The increase in the performance of the regression model, reflected by higher values of NSC and lower values of RMSE for NONLIN_Q compared to NONLIN, was found for 87% of the GEMS/Water stations (for 84% of the stations with daily fits and 97% with monthly fits). To show differences in estimated water temperatures between both regression models, the mean annual cycle of observed and estimated water temperatures with NONLIN and NONLIN_Q are presented for a selection of GEMS/Water stations (Figure 2.4). The regression model was fitted and the performance was tested on a daily basis for the majority of river stations presented, except for the Murray, Parana and Yangtze. However, monthly averages are shown for all stations because of the limited amount of observed water temperature data to calculate the mean thermal regime on a daily time step. Comparing the calculated water temperatures of NONLIN_Q and NONLIN, we find the strongest improvements for the

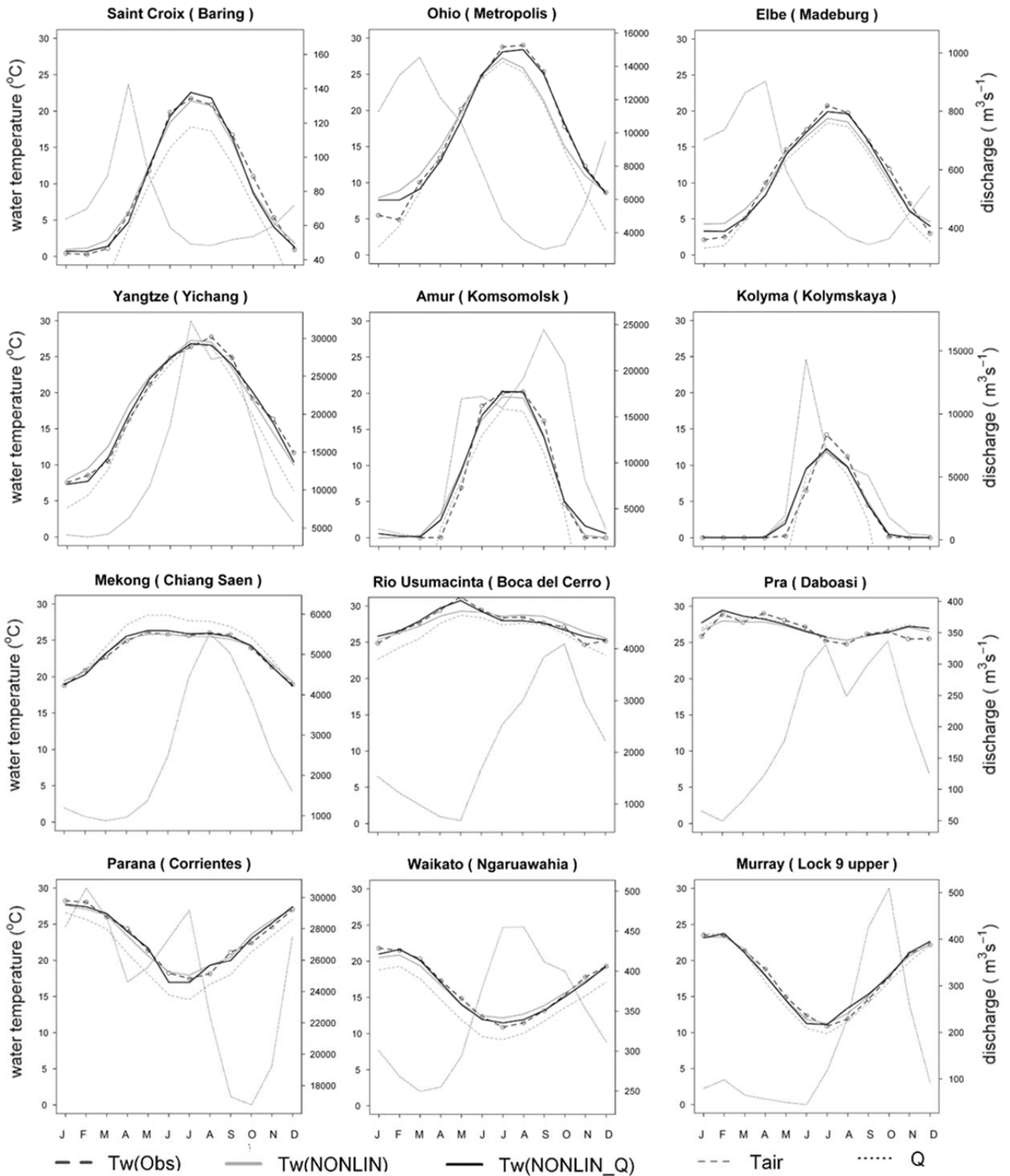


Figure 2.4: Mean annual cycles of observed daily water temperatures (Tw(Obs)) and simulated daily water temperatures for the original regression model with time lag included (Tw(NONLIN)) and for the adapted regression model including time lag and discharge (Tw(NONLIN_Q)) for a selection of GEMS/Water stations of the Saint Croix (Canada), Ohio (USA), Elbe (Germany), Yangtze (China), Amur (Russia), Kolyma (Russia), Mekong (Thailand), Rio Usumacinta (Mexico), Pra (Ghana), Parana (Argentina), Waikato (New Zealand) and Murray (Australia) averaged per month over the 1980-1999 period.

Ohio, Elbe, Rio Usumacinta and Waikato, which are rivers characterized by typical low flow conditions during summer and high flow conditions during winter or early spring. For rivers with a peak in discharge during the period with high water temperatures, like the Yangtze, Amur, Kolyma and Mekong, less distinct or no improvements were found by introducing discharge as an additional variable in the regression model. No distinct inverse empirical relations between water temperature and discharge were found for these river stations.

The boxplots with the distribution of NSC and RMSE values for GEMS/Water stations (Figure 2.5) generally show a higher performance for NONLIN_Q compared to NONLIN both for daily and monthly fitted stations. Results of Wilcoxon Rank Sum tests indicated that NSC for NONLIN_Q is significantly higher ($p < 0.01$) than for NONLIN with an overall median NSC of 0.86 versus 0.83 on a daily basis, and 0.93 versus 0.89 on a monthly basis. The values of RMSE are significantly lower ($p < 0.01$) for NONLIN_Q, especially for the stations with monthly fits. The median value of RMSE for NONLIN_Q and NONLIN is 1.8°C versus 2.0°C on a daily basis and 1.4°C versus 2.1°C on a monthly basis. The higher performance of the regression model for monthly data compared to daily data is expected because the correlation between water temperature and air temperature increases from a daily to a monthly time step (Erickson et al., 2000; Pilgrim et al., 1998).

For 38% of the stations, NSC was higher when the regression model was plotted for the rising and falling limb separately, implying that these stations exhibited seasonal hysteresis. For 21% of the stations, the amount of water temperature measurements was, however, too low

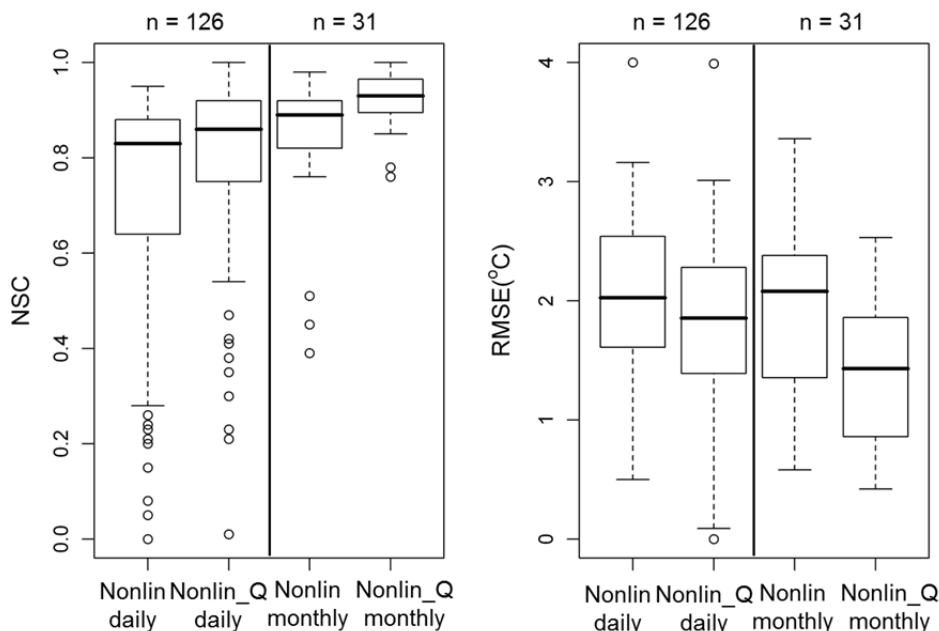


Figure 2.5: Boxplots of the Nash-Sutcliffe coefficients (NSC) and root mean squared errors (RMSE) based on all GEMS/Water stations for the original regression model with time lag included (NONLIN) and for the adapted regression model including time lag and discharge (NONLIN_Q) presented for the daily and monthly fitted stations separately. The boxplots present the median, lower and upper quartile, minimum, maximum and outliers (specified as more than 1.5 * interquartile range).

to fit the regression model for the rising and falling limb separately. The calculated optimal time lags are between 1 and 15 days, and the overall mean of all stations is 6 days. A positive relation was found between time lag and mean annual discharge, reflecting a higher thermal inertia under higher river discharge, although the explained variance was low ($R^2=0.10$).

Considering the spatial distribution of the relative increase in NSC between NONLIN_Q and NONLIN (Figure 2.6), improvements in model performance were generally largest for river stations at middle and low latitudes. This can be explained by the flow regime of these river stations, which is generally characterized by low flow conditions during summer and high flow conditions during winter and spring, or by moderate river discharge variability throughout the year. For river stations at high northern latitudes, the influence of discharge on the model performance is highly variable. This is mainly dependent on the timing of the snowmelt peak in relation to the peak in water temperatures. For several stations at high latitude, the peaks in flow and thermal regimes coincide and inverse empirical relations between water temperature and discharge were therefore not found for these stations. Introduction of discharge in the regression model did not improve or slightly decreased the performance of the regression model for these river stations. However, the relative decrease in NSC was smaller than 2%. For several stations in North America, the introduction of discharge in the regression model also did not result in better estimates of river temperature. This may be explained by the presence of many deep reservoirs that affect river temperatures downstream. For these stations, river temperatures highly depend on reservoir thermal stratification and reservoir operation (Sinokrot et al., 1995).

Regarding the absolute NSC values for NONLIN_Q for the selected GEMS/Water global stations (Figure 2.6), a high model performance with $NSC > 0.90$ was found for 41% of the stations (32% for stations fitted on a daily basis; 74% on a monthly basis). In addition, NSC was between 0.80 and 0.90 for 35% of the stations (40% for daily fitted stations; 18% for monthly fits). For 12% of the stations (16% on a daily basis, 3% on a monthly basis), the model performance was poorer with $NSC < 0.6$. These stations are situated in rivers in northern Canada (Mackenzie, Saskatchewan and Churchill), Southwest United States and Mexico (Colorado, Rio Panuca), Southeast Asia (Mekong) and West Africa (White Volta and Pra). Although river temperatures at many stations are influenced by other factors than air temperature and discharge (e.g. reservoirs, thermal pollution), only weak relations were found between the NSC and RMSE values and river basin characteristics like contributing basin area (mean $R^2 = 0.02$) and latitude (mean $R^2 = 0.04$). In addition, the large-scale spatial patterns in NSC and RMSE did not show a clear correspondence with the global distribution in climate zones, melt water fluxes, thermal effluents and location of dams and reservoirs. An explanation for the lower model performance for these river stations could be the limited availability (and quality) of river temperature data, as a low number of measurements ($n < 200$) was available for all stations with $NSC < 0.6$ (Figure 2.1; Figure 2.6). In addition, a positive relation between NSC and data availability was found, and RMSE negatively related to the number of measurements (mean $R^2 = 0.12$).

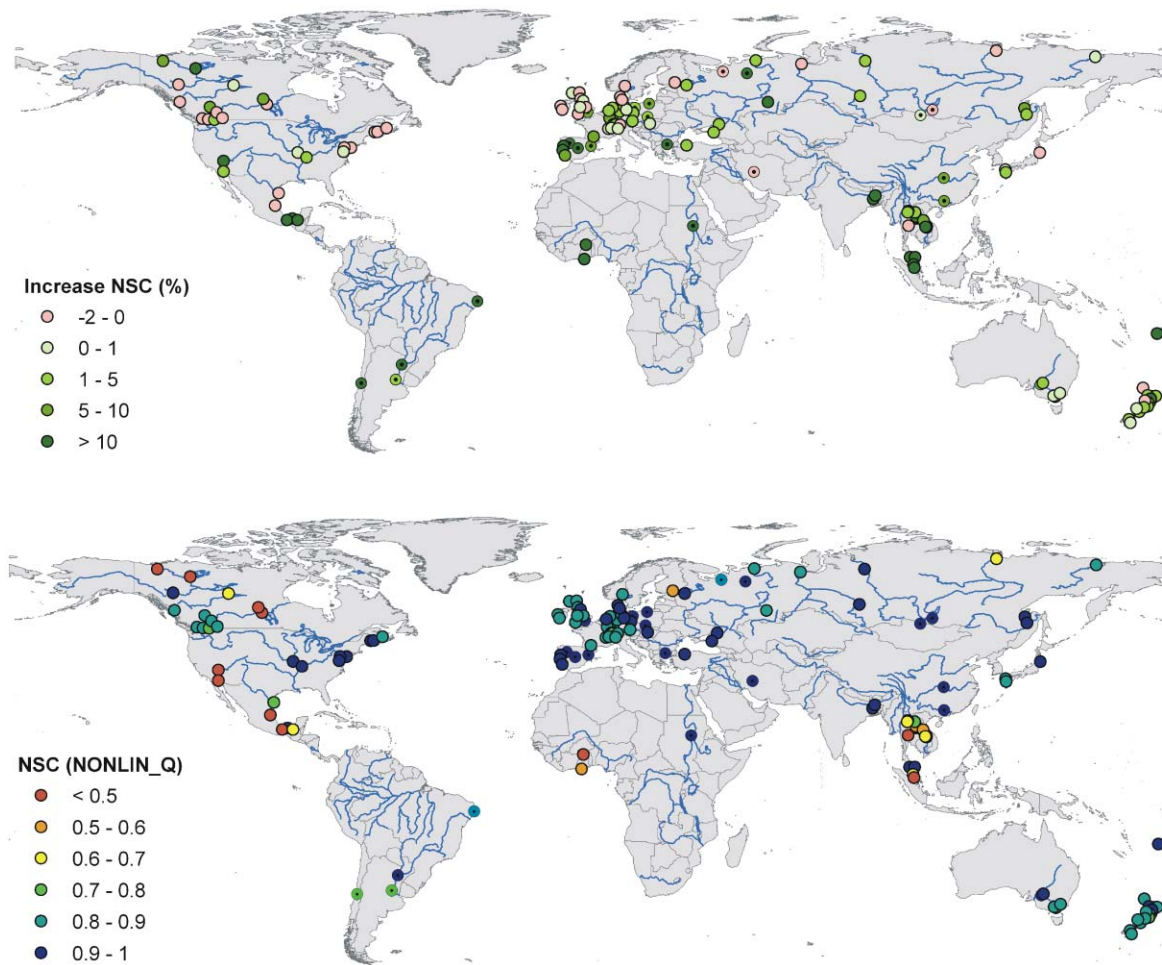


Figure 2.6: Global distribution of relative increase in Nash-Sutcliffe coefficients (NSC) (%) for the regression model including discharge (NONLIN_Q) compared to the regression model without discharge (NONLIN), and absolute values of NSC for NONLIN_Q for all selected GEMS/Water stations. The circles with black dots indicate river stations fitted using monthly data.

2.4 Sensitivity of river temperature to changes in air temperature and river discharge

2.4.1 Sensitivity of river temperatures at study basin stations

For all study basin stations, annual mean water temperature increases linearly under air temperature increases of +2°C, +4°C and +6°C, with an annual mean (range) increase of 1.4 (0.6 to 1.8)°C, 2.7 (1.2 to 3.6)°C, and 4.0 (1.8 to 5.3)°C, respectively (Table 2.5). Although the slopes at the inflection point ($\tan \theta$) are on average larger than 1 for all study basin stations (except for the Lena (Kusur)), the overall average slopes are smaller and decrease in the high temperature range resulting in a less strong increase in water temperature under specific air temperature increases.

Considering the sensitivity of water temperature to discharge changes, an increase in discharge of +20% generally reduced water temperature increases, while decreases of 20% and 40% in discharge intensified water temperature increases for the majority of river

stations. This partly reflects the higher thermal capacity of a river under increased discharges (water volumes) and lower thermal capacity when discharges are reduced. In addition, water temperature increases in thermally polluted rivers are also influenced by river flow changes due to impacts on dilution capacity for thermal effluents. However, for stations of the Missouri, Orange, Darling, Lena and Ob rivers, slightly higher water temperatures under an increase in discharge and lower water temperatures under a discharge decrease were observed. As previously mentioned (Section 2.3.1), the flow regime at these river stations are characterized by generally high flow conditions during summer and low flow conditions during winter, implying that the peaks in flow regime and thermal regime coincide. The influence of changes in thermal capacity on water temperature is therefore not well reflected by the empirical relation between water temperature and discharge for these study basin stations. This regression modelling approach is therefore less suitable to study the impact of discharge changes on water temperature for these river stations.

For the majority of study basin stations, mean annual water temperatures were most sensitive to an air temperature increase of +6°C, with a greatest increase of 5.3°C for the Potomac (Washington D.C.) and lowest increase of 1.8°C for the Lena (Kusur). For the river stations in the Columbia and Yenisey, however, water temperature increases were highest for a +4°C air temperature increase in combination with a 40% decrease in discharge, resulting in water temperature increases which are more than 1.5°C higher than under a +4°C air temperature increase without discharge changes.

Table 2.5: Mean annual river temperature increase (°C) under different air temperature increases and changes in river discharge for study basin stations. Values in bold indicate the highest mean annual water temperature increase.

river	station	+2°C	+4°C	+6°C	+4°C +20% Q	+4°C -20%Q	+4°C -40% Q
Columbia	The Dalles	1.2	2.3	3.4	1.6	3.4	5.2
Mississippi	Clinton	1.5	3.0	4.5	3.0	3.1	3.2
Missouri	Omaha	1.4	2.8	4.1	3.1	2.4	1.7
Potomac	Washington D.C.	1.8	3.6	5.3	3.3	3.9	4.5
San Joaquin	Vernalis	1.6	3.0	4.4	2.9	3.2	3.6
Danube	Bratislava	1.3	2.6	3.8	2.4	2.8	3.2
Danube	Budapest	1.5	2.9	4.4	2.7	3.3	3.8
Meuse	Eijsden	1.7	3.3	4.8	3.2	3.4	3.6
Rhine	Lobith	1.7	3.4	5.0	3.1	4.0	4.9
Orange	Oranjedraai	1.1	2.2	3.1	2.3	2.1	1.9
Darling	Burtundy	1.7	3.2	4.6	3.3	3.1	2.9
Lena	Kusur*	0.6	1.2	1.8	1.3	1.2	1.1
Ob	Salekhard *	1.2	2.3	3.4	2.3	2.3	2.3
Yenisey	Igarka *	1.3	2.5	3.6	2.2	3.0	4.0

* Stations fitted on 10-day mean basis instead of daily basis

In order to get more detailed insight into the sensitivity of river temperature on a daily basis, density plots are presented for the San Joaquin (Vernalis), Potomac (Washington D.C.), Rhine (Lobith) and Danube (Bratislava), showing the distribution of daily water temperatures under air temperature increases of +4°C, +6°C, and under an air temperature increase of +4°C combined with a 40% decrease in discharge (Figure 2.7). Although the increase in mean annual water temperature is highest under an air temperature increase of +6°C, the density plots for these stations indicate that an air temperature increase of +4°C combined with a 40% decrease in discharge results in higher maximum water temperatures than those found for an air temperature increase of +6°C. The impact of a 40% discharge decrease is most pronounced for the Rhine (Lobith), resulting in a considerably higher 99th percentile water temperature of 27.0°C, compared to 24.6°C under an air temperature increase of +4°C, and 25.0°C under an air temperature increase of +6°C without any discharge change.

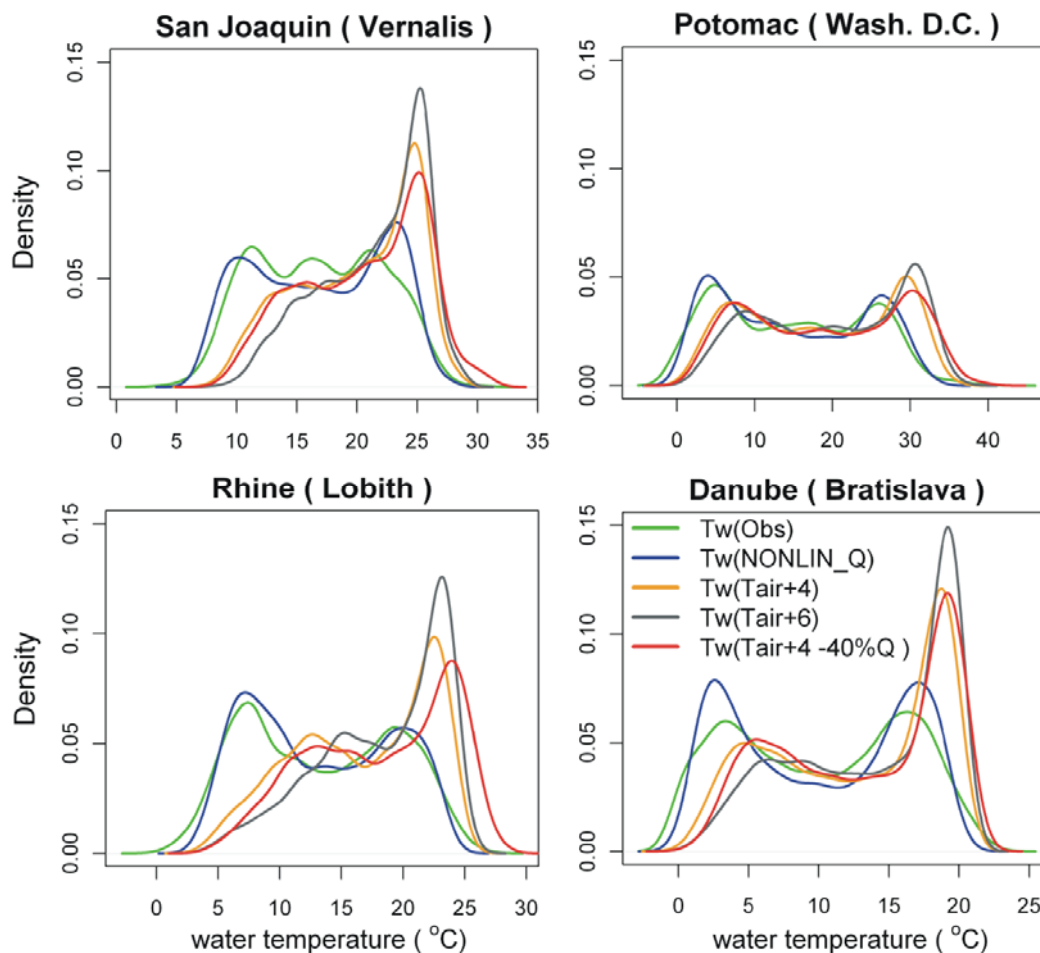


Figure 2.7: Density functions of observed daily water temperature (Tw(obs)) and simulated daily water temperature for the adapted regression model including time lag and discharge (Tw(NONLIN_Q)) for the reference period 1980-1999 and under an air temperature increase of +4°C (Tw(Tair+4)) and +6°C (Tw(Tair+6)), and under an air temperature increase of +4°C in combination with a decrease in discharge of 40% (Tw(Tair+4 -40%Q)).

2.4.2 Sensitivity of river temperatures at global GEMS/Water stations

Considering the mean annual water temperature increases for the GEMS/Water stations, the overall average values (1 to 99 percentile range) under a +2°C, +4°C and +6°C air temperature increase are 1.3 (0.1 to 2.3)°C, 2.6 (0.1 to 4.7)°C and 3.8 (0.2 to 7.0)°C, respectively. Considering the calculated water temperature increases of the individual stations under these warming rates (Figure 2.8), river stations at high northern latitude (northern Canada and Siberia) show a relatively moderate water temperature increase compared to the middle and low latitude zones. This is mainly because water temperatures for these stations remain around freezing point for a large part of the year, resulting in smaller mean annual water temperature increases. Furthermore, generally low slopes at the inflection point were fitted for these high northern latitude stations, resulting in less strong water temperature increases.

To address the sensitivity of water temperature to changes in discharge, we focused on 102 GEMS/Water stations showing distinct inverse relations between water temperature and discharge, and thus excluded stations for which our regression model is less suitable to address the sensitivity to river discharge changes (see previous section). Comparing the annual mean water temperature increases under an air temperature increase of +4°C with the results under this air temperature increase combined with discharge changes, we found that an increase in discharge of 20% reduced the annual water temperature increase by a mean (1 to 99 percentile range) of 0.2 (0.0 to 0.7)°C. In contrast, a decrease in discharge of 20% and 40% exacerbated the increase in water temperatures by 0.3 (0.0 to 1.0)°C and 0.8 (0.0 to 2.6)°C, respectively. In general, water temperatures showed higher sensitivity to a 20% decrease in discharge than a 20% increase in discharge. Considering the increase in mean annual river temperatures for the selected GEMS/Water stations individually (Figure 2.9), a high sensitivity to discharge decreases of 20% and 40% was found for stations in the Ganges, Ob, Yenisey, Ohio/Mississippi, and in several rivers in Europe (e.g. Rhine, Danube, Elbe, Rhone and Guadiana). Estimated river temperature increases under an air temperature increase of +4°C in combination with a change in discharge of -40% (Figure 2.10), indicate highest mean annual water temperature increases (more than 4°C) for river stations in western Europe and the eastern part of the United States (Figure 2.10). The overall average in maximum river temperature increase (on a daily basis) under this air temperature and discharge change is 4.4°C, with strongest maximum water temperature increases for rivers in western Europe, the eastern part of the United States and Russia.

2.5 Discussion and conclusions

The performance of the nonlinear regression model of Mohseni et al. (1998) for weekly water temperatures was generally improved by the introduction of river discharge as an additional variable, and the model was successfully applied on a daily basis by incorporating a time lag. For 76% of the GEMS/Water stations NSC values were higher than 0.8 (Figure 2.6), indicating the usefulness of the modified water temperature regression model to estimate water

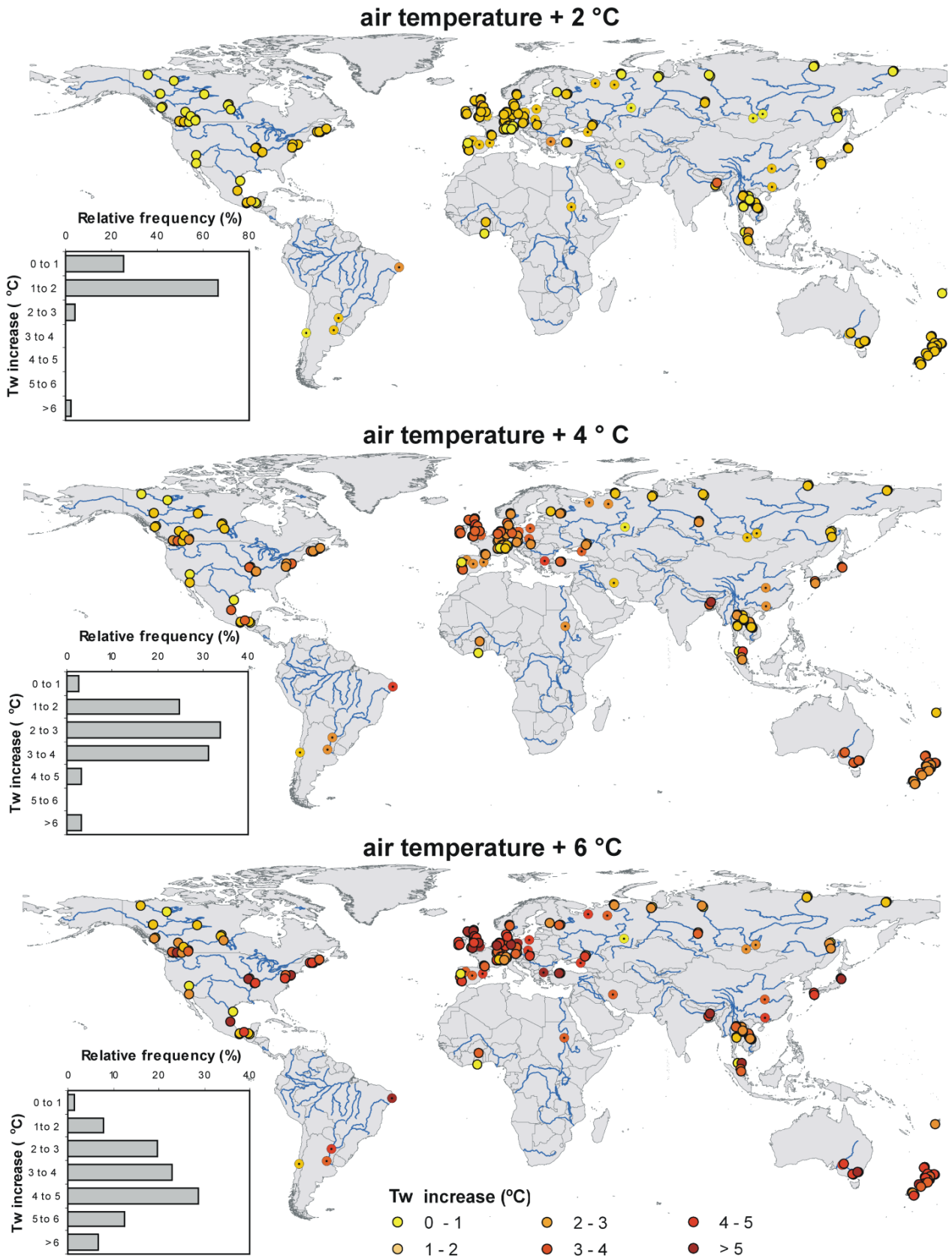


Figure 2.8: Mean annual river temperature increase (°C) under air temperature increases of +2°C, +4°C and +6°C for the selected GEMS/Water stations. The circles with black dots indicate river stations fitted using monthly data.

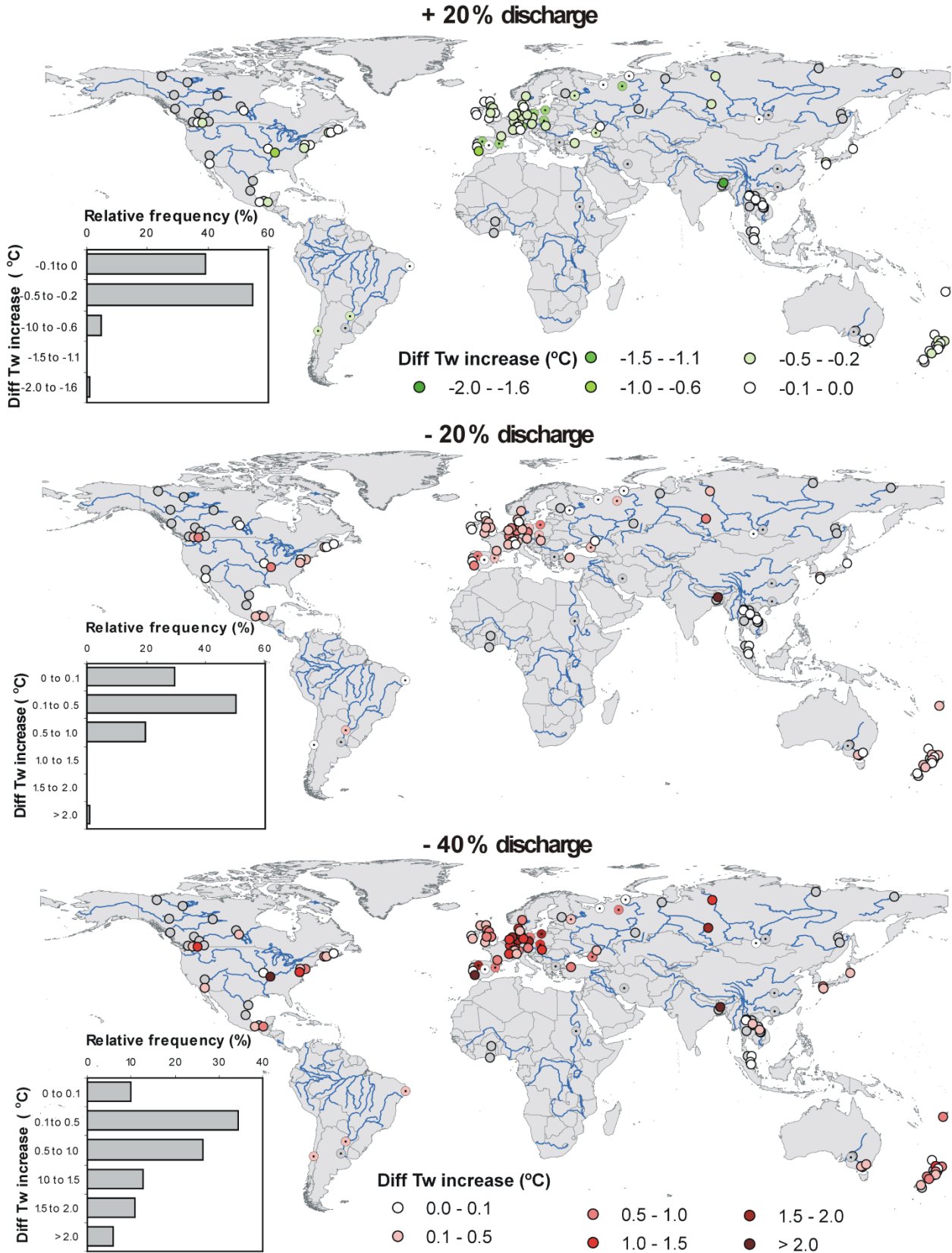


Figure 2.9: Difference in mean annual river temperature increase (°C) under an air temperature increase of +4°C in combination with a change in discharge of +20, -20% and -40% relative to an air temperature increase of +4°C without discharge changes for the selected GEMS/Water stations. The circles with black dots indicate river stations fitted using monthly data.

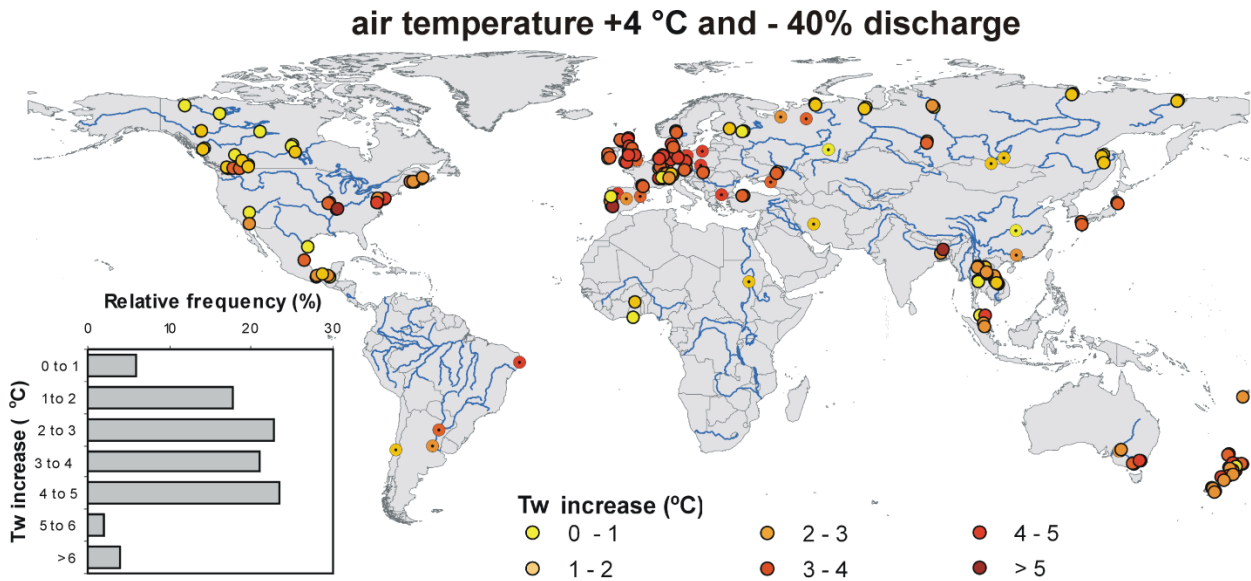


Figure 2.10: Mean annual river temperature increase (°C) under an air temperature increase of +4°C combined with a change in discharge of -40% for the selected GEMS/Water stations. The circles with black dots indicate river stations fitted using monthly data.

temperatures on a daily basis for river stations on a global scale. Positive relations were found between model performance and the availability of water temperature data to fit the regression model, while only weak relations were observed between the NSC and RMSE values and river basin characteristics (latitude and basin area). A distinct improvement in the model performance by the introduction of river discharge was found for 87% of the GEMS/Water stations globally. This improvement was most pronounced for stations with typically high winter discharges and low summer discharges. Less distinct increases in model performance, however, were obtained for river stations affected by reservoir operations or characterized by distinct snowmelt peaks during spring and summer. The improvement in model performance by the introduction of discharge was highest during extreme dry and warm spells (droughts and heat waves), when water temperatures are most sensitive to atmospheric influences and can reach high values.

Comparing our results with previous studies addressing the influence of river discharge on stream and river temperatures (e.g. Crisp and Howson, 1982; Mohseni et al., 1999), a generally higher impact of river discharge on water temperatures was found in our study. A multiple regression analysis of Webb et al. (2003), however, also indicated that inverse relations between water temperature and discharge were found, with greater impact of discharge on water temperatures at shorter time-scales and in larger catchments. This may explain that results of our study, in which a water temperature regression model applied to stations of generally large river basins on a daily basis showed a greater improvement by introduction of discharge than was found in previous studies that focused on stream stations in catchments or small river basins with weekly or monthly mean water temperatures.

Studies that previously applied the water temperature regression model of Mohseni et al. (1998) found an underestimation of the upper bound water temperature (α) with least squares regression, resulting in an underestimation of the calculated maximum water temperature (Bogan et al., 2006; Mantua et al., 2010; Mohseni et al., 1999; Mohseni et al., 1998). Although we generally obtained lower values of α for our modified water temperature regression model compared to the original model, the underestimation in river temperatures during summer periods was, however, less for the modified model including river discharge. Furthermore, results of calculated water temperatures for the European study basin stations during the heat wave and drought of 2003 (Figure 2.3) showed that the underestimation was greatly reduced by the introduction of discharge. This indicates that the regression model is less biased by an underestimation of the upper bound water temperature.

Results of our sensitivity analyses with water temperature changes under air temperature increases and changes in river discharge indicated that the impact of discharge changes were generally moderate compared to air temperature increases on a mean annual basis. The calculated changes in mean annual water temperature averaged for all selected GEMS/Water stations are +1.3°C, +2.6°C and +3.8°C under an air temperature increase of +2°C, +4°C and +6°C respectively. An increase in discharge with 20% resulted in a slight decrease in mean annual water temperature increase of -0.2°C, while decreases in discharge of 20% and 40% slightly exacerbated the water temperature increase by +0.3°C and +0.8°C on average. Although the contribution of discharge is moderate on an annual mean basis, relevant impacts of discharge changes were found especially for maximum water temperatures on a daily basis. For the study basin stations of San Joaquin, Potomac, Rhine and Danube (Figure 2.7), higher maximum water temperatures were found under an air temperature increase of +4°C in combination with a decrease in discharge of 40% than under an air temperature increase of +6°C (without discharge changes). This indicates that a strong decrease in river discharge under warm atmospheric conditions can have a greater impact on rising water temperatures than an extra air temperature increase of 2°C under these conditions. The relatively high sensitivity of daily water temperatures to discharge changes during dry and warm spells is relevant, as water temperatures can reach critically high values during these periods, with possibly negative environmental effects (e.g. exceeded water temperature tolerance values of freshwater species) and economic consequences (e.g. reduced cooling water potential for industries and thermal power plants). Considering the estimated water temperature increases of the Rhine (Lobith) (Section 2.4.1), the mean number of days per year that the critical limit of 23°C for cooling water use by thermal power plants (EEA, 2008a) is exceeded, is 16 days for the reference situation, 47 days and 83 days under air temperature increases of + 4°C and + 6°C, respectively, and 104 days per year under an air temperature increase of + 4°C in combination with a decrease in discharge of 40%. Although this is a rough estimation, it emphasizes the relevant contribution of decreasing discharges (reduced thermal capacity, limited dilution capacity for thermal effluents) to water temperature increases on a daily time step, and the associated impacts for cooling water purposes.

Results of our study are preliminary rough estimates of the sensitivity of river temperatures to air temperature increases and changes in river flow on a global scale. Although the selected air temperature increases and changes in river flow are realistic in the context of climate change, further research is needed to address the impact of climate change and changes in anthropogenic influences in detail. A limitation of the model approach for future projections is the fixed value of parameter estimates. It is likely that the upper bound in water temperature (α) and possibly also other parameters of the regression model may change as a result of climate change and anthropogenic changes (e.g. cooling water discharges, reservoir operations). The use of daily climate change and river discharge scenarios as input into a large-scale deterministic water temperature model can be a next step to produce more detailed and realistic estimates of river temperature under climate change conditions for a specific future period.

Despite these preliminary estimates, the outcomes of our study clearly demonstrate the relevant contribution of low river discharge in accounting for high water temperatures during dry, warm periods. As previous studies demonstrated an increase in flow seasonality as a result of climate change, with lower flows during the low-flow season in many rain-dominated catchments (Arnell, 2003a; Arnell, 2003b; Burlando and Rosso, 2002; Menzel and Burger, 2002), we expect that the relative impact of river discharge on water temperatures will increase in the future. Moreover, climate variability is expected to increase, resulting in increased risks of droughts and heat waves (Easterling et al., 2000; Schar et al., 2004; Stott et al., 2004; Wetherald and Manabe, 1999). The combined effects of both atmospheric warming and changes in river flow should therefore be considered in order to produce more realistic projections of future changes in river temperature under climate change.

To conclude, the outcomes of our study demonstrated that a nonlinear regression model with air temperature, river discharge and time lag included, is a simple and robust method to estimate river temperatures on a daily basis for monitoring stations in different river basins globally. The performance of the regression model improved for 87% of the global GEMS/Water river stations where discharge was introduced as an additional variable. Results showed that the impact of discharge changes generally increases during dry, warm periods, when rivers have a lower thermal capacity and are thus more sensitive to warm atmospheric conditions. This high sensitivity of daily water temperatures to discharge changes during dry (low flow) and warm spells is important, as water temperatures can reach critically high values for freshwater ecosystems and several usage functions (e.g. cooling for thermal power plants and industries, drinking water production, recreation) during these periods. Impacts of river discharge on water temperatures should thus be incorporated to provide more accurate estimates of high river temperatures during historical and future projected dry, warm spells.

Acknowledgements

This research was financially supported by the European Commission through the FP6 Water and Global Change (WATCH) project. GPW was supported by the Joint DECC and Defra Integrated Climate Programme - DECC/Defra (GA01101). We gratefully acknowledge Kelly Hodgson of the United Nations Environment Programme Global Environment Monitoring System (GEMS/Water) for providing water temperature data and the Global Runoff Data Centre (GRDC) for supplying discharge data of river stations globally. Pavla Pekarova of the Institute of Hydrology in Slovakia, Zsolt Kozma of Budapest University of Technology and Economics, Richard Lammers of University of New Hampshire and Erasmus Marica of the Department of Water Affairs and Forestry in South Africa are kindly acknowledged for providing river temperature data for the selected study basins stations. Finally, we would like to thank Nick Gorski of KWR Watercycle Research Institute and three anonymous reviewers for their constructive and valuable comments.

Coupled Daily Streamflow and Water Temperature Modelling in Large River Basins

Abstract

Realistic estimates of daily streamflow and water temperature are required for effective management of water resources (e.g. for electricity and drinking water production) and freshwater ecosystems. Although hydrological and process-based water temperature modelling approaches have been successfully applied to small catchments and short time periods, much less work has been done at large spatial and temporal scales. We present a physically-based modelling framework for daily river discharge and water temperature simulations applicable to large river systems on a global scale. Model performance was tested globally at $1/2^\circ \times 1/2^\circ$ spatial resolution and a daily time step for the period 1971-2000. We made specific evaluations on large river basins situated in different hydro-climatic zones and characterized by different anthropogenic impacts. Effects of anthropogenic heat discharges on simulated water temperatures were incorporated by using global gridded thermoelectric water use data sets and representing thermal discharges as point sources into the heat-advection equation. This resulted in a significant increase in the quality of the water temperature simulations for thermally polluted basins (Rhine, Meuse, Danube and Mississippi). Due to large reservoirs in the Columbia which affect streamflow and thermal regimes, a reservoir routing model was used. This resulted in a significant improvement in the performance of the river discharge and water temperature modelling. Overall, realistic estimates were obtained at daily time step for both river discharge (median normalized BIAS=0.3; normalized RMSE=1.2; $r=0.76$) and water temperature (median BIAS=-0.3°C; RMSE=2.8°C; $r=0.91$) for the entire validation period, with similar performance during warm, dry periods. Simulated water temperatures are sensitive to headwater temperature, depending on resolution and flow velocity. A high sensitivity of water temperature to river discharge (thermal capacity) was found during warm, dry conditions. The modelling approach has potential to be used for risk analyses and studying impacts of climate change and other anthropogenic effects (e.g. thermal pollution, dams and reservoir regulation) on large rivers.

This chapter has been published as:

van Vliet, M.T.H., J.R. Yearsley, W.H.P. Franssen, F. Ludwig, I. Haddeland, D.P. Lettenmaier, and P. Kabat (2012), Coupled daily streamflow and water temperature modelling in large river basins, Hydrology and Earth System Sciences 16, 4303–4321, doi:10.5194/hess-16-4303-2012

3.1 Introduction

Streamflow and water temperature affect many aspects of water quality (Ducharne, 2008; Haag and Westrich, 2002; Kaushal et al., 2010; van Vliet and Zwolsman, 2008) and are among the most important parameters characterizing the physical conditions of freshwater ecosystems (e.g. Bartholow, 1991; Rundquist and Baldrige, 1990). Hence, the distribution of fish and other aquatic organisms is directly influenced by the hydrological and thermal regime of rivers (e.g. Eaton and Scheller, 1996; Ebersole et al., 2001). In addition, river discharge and water temperature influence the potential for cooling water use, and as a result are key factors for thermoelectric power production (IPPC, 2001; Segrave, 2009).

Realistic estimates of river discharge and water temperature are needed for water management. In particular during periods with high water temperature and low streamflow, conflicts may arise between protecting freshwater ecosystems by enforcing ecological water temperature standards and risks to thermoelectric power production due to cooling water shortages. This has been reported for example for the River Rhine (Rutten et al., 2008), and for the Loire and Rhone Rivers (Manoha et al., 2008) during the recent warm summers of 2003 and 2006 in Europe. In addition, significant impacts of water temperature of the River Rhine on electricity prices were found when water temperatures are above 22-23°C (Boogert and Dupont, 2005).

For effective management of water and freshwater ecosystems, estimates of river discharge and water temperature at high temporal resolution, preferably on daily basis, are required. Both data (statistical) and process (physically-based) models have been used to estimate river discharge and water temperature using climatic forcings. Statistical models (e.g. regression, stochastic models and neural networks) are appealing because they require only limited input variables (e.g. Ahmadi-Nedushan et al., 2007; Augustin et al., 2008; Chenard and Caissie, 2008; Mohseni et al., 1998; Muttiah et al., 1997). However, they are fitted for a specific historical period and, therefore, are limited in their application for forecasting and scenario studies, such as climate change impact assessments. In contrast, process models represent the physical processes that affect river discharge and water temperature and have been particularly useful for predictions of the effects of anthropogenic perturbations of model forcings and boundary conditions (land use change, thermal pollution, flow regulation) (e.g. Haag and Luce, 2008; Risley et al., 2010; St-Hilaire et al., 2003) and climate change (e.g. Ferrari et al., 2007; Morrison et al., 2002).

Although water temperature is generally most sensitive to the heat exchange processes at the air - water surface interface, changes in streamflow significantly affect water temperatures due to changes in thermal capacity (Edinger et al., 1968b) and travel time, and dilution capacity for thermal effluents (Moatar and Gailhard, 2006; Sinokrot and Gulliver, 2000; van Vliet et al., 2011; Webb et al., 2003). Therefore, an integrated hydrological and river temperature modelling approach is preferred which includes both heat exchange processes at the air - water surface interface and changes in thermal capacity and travel times due to

streamflow changes. Although hydrological and process-based water temperature modelling approaches have been successfully applied for small-scale catchments and subbasins (e.g. Caissie et al., 2007; Haag and Luce, 2008; St-Hilaire et al., 2000), considerably less work has been done at large scales. To our knowledge, water temperature simulations on macro-hydrological scale have only been performed by van Beek et al. (2012). Limited studies have simulated both river discharge and water temperature for long (>20-30 year) time periods, which is required for scenario analyses and climate change impact assessments. In addition, realistic simulations of water temperature and discharge of rivers with different basin characteristics and anthropogenic impacts are needed to address large-scale water management issues.

In this study, we test the performance of an integrated framework with a physically (process) based hydrological and water temperature model to simulate daily river discharge and water temperature of large river basins in different hydro-climatic regions and with different anthropogenic impacts. A spatial resolution of $1/2^\circ \times 1/2^\circ$ was used as in Haddeland et al. (2011) and for which global forcing data are available (Weedon et al., 2011). Several macro-scale hydrological models have simulated river discharge at this spatial resolution (e.g. Alcamo et al., 2003a; Arnell, 1999c; Oki et al., 2001), but most studies focus on monthly or annual mean estimates of river discharge.

Our modelling framework is based on the Variable Infiltration Capacity (VIC) macro-scale hydrological model (Liang et al., 1994) and the particle tracking River Basin Model (RBM) for water temperature (Yearsley, 2009) (Section 3.2.2). The modelling framework was applied globally, however we focus on rivers situated in different hydro-climatic zones and characterized by different anthropogenic influences (Section 3.2.1). The performance of VIC-RBM was tested for a historical period 1971-2000 (Section 3.3.1 and 3.3.2). In addition, we tested the modelling framework for the Rhine and Columbia during warm, dry summer periods, and during the second half of the 20th century (Section 3.3.3). The sensitivity of simulated water temperatures to the boundary conditions (headwater temperature estimates) was studied (Section 3.3.4), as well as the sensitivity to streamflow (Section 3.3.5). The overall performance and major uncertainties of the hydrological - water temperature modelling approach for large-scale applications are discussed in Section 3.4.

3.2 Methodology

3.2.1 Study basins

We focused on the Columbia, Mississippi (North America), Parana (South America), Rhine, Meuse, Danube (Europe), Orange (Africa), Ob, Yenisey, Lena (Arctic Asia), Mekong, Yangtze, Yellow (Southeast Asia) and Murray-Darling (Australia) to test the performance of the hydrological - water temperature modelling approach. These basins are situated in different hydro-climatic zones with different anthropogenic influences, and therefore represent different hydrological and thermal regimes (Table 3.1). The Columbia, Mississippi, Rhine,

Meuse, Danube, Yangtze and Yellow basin are situated in the temperate climate zone and are influenced by transient runoff (mix of rainfall and springtime snowmelt), while the Murray-Darling and Orange are mainly fed by rainwater. The Parana and Mekong are rain (monsoon) fed rivers located in the tropical climate zone, while the Ob, Yenisey and Lena are Arctic rivers that are strongly affected by melt water during spring and summer. River discharge and water temperatures of the Columbia are heavily influenced by reservoirs, and parts of the Rhine, Meuse, Danube and Mississippi have a high level of thermal pollution due to cooling water discharges from thermoelectric power plants. The river basins vary in size, from almost 3.0 million km² (Mississippi and Ob) to 36,000 km² (Meuse). Another important criterion for selecting these study basins was the availability of monitoring stations with daily river discharge and water temperature records suitable for evaluating the performance of the modelling framework.

3.2.2 Concept of hydrological and water temperature modelling approach

Figure 3.1 shows linkages between the component models in the hydrological - water temperature modelling framework, along with required model input and model output. Conceptual background for the VIC hydrological model, RBM water temperature model, and the regression model used to estimate the headwater temperature are given below.

In brief, climate forcings and soil and vegetation parameters are used as input into VIC, resulting in simulated surface runoff and baseflow. The output (surface runoff and baseflow) is then provided to an offline routing model to simulate channel flows, depth, width and flow velocity on a stream reach basis. A routing model with a reservoir scheme simulates river discharge in the strongly regulated Columbia River. Climate forcings include air temperature, shortwave and long wave radiation, vapor pressure, density, pressure and wind speed disaggregated to the VIC grid cell and RBM reach level at a 3-hourly time step. In addition, daily channel flows, width, depth and flow velocity are used to force RBM. Other required inputs are an ordered stream network with defined river reaches (Yearsley, 2012), estimates of anthropogenic point heat sources and daily headwater stream temperature estimates (boundary conditions). The integrated modelling system simulates streamflow and water temperature in each of the grid cells.

Variable Infiltration Capacity (VIC) model and routing model

The Variable Infiltration Capacity (VIC) (Liang et al., 1994) is a grid-based macro-scale hydrological model that solves both the surface energy and water balance equations. The model represents subgrid variability in vegetation, elevation, and soils by partitioning each grid cell into multiple land cover (vegetation) and elevation classes. The soil column is commonly divided into three soil layers. Surface runoff and baseflow are routed along the stream network to the basin outlet with an offline routing model that uses the unit hydrograph principle within the grid cells and linearized St. Venant's equations to simulate

Table 3.1: Major characteristics of selected study basins, data sources and number of monitoring stations with river discharge (Q) and water temperature (Tw) data used for validation of modelling approach.

study basin	drain. area (*10 ³ km ²)	river length (km)	climate (Köppen) zone	dominant source water	human impacts	data source Q stations	data source Tw stations
North America							
Columbia	668	2,000	temperate (Ds, Cs)	mix rain/melt water	many dams, reservoirs	GRDC (n=47)	Streamnet, GEMS/Water (n=18)
Mississippi	2,981	3,734	temperate (Df, Cf)	mix rain/melt water	thermally polluted, dams	GRDC (n=104)	USGS, GEMS/Water (n=33)
South America							
Parana	2,583	4,880	tropical (Aw, Cf)	rain water	several dams	GRDC (n=4)	GEMS/Water (n=3)
Europe							
Rhine	170	1,232	temperate (Cf)	mix rain/melt water	thermally polluted, one reservoir	GRDC (n=19)	LU, BG, Waterbase, GEMS/Water (n=21)
Meuse	36	935	temperate (Cf)	rain (and melt) water	thermally polluted	GRDC (n=5)	Waterbase, GEMS/Water (n=5)
Danube	817	2,860	temperate (Df)	mix rain/melt water	moderate thermal pollution, dams	GRDC (n=26)	ICPD, GEMS/Water (n=13)
Africa							
Orange	973	2,200	temperate (BW, BS, Cf)	rain water	several dams, water withdr.	GRDC (n=3)	DWAF (n=3)
Northern Asia (Arctic)							
Ob	2,972	2,962	arctic (Df)	melt water	dams, moderate thermal pollution	GRDC (n=5)	GEMS/Water, Lammers et al. (2007)(n=3)
Yenisey	2,580	5,539	arctic (Df, ET)	melt water	low number of reservoirs	GRDC (n=5) daily	GEMS/Water, Lammers et al. (2007) (n=1)
Lena	2,490	4,472	arctic (Df, ET)	melt water	low number of reservoirs	GRDC (n=6)	GEMS/Water, Lammers et al. (2007)(n=1)
Southeast Asia							
Mekong	795	4,909	tropical (Am, Aw, Cw)	rain (monsoon)	low number of reservoirs	GRDC (n=14)	GEMS/Water (n=9)
Yangtze	1,809	6,300	temperate (Cw)	mix rain/melt water	several dams	GRDC (n=4) monthly	GEMS/Water (n=3)
Yellow	752	5,464	temperate (Cw, Dw)	mix rain/melt water	several dams	GRDC (n=3)	GEMS/Water (n=2)
Australia							
Murray-Darling	1,061	2,589 3,375	temperate (BS, BW, Cs)	rain water	much water withdrawal	GRDC (n=12)	MDBC, GEMS/Water (n=6)

(LU = Landesanstalt für Umwelt Germany, BG = Bundesanstalt für Gewässerkunde Germany, ICDR = International Commission for the Protection of the Danube, DWAF = Department of Water Affairs and Forestry South-Africa; MDBC=Murray-Darling Basin Commission)

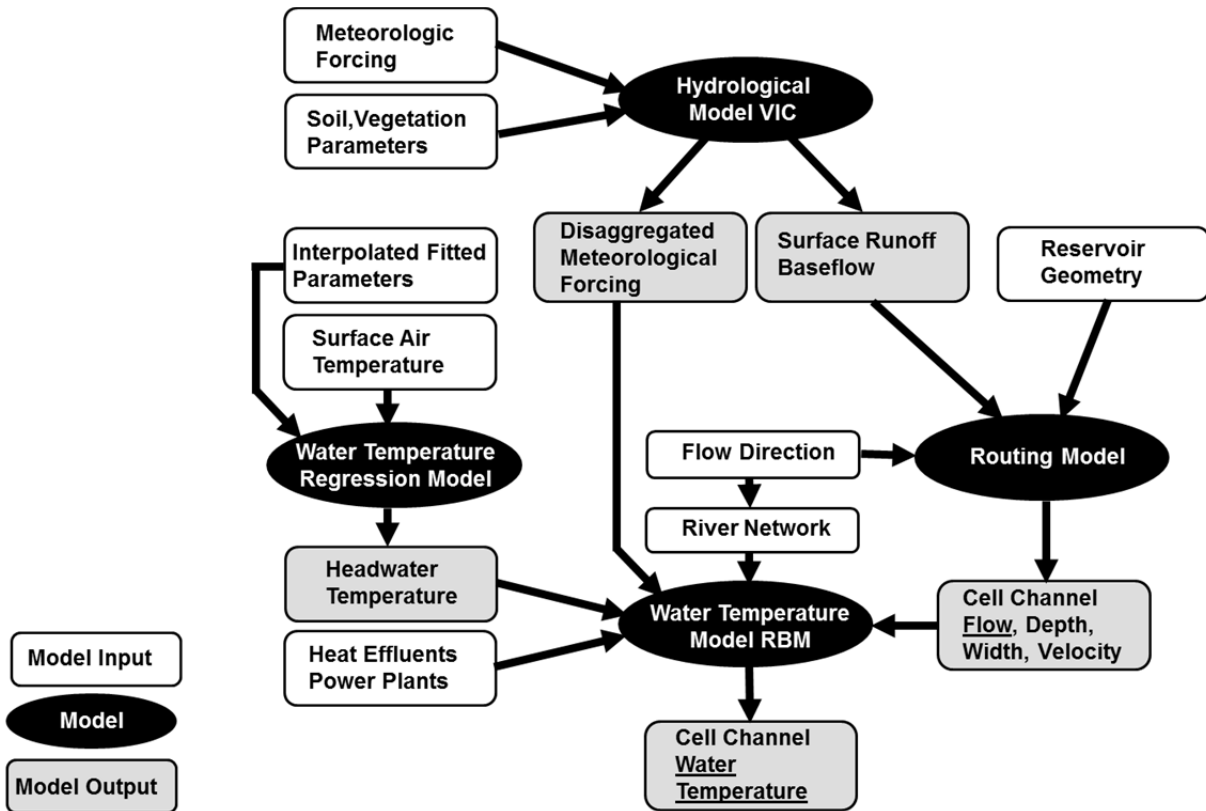


Figure 3.1: Flowchart of the hydrological - water temperature modelling framework, presenting the links between the hydrological model (VIC), routing model, process-based water temperature model (RBM), water temperature regression model used to assess headwater temperatures (boundary conditions), and model input and output.

river flow through the stream channel (Lohmann et al., 1998). For the Columbia River, which is highly affected by dams and reservoirs, we used the reservoir scheme of Haddeland et al. (2006), which is combined with the routing scheme of Lohmann et al. (1998) to obtain a more realistic representation of streamflow below the major reservoirs. The reservoir scheme runs at a daily time step, but was originally developed for analyses at coarser time scales. Hence, we calculated 10-day moving averages of daily regulated river discharge.

Information about daily river depth, width and velocity is required for the water temperature simulations. The original VIC routing model (Lohmann et al., 1998) was therefore modified to calculate hydraulic characteristics based on power equations relating mean velocity, cross-sectional area and width to river discharge (Leopold and Maddock, 1953). Allen et al. (1994) obtained coefficients for these equations by fitting empirical relationships with river discharge using data from 674 stream discharge stations across the United States (equation 3.1a and 3.1b). As these stations are situated in a wide range of hydro-climatic zones, the assumption was made that these fitted relations can be applied to estimate the hydraulic characteristic of rivers in other regions as well and under different flow conditions. Flow velocity was estimated based on river discharge and cross-sectional area (equation 3.1c).

$$D = 0.34Q^{0.341} \tag{3.1a}$$

$$W = 1.22Q^{0.557} \quad (3.1b)$$

$$U = \frac{Q}{WD} \quad (3.1c)$$

Where: D = river depth [m]; Q = river discharge [m³s⁻¹]; W = river width [m]; U= river flow velocity [m s⁻¹].

For the river reaches controlled by reservoirs, we assumed water surface elevation, and as a result the depth (D_{res}) and width (W_{res}) to remain constant in time. In these river reaches equation 3.1c becomes:

$$U = \frac{Q}{W_{res} D_{res}} \quad (3.2)$$

VIC and its routing model have been applied in the recent past at spatial scales ranging from 1/16° (Elsner et al., 2010) to 1° (Nijssen et al., 2001b). The temporal resolution is flexible between hourly to daily step. The 1/2° spatial resolution used in this study was selected as a compromise between the ability to resolve variations in river basin contributing areas and channel variations, and computational efficiency.

Stream temperature model RBM

RBM is a process-based one-dimensional stream temperature model that solves the 1D-heat advection equation using the semi-Lagrangian (mixed Eulerian-Lagrangian) approach (Yearsley, 2009). Because of the large-scale application, the advection term dominates, and dispersion was for that reason neglected. Water temperature is calculated for a specific stream segment based on the upstream water temperature and inflow into the stream segment, the dominant heat exchange at the air - water surface, and the inflow and temperature of water advected from tributaries. RBM was developed for subbasins of the Columbia River and has been applied by Yearsley (2012) to the Salmon subbasin (36,325 km²) on a 1/16° spatial resolution. In this study, modifications were made to apply RBM to larger river basins characterized by different thermal and hydrological regimes and anthropogenic impacts. To use RBM for thermally polluted river basins, modifications were made to incorporate anthropogenic heat discharges of thermoelectric power plants as advected heat sources. This results in the following 1D-heat advection equation:

$$\rho_w C_p \frac{\delta(T_w A_x)}{\delta t} = H_{air-water} w_x + \frac{\rho_w C_p Q_{trb} \Delta T_{trb}}{\delta x} + \frac{\rho_w C_p Q_{effl} \Delta T_{effl}}{\delta x} \quad (3.3)$$

Where: ρ_w = density of water [kg m⁻³]; C_p = specific heat capacity of water [J kg⁻¹°C⁻¹]; T_w = water temperature [°C]; A_x = cross-sectional area of river at distance x [m²]; $H_{air-water}$ = heat flux at air - water interface [J m⁻² s⁻¹]; w_x = stream width at distance x [m]; Q_{trb} = advected flow from tributaries or subsurface [m³ s⁻¹]; ΔT_{trb} = the difference between advected temperature

from tributaries or subsurface, T_{tbr} , and T_w [°C]; Q_{effl} = advected flow from heat dumps of thermoelectric power plants [$m^3 s^{-1}$]; ΔT_{effl} = the difference between the advected temperature from heat dumps of thermoelectric power plants, T_{effl} , and T_w [°C]; x = longitudinal distance along the axis of the river [m]; t = time [s].

The net exchange of thermal energy across the air - water interface ($H_{air-water}$) is determined using a one dimensional implementation of the stream energy balance equation Wunderlich and Gras (1967):

$$H_{air-water} = (H_s - H_{rs}) + (H_a - H_{ar}) + H_{evap} + H_{cond} + H_{back} \quad (3.4)$$

Where: $H_{air-water}$ = net exchange of thermal energy across the air - water interface [$J m^{-2} s^{-1}$]; H_s = shortwave solar radiation [$J m^{-2} s^{-1}$]; H_{rs} = reflected shortwave solar radiation [$J m^{-2} s^{-1}$]; H_a = longwave atmospheric radiation [$J m^{-2} s^{-1}$]; H_{ar} = reflected atmospheric radiation [$J m^{-2} s^{-1}$]; H_{evap} = evaporative heat flux [$J m^{-2} s^{-1}$]; H_{cond} = conductive or convective heat flux [$J m^{-2} s^{-1}$] (the flux resulting from temperature differences between the atmosphere and river); H_{back} = blackbody radiation from the water surface [$J m^{-2} s^{-1}$].

Estimation of the boundary conditions (headwater temperatures)

As part of the study described in Yearsley (2012), two methods for headwater temperature estimation were compared for the Salmon River (subbasin of the Columbia). One method uses daily soil temperature from VIC and another method uses a nonlinear water temperature regression model (Mohseni et al., 1998) based on air temperature. Overall, the performance of the RBM model did not improve by using soil temperature to estimate headwater temperature. Given the widespread use of the regression model of Mohseni et al. (1998), we decided to use the latter approach for this study to estimate headwater temperature. The water temperature regression model of Mohseni et al. (1998) describes the S-curve relationship between weekly water temperature and weekly air temperature according to:

$$T_{w_{head}} = \mu + \frac{\alpha - \mu}{(1 + e^{\gamma(\beta - T_{air})})} \quad (3.5)$$

$$\text{with: } \gamma = \frac{4 \tan \theta}{\alpha - \mu}$$

Where: μ = lower bound of water temperature [°C]; α = upper bound of water temperature [°C]; γ = measure of the slope at inflection point (steepest slope) of the S-shaped relation [°C⁻¹]; β = air temperature at inflection point [°C]; $T_{w_{head}}$ = headwater temperature [°C]; T_{air} = air temperature [°C]; $\tan \theta$ = slope at inflection point [-].

The four parameters of the regression model and time lag were fitted for 333 Global Environment Monitoring System (GEMS)/Water stations globally for the period 1980-2000 using least squares regression. We applied the nonlinear water temperature regression model

on a daily time step by including a lag effect, as water temperature variations lag behind air temperature fluctuations at short time scale (hourly, daily basis) (Erickson et al., 2000; Jeppesen and Iversen, 1987). For each station, the optimal lag parameter was estimated by calculating correlation coefficients between water temperature and smoothed air temperature ($T_{air_{smooth}}$) for various lag parameter values (λ) using equation 3.6, and selecting the λ for which the correlation coefficient was highest.

$$T_{air_{smooth}} = (1 - \lambda)T_{air}(t - 1) + \lambda T_{air}(t) \quad (3.6)$$

In a next step, the fitted parameter values μ , α , γ and β were interpolated using ordinary kriging, resulting in $1/2^\circ \times 1/2^\circ$ interpolated grids. The time lag at which water temperature variations follow air temperature variations increases with stream depth (Stefan and Preudhomme, 1993) and thus with river discharge. The lag parameter was, therefore, spatially interpolated using gridded river discharge simulations produced by VIC in combination with an empirical relationship between lag parameter and river discharge (fitted for all stations). An overview of the mean and range (minimum-maximum) in fitted parameters for all study basins (Table 3.2) shows that the fitted values of the Mohseni parameters vary between the different study basins (in particular μ). The lag parameter (λ) is generally constant within and between the different basins (between 0.09 - 0.12 for all basins).

3.2.3 Application of hydrological - water temperature modelling framework

To test the performance of the modelling framework, the VIC-RBM framework was applied globally for the period 1970-2001 (including a spin-up period of one year). The models were forced with daily (24h mean) values of precipitation, minimum and maximum surface air

Table 3.2: Mean values and range (minimum-maximum) of interpolated parameters of nonlinear water temperature regression model and time lag used for estimating daily headwater temperature in the study basins.

study basin	μ (°C)	α (°C)	β (°C)	γ (°C ⁻¹)	λ (day ⁻¹)
	mean [range]	mean [range]	mean [range]	mean [range]	mean [range]
Columbia	3.0 [0.5 - 5.3]	16.4 [13.9 - 18.8]	5.6 [2.3 - 8.3]	0.27 [0.24 - 0.31]	0.10 [0.09 - 0.11]
Mississippi	4.0 [0.8 - 10.4]	22.7 [16.0 - 26.2]	10.3 [4.2 - 18.6]	0.27 [0.18 - 0.55]	0.10 [0.09 - 0.11]
Parana	19.2 [16.4 - 20.2]	25.2 [24.8 - 25.6]	18.1 [17.2 - 18.7]	0.44 [0.40 - 0.50]	0.10 [0.09 - 0.12]
Rhine	4.5 [2.6 - 5.6]	19.8 [19.3 - 20.4]	8.8 [7.9 - 9.8]	0.30 [0.28 - 0.39]	0.10 [0.09 - 0.11]
Meuse	4.7 [3.7 - 6.7]	19.8 [19.4 - 20.0]	8.9 [8.5 - 9.4]	0.34 [0.29 - 0.44]	0.10 [0.10 - 0.11]
Danube	2.6 [0.6 - 5.3]	20.9 [19.5 - 22.2]	9.1 [7.5 - 11.5]	0.25 [0.07 - 0.40]	0.10 [0.09 - 0.11]
Orange	14.2 [9.4 - 18.0]	25.4 [24.2 - 26.4]	18.8 [17.2 - 20.1]	0.60 [0.49 - 0.77]	0.11 [0.09 - 0.12]
Ob	0.0 [0.0 - 0.0]	19.0 [15.4 - 22.3]	6.5 [0.0 - 12.9]	0.18 [0.09 - 0.41]	0.11 [0.09 - 0.12]
Yenisey	0.0 [0.0 - 0.0]	17.7 [13.8 - 21.3]	4.8 [0.1 - 9.3]	0.22 [0.05 - 0.51]	0.11 [0.09 - 0.12]
Lena	0.0 [0.0 - 0.0]	17.6 [14.4 - 20.7]	5.3 [2.3 - 6.9]	0.19 [0.11 - 0.35]	0.11 [0.09 - 0.11]
Mekong	21.0 [3.9 - 28.6]	28.5 [25.5 - 30.0]	23.0 [16.2 - 28.2]	1.02 [0.48 - 1.31]	0.10 [0.09 - 0.11]
Yangtze	7.3 [0.6 - 15.1]	27.4 [24.9 - 29.0]	16.8 [14.2 - 19.7]	0.27 [0.24 - 0.31]	0.10 [0.09 - 0.11]
Yellow	0.6 [0.0 - 5.8]	16.4 [13.9 - 18.8]	5.6 [2.3 - 8.3]	0.27 [0.18 - 0.55]	0.10 [0.09 - 0.12]
Murray-Darling	3.0 [0.5 - 5.3]	22.7 [16.0 - 26.2]	10.3 [4.2 - 18.6]	0.44 [0.40 - 0.50]	0.10 [0.09 - 0.11]

temperature and wind speed from the global gridded $1/2^\circ \times 1/2^\circ$ meteorological dataset developed within the EU FP6 Water and Global Change (WATCH) project (Weedon et al., 2010; Weedon et al., 2011). VIC was applied using the elevation and land cover classifications (elevation, vegetation, and soil characteristics) described in Nijssen et al. (2001b), disaggregated to $1/2^\circ \times 1/2^\circ$ spatial resolution. In their study, calibration on soil characteristics was performed for selected large river basins globally (including the Mississippi, Columbia, Danube, Parana, Yellow, Yangtze, Mekong, Yenisey, Lena and Ob). Calibrated parameters values were subsequently transferred to other basins based on climate characteristics. The global DDM30 routing network (Döll and Lehner, 2002) was used for the lateral routing of streamflow and to create an ordered river network for the RBM water temperature simulations. For the Columbia basin where river discharge and water temperature is highly impacted by reservoirs, we used information about dams from the University of New Hampshire updated according to the World Register of Dams (ICOLD, 2003), as described by Haddeland et al. (2006).

To get realistic water temperature simulations in thermally polluted river basins (Mississippi, Rhine, Meuse, Danube), estimates of thermal discharges of thermoelectric power plants are required as input into RBM. We used gridded ($1/2^\circ \times 1/2^\circ$) estimates of global thermoelectric water consumption and water withdrawal for the 20th century (Flörke et al., 2011; Voß and Flörke, 2010) to estimate return flows from thermoelectric water diversions (Q_{effl}). Because, gridded data for the difference in temperature between return water temperature and inlet water temperature were not available, we assumed that the temperature of return flow (T_{effl}) was on average 3°C higher than the inlet river water temperature (T_w). This value was also selected based on an average estimate for the Rhine River (Icke et al., 2006) and based on standards for heat discharges in the U.S., which are written under the requirements of the Clean Water Act, and limit the ΔT_{effl} to 3°C for most states. In addition, overall best results of daily simulated water temperature were obtained under a ΔT_{effl} of 3°C when we tested this for the thermally polluted basins Mississippi, Rhine, Meuse and Danube with values ranging from 2 to 10°C (van Vliet et al., 2012). Using information about the dominant cooling type in each grid cell, Q_{effl} and ΔT_{effl} , gridded ($1/2^\circ \times 1/2^\circ$) datasets of thermal discharge were calculated for the period 1971-2000 and these were used as input into RBM.

3.2.4 Evaluation of hydrological - water temperature modelling framework

Observed daily river discharge and water temperature records for selected monitoring stations in the study basins were used to evaluate the VIC-RBM simulations. Daily mean series of river discharge were provided by the Global Runoff Data Centre (GRDC; <http://grdc.bafg.de/>) for the period 1971-2000. For the Yangtze River, we tested the performance of VIC on a monthly time step, because daily discharge series were not available. For water temperature, we used observed records for the period 1980-2000 provided by the United Nations Environment Programme (UNEP) Global Environment Monitoring System (GEMS/Water; <http://www.gemswater.org>) in combination with daily water temperature series provided by different sources (Table 3.1). In general, the water temperature

observations represent daily instantaneous (spot) measurements, taken approximately 0-1 m below the water surface around mid-day. These instantaneous water temperature measurements that are taken at the water surface were related to simulated water temperature, which are cross-sectional averages of mean daily water temperature. Although there are vertical variations in water temperature, previous studies have shown that instantaneous observations of water temperature taken near surface are generally representative of the mean water temperature as vertical and lateral mixing of water is often very strong in large rivers (Liu et al., 2005; Mackay and Mackay, 1975).

To quantify the performance of VIC and RBM for daily river discharge and water temperature simulations we used the root mean squared error (*RMSE*) and mean bias (*BIAS*). In addition, the Pearson correlation coefficient (*r*) was calculated to quantify the linear dependence between simulations and observations values. For river discharge, normalized values of *RMSE* and *BIAS* were calculated (*NRMSE* and *NBIAS* henceforth) by dividing by the mean observed river discharge values. The equations for the selected performance coefficients are:

$$RMSE = \sqrt{\frac{\sum_{i=1}^n (P_i - O_i)^2}{n}} \quad (3.7)$$

$$BIAS = \frac{\sum_{i=1}^n (P_i - O_i)}{n} = \bar{P} - \bar{O} \quad (3.8)$$

$$r = \frac{\sum_{i=1}^n (O_i - \bar{O})(P_i - \bar{P})}{\sqrt{\sum_{i=1}^n (O_i - \bar{O})^2} \sqrt{\sum_{i=1}^n (P_i - \bar{P})^2}} \quad (3.9)$$

Where: P_i = predicted value at time step I [°C]; O_i = observed value at time step I [°C]; \bar{O} = average of daily observed value [°C]; \bar{P} = average of daily predicted value [°C]; n = number of data pairs to be compared.

For the Columbia and Rhine basins, more detailed and longer term daily water temperature datasets were available. This allows a validation over the simulated water temperature trends over the entire 1971-2000 period and for warm, dry summers, specifically, when critically high water temperatures and low water availability occur. We focused on the warm summers of 1992 and 1994 in the Rhine, and the summers of 1998 and 1999 in the Columbia. These summers were selected, as highest water temperature values were observed, considering the average of all water temperature records in the river basin.

3.2.5 Sensitivity of simulated water temperature to headwater temperature

For coarse spatial resolution, uncertainties in the estimates of the boundary conditions are expected to propagate over large distances. A sensitivity analysis was therefore performed to assess the impact of uncertainties in headwater temperature estimates on simulated water temperatures at different spatial resolutions; $1/2^\circ$, $1/4^\circ$ and $1/8^\circ$. We focused on the Rhine and Meuse basins in Western Europe, because these basins are the smallest study basins and have reasonable running times at $1/8^\circ$ resolution. The routing and water temperature simulations for the Rhine and Meuse on $1/4^\circ$ and $1/8^\circ$ were performed by using the river routing networks derived from HYDRO1K (Wu et al., 2011). We compared water temperature simulations produced by using an overestimated headwater temperature of $+2.0^\circ\text{C}$ with simulations based on the original gridded headwater temperature estimates (reference case) at $1/2^\circ$, $1/4^\circ$ and $1/8^\circ$ resolutions for the period 1971-2000.

3.2.6 Sensitivity of simulated water temperature to river discharge

In addition to headwater temperature, we assessed the impact of uncertainties associated with the hydrological model output and changes in river discharge on the simulated daily water temperature. We compared simulated water temperature for the reference case with simulated water temperature under a change in streamflow of -25%, -50%, +25% and +50%. Simulations with RBM were performed for the period 1970-2000 (including one year spin-up) assuming a constant decrease and increase in both daily simulated runoff and baseflow from VIC of -25%, -50%, +25% and +50% compared to the reference conditions.

3.3 Results

3.3.1 Performance of daily river discharge simulations

The spatial patterns of simulated mean annual river discharge of the study basins (Figure 3.2) generally show a close correspondence with the mean observed river discharge (small circles). For some downstream stations in the Orange and Murray-Darling basins, VIC overestimated river discharge. Part of this overestimation can be explained by anthropogenic water withdrawals (e.g. for agriculture, energy, manufacturing and domestic water use) which are relatively high in these basins. This results in lower observed river discharge values compared to the simulated values (which do not include anthropogenic water extractions). This overestimation is also reflected by relatively high values in NBIAS (>2) and high values in the NRMSE (>3) for both the Murray-Darling and the Orange river basins (Table 3.3). For the Ob, Yenisey, Lena, Mekong and Yangtze, a slight underestimation was found resulting in small negative values of NBIAS. However, values of NRMSE were generally low and r was relatively high ($r > 0.75$ for most of these basins). The use of the reservoir scheme resulted in a distinct improvement (significantly smaller bias; $p < 0.05$ using paired t-test) in the simulated river discharge of the highly regulated Columbia River (Figure 3.3). This is reflected by a lower value of mean NBIAS and NRMSE ($+0.3$ and 1.4 , respectively) compared to the simulation without the reservoir scheme ($+0.5$ and 2.0 , respectively). Although the onset of the discharge

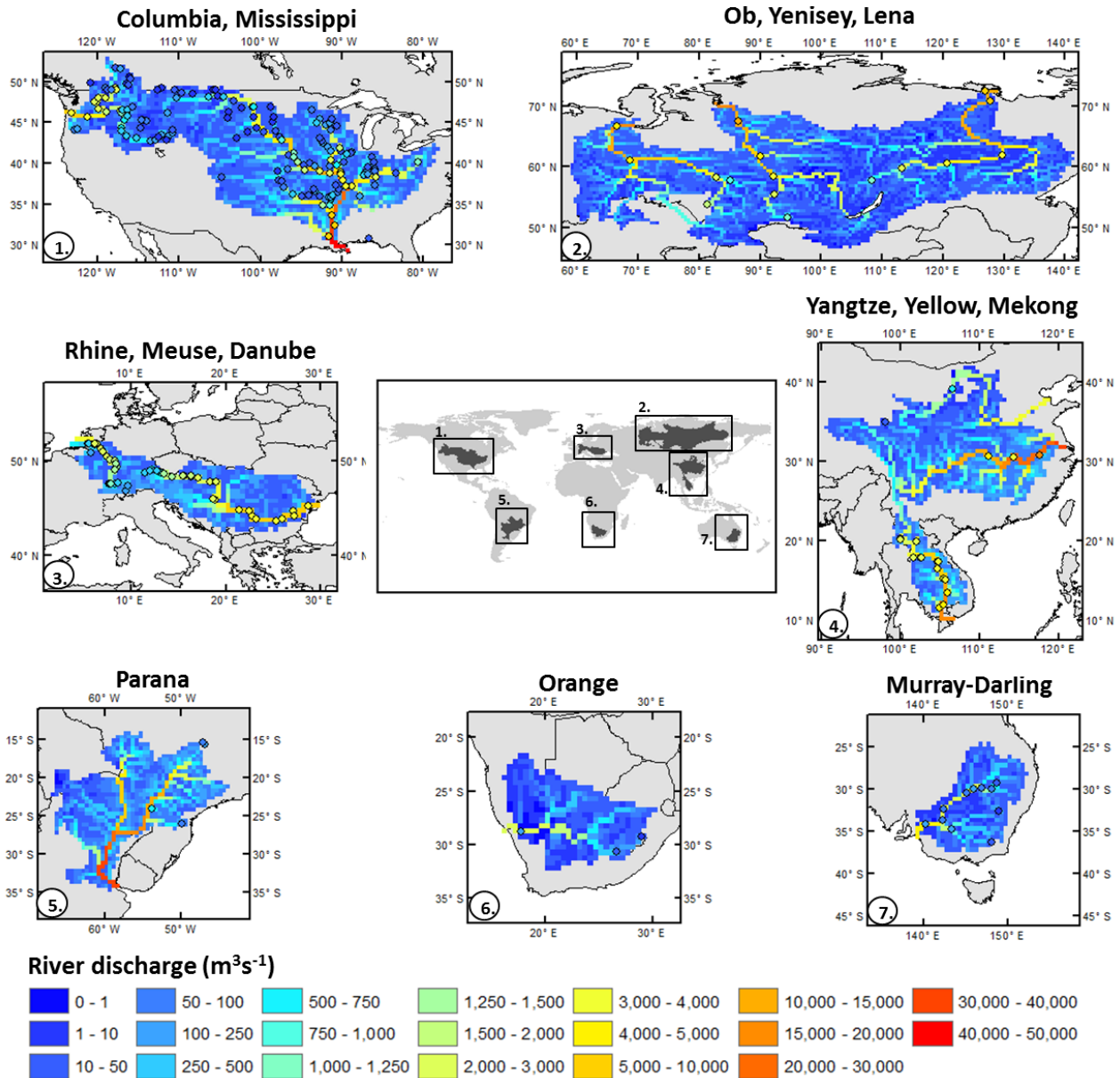


Figure 3.2: Spatial patterns of simulated (grid cells) and observed (circles) mean annual river discharge for study basins.

peak in spring is somewhat too early e.g. at the Dalles (Figure 3.3), the hydrologic regime is represented more realistically when the reservoir scheme is included. Although the hydrologic regimes of some other rivers, like the Mekong and Ob, are also slightly impacted by reservoirs, we obtained a quite realistic representation of daily river discharge with VIC without the use of a reservoir scheme for these rivers (mean NBIAS= -0.1; $r=0.91$ for Mekong; NBIAS= -0.1; $r=0.76$ for Ob; Figure 3.3). Daily variability in river discharge was slightly underestimated for some upstream stations in the River Rhine (Figure 3.3), but in general a realistic representation was found (mean NBIAS=+0.1; $r=0.76$). This indicates that the hydrological model is suitable for simulating daily discharge in river basins situated in different climate zones (temperate, tropical and arctic) and with different anthropogenic impacts.

Table 3.3: Mean and range of bias (BIAS), root mean squared error (RMSE) and Pearson-correlation coefficient (r) of daily river discharge (a) and water temperature simulations (b) for study basins. For river discharge, normalized values are presented for root mean squared error (NRMSE) and mean bias (NBIAS).

a) Daily river discharge (Q)

river basin	NBIAS		NRMSE		r	
	mean	range	mean	range	mean	range
Columbia*	+0.3	[-0.7, +4.6]	1.4	[0.3, 6.2]	0.65	[0.32, 0.89]
Mississippi	+1.2	[-1.0, +3.5]	2.6	[0.5, 4.9]	0.60	[0.28, 0.89]
Parana	+1.2	[+0.8, +1.6]	1.9	[1.4, 2.4]	0.79	[0.39, 0.86]
Rhine	+0.1	[-1.0, +1.7]	0.6	[0.3, 1.9]	0.76	[0.53, 0.86]
Meuse	+0.9	[-0.3, +6.0]	1.6	[0.8, 3.5]	0.81	[0.71, 0.85]
Danube	+0.3	[-1.0, +1.5]	0.6	[0.3, 1.7]	0.75	[0.47, 0.84]
Orange	+2.5	[+1.1, +9.2]	3.1	[1.5, 3.8]	0.52	[0.31, 0.73]
Ob	-0.1	[-1.0, +0.3]	0.8	[0.5, 1.6]	0.76	[0.60, 0.87]
Yenisey	-0.5	[-1.0, -0.2]	0.8	[0.4, 1.6]	0.68	[0.30, 0.90]
Lena	-0.5	[-1.0, -0.2]	1.0	[0.8, 1.7]	0.76	[0.65, 0.83]
Mekong	-0.1	[-0.9, +0.2]	0.5	[0.3, 1.3]	0.91	[0.80, 0.95]
Yangtze**	-0.1	[-0.2, +0.0]	0.3	[0.2, 0.3]	0.95	[0.93, 0.97]
Yellow	+1.9	[+0.2, +2.9]	1.8	[1.3, 3.9]	0.57	[0.51, 0.66]
Murray-Darling	+4.0	[-1.0, +8.8]	3.5	[1.8, 8.3]	0.54	[0.20, 0.80]

b) Daily water temperature (Tw)

river basin	BIAS (°C)		RMSE (°C)		r	
	mean	range	mean	range	mean	range
Columbia*	-2.3	[-3.1, +1.0]	2.8	[2.0, 4.0]	0.88	[0.80, 0.95]
Mississippi	-0.3	[-4.7, +3.8]	3.2	[1.7, 6.7]	0.93	[0.48, 0.98]
Parana	-0.2	[-2.3, +0.9]	2.8	[2.6, 3.0]	0.80	[0.65, 0.88]
Rhine	-0.6	[-1.4, +0.3]	2.3	[1.6, 3.4]	0.94	[0.90, 0.97]
Meuse	+0.7	[+0.3, +1.2]	2.2	[1.6, 3.1]	0.95	[0.92, 0.97]
Danube	-0.3	[-2.3, +1.0]	2.5	[1.7, 3.4]	0.95	[0.93, 0.97]
Orange	-1.5	[-2.8, +0.1]	4.8	[3.6, 5.8]	0.56	[0.39, 0.78]
Ob	-2.4	[-5.8, +0.3]	4.1	[3.6, 6.5]	0.76	[0.46, 0.93]
Yenisey	-0.2	[-0.2, -0.2]	2.8	[2.8, 2.8]	0.95	[0.95, 0.95]
Lena	-1.2	[-1.2, -1.2]	3.2	[3.2, 3.2]	0.87	[0.87, 0.87]
Mekong	+1.5	[+0.6, +2.8]	2.5	[1.9, 3.2]	0.77	[0.65, 0.87]
Yangtze	-0.2	[-0.3, +0.1]	2.8	[2.1, 3.2]	0.94	[0.92, 0.97]
Yellow	+2.7	[+2.0, +3.5]	3.9	[2.6, 5.2]	0.94	[0.89, 0.98]
Murray-Darling	-0.1	[-1.1, +1.0]	3.5	[2.4, 6.4]	0.80	[0.50, 0.98]

* Reservoir scheme and modified geometry - streamflow relations were used for these simulations; ** Monthly river discharge data used for validation of river flow modelling, because daily discharge observations were not available.

3.3.2 Performance of daily water temperature simulations

The spatial patterns of simulated mean annual water temperatures within the study basins averaged over the period 1980-2000 (Figure 3.4) show pronounced increases in water temperature from the upstream to the downstream parts of most river basins (except for the Lena, Ob and Yenisey and Parana River that flow to high latitude). In general, the simulated values of the grid cells correspond closely with the observed mean annual water temperatures for the different stations (circles) along the streams.

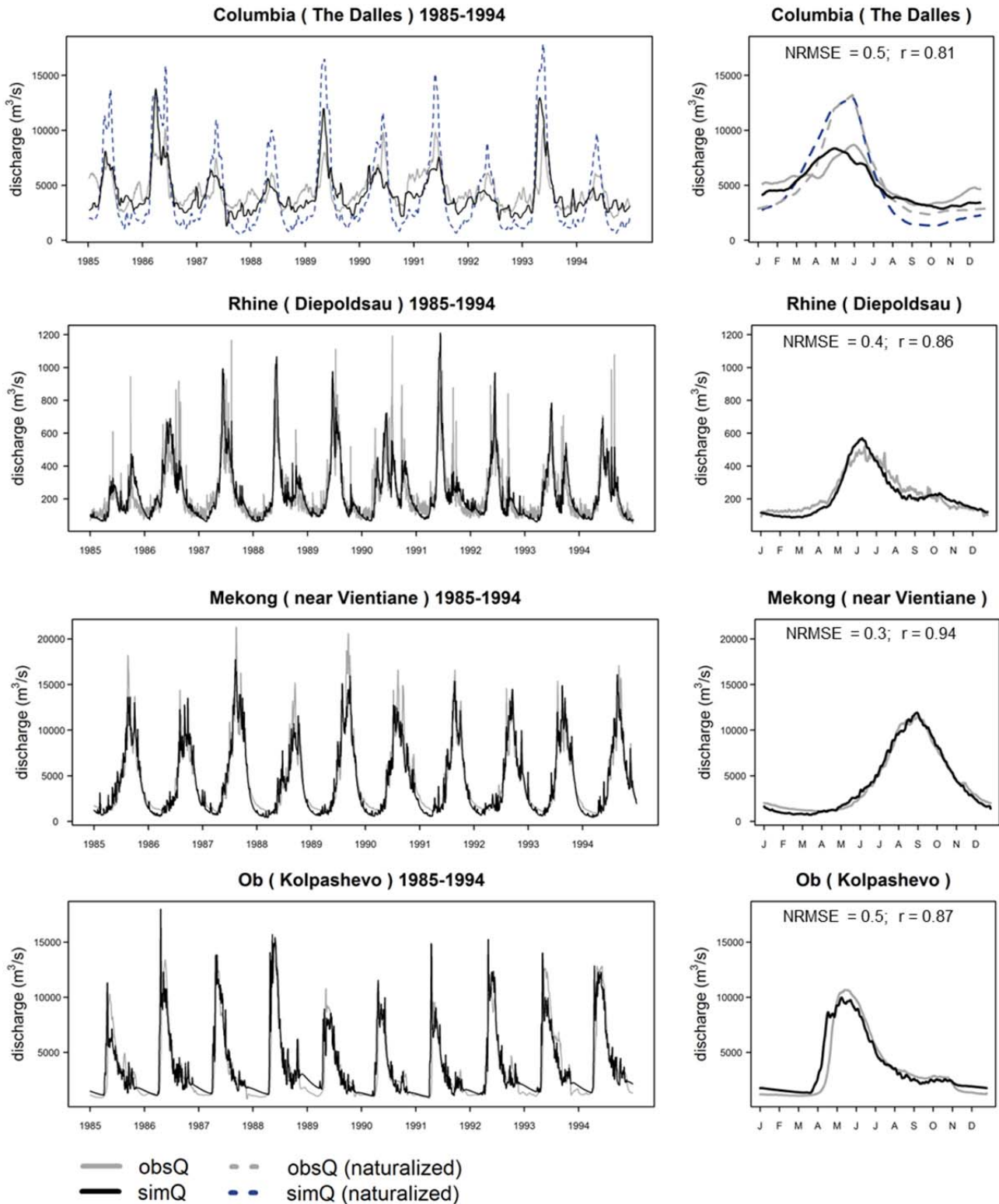


Figure 3.3: Daily time series for 1985-1994 and mean annual cycles of observed and simulated daily river discharge for selected monitoring stations for the period 1971-2000. The stations are situated in river basins with different hydroclimatic zones and anthropogenic impacts and are characterized by an overall good model performance. The normalized root mean squared error (NRMSE) and correlation coefficient (r) are calculated for daily time series for 1971-2000. For the Columbia (The Dalles), 10-day moving average series are presented and used for calculation of the performance coefficients.

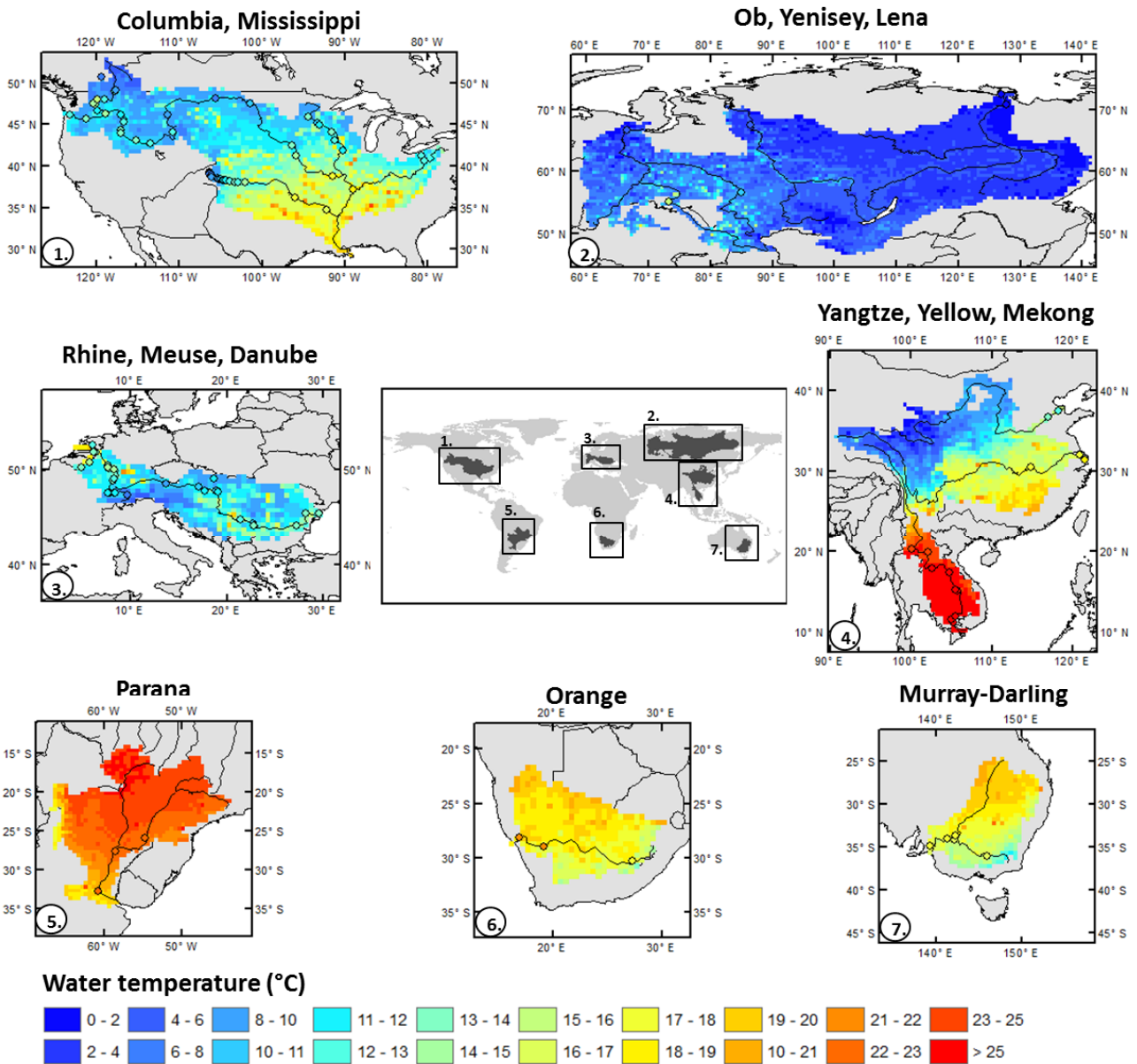


Figure 3.4: Spatial patterns of simulated (grid cells) and observed (circles) mean annual water temperatures for study basins.

For the Columbia River a significant improvement ($p=0.03$) was found by using corrected geometry – streamflow relations (equation 3.2; Section 3.2.2) for the grid cells where reservoirs are located. Without these corrected relationships, the onset of the rising and falling limb in the simulated thermal regime is too early in the season (see Figure 3.5, station Grand Coulee), because the calculated depth and width are underestimated, resulting in an underestimation of the thermal capacity of the stream segment. Furthermore, flow velocity is overestimated, which can result in greater influence of uncertainties in headwater temperature estimates on simulated water temperature. The improvement in model performance was also reflected by lower values of RMSE (mean value of 2.8°C versus 3.5°C) and higher values of r (0.88 versus 0.77) for a model run with corrected relations

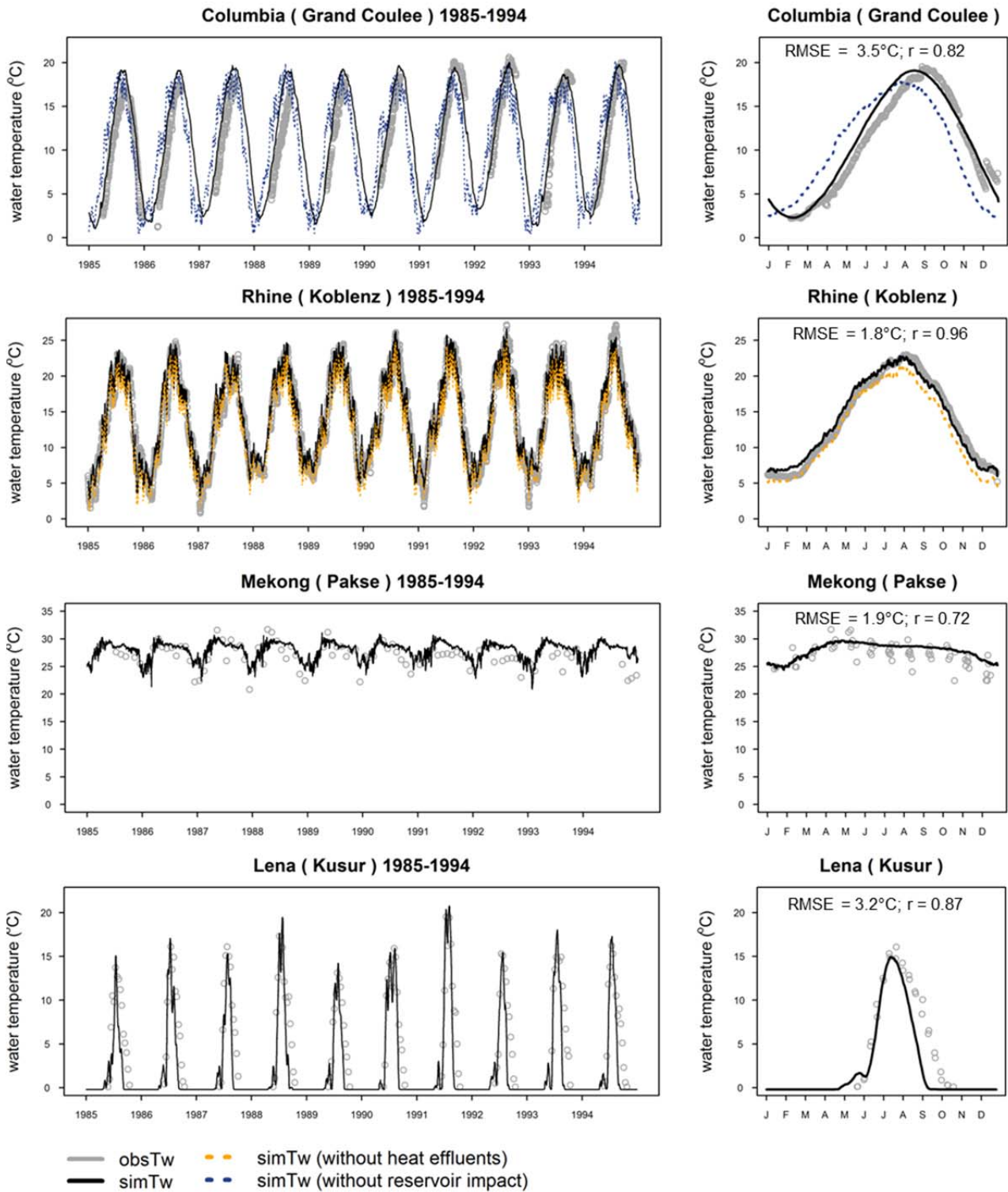


Figure 3.5: Daily time series for 1985-1994 and mean annual cycles of daily observed and simulated river temperature over the period 1980-2000 for selected stations. The stations are situated in river basins with different hydro-climatic zones and anthropogenic impacts and are characterized by an overall good model performance. The root mean squared error (RMSE) and correlation coefficient (r) are calculated for daily time series for 1980-2000. Grey circles in the figures at the right indicate individual measurements, rather than multi-annual averages because of limited availability of observed water temperature data.

(equation 3.2) compared to the run based on uniform geometry – streamflow relations (equation 3.1). The implementation of point sources of heat effluents also resulted in a significant ($p < 0.05$) improvement in model performance for thermally polluted rivers like the Rhine, Meuse, Danube and Mississippi. Without implementation of heat effluents, the simulated water temperatures are underestimated (negative bias) compared to observed water temperature, as these reflect the “naturalized” water temperature (see Figure 3.5, Rhine (Koblenz)). The improvement was reflected by decreases in negative BIAS, lower RMSE and slightly higher values of r for these river basins.

For some of the tropical and arctic basins, like the Mekong and Lena, only a limited number of water temperature measurements was available to test the performance of RBM on a daily time step. However, the simulated water temperature series generally fell between the observations and the variability in water temperature throughout the year was well simulated, as shown for the Mekong (Pakse) (Figure 3.5). This was also found for the other eight water temperature monitoring stations along the Mekong, although slightly overestimations occurred for the most upstream stations (mean BIAS = $+1.5^{\circ}\text{C}$). For the Lena, which is strongly affected by melt water, the annual cycles in water temperature were simulated realistically during the snowmelt period. However, the steepness of the falling limb during August-October was on average too high and the decrease started too early in the season. This might be explained by an underestimation of the discharge peak for the Lena during summer (reflected by negative NBIAS; Table 3.3), and associated underestimation of the thermal capacity. Due to ice and melt water inflow, water temperatures in spring were slightly overestimated for some years, but overall, the timing and magnitude of the rise in water temperature of the Lena during summer were simulated realistically for most of the years during the evaluation period.

The scatterplots and histograms of the simulated versus observed daily water temperature (Figure 3.6) show that simulated water temperature values match the observed values reasonably well for most of the stations. For some stations the correlation coefficients are high ($r > 0.80$; Yellow, Murray-Darling) or very high ($r > 0.90$; Snake (Columbia), Missouri, Arkansas (Mississippi), Rhine, Meuse). For the Mekong and Orange, the correlations were somewhat lower ($r = 0.72$ and $r = 0.78$), although the distributions of daily simulated and observed values correspond closely. In addition, the seasonal signal in water temperature for both rivers is weaker, resulting in a lower signal-to-noise ratio and thus a lower correlation coefficient.

3.3.3 Long-term water temperature 1971-2000 and performance for warm, dry summers

For the evaluation of the simulated water temperature for the Columbia and Rhine basins during the entire 1971-2000 period, we focused on the stations Anatone and Lobith for which long-term daily observed water temperature series were available. Annual mean (\pm one standard deviation), and annual maximum values in simulated and observed water

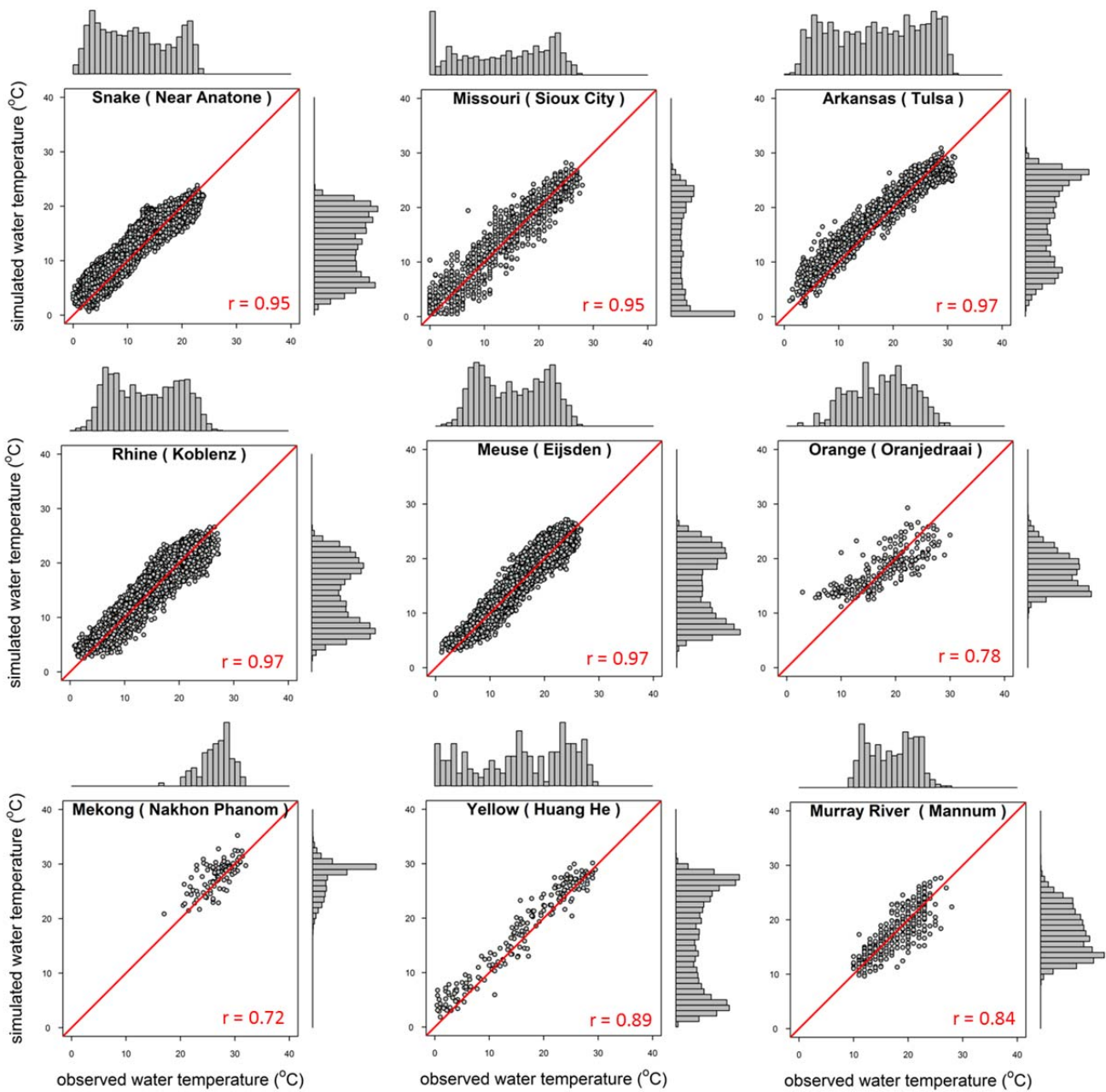


Figure 3.6: Scatter plots and histograms of daily simulated river temperature versus daily observed river temperature for selected stations in the study basins for 1980-2000 period. Histograms on the vertical axis are for simulated values and histograms on horizontal axis for the observed water temperature.

temperature are shown for both stations for the period 1971-2000 (Figure 3.7; left). The annual simulated water temperatures match closely with the observations for the entire period.

The simulated daily water temperature and river discharge during the warm summers of 1998 and 1999 in the Columbia River and summers of 1992 and 1994 in the Rhine River also showed an overall realistic performance of the modelling approach. For the Rhine, the

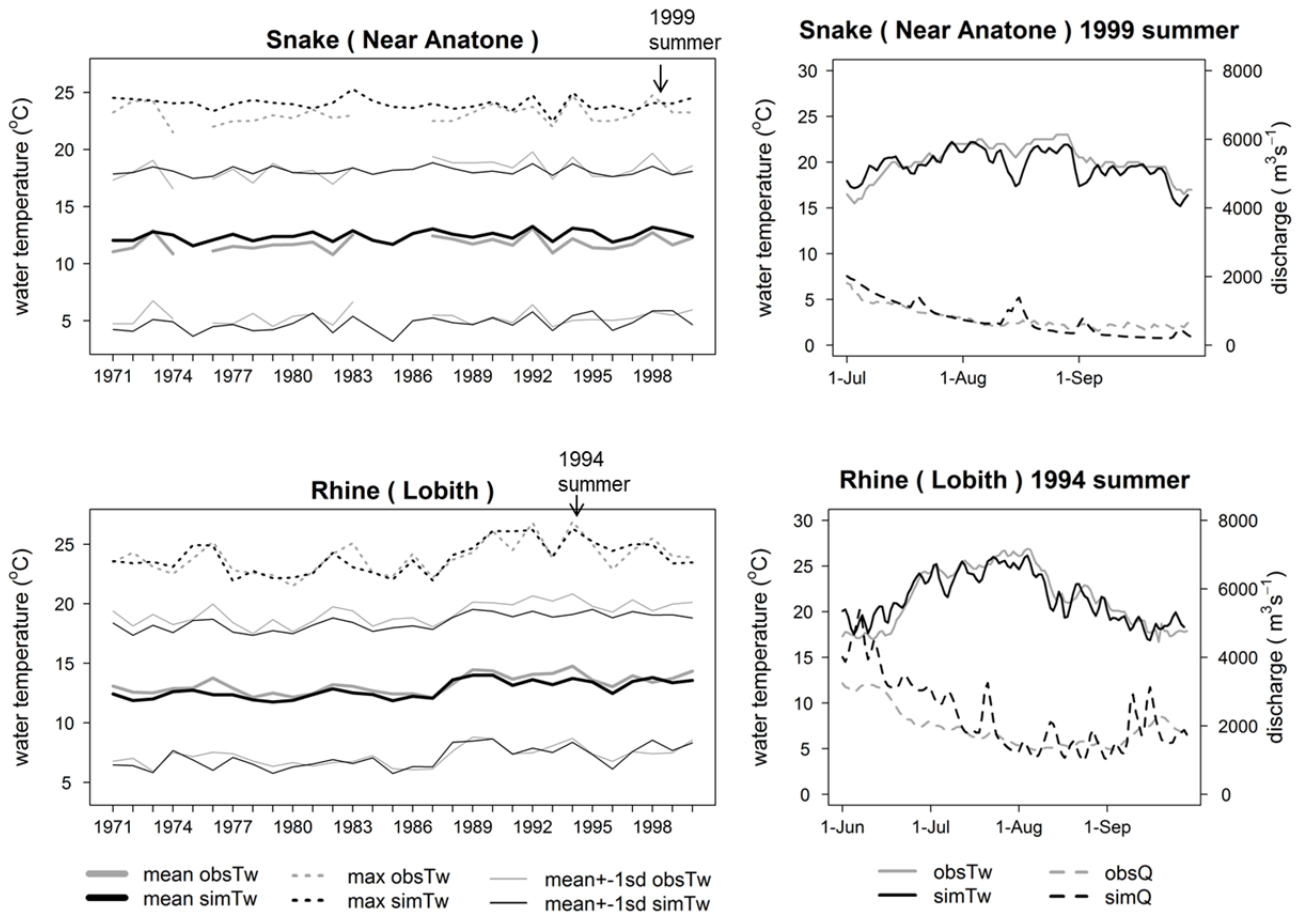


Figure 3.7: Long term mean, and max annual observed and simulated water temperature for 1971-2000. The thin lines indicate the mean \pm one standard deviation for observed and simulated water temperature. Figures at the right show the simulated and observed daily river temperature and discharge during a selected dry, warm summer in the Snake (near Anatone) and Rhine (Lobith). Scales on left and right figures are different.

variability in river discharge and water temperature was slightly overestimated (Figure 3.7; right). In addition, the simulated water temperature values were slightly underestimated for some downstream stations in the Rhine during the period with the highest water temperatures (mean BIAS of -1.2°C). This was also found for some stations in the Columbia and Snake Rivers (overall mean BIAS for all stations of -0.8°C). River discharge was also simulated realistically (mean NBIAS for both summers of $+0.05$ for the Columbia and $+0.18$ for the Rhine), resulting in an overall a realistic performance of the hydrological - water temperature modelling framework for warm summers.

3.3.4 Sensitivity of water temperature to headwater temperature estimates

The impact of a positive bias in headwater temperature of $+2.0^{\circ}\text{C}$ generally shows the largest impact in the upstream parts of the Rhine and Meuse Rivers and declines in the downstream direction more rapidly for the finer resolution simulations ($1/4^{\circ}$) compared to the coarse resolution simulations ($1/2^{\circ}$) (Figure 3.8a-b). In particular for the Meuse, which is the smallest basin, the impact of biases in headwater temperature estimates differs for the $1/2^{\circ}$,

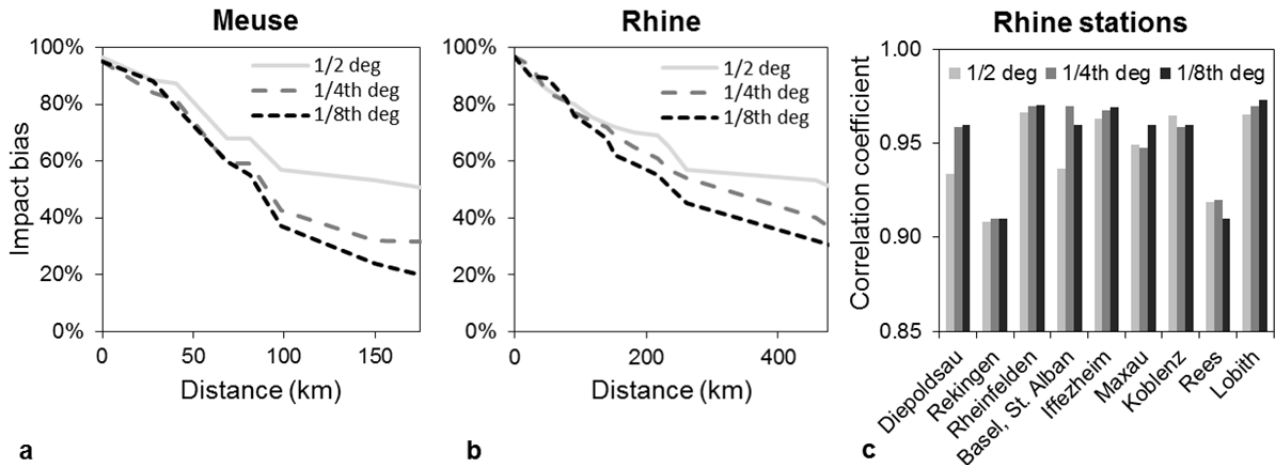


Figure 3.8: Impacts of spatial resolution on propagation of uncertainties in headwater temperature estimates on simulated water temperature along the river course for the Rhine and Meuse, and correlation coefficients between daily simulated and observed water temperature for stations in the Rhine (from upstream station Diepoldsau to most downstream station Lobith) at 1/2°, 1/4° and 1/8° spatial resolution.

1/4° and 1/8° simulations. Assuming a positive bias in headwater temperature of +2.0°C, the impact on simulated water temperature 175 km downstream in the Meuse is on average +1.0°C (51%) for the 1/2° simulations compared to +0.4°C (20%) for the 1/8° simulations. For the Rhine, the impact at 175 km downstream is larger; +1.4°C (71%) and +1.2°C (59%) for the 1/2° and 1/8° resolution simulations, respectively. This is due to the higher flow velocities of the Rhine compared to the Meuse, which results in shorter travel times from headwaters to the downstream site. In addition, higher water depths for the Rhine compared to the Meuse results in slower response rates to atmospheric conditions, and consequently, larger propagation of uncertainties in head water temperatures along a longitudinal section.

Higher resolution simulations also resulted in an overall higher quality of the daily water temperature simulations, although the differences are small. The mean RMSE for the stations in the Rhine decreased from 2.3°C (at 1/2° spatial resolution), to 2.1°C (1/4°) and 2.0°C (1/8°). The correlation coefficients between the observed and simulated daily values were also higher for most stations along the Rhine for the 1/8° compared to 1/2° resolution simulations, although the differences were very small (mean r of 0.944 (at 1/2° spatial resolution), 0.952 (1/4°) and 0.953 (1/8°); Figure 3.8c).

3.3.5 Sensitivity of water temperature to river discharge simulations

Results of the sensitivity analyses showed moderate impacts of changes in river discharge on mean annual water temperature (average value for all basins of +0.2°C for -50% change in river runoff and -0.1°C for +50% change; Figure 3.9). However, pronounced impacts in the low and high water temperature range were found. A decrease in river runoff of 25% and 50% results in significantly ($p < 0.01$; paired t-test) lower minimum water temperatures during winter (average impact of 50% runoff decrease is -0.4°C) and significantly ($p < 0.01$) higher maximum water temperature during summer (average impact of 50% decrease is

+1.2°C). This is mainly due to a smaller thermal capacity, which increases the sensitivity to atmospheric warming and cooling. The impacts of changes in river runoff on minimum water temperatures are very limited for basins at high northern latitude because minimum water temperature values remain around freezing point. An increase in streamflow has an opposite impact on water temperature. An +50% increase in river runoff results in an average impact for all basins of +0.3°C in minimum water temperature and -0.6°C in maximum water temperature, which is also significant ($p < 0.01$). Probability distributions of daily water temperature for the reference case and under a change in river runoff of -50%, -25%, +25% and +50% also show highest impact of changes in streamflow in the low and high water temperature range (Figure 3.10). In particular, decreases in streamflow result in substantial increases in water temperature in the high range. For the Danube station, a decrease in river runoff results in higher (rather than lower) minimum water temperatures, and strong increases in high water temperatures were found. This was also found for several other stations in thermally polluted basins, and this could be explained by a reduced dilution capacity for thermal effluents under decreasing runoff.

3.4 Discussion and conclusions

We used a physically-based modelling framework with the VIC macro-scale hydrological model and process-based water temperature model RBM. The modelling framework was modified to include impacts of reservoirs and heat effluents of thermoelectric power plants and was tested for large river basins in different hydro-climatic zones and with different anthropogenic impacts.

Based on our analysis, we conclude that the coupled hydrological - water temperature modelling framework is suitable to simulate daily river discharge (median normalized BIAS=0.3; normalized RMSE=1.2; $r=0.76$) and water temperatures (median BIAS=-0.3°C; RMSE=2.8°C; $r=0.91$) realistically on daily time step over long (>20 year) periods and on large spatial scales. A similar performance was found during critical periods (warm, dry summers), which indicates that the modelling approach has potential for risk assessments and studying climate change and other anthropogenic impacts on daily river discharge and water temperature in large river basins. In addition, the modelling framework shows possibilities for incorporating other water quality parameters. Yearsley (2012) compared the performance of the VIC-RBM modelling framework applied to the Salmon (subbasin Columbia) with other previous catchment-scale water temperature modelling studies, and concluded that the modelling framework performs as well or better than statistical water temperature models and within the range of site-specific applications of process-based models. Van Beek et al. (2012) simulated water temperature on a global scale (without calibration) with mean absolute errors in daily simulations ranging from 1.6 to 7.6°C, which are comparable or slightly higher than obtained in our study.

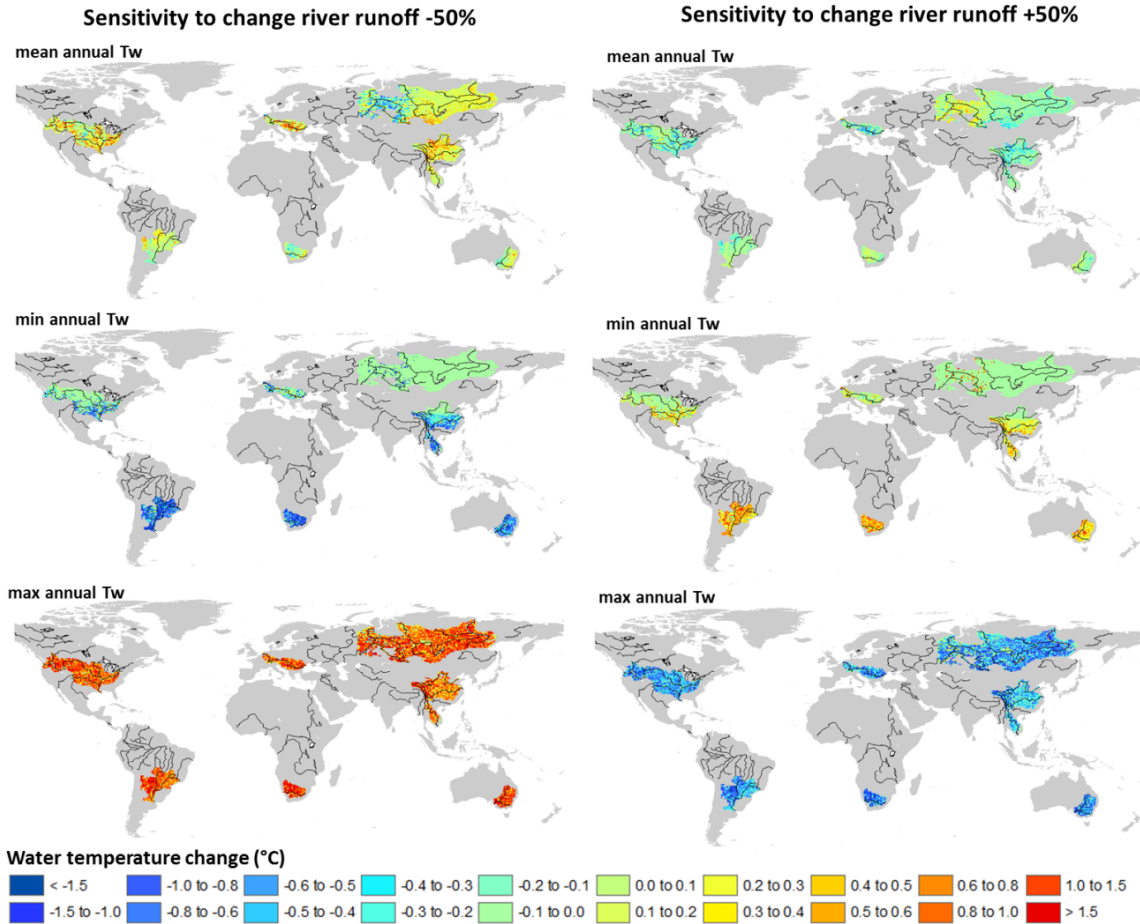


Figure 3.9: Impacts of changes in river runoff of -50% and +50% on mean, minimum and maximum annual water temperature.

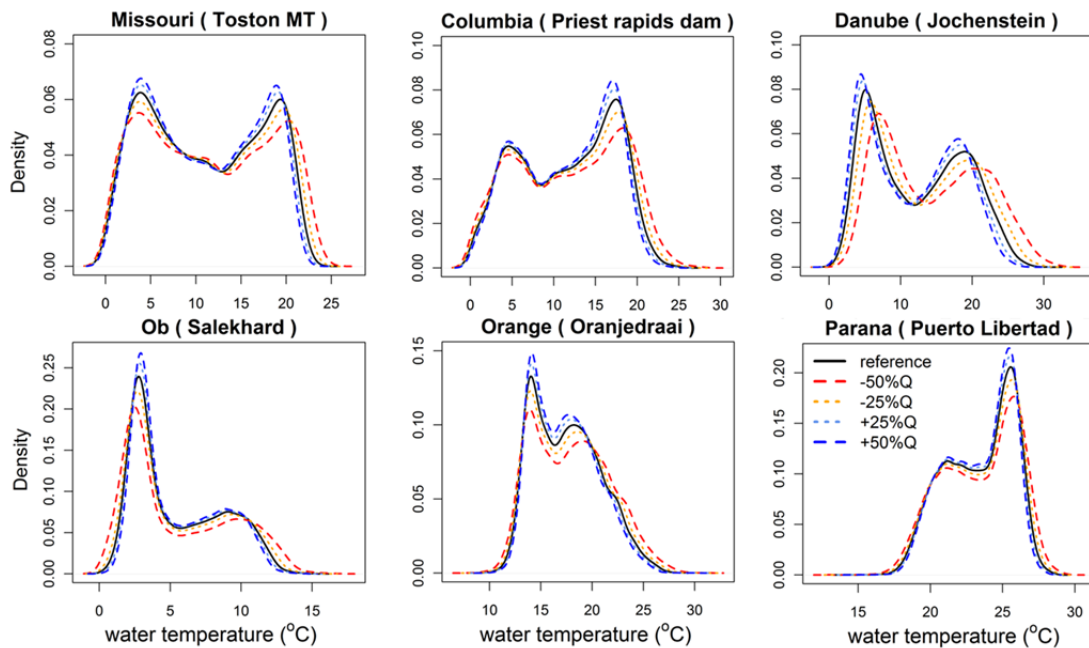


Figure 3.10: Probability distribution functions of daily simulated water temperature for the reference situation 1971-2000 and under a change in river runoff of -50%, -25%, +25% and +50% for selected stations in the study basins.

As the focus of our study is on global river basins, local conditions such as effects of topography, vegetation and groundwater recharge, which can significantly influence river discharge and water temperature in small streams (e.g. Brown, 1969; Cristea and Burges, 2009; Sridhar et al., 2004), were disregarded. Although this contributes to uncertainties in river discharge and water temperature simulations, impacts of processes like groundwater advection, energy exchange between river bed and water interface, dispersion of heat and local conditions (topography and vegetation) in the main river are relatively small at this large scale (Caissie, 2006; Liu et al., 2005).

For river flow, major sources of uncertainties are from meteorological forcing data and the parameterization of the soil and land cover (vegetation) characteristics. Uncertainties in simulated river flow then affect simulated water temperatures, especially during warm, dry conditions. Results of the sensitivity analyses showed significant impacts of river discharge (thermal capacity) on water temperature in the low and, especially high water temperature range (Section 3.3.5; Figure 3.9 and 3.10). These results correspond with previous physically-based and statistical water temperature modelling studies that have found a pronounced impact of river discharge on especially high temperatures (Bartholow, 1991; Sinokrot and Gulliver, 2000; van Vliet et al., 2011).

For water temperature, we also found a relatively high sensitivity of simulated water temperatures to the boundary conditions (headwater temperatures) on a $1/2^\circ$ spatial resolution (Section 3.3.4). This highlights the importance of realistic estimates of headwater temperature for large-scale applications and coarse spatial resolutions. The effects of headwater temperature are larger in the upstream parts of the basins, although the magnitude of impact also increases with higher flow velocity due to the shorter travel time from headwater to the downstream site (Yearsley, 2012). Both the scale and time of travel from the headwaters determine the propagation and impact of incorrect values of the boundary conditions on the simulated water temperatures downstream. Increasing the spatial resolution would probably improve the quality of the water temperature simulations, by decreasing the impact of biases in headwater temperature estimates on the downstream reaches. However, only relatively small improvements in model performance were found for the Rhine and Meuse on $1/4^\circ$ and $1/8^\circ$ compared to $1/2^\circ$ while storage of input and output data and running times drastically increased.

We conclude that the integrated physically-based VIC-RBM modelling framework is suitable to simulate daily river discharge and water temperatures in large basins realistically. The modelling approach has potential for decision support (for example for water quality planning on a large scale) and to perform risk analyses and studying climate change impacts for large river basins and on a continental and global scale.

Acknowledgements

This study was funded by the European Commission through the FP6 Water and Global Change (WATCH) project. The Global Runoff Data Centre, 56068 Koblenz, Germany, and United Nations Global Environment Monitoring System are kindly acknowledged for supplying daily observed river discharge and water temperature data for river stations in the study basins. We would like to thank Jennifer Adam of Washington State University for the global elevation and land cover classification files for the VIC hydrological model. Martina Flörke and Frank Voß of University of Kassel are kindly acknowledged for supplying global datasets of thermoelectric water uses for the 20th century.

Global River Discharge and Water Temperature under Climate Change

Abstract

Climate change will affect hydrologic and thermal regimes of rivers, having a direct impact on freshwater ecosystems and human water use. Here we assess the impact of climate change on global river flows and water temperatures, and identify regions that might become more critical for freshwater ecosystems and water use sectors. We used a global physically-based hydrological and water temperature modelling framework forced with an ensemble of bias-corrected general circulation model (GCM) output for both the SRES A2 and B1 emissions scenario. This resulted in global projections of daily river discharge and water temperature under future climate. Our results show an increase in the seasonality of river discharge (both increase in high flow and decrease in low flow) for about one-third of the global land surface area for 2071-2100 relative to 1971-2000. Consistent increases in mean river flow are projected for the high northern latitudes and parts of the tropical region, and consistent decreases for the United States, southern and central Europe, Southeast Asia and the southern parts of South America, Africa and Australia. Global mean and high (95th percentile) river water temperatures are projected to increase on average by 0.8–1.6 (1.0–2.2)°C for the SRES B1-A2 scenario for 2071-2100 relative to 1971-2000. The largest water temperature increases are projected for the United States, Europe, eastern China and parts of southern Africa and Australia. In these regions, the sensitivities are exacerbated by projected decreases in low flows (resulting in a reduced thermal capacity). A combination of large increases in river temperature and decreases in low flows are projected for the south-eastern United States, Europe, eastern China, southern Africa and southern Australia. These regions could potentially be affected by increased deterioration of water quality and freshwater habitats, and reduced water available for human uses such as thermoelectric power and drinking water production.

This chapter has been published as:

van Vliet, M.T.H., W.H.P. Franssen, J.R. Yearsley, F. Ludwig, I. Haddeland, D.P. Lettenmaier, and P. Kabat (in press), Global river discharge and water temperature under climate change, Global Environmental Change, doi:10.1016/j.gloenvcha.2012.11.002

4.1 Introduction

Hydrologic and thermal regimes of rivers are of major importance for freshwater ecosystems and human water use. Both river discharge and water temperature directly affect water quality (Ducharne, 2008; Haag and Westrich, 2002; Ozaki et al., 2003), and the growth rate and distribution of freshwater organisms (Eaton and Scheller, 1996; Ebersole et al., 2001; Mohseni et al., 2003). In addition, water temperature and availability are economically important, for example for thermoelectric power production (Forster and Lilliestam, 2011; Koch and Vögele, 2009; Manoha et al., 2008), drinking water production (Ramaker et al., 2005; Senhorst and Zwolsman, 2005), fisheries (Bartholow, 1991; FAO, 2008; Ficke et al., 2007) and recreation (EEA, 2008b; Webb et al., 2008).

Due to climate change, hydrological and thermal regimes of rivers are expected to change. This will have direct consequences for freshwater ecosystems, water quality and human water use. Many previous macro-scale hydrological modelling studies have been carried out to assess the impact of climate change on water availability at continental (Arnell, 1999b; Lehner et al., 2006) and global scales (e.g. Arnell, 1999a; Döll and Zhang, 2010; Sperna Weiland et al., 2012; Vörösmarty et al., 2000). However, most of these studies ignore changes in water temperature (or water quality in general) and focus on monthly or annual mean estimates of river discharge, while higher temporal resolution (e.g. daily) estimates are commonly required to address impacts for freshwater ecosystems and water use sectors.

For water temperature, both statistical (e.g. Mantua et al., 2010; Pilgrim et al., 1998) and process-based modelling approaches (e.g. Gooseff et al., 2005; Sinokrot et al., 1995; Stefan and Sinokrot, 1993) have been applied to project the effects of future climate on catchment scale river temperatures. Less work has been done on modelling climate change impact on river temperatures at larger scales, although some regression studies have addressed the sensitivity of water temperatures to air temperature increases in the United States (Mohseni et al., 1999) and the combined impacts of river flow changes on river temperatures at the global scale (van Vliet et al., 2011).

Although river temperatures are generally most sensitive to atmospheric conditions, changes in streamflow also significantly affect water temperatures, especially during warm, dry periods with low river flows (Sinokrot and Gulliver, 2000; van Vliet et al., 2011). Combined effects of atmospheric warming and changes in river flow should therefore be considered in modelling future climate change impacts on river water temperature.

Here we assess the impact of climate change on daily river discharge and water temperature on a global scale, by using a physically-based hydrological and water temperature modelling framework forced with an ensemble of daily bias-corrected general circulation model (GCM) output. The daily projections were used to assess the magnitude and significance of changes in mean and extremes in river flow and water temperature on both global and river basin scales. We then used the global river discharge and water temperature projections to identify regions characterized by substantial decreases in low flow in combination with large

increases in water temperature, because these regions could potentially experience increased deterioration of freshwater habitats and reduced potential for human water use.

The global hydrological - water temperature modelling framework consists of the Variable Infiltration Capacity (VIC) macro-scale hydrological model (Liang et al., 1994) and stream temperature River Basin Model (RBM) (Yearsley, 2009). The modelling framework includes anthropogenic impacts of thermal discharges from thermoelectric power plants on water temperatures, and the modelling performance has been evaluated for 14 large river basins globally, situated in different hydro-climatic zones and with different anthropogenic impacts (van Vliet et al., 2012a). Overall, a realistic representation of daily river discharge and water temperature was found for the historical period 1971-2000, with a similar performance during warm, dry summer periods.

In this study, future projections of daily river discharge and water temperature under climate change were produced on a global scale by forcing the global hydrological - water temperature modelling framework (Section 4.2.1) with statistically bias-corrected GCM output for both the SRES A2 and B1 scenario for 2071-2100 and for 1971-2000 (Section 4.2.2). These global projections were used to quantify changes in river discharge (Section 4.3.2) and water temperature (Section 4.3.3) and to identify regions characterized by a strong increase in river water temperature and decreases in river discharge (water availability) (Section 4.3.4).

4.2 Material and methods

The methodological framework for this study is shown in Figure 4.1. Bias-corrected output from three GCMs for both the SRES A2 (red) and B1 (orange) global emissions scenarios (Nakicenovic, 2000) for 2071-2100 and for 1971-2000 (control; blue) were used to force the global hydrological and water temperature modelling framework. The resulting daily simulations of global river flow and water temperature were used in three control experiments and six future GCM experiments. The background of the hydrological - water temperature modelling framework, climate scenarios and bias-correction are described in Sections 4.2.1 and 4.2.2.

4.2.1 Hydrological - water temperature modelling framework

The hydrological - water temperature modelling framework consists of the physically-based Variable Infiltration Capacity (VIC) model (Liang et al., 1994) and the one-dimensional stream temperature model RBM (Yearsley, 2009; Yearsley, 2012). VIC is a grid-based water - energy balance model and is used with an offline routing model (Lohmann et al., 1998) to simulate daily streamflow. The VIC hydrological model was applied using the elevation and land cover classification as described in Nijssen et al. (2001b) and using the DDM30 routing network (Döll and Lehner, 2002) for lateral routing of streamflow.

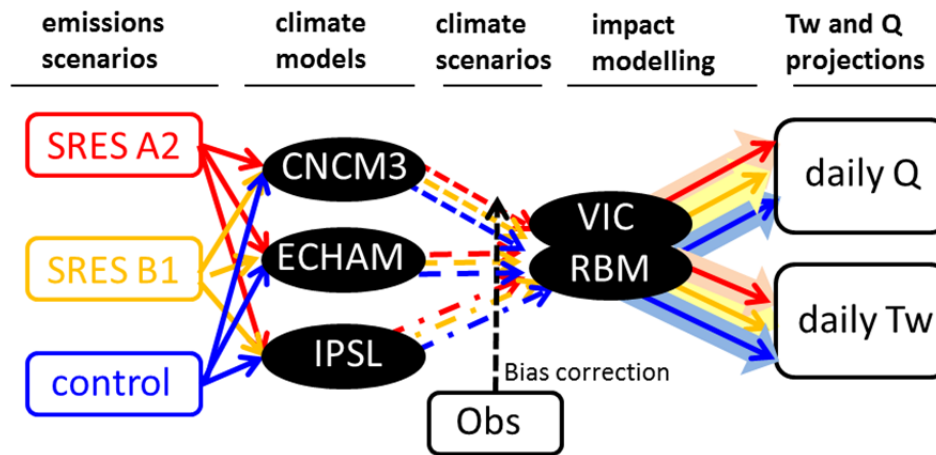


Figure 4.1: Schematic representation of the modelling framework with selected emission scenarios and GCMs, and bias-correction of GCM output with observed meteorological dataset (Obs). These data were used to force the physically-based hydrological - water temperature (VIC-RBM) modelling framework, resulting in daily simulations of river flow (Q) and water temperature (Tw) under control (reference) and future climate.

RBM is a process-based computationally-efficient water temperature model that solves the 1D-heat advection equation using the semi-Lagrangian approach (Yearsley, 2009). Daily river water temperature is simulated using climate forcings (air temperature, shortwave and long wave radiation, vapor pressure, density, pressure and wind speed) disaggregated to a 3-hourly time step and daily channel flows, width, depth and flow velocity from VIC and the routing model (see Yearsley (2012) and van Vliet et al. (2012a) for a description of the linkages between the components in the modelling framework).

The VIC-RBM modelling framework has been implemented on a global scale on a $0.5^\circ \times 0.5^\circ$ spatial resolution (van Vliet et al., 2012a). The model system runs on a daily time step. Impacts of anthropogenic heat effluents from thermoelectric power plants on water temperature were incorporated by using global gridded thermoelectric water use datasets (Flörke et al., 2011; Vassolo and Döll, 2005; Voß and Flörke, 2010) and representing thermal discharges as point sources in the heat-advection equation (see van Vliet et al. (2012b) for details). The headwater temperatures were estimated using the nonlinear water temperature regression model of Mohseni et al. (1998) for 333 GEMS/Water stations for 1980-2000. The estimated parameters were then interpolated to $0.5^\circ \times 0.5^\circ$ global grids using ordinary kriging. For the headwater grid cells in RBM, water temperatures were estimated based on daily air temperature and the parameter values for these headwater grid cells (van Vliet et al., 2012b).

4.2.2 Climate change scenarios

Daily output of the three coupled atmosphere/ocean general circulation models (GCMs) ECHAM5/MPIOM (Jungclaus et al., 2006; Roeckner and Coauthors, 2003), CNRM-CM3 (Déqué et al., 1994; Madec et al., 1998; Salas-Méla, 2002) and IPSL-CM4 (Fichefet and Morales Maqueda, 1997; Goosse and Fichefet, 1999; Hourdin et al., 2006) for both the SRES A2 and B1

emissions scenario (Nakicenovic, 2000) from the CMIP3 archive were used to force the global hydrological - water temperature modelling framework. These three GCMs, denoted as ECHAM, CNRM3 and IPSL henceforth, were selected mainly because of the availability of archived output on a daily time step (Hagemann et al., 2011). For an evaluation of these GCMs and projected changes in climate in relation to the other GCMs for which model output was archived for CMIP3 we refer to Randall et al. (2007) and Meehl et al. (2007). We used climate data for both the SRES A2 and B1 emissions scenario (Nakicenovic, 2000). The two SRES scenarios represent contrasting storylines and emissions scenarios, which results in the largest range from the four IPCC SRES main emissions scenarios.

Because of significant systematic biases in the ability of GCMs for simulations of observed climate (Randall et al., 2007) a bias correction on GCM output is needed to produce suitable forcings for use in hydrological models. Several previous studies that assessed the impact of climate change on global hydrology (e.g. Alcamo et al., 2007; Arnell, 2004; Nijssen et al., 2001a) used the 'change factor' ('delta-change') approach (Diaz-Nieto and Wilby, 2005). In this approach, differences between control and future climate model simulations are applied to baseline climate observations by simply adding or scaling the mean change factors for each day to produce forcings for hydrology models (Fowler et al., 2007b). Among the limitations of this approach are the assumption of a constant bias through time, which ignores possible changes in variability, and the assumption that spatial patterns of climate will remain constant (Diaz-Nieto and Wilby, 2005). In addition, for precipitation the temporal sequence of wet days remains unchanged, which ignores changes in dry and wet periods expected under climate change (Fowler et al., 2007b). To obtain more reliable estimates of changes in hydrological variability and extremes, more sophisticated statistical bias correction methods have been developed (e.g. Ines and Hansen, 2006; Li et al., 2010; Piani et al., 2010), as well as dynamical approaches which use regional climate models with boundary conditions provided by a GCM (e.g. Jacob et al., 2007) and combination of dynamical and statistical approaches (e.g. Wood et al., 2004).

Within the FP6 Water and Global Change (WATCH) project, a statistical bias correction procedure was performed on daily precipitation, mean, minimum and maximum surface air temperature for the GCM experiments described above (Hagemann et al., 2011). The method is based on transfer functions that describe the relationship between the daily modelled (corrected) and daily observed time series. These transfer functions are fitted at grid cell level and are used to adjust the probability distribution function of intensity for these simulated variables (Piani et al., 2010). Note that this method does not correct directly for some changes in timing of precipitation (e.g. in the onset of the monsoon (Hagemann et al., 2011)). Other shortcomings are that the assumed bias for the future period is similar to the bias in the control (historical) period to which the transfer functions are fitted, and the quality of the bias correction highly depends on the quality of observations used as the reference. Nonetheless, the application of this bias correction method has shown that it effectively improves both the mean and variance of the daily precipitation and temperature fields for the control period, and can also correct higher moments of the precipitation distribution (Hagemann et al., 2011;

Piani et al., 2010). The global gridded $0.5^\circ \times 0.5^\circ$ WATCH forcing dataset (WFD) (Weedon et al., 2011) was used as the reference (observed) data for the statistical bias correction. The bias correction transfer function for each grid cell was derived for the 1960-1999 period and was subsequently applied to 1960-2100 under an assumption that the biases in GCM output for the future period are similar as for the control period. Before the actual bias correction of precipitation and surface air temperature, a statistical downscaling was conducted on all forcing variables to produce fields at $0.5^\circ \times 0.5^\circ$ spatial resolution (for details see Hagemann et al. (2011)).

The VIC-RBM hydrological - water temperature modelling framework was forced with daily bias-corrected precipitation, daily minimum and maximum temperature and with (uncorrected) wind speed to produce projections of daily river flow and water temperature for the 21st century. As vapor pressure, incoming shortwave and net longwave radiation are not supplied directly to VIC, these forcing variables are calculated internally based on bias-corrected daily minimum and maximum temperature and daily precipitation, using the algorithms of Kimball et al. (1997) and Thornton and Running (1999) (for details see Nijssen et al. (2001b)). For the analyses we focussed on the control period 1971-2000 and future period 2071-2100.

4.3 Results

4.3.1 Evaluation of control simulations of river discharge and water temperature

To address impacts of uncertainties from the (bias-corrected) GCM output on daily river flow and water temperature, we compared the simulated results for the control runs of the three GCMs with those based on the historical WATCH forcing data for the period 1971-2000. In addition, the simulated river discharge and water temperature were also compared with observed values to evaluate the overall performance of the VIC-RBM modelling framework. For both river discharge and water temperature, boxplots are shown in Figure 4.2 which summarize the distribution in the observed mean values (OBS) and simulated mean values based on the WATCH forcing data (WFD) along with the control runs of the three GCMs (CNRM3, ECHAM, IPSL) for river stations grouped per Köppen climate zone (tropical (A), dry (arid and semiarid; B), temperate (C), continental (D) and polar (E)) (Köppen, 1923). For river discharge, we used daily observed series of 1612 stations (see Figure 4.2a) provided by the Global Runoff Data Centre (GRDC) for the period 1971-2000. For water temperature, we used daily records of 347 river stations (see Figure 4.2b) of the United Nations Environment Programme (GEMS/Water) for 1980-2000 and compared with simulated daily mean water temperatures for the same period. The Supplementary Figures A1-A3 provide more details about the performance of the VIC-RBM hydrological and water temperature modelling framework using different performance coefficients.

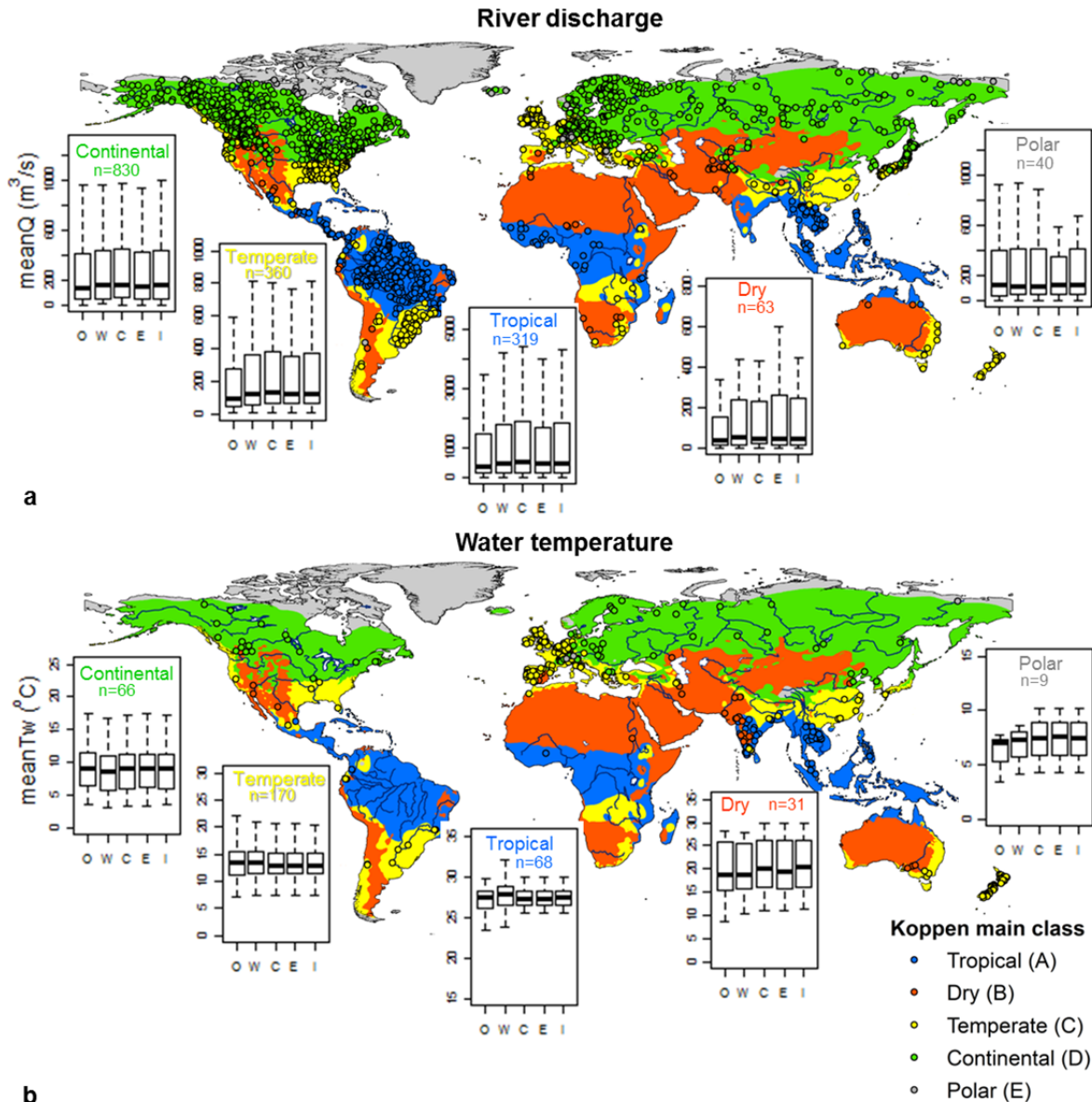


Figure 4.2: Location of selected GRDC river discharge stations (a) and GEMS water temperature stations (b) and boxplots of mean observed (O) and mean simulated values using WATCH forcing data (W) and three control simulations of the CNM3 (C), ECHAM (E) and IPSL (I) GCMs for river discharge (1971-2000) (a) and for water temperature (1980-2000) (b) per main Köppen climate class.

Boxplots for simulated mean river discharge values (Figure 4.2a) based on WFD correspond well with the boxplots of the observed mean discharge values, although the median, upper quartile and upper range (1.5* interquartile range) of simulated means for river stations in the tropical, dry and temperate climate zone are slightly overestimated compared to the observations. This corresponds with the overall positive normalized bias that we found for the discharge stations in these three climate zones (see Supplementary Figure A3a). The overall overestimation in river discharge in dry and tropical basins was also found for several other global hydrological models and land surface schemes which were run using the same forcing data (WFD) as part of the EU FP6 WATCH global modelling framework. This overestimation is partly due to the neglect of water extractions and complicated wetland

dynamics (Haddeland, 2011). The boxplots of simulated river discharge for the three control simulations (CNCM3, ECHAM, IPSL) correspond closely with the boxplots for WFD (Figure 4.2a), which indicates that no distinct impacts of biases (uncertainties) in GCM output on the control river flow simulations were found.

An overall close correspondence between boxplots of observed (OBS) and simulated water temperature (WFD) was found (Figure 4.2b), although simulated mean water temperatures in the tropical region were slightly overestimated probably due to neglect of vegetation shading effects. Slightly lower model performance for stations in the high latitude region (Supplementary Figure A2-A3) is probably due to the neglect of impacts of complex snowmelt processes on the water temperature simulations. Boxplots of mean water temperature for the control simulations of CNCM3, ECHAM and IPSL also match closely with those for WFD. While discharge simulations are used as input into the water temperature model, we found an overall greater persistence of the system under uncertainties in input (robustness) for the water temperature predictions compared to the discharge predictions. This is mainly because water temperature is more strongly impacted by radiation and air temperature than by precipitation. Water temperature is therefore less sensitive to uncertainties in precipitation, while these uncertainties potentially have a large impact on simulated river discharge (Biemans et al., 2009; Fekete et al., 2004; Voisin et al., 2008).

4.3.2 Global changes in river discharge under future climate

Based on the daily river discharge projections for all GCM experiments, we calculated spatial patterns of ensemble mean changes in daily river discharge for the period 2071-2100 for both the SRES A2 and B1 emissions scenarios relative to the ensemble mean control simulations for 1971-2000. Our results show an increase in mean annual river discharge in the high northern latitudes and large parts of the tropical (monsoon) region. A decrease in river discharge on a mean annual basis is projected for the mid-northern latitudes (U.S., Central America, southern and central Europe, and Southeast Asia) and the southern latitudes (southern parts of South America, Africa and Australia) (Figure 4.3a). Projected changes in river discharge are generally larger for GCM experiments based on the SRES A2 (medium-high) compared to B1 (low), because of the larger changes in projected precipitation and meteorological forcing variables affecting evaporation. The Supplementary Figures A4 and A5 present global patterns with mean annual changes of meteorological forcing and water balance components simulated with VIC for both SRES A2 and B1 for the period 2071-2100 relative to 1971-2000. Overall, the spatial patterns of projected changes in mean river discharge (Figure 4.3a) and total runoff (Supplementary Figure A5) correspond closely with projected changes in mean precipitation (Supplementary Figure A5).

Although projected changes in river discharge are larger for the SRES A2 than for B1 and differences exist between the three GCM projections (see Supplementary Figure A6), the signal of changes in mean river discharge among the six GCM experiments is consistent for about 60% of the grid cells globally (see regions with black dots in Figure 4.3). In addition, we

found a high signal-to-noise ratio (SNR), defined as the ratio of mean change in river discharge to standard deviation of change in river discharge for the three GCMs. On a global average basis the SNR is 10-11 for the SRES B1-A2.

In addition to changes in mean river flow, we focussed on spatial patterns of changes in high and low flows (Figure 4.3b-c). For high flows, we calculated changes in the 95th percentile of the daily distribution (Q_{95}) rather than the maximum annual discharge, because the 95th percentile is less sensitive to outliers in the simulated daily discharge series. For low flows, we used the 10th percentile of the daily distribution (Q_{10}) which is a widely used low flow index (Pyrce, 2004; Smakhtin, 2001; Tharme, 2003). Overall, high flows are also projected to increase for a large part of the global land surface area, with similar patterns as for changes in mean flow (Figure 4.3a-b). In contrast, low flows are projected to decrease, especially in the southern U.S., Central America, Europe (except northern part), Southeast Asia, Australia and southern parts of South America and Africa (Figure 4.3c). For about 24% of the global land surface area there were consistent decreases in low flow projected for all GCM experiments. A distinctly higher signal-to-noise ratio (SNR) in low flows was found for the A2 compared to the B1 scenario (global average SNR of 39 compared to 10, respectively).

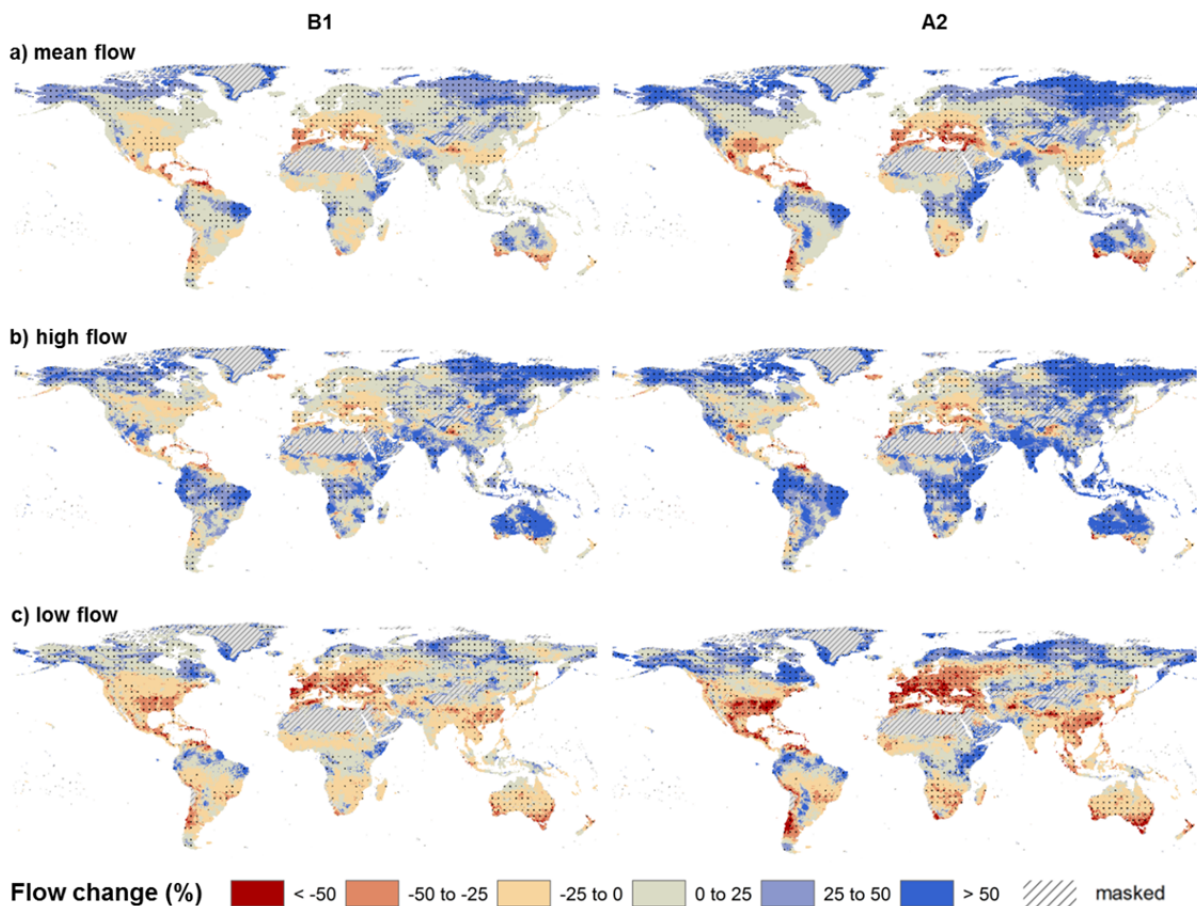


Figure 4.3: Global projected changes in mean flow (a), high flow (Q_{95}) (b) and low flow (Q_{10}) (c) for 2071-2100 relative to 1971-2000 averaged for the three selected GCMs for both the SRES A2 and B1 emissions scenario. Black dots indicate regions with consistent signal of change between the three GCMs. Regions with mean flow less than $1 \text{ m}^3 \text{ s}^{-1}$ are masked.

Considering the changes in daily river discharge, we found an increase in river discharge seasonality, which we defined as increasingly higher 95th percentile flows and decreasingly lower 10th percentile flows, with values ranging between 58% and 64% of the global land surface area for the different GCM experiments. Using the ensemble mean discharge changes, an increase in discharge seasonality is projected for 27-30% of the global land surface area for SRES B1-A2. Increases in discharge seasonality were found for different hydro-climatic regions, but overall highest increases were found for the temperate zone and continental climate zone (Figure 4.4).

Mean annual cycles of projected changes in river flow (Figure 4.5) also show an increase in discharge seasonality for 2071-2100 relative to 1971-2000. Examples are shown for the Mekong, Rhone and Ob Rivers, which are situated in different hydro-climatic zones. In addition, the mean annual cycles show an earlier start of the snowmelt peak in spring for the snowmelt dominated Ob River, and transient (mixture of snowmelt- and rain-fed) Rhone River. A decrease in snowmelt peak and transition to a more rain-fed dominated discharge regime is also shown for the Rhone. Projected changes in mean, low (Q_{10}) and high (Q_{95}) river flows for 24 large river basins (Table 4.1) show the highest increase in river discharge seasonality for the Mekong (mean change in Q_{10} : -22% vs. Q_{95} : +7%), Yangtze (-18% vs. +5%), Ganges-Brahmaputra (-13% vs. +5%) and Columbia (-8% vs. +20%) river basins. For several basins in Europe, we found strong and significant (paired t-test; $p < 0.01$) decreases in low flow (Q_{10}) (e.g. Loire -53%, Rhone -46%, Danube -43%, Rhine -37%) and overall decreases in mean annual river flow. In contrast, significant increases in mean and high flow (Q_{95}) were found for the Arctic basins due to large increases in precipitation and snowmelt at high northern latitude. Significant increases in Q_{mean} and Q_{95} were also found for several tropical basins (Amazon, Congo, Indus) because of projected strong increases in monsoon rainfall.

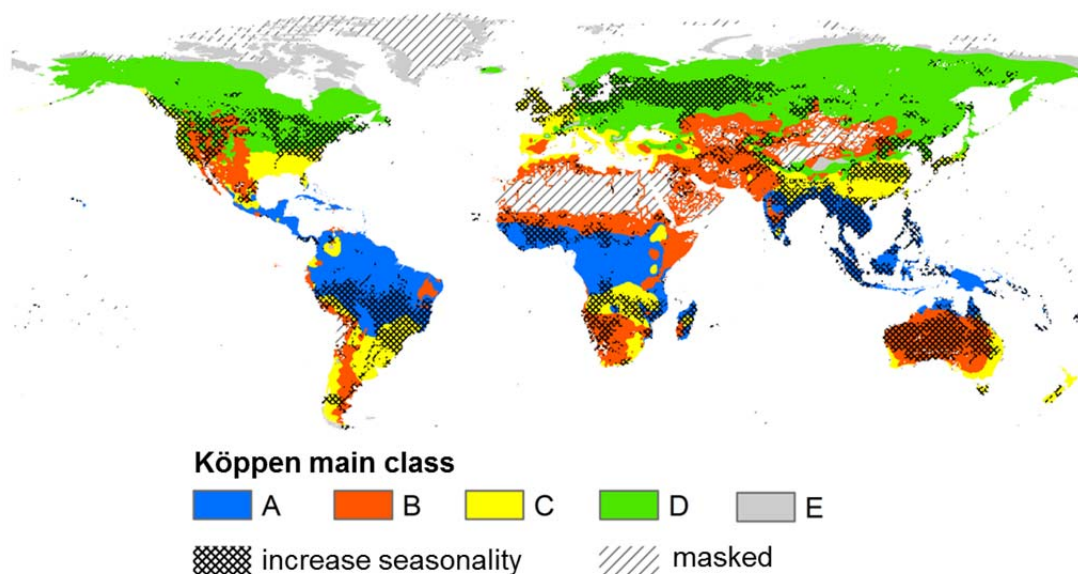


Figure 4.4: Global projections of areas with increase in river discharge seasonality (defined as both increasing high flows (95th percentile, Q_{95}) and decreasing low flows (10th percentile, Q_{10}) for 2071-2100 relative to 1971-2000 (consistent for SRES A2 and B1) plotted on the Köppen main climate zones (tropical (A), dry (B), temperate (C), continental (D) and polar (E)). Regions with mean flow less than $1 \text{ m}^3 \text{ s}^{-1}$ are masked.

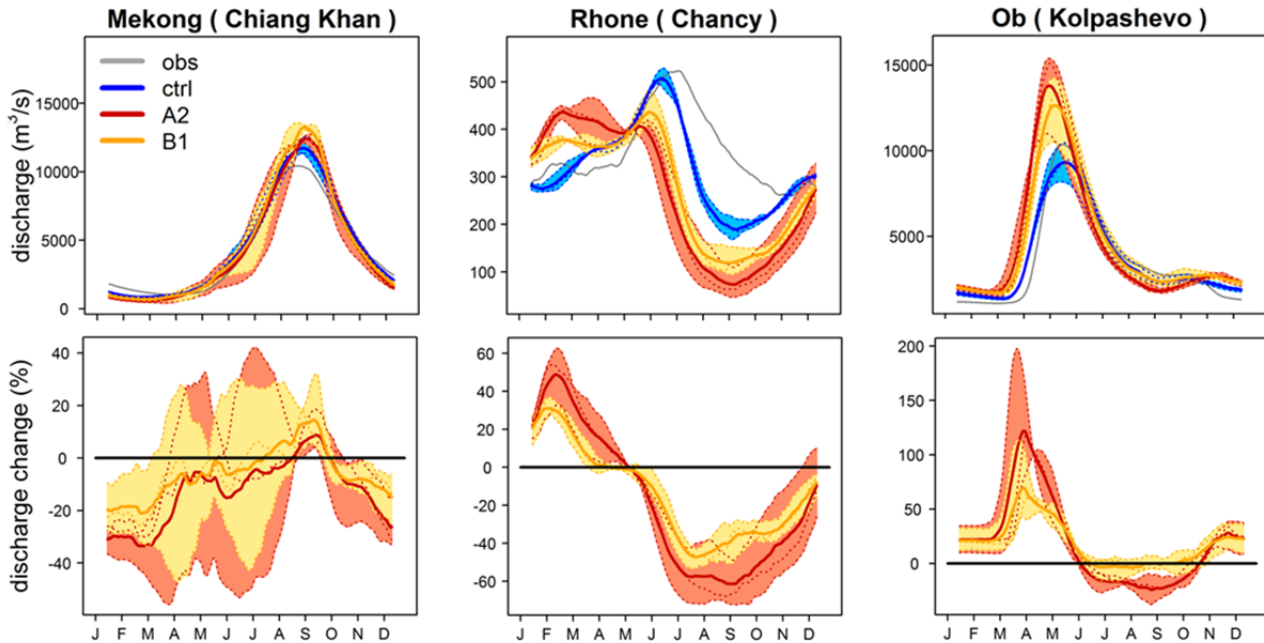


Figure 4.5: Mean annual cycles of projected changes in 30-day moving average of river discharge for GRDC stations in different hydro-climatic zones for 2071-2100 relative to 1971-2000. Observed (obs; grey) and control simulations of river discharge (ctrl; blue) are for 1971-2000 and future simulations for the SRES A2 (red) and B1 (orange) emissions scenarios are for 2071-2100. Dotted lines show the results for the three GCMs individually, coloured polygons show the range in results across the GCMs, and the thick line shows the overall GCM mean results for the control run and for the SRES A2 and B1 scenario.

4.3.3 Global changes in river temperature under future climate

Similar to river flow, global patterns of changes in projected mean water temperature for the period 2071-2100 relative to 1971-2000 were calculated (Figure 4.6). Overall, the patterns of projected change in mean annual water temperature between the different GCMs are consistent, but the magnitude of water temperature increases are higher for CNRM3 (global mean increase of 0.9-1.8°C for SRES B1-A2) and IPSL (1.1-1.9°C) than for ECHAM (0.4-1.0°C). Regions for which largest increases in mean water temperature are projected are the U.S., Europe, eastern China and parts of southern Africa and Australia (all of which have mean increases larger than 2°C). The basin average increases in mean water temperature based on all six GCM experiments are 2.4°C for the Mississippi, 1.9°C for the Colorado, 2.1°C for the Danube, 1.9°C for the Rhine, and 2.1°C for the Rhone (see Table 4.1). For these basins large increases were found in high water temperatures (95th percentile in daily distribution; T_{w95}) of 2.6-2.8°C. Overall, the regions for which strongest increases in water temperature are projected also experience the greatest declines in low flow (Figures 4.3c and 4.6). While the largest relative increases in incoming longwave radiation and air temperature are found for the high northern latitude regions (Supplementary Figure A4), simulated mean water temperature increases are generally low on a mean annual basis for the northern river basins (e.g. Lena 1.1°C, Ob 0.9°C and Mackenzie 1.1°C; Table 4.1). This is mainly because rivers are still frozen during a large part of the winter period (simulated water temperatures values

Table 4.1: Projected changes in mean flow (Q_{mean}), low flow (10th percentile; Q_{10}) and high flow (95th percentile; Q_{95}) and changes in mean ($T_{w_{\text{mean}}}$) and high (95th percentile; $T_{w_{95}}$) water temperatures for 2071-2100 relative to 1971-2000. Changes are averages for all grid cells in the river basin and are averaged for all six GCM experiments (A2 and B1 experiments are combined). Significance of change was tested using paired t-tests for the gridcells in each basin. Changes at 99% significance level are bold. Values between brackets indicate changes in mean summer (JJA) water temperatures for rivers which are frozen during a large part of the year.

river basin	dQ_{mean} [%]	dQ_{10} [%]	dQ_{95} [%]	$dT_{w_{\text{mean}}}$ [°C]	$dT_{w_{95}}$ [°C]
North America					
Mackenzie	+22	+24	+20	+1.1 (+1.4)	+2.2
Mississippi	-6	-20	-3	+2.4	+2.7
Columbia	+25	-8	+20	+1.6	+1.9
Colorado	-1	-15	+2	+1.9	+2.6
Rio Grande	-13	-27	-15	+1.6	+1.4
South America					
Amazon	+21	+12	+23	+0.5	+0.7
Parana	+12	-2	+16	+1.0	+1.2
Europe					
Danube	-20	-43	-14	+2.1	+2.7
Rhine	-8	-37	+1	+1.9	+2.8
Loire	-23	-53	-7	+1.6	+1.8
Rhone	-11	-46	+1	+2.1	+2.8
Africa					
Congo	+20	+12	+24	+1.4	+1.2
Zambezi	+1	-10	+4	+1.5	+1.3
Niger	+9	-1	+11	+1.3	+1.7
Orange	+8	+1	+11	+1.3	+1.0
Asia					
Ganges-Brahmaputra	+4	-13	+5	+1.2	+1.5
Indus	+65	+30	+78	+1.3	+0.8
Mekong	+3	-22	+7	+0.9	+0.9
Yangtze	-1	-18	+5	+1.8	+1.8
Yellow	+22	+10	+28	+1.8	+2.3
Asia (Arctic)					
Lena	+48	+31	+55	+1.1 (+2.1)	+2.3
Ob	+17	+5	+21	+0.9 (+1.3)	+1.2
Amur	+23	+10	+27	+1.5 (+2.0)	+2.2
Oceania					
Murray-Darling	-10	-25	-8	+1.3	+1.3

remain around freezing point). In addition, large increases in mean river discharge are projected (Table 4.1) which increases the thermal capacity of these arctic rivers and reduces the sensitivity of river temperatures to atmospheric warming. Increases in water temperature in summer (JJA) are higher than in the annual mean values for the northern basins, and increases in T_{w95} are more than twice as large as increases in mean water temperature (Table 4.1). Overall moderate increases in mean and high water temperatures (T_{w95}) are projected for river basins in the central parts of South America and Asia with mean water temperature increases between 0.5°C (Amazon) and 1.3°C (Indus) (Table 4.1). A possible reason for these moderate water temperature increases is the dominant impact of increased evaporative cooling (latent heat flux) and back radiation (blackbody radiation from the water surface) under warmer conditions in these tropical basins, in combination with strong increases in projected mean annual river flow (thermal capacity) for most tropical basins (Table 4.1). These processes reduce the magnitude of water temperature rises under increased atmospheric energy input.

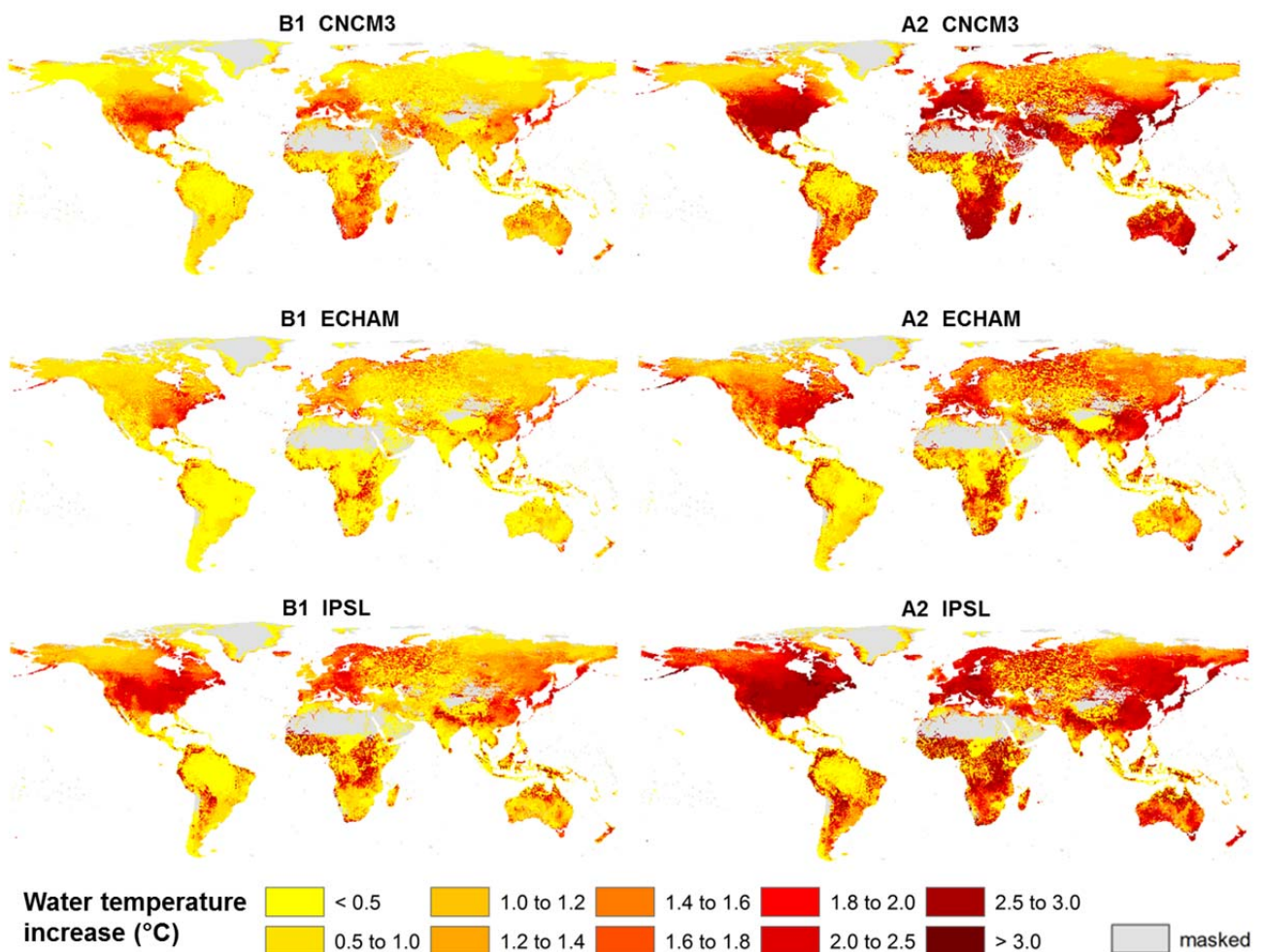


Figure 4.6: Global projected changes in mean water temperature for 2071-2100 relative to 1971-2000 for the three GCMs for both the SRES A2 and B1 scenario. Regions with mean flow less than $1 \text{ m}^3 \text{ s}^{-1}$ are masked.

Annual mean cycles and probability distribution functions of simulated water temperature also show stronger increases for the Danube and Missouri Rivers (temperate zone) than for the Mekong (tropical zone) (Figure 4.7). For the Missouri and Danube Rivers, the distribution of water temperature is bimodal, with maxima around $\sim 0-5^{\circ}\text{C}$ and $\sim 20-25^{\circ}\text{C}$. These values indicate the ranges when water temperature starts to show a nonlinear response to atmospheric cooling (because of freezing) and warming (because of increased evaporative cooling and back radiation) (Mohseni and Stefan, 1999). For the Danube, and to a lesser extent the Missouri, the increase in water temperature is largest during summer, while a moderate increase in the high water temperature range would be expected due to increased evaporative cooling. The strong increase in high water temperature during summer is partly due to the strong declines in summer flow for these basins, which reduces the thermal capacity and increases the sensitivity to increased incoming radiation and increased air temperature. In addition, declines in river flow exacerbate water temperature rises in thermally polluted rivers by reducing the dilution capacity for thermal effluents. Especially for the SRES A2 scenario, a strong increase in high river temperatures is projected for 2071-2100 as shown by the probability distribution functions of simulated water temperature (Figure 4.7 lower panel).

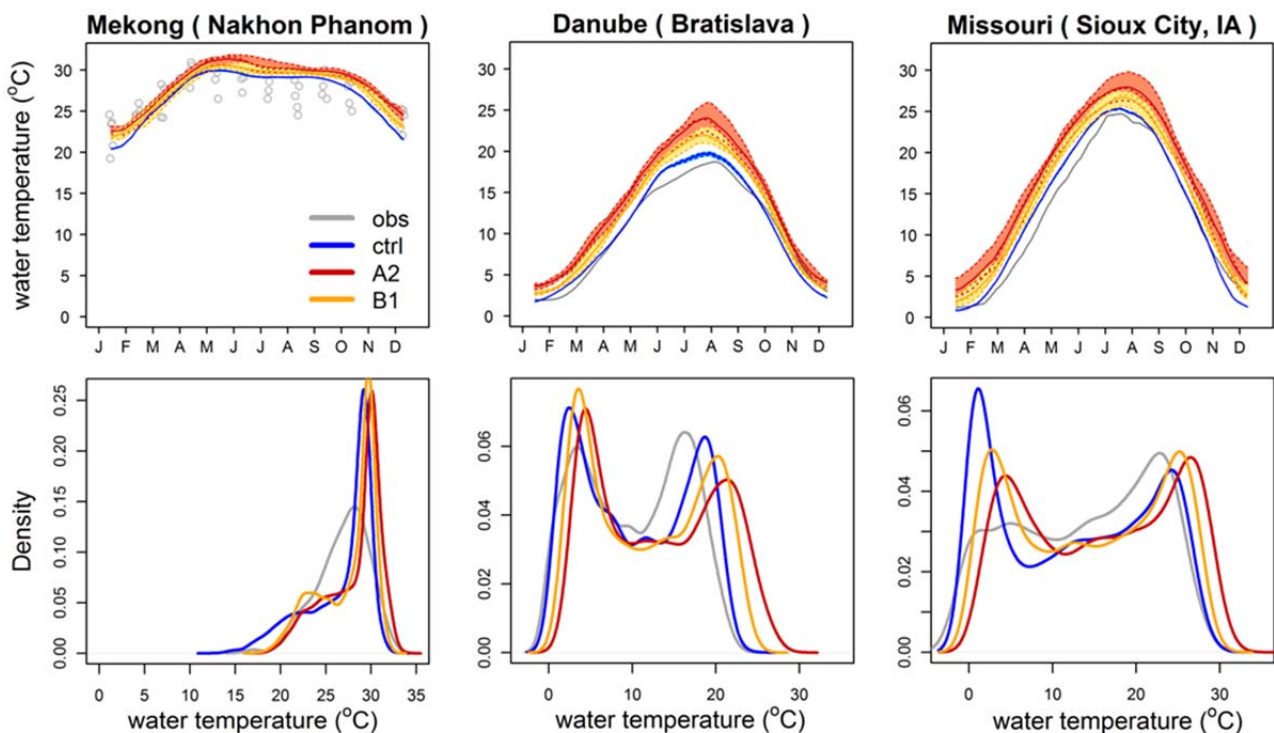


Figure 4.7: Mean annual cycles of projected daily river temperature and probability distribution functions for monitoring stations in different hydro-climatic zones for 2071-2100 relative to 1971-2000. Mean annual cycles are based on 30-day moving averages. Observed (obs; grey) and control simulations of water temperature (ctrl; blue) are for 1971-2000 and future simulations for the SRES A2 (red) and B1 (orange) emissions scenario are for 2071-2100. Dotted lines show the results for the three GCMs individually, coloured polygons show the range in results across the GCMs and the thick line shows the overall GCM mean results for the control run and for the SRES A2 and B1.

4.3.4 Critical regions for global freshwater ecosystems and human water use

Regions characterized by a combination of large reductions in (low) river flows and increases in water temperatures under future climate, could potentially experience increased deterioration of water quality, freshwater habitats and reduced potentials for human water use in the future compared to the current situation.

In the case of water quality, declining river flows decrease their dilution capacity, resulting in increased concentrations of effluents from point sources (Caruso, 2002; Moore et al., 1997; van Vliet and Zwolsman, 2008). In addition, rising water temperatures decrease oxygen solubility and concentrations (Kundzewicz and Krysanova, 2010; Murdoch et al., 2000) and increase the toxicity of pollutants (e.g. heavy metals and organophosphates) to fish and other freshwater species (Ficke et al., 2007). Freshwater organisms might also experience increased stress due to lower summer flows that decrease available habitats (Isaak et al., 2012; Sabo and Post, 2008) and the exceedances of critical water temperature thresholds (Eaton and Scheller, 1996; Mantua et al., 2010; Mohseni et al., 2003).

Increases in the occurrence of low flow and high water temperature events may also have adverse socio-economic impacts such as through reduced thermoelectric power production (Forster and Lilliestam, 2011; Koch and Vögele, 2009; van Vliet et al., 2012b). Rising water temperatures are also expected to increase risks of health impacts due to increased concentrations of microbiological pollutants (e.g. *Legionella Campylobacter*, *Vibrio cholerae*). This could result in increased costs of water treatment to produce potable drinking water (Delpla et al., 2009; Schindler, 2001; WHO, 2011).

To get a first impression of regions that could potentially experience deterioration of water quality, freshwater habitat and reduced potential for human water use under future climate, we combined spatial patterns of projected changes in low river flow with patterns of changes in mean water temperature for 2071-2100. Based on this, we identified regions for which a strong decrease in low flow (change of $< -25\%$ in the 10th percentile of daily river discharge) and large increases in mean water temperature ($>2.0^{\circ}\text{C}$) for 2071-2100 relative to 1971-2000 are projected. Overall, the extent of such regions is larger for the SRES A2 than B1 emissions scenario (Figure 4.8). Regions where both conditions are projected to occur are located in the south-eastern U.S., Europe (except the northern part), eastern China, southern Africa and southern Australia.

In addition to these spatial patterns, we explored whether the timing of low flow periods and high water temperature periods correspond, because most critical impacts for freshwater ecosystems and human water use occur when low flow and high water temperature events coincide. Therefore, we tested for each grid cell whether the month with the highest water temperature corresponds to the month of lowest river flow (\pm one month deviation) using the daily simulated water temperature and river flow under both historical (1971-2000) and future climate (2071-2100). For 18% of the global land surface area (17% for SRES B1 and 19% for SRES A2) the timing of high water temperature and low flow periods coincide (Figure

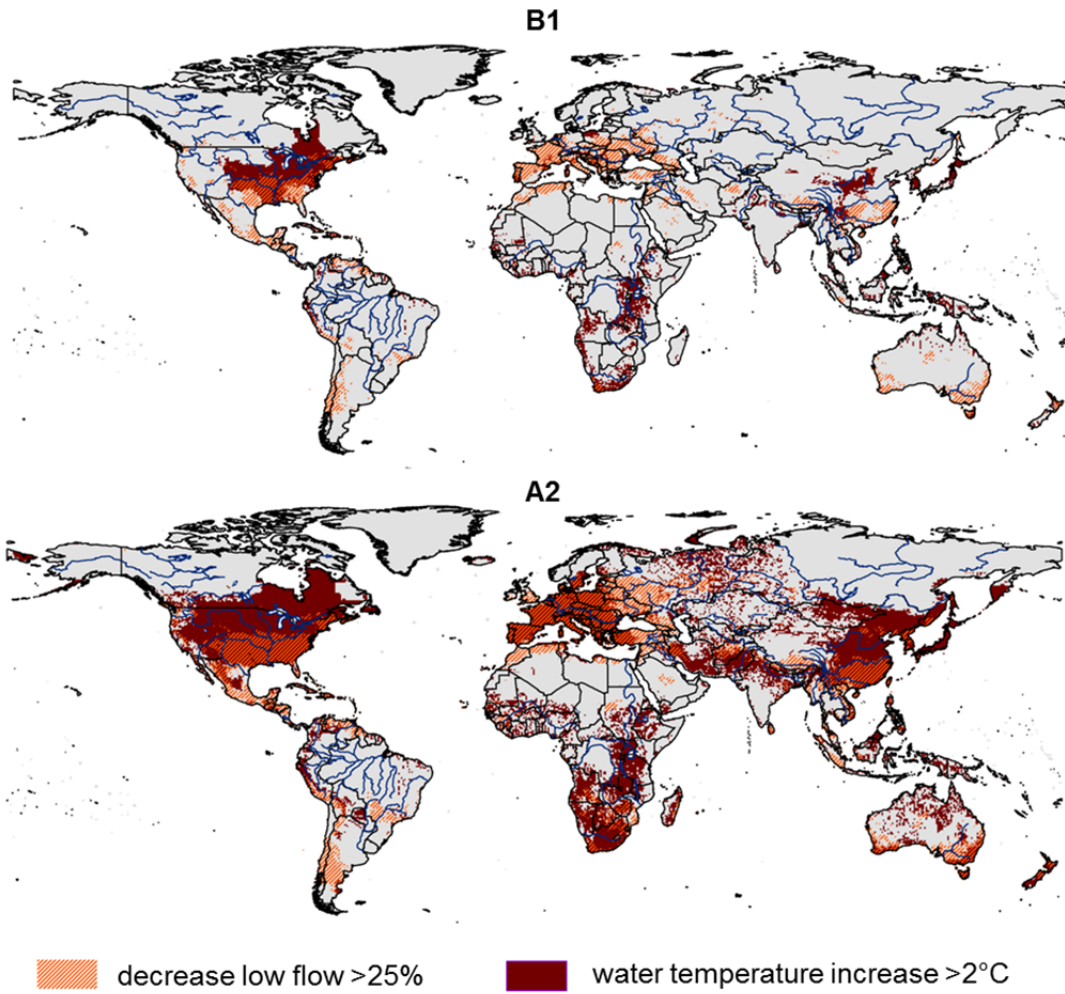


Figure 4.8: Regions characterized by strong decreases in low (10th percentile) river flow (orange), high water temperature rises (>2.0°C) (brown) and combination of both changes for 2071-2100 using averages for both the SRES A2 and B1 scenario.

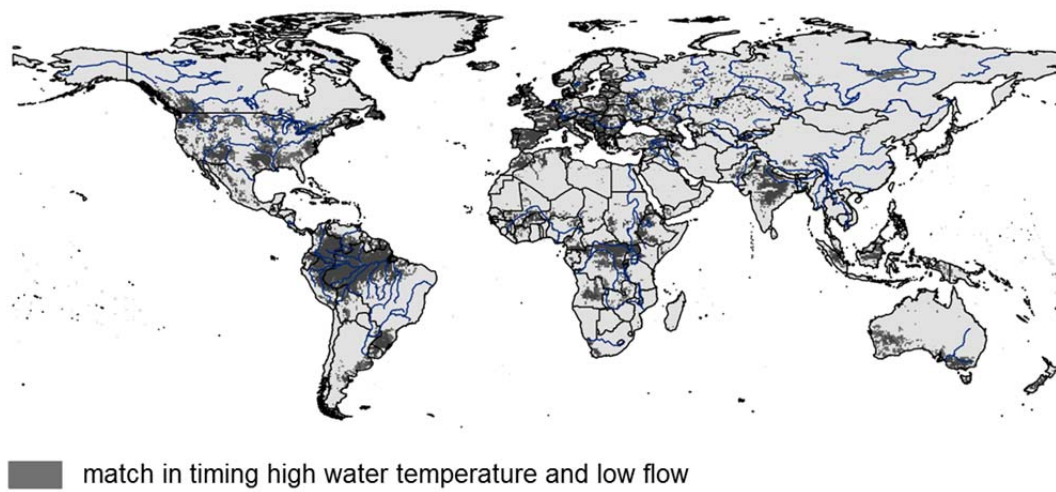


Figure 4.9: Regions for which the month with the highest water temperature coincides with the month with lowest flow (± one month deviation) for 2071-2100 consistently for all six GCMs.

4.9). These global maps with areas for which high water temperature and low flow period coincide (condition 1) were combined with global maps showing regions with projected large (>25%) decreases in low flow (condition 2) and large increases in water temperature (>2°C) (condition 3). Areas where all three conditions occur are southern and central Europe, south-eastern U.S. and parts of south-eastern Australia and southern Africa (Figure 4.10). These regions could potentially experience a deterioration of water quality and freshwater ecosystems, as well as reduced human water use as a result of climate change.

To illustrate some potential effects of the projected changes in thermal and hydrologic regimes, the lower panel of Figure 4.10 shows mean annual cycles of daily water temperature and river discharge changes for a station in the Snake (Columbia Basin), Rhine, and Mekong basins for 2071-2100 relative to 1971-2000. Considering the projected rises in water temperature in combination with relevant water temperature thresholds for these basins, there is a distinct increase in probability and magnitude of exceeded water temperature thresholds. For instance, the maximum temperature tolerance value for pink salmon of 21°C (Eaton and Scheller, 1996; Mantua et al., 2010) in the Columbia, show a distinct increase in duration and magnitude of exceedance for summer. We found comparable results when we considered the water temperature projections for the Rhine with the 23°C limit of reduced cooling water discharge potential for European rivers (EEA, 2008a). In addition, for river basins in Asia like the Mekong, an increase is projected in the duration of the period that the 25°C WHO water quality and health standard is exceeded (WHO, 2011). Although the projected increases in water temperature are moderate compared to air temperature increases, these examples illustrate that projected water temperature rises may have diverse and adverse consequences, especially when they coincide with decreases in river flow during the same period.

4.4 Discussion and conclusions

4.4.1 Impact of uncertainties in modelling framework

The physically-based hydrological and water temperature modelling framework VIC-RBM was forced with different socio-economic and climate change scenarios for 2071-2100 to quantify how climate change will affect both daily river discharge and water temperature on a global scale. Output of three GCMs for both the SRES A2 and B1 emissions scenario was used to reflect some uncertainties arising from different socio-economic storylines, climate model structures and parameterizations, notwithstanding that the use of a larger number of GCM outputs would better represent the structural uncertainty in climate models (Tebaldi and Knutti, 2007).

The use of a cascade of impact models (VIC hydrological model – routing model – RBM water temperature model) forced with climate model output results in a ‘cascade of uncertainty’ (Schneider, 1983). This can be described as the process whereby uncertainty accumulates

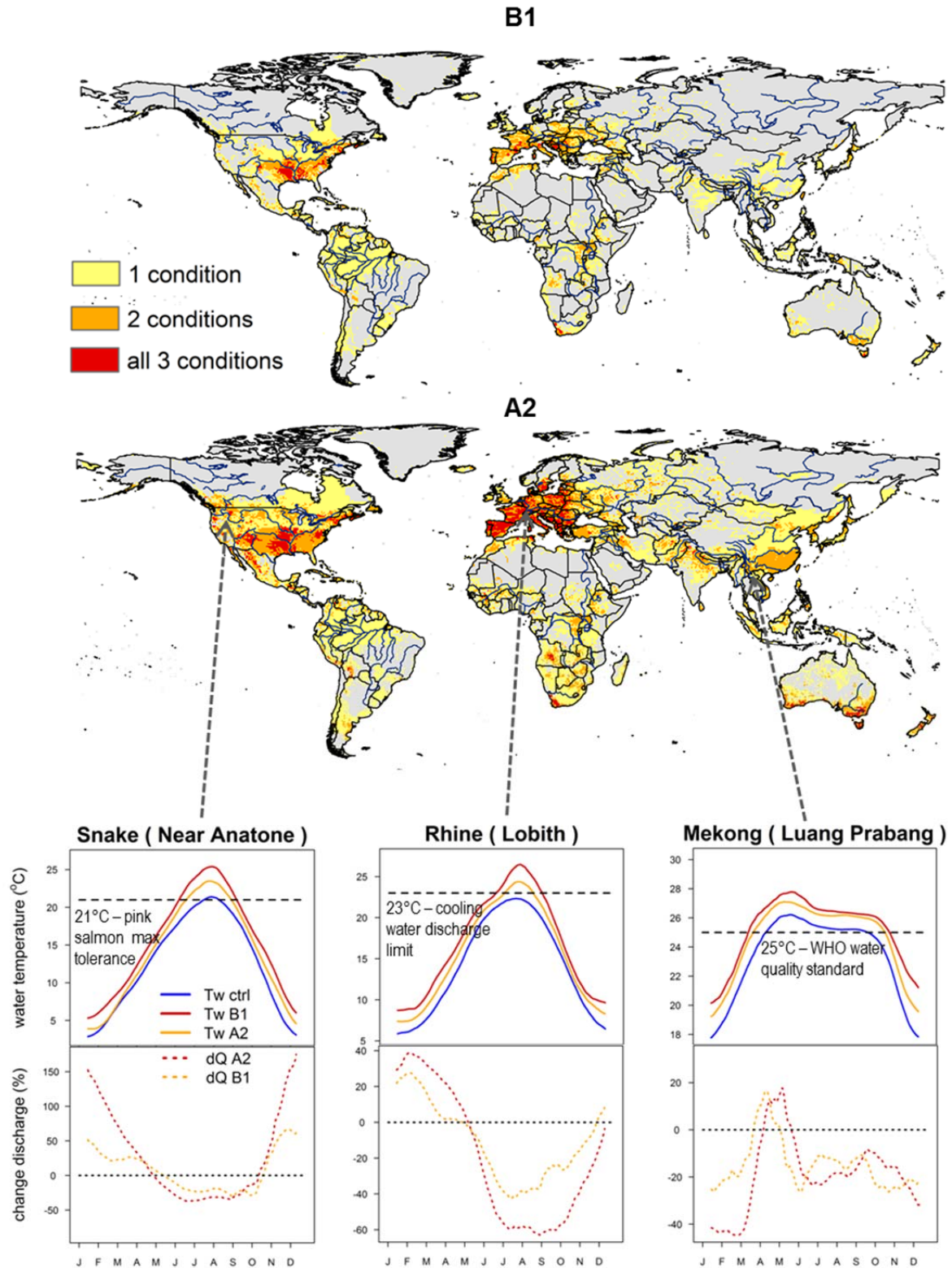


Figure 4.10: Maps with regions for which the month with the highest water temperature and lowest flow coincides and/or where a strong decrease (>25%) in low flow and/or high water temperature increase (>2°C) is projected for 2071-2100 relative to 1971-2000 for the SRES A2 and B1 scenarios. Regions where one or two out of these three conditions are projected are shown in yellow and orange. Regions where all three conditions occur are in red. Lower figures show mean annual cycles of 30-day moving averages in water temperature (Tw) and river discharge changes (dQ) for a station in the Snake (Columbia), Rhine and Mekong with water temperature thresholds relevant for these river basins.

throughout the process of climate change projections (socio-economic storylines – emission scenarios – biogeochemical models – general circulation models / regional climate models) and impact assessment (Jones, 2000). Uncertainties related to the structure and parameterization of the hydrological - water temperature modelling framework are discussed in Yearsley (2012) and van Vliet et al. (2012a). These studies showed that uncertainties are mainly attributed to heterogeneity in hydraulic characteristics and estimates of the boundary conditions (headwater temperatures). To reduce uncertainties from GCM output we used statistically bias-corrected GCM output of precipitation and air temperature to force the VIC-RBM modelling framework. Haddeland et al. (2012) used the same data set in combination with GCM output of radiation, humidity and wind speed data to force four global hydrological models. Their results showed that the direct use of (non-bias corrected) radiation, humidity and wind speed can result in different evapotranspiration and runoff estimates than those based on observational data. In our study, we used in addition to bias-corrected precipitation and temperature only uncorrected wind speed as forcing. Although this might affect river discharge and water temperature simulations (as a result of their impacts on evapotranspiration and evaporative heat flux), our results did not show distinct impacts of biases in GCM output on simulated results (Section 4.3.1). The statistics for simulated river flow and water temperature for the control simulations of the GCMs generally correspond well with the simulations based on the observed meteorological dataset and observed values (Figure 4.2).

4.4.2 Evaluation of projected changes in daily river discharge and water temperature

Forcing the VIC-RBM framework with daily bias-corrected GCM output allows quantification of potential changes in daily river flow and water temperature over the entire probability distribution, rather than just mean values. Our results show an increase in river discharge seasonality, with increasing high flows (95th percentile of the daily distribution) and decreasing low flows (10th percentile) for 27-30% of the global land surface area (SRES B1-A2). On an annual basis, river discharge is projected to increase in the high northern latitude region due to increased precipitation, with seasonal shifts (earlier start of the snowmelt peak). Discharge will also increase on annual basis in large parts of the tropical zone due to increases in monsoon rainfall. However, an overall decrease in river flow is found for river basins in the mid-northern latitude region (U.S., Central America, southern and central Europe, Southeast Asia) and the southern latitudes (southern parts of South America, Africa and Australia). These spatial patterns of projected change largely correspond with the outcomes of previous global hydrological model studies (e.g. Arnell, 2003a; Milly et al., 2005; Nijssen et al., 2001a; Sperna Weiland et al., 2012) despite different choices of emission scenarios and GCMs and different hydrological models that were used. Döll and Zhang (2010) found an increase in mean annual discharge for one half of the global land surface area and a decrease in monthly low flow (monthly 10th percentile flow) for one quarter of the land surface area (e.g. Mediterranean, southern Africa, eastern China) for the 2050s. The total extent of land surface where river flow is affected by climate change largely corresponds with our results (consistent increase in mean discharge for 50% and decrease in low flow for 24%

of global land surface area), although some discrepancies exist in regions characterized by strong declines in low flow due to different model choices.

With respect to water temperature, the greatest increases are projected for river basins in the U.S., Europe, Southeast Asia, South Africa and Australia. In these regions, the sensitivity of the river water to warming is exacerbated due to the reductions in low flows (resulting in a reduced thermal carrying capacity and limited dilution capacity for thermal effluents).

Moderate water temperature increases are projected for the tropical basins due to dominant impacts of increased evaporative cooling and back radiation under warmer conditions. On a global mean basis, the increases in mean (95th percentile) water temperature are 0.8–1.6 (1.0–2.2)°C for SRES B1-A2 for 2071-2100. This increase seems moderate compared to projected increases in global mean air temperature of 3.0–4.9°C for the selected GCM experiments, but can be important when considered in combination with relevant water temperature thresholds for specific basins (Section 4.3.4).

4.4.3 Outlook and potential impacts for human water use and freshwater ecosystems

The combination of projected rises in river temperature and decreases in river flow may have important consequences for water quality, freshwater ecosystems and human water use (e.g. thermoelectric power and drinking water production, fisheries and recreation). Regions where low flow and high water temperature periods typically coincide and for which strong increases in water temperature and combined with declines in (low) river flow are projected are the south-eastern U.S., Europe (except northern part) and parts of south-eastern Australia and southern Africa. Combination of strong increases in water temperature and decreases in river flow were also found for the eastern part of China. In these regions, the economic impact of limited water availability and increased water temperatures for water use sectors (like thermoelectric power and drinking water production) is generally high. For example, during the recent warm, dry summers in Europe (2003 and 2006) and the U.S. (2007-2008), several thermoelectric power plants were forced to reduce production or shut down, due to a lack of surface water for cooling and environment restrictions on thermal discharges (Forster and Lilliestam, 2011; Macknick et al., 2011). In Europe, this led to significant rises in electricity prices (Boogert and Dupont, 2005; McDermott and Nilsen, 2011).

Some water use sectors require not only sufficient water availability (quantity), but also suitable water quality (e.g. water temperature for cooling water use of thermoelectric power plants and industries or limited salinity for agricultural and domestic (drinking) water use). There has been a growing recognition of the need to expand hydrological impact assessments to incorporate water quality issues (Kundzewicz and Krysanova, 2010; Whitehead et al., 2009). Implementation of water quality in large-scale (global) hydrological models and land surface schemes could be an important step toward obtaining more realistic projections of large-scale water resources in relation to global change. Although the focus of our study has been limited to climate change impacts on global river flow and water temperature, the VIC-

RBM modelling framework used in our study has the potential to incorporate other water quality parameters as well, and to address impacts of other aspects of global change (e.g. land use change) that are likely to affect freshwater ecosystems and human water use in the 21st century.

Acknowledgements

This study was funded by the European Commission through the FP6 WATCH project and through the FP7 ECLISE project to Wageningen University, and by funding from the U.S. Environmental Protection Agency to University of Washington. The Global Runoff Data Centre, 56068 Koblenz, Germany, and United Nations Global Environment Monitoring System are kindly acknowledged for supplying daily observed river flow and water temperature data for river stations globally.

Vulnerability of U.S. and European Electricity Supply to Climate Change

Abstract

In the United States and Europe, at present 91% and 78% (EIA, accessed 2011) of the total electricity is produced by thermoelectric (nuclear and fossil-fuelled) power plants, which directly depend on the availability and temperature of water resources for cooling. During recent warm, dry summers several thermoelectric power plants in Europe and the south-eastern United States were forced to reduce production owing to cooling-water scarcity (Forster and Lilliestam, 2011; Macknick et al., 2011; NETL, 2009). Here we show that thermoelectric power in Europe and the United States is vulnerable to climate change due to the combined impacts of lower summer river flows and higher river water temperatures. Using a physically-based hydrological and water temperature modelling framework in combination with an electricity production model, we show a summer average decrease in capacity of power plants of 6.3–19% in Europe and 4.4–16% in the United States depending on cooling system type and climate scenario for 2031–2060. In addition, probabilities of extreme (>90%) reductions in thermoelectric power production will on average increase by a factor of three. Considering the increase in future electricity demand, there is a strong need for improved climate adaptation strategies in the thermoelectric power sector to assure future energy security.

This chapter has been published as:

van Vliet, M.T.H., J.R. Yearsley, F. Ludwig, S. Vögele, D.P. Lettenmaier, and P. Kabat (2012), Vulnerability of US and European electricity supply to climate change, Nature Climate Change, 2(9), 676–681, doi:10.1038/nclimate1546.

Worldwide, freshwater withdrawals for cooling of coal-, gas-, and nuclear-fuelled power plants are highest in North America ($224 \text{ km}^3 \text{ yr}^{-1}$), followed by Europe ($121 \text{ km}^3 \text{ yr}^{-1}$), which together represent about 86% of the global thermoelectric water withdrawals (Vassolo and Döll, 2005). When compared with other sectors, thermoelectric power is one of the largest water users in both the U.S. (40%)(King et al., 2008) and Europe (43% of total surface water withdrawals)(Rubbelke and Vögele, 2011).

Changes in water availability and surface water temperature directly affect thermoelectric power generation potential and reliability. During recent warm, dry summers in 2003, 2006 and 2009 several thermoelectric power plants in Europe were forced to reduce production, because of restricted availability of cooling water (Forster and Lilliestam, 2011). The limited supply of electricity in combination with increased production costs lead to significant rises in electricity prices (Boogert and Dupont, 2005; McDermott and Nilsen, 2011). In the U.S. a similar event in 2007-2008 caused several power plants to reduce production, or shut down for several days owing to a lack of surface water for cooling and environmental restrictions on thermal discharges (Macknick et al., 2011; NETL, 2009).

In both Europe and the U.S., power plants are highly regulated (European Fish Directive, Water Framework Directive, and U.S. Clean Water Act) with restrictions on the amount of water withdrawn and temperatures of the water discharged. It is especially during warm periods with low river flows that conflicts arise between environmental standards of receiving waters and economic consequences of reduced electricity production. Owing to the long lifetime of thermoelectric power plants and magnitude of investments, it is important for the electricity sector to have realistic projections of both water availability and water temperature to be able to anticipate and adapt to changes in cooling water availability. Although several previous large-scale modelling assessments have been made that evaluate the impact of climate change on freshwater availability on continental and global scales (Alcamo et al., 2007; Arnell, 1999a; Oki and Kanae, 2006), most of these studies focus on monthly or annual mean estimates of river flow, and ignore changes in water temperature. Shorter term (e.g. daily) estimates are required to address impacts on aquatic ecosystems and water users, such as thermoelectric power.

We used a physically-based hydrological and water temperature modelling framework (Supplementary Section B1) to produce a multi-model ensemble of daily river flow and water temperature projections for Europe and the United States over the 21st century. We evaluated the modelling estimates using observed daily river flow and water temperatures, which showed an overall realistic representation of observed conditions for the historical period 1971-2000 (Supplementary Section B2, Figure B2-B5). We then produced daily simulations of river flow and water temperature for the periods 1971-2000 (control), 2031-2060 (2040s) and 2071-2100 (2080s) by forcing the coupled hydrological - water temperature model with bias-corrected (Hagemann et al., 2011) general circulation model (GCM) outputs for both the Intergovernmental Panel on Climate Change (IPCC) Special Report on Emissions Scenarios SRES A2 and B1 global emissions scenarios (Nakicenovic, 2000) (Supplementary Section B3).

The A2 scenario considers a world of fragmented and slow technological change, whereas the B1 scenario assumes environmental sustainability and a much more rapid introduction of renewables (Nakicenovic, 2000). Both SRES A2 and B1 were selected, because they represent contrasting storylines and indicate the largest range from the four IPCC SRES main emissions scenarios.

Based on the daily river flow simulations for six GCM experiments, we calculated spatial patterns of relative changes in low flows for the future periods relative to the control period. To account for uncertainty in GCM output, we present the changes in the ensemble mean daily flow for both the SRES A2 and B1 emissions scenarios relative to the ensemble mean control simulations of the three selected GCMs. We focused our analyses on the mainland U.S. (excluding Alaska) and the European continent (excluding the Ural region and northern islands). Overall, a decrease in low flows (10th percentile of daily distribution) for Europe (except Scandinavia) is projected with an average decrease of 13-15% (16-23%) for the B1-A2 scenario for the 2040s (2080s) (Figure 5.1a). For the U.S., a decrease in low flows of 4-12% (15-19%) is simulated with the largest changes in the southern and south-eastern states. Along with decreases in the 10th percentile of daily river flow, the probability of flows below a given threshold will increase substantially (Figure 5.1b).

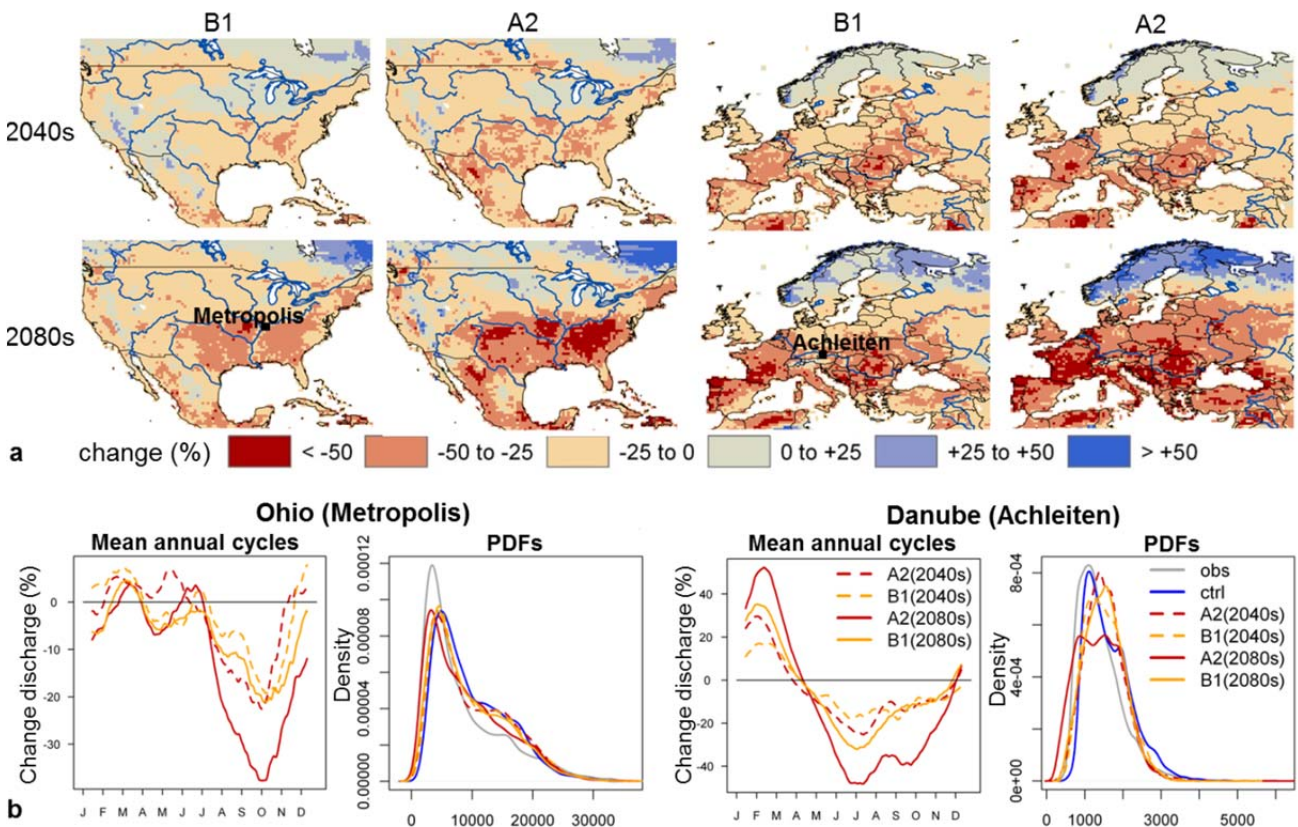


Figure 5.1: Changes in low river flows. Projected changes in low flows (10th percentile of daily distribution of river flow) for the 2040s (2031-2060) and 2080s (2071-2100) relative to the control period (1971-2000) in the U.S. and Europe (a) and mean annual cycles and probability distribution functions (PDFs) of daily river flow for a selected station in the Ohio River (U.S.) and Danube River (Europe) for the control and future periods (b).

As for river flow, we calculated changes in daily water temperature for the 2040s and 2080s. The overall projected increase in mean summer (21 Jun-20 Sep) water temperatures is 0.7-0.9 (1.4-2.4)°C for the U.S. and 0.8-1.0 (1.4-2.3)°C for Europe for the B1-A2 scenario for the 2040s (2080s). This is on average 0.2°C higher than the mean annual water temperature increase (Figure 5.2a). Probability distributions of daily water temperature (Figure 5.2c) indicate larger increases in the high water temperature range than in mean values (see e.g. Danube River for which the basin average increase in 95th percentile water temperature is 0.7°C higher than in mean water temperature for the 2080s). In the U.S., the largest water temperature increases are projected for the southern part of the Mississippi basin and along the east coast. In Europe, projected water temperature increases are highest in the south-western and south-eastern parts.

For cooling water use, the combination of declines in low river flows and increases in (especially high) water temperature is problematic. We used daily water temperature projections to calculate the mean number of days per year that water temperature is predicted to exceed the inlet limits of river water for cooling water use of 23°C (Europe)(EEA, 2008a) and 27°C (U.S., derived on basis of regulations for different states) (Supplementary Section B4). The increase in the number of days per year with water temperature exceeding 23°C is generally highest for southern Europe (median of 44-48 (59-82) days per year for B1-A2 scenario for the 2040s (2080s) relative to 23 days for 1971-2000; Figure 5.2b). The same magnitude of increase in number of days with water temperatures exceeding 27°C is found for the south and south-eastern U.S.. Combined with projected decreases in low river flows of more than 25% in these regions, cooling water problems are expected to be exacerbated substantially in the future.

To quantify climate change impacts on usable capacity of existing thermoelectric power plants, we used daily water temperature and river flow projections in combination with power plant specific data of cooling system, efficiency and environmental restrictions for 61 power plants in the U.S. and 35 in Europe. In the U.S., we focus on power plants located in the central and eastern part of the country for which the most data were available. The power plants contribute to 11% of the total electricity production for the entire U.S. and 10% in Europe. Both fossil-fuelled and nuclear power plants with different cooling systems (once-through, recirculation and combination cooling) were included (see Supplementary Section B5). Assuming an average lifetime of thermoelectric power plants of 50-60 years (IEA-NEA, 2010) more than 60% of the power plants in our data set will still be operating in 2030. Usable capacity of each thermoelectric power plant was quantified on the basis of calculated daily required water withdrawal, river flow and water temperature simulations for the power plant site and environmental (water temperature and water withdrawal) limitations (see Supplementary Section B5). An evaluation of the impacts of biases in water temperature and river flow simulations on the usable capacity of power plants showed that the strength in climate signal is on average a factor of three higher when compared with the effects of biases (see Supplementary Section B5).

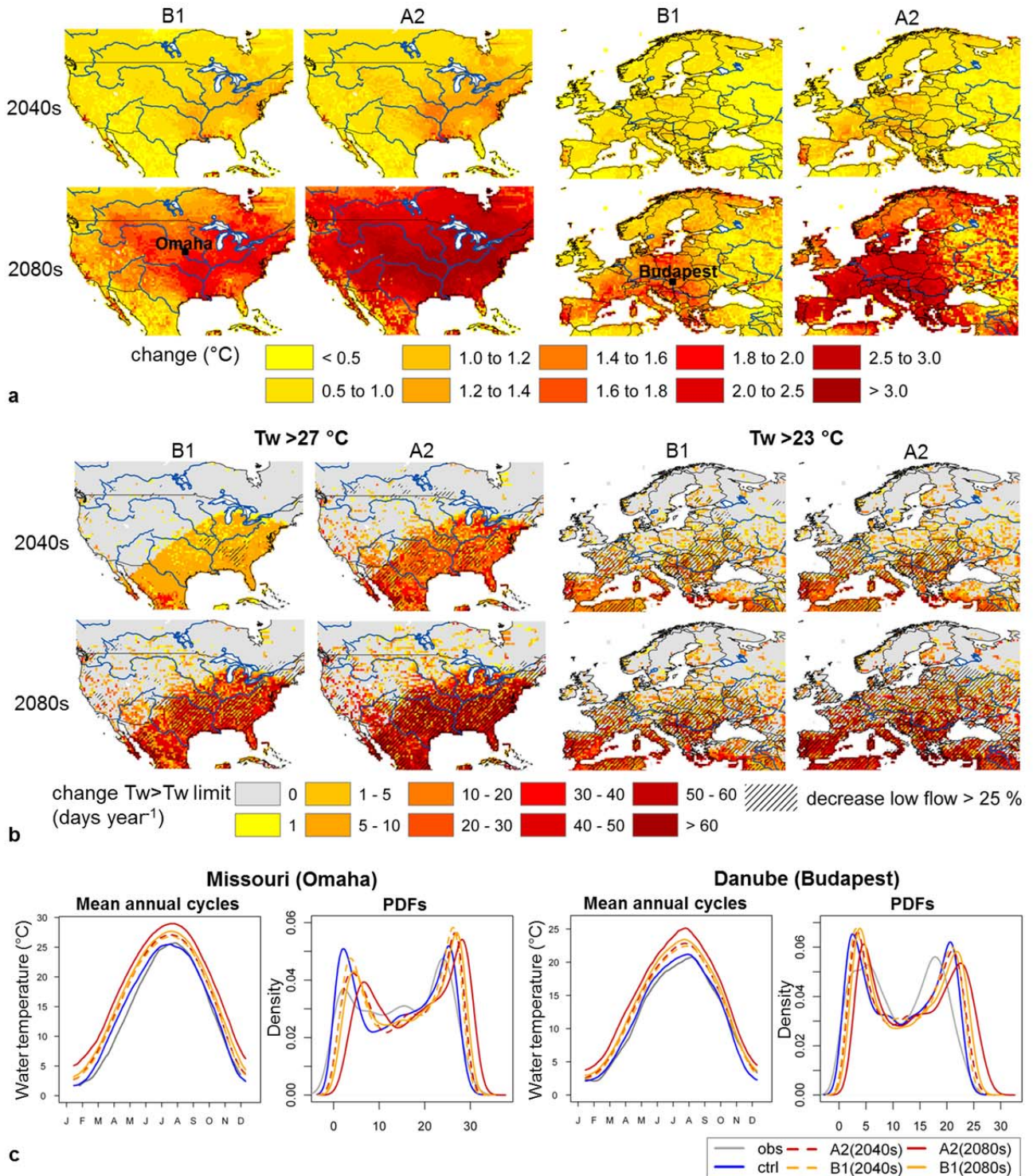


Figure 5.2: Increases in river water temperatures and exceeded water temperature limits. Projected changes in mean river water temperature (a) and mean number of days per year that the 23°C (for Europe) and 27°C (for the U.S.) inlet water temperature limit is exceeded for the 2040s (2031-2060) and 2080s (2071-2100) relative to the control period (1971-2000) (b). Regions with projected decreases in low flows of more than 25% are hatched. Mean annual cycles of daily water temperature and probability distribution functions (PDFs) of water temperature for selected stations in the Missouri River (U.S.) and Danube River (Europe) for the control and future periods (c).

For 76% of the power plants with once-through or combination cooling systems (n=37) and 41% of the power plants with recirculation systems (n=59), electricity production potential will be reduced significantly ($p < 0.01$; Wilcoxon Rank Sum tests) as a result of the projected increases in daily water temperature and decreases in summer flows for the 2040s. The summer average usable capacity of power plants with once-through or combination cooling systems is projected to decrease by 12-16% (U.S.) and 13-19% (Europe) for the 2040s (for B1-A2 SRES emissions scenario) (Figure 5.3a). The occurrence of periods with large reductions in usable capacity will increase in the 2040s, as shown by the return period plots for the power plants New Madrid (U.S.) and Civaux (France) (Figure 5.3b). These power plants extract water from large rivers (Mississippi and Vienne (Loire)) and are illustrative by showing impacts on usable capacity that are close to the overall average impacts for power plants with once-through and recirculation cooling systems in these regions. For recirculation (tower) cooling systems, the decrease in usable capacity during summer is much lower, but non-negligible (on average 6.3-8.0% for power plants in Europe and 4.4-5.9% in the U.S.). Although power plants with recirculation systems have relatively low water demand, a part of the water withdrawn is also discharged back to the river and affects river water temperatures. Therefore, both limitations in water availability and exceeded water temperature limits can reduce the usable capacity, but the mean number of days per year with production limitations is lower compared to power plants with once-through systems (Table 5.1). However, similar factors of increases in the probability of large capacity reductions are found for power plants with once-through and recirculation cooling systems. The probability of capacity reductions $>50\%$ will increase by a factor of 1.4 for the 2040s. Capacity reductions of $>90\%$ are projected to increase by a factor of 2.8. However, these probability values are low and are more sensitive to uncertainties in the modelling framework than the probability values for moderate capacity reductions. Overall, the results present a higher increase in the occurrence of extreme reductions ($>90\%$) in thermoelectric power production than in the occurrence of moderate reductions (10-25%), showing a nonlinearity of the system.

We studied the impact of climate change on thermoelectric power production in Europe and the U.S. using river flow and water temperature projections that were produced on continental scale and $0.5^\circ \times 0.5^\circ$ spatial resolution. Although the parameterizations of the hydrological and water temperature model are suited to this coarse spatial resolution resulting in a realistic representation of the observed conditions, our results do not reveal the vulnerability of any particular power plant. Under both the SRES A2 and B1 scenario (Nakicenovic, 2000) there will be substantial impacts of climate change on the usable capacity of power plants. However, the adaptive capacity of the energy sector will be much lower for the SRES A2 storyline, which considers a slow technological change with many fossil-fuelled power plants in need of cooling water, compared with B1, which assumes a much more rapid introduction of renewables (Nakicenovic, 2000). The vulnerability of the thermoelectric power sector to climate change under the A2 scenario will therefore be higher when compared with the B1 storyline.

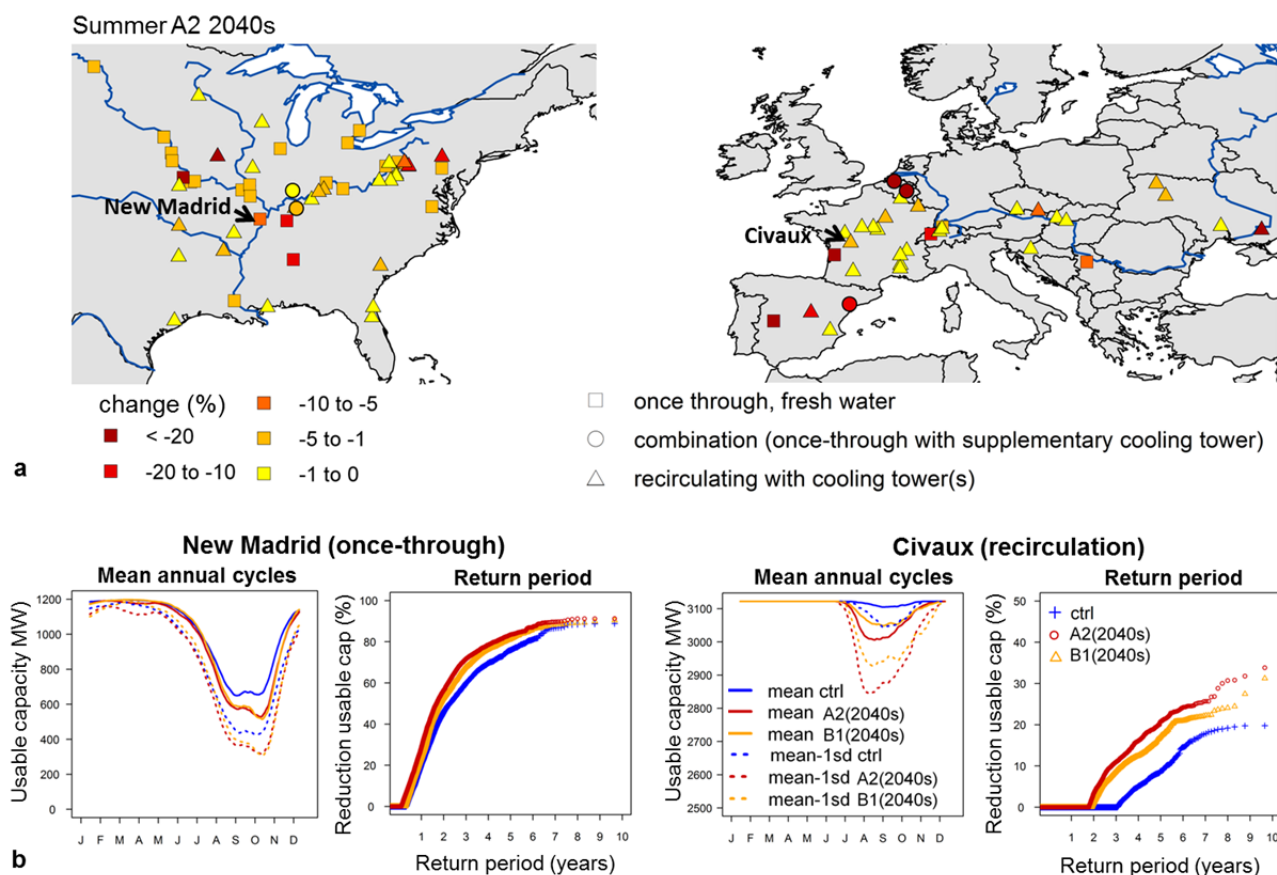


Figure 5.3: Changes in usable capacity of thermoelectric power plants. Projected changes in summer mean usable capacity of power plants in the U.S. and Europe for the SRES A2 emissions scenario for the 2040s (2031-2060) relative to the control period (1971-2000) (a). Mean annual cycles of usable capacity and return periods of production reductions for the New Madrid power station in the U.S. (coal power plant with installed capacity of 1200 MW using once-through cooling with water from Mississippi River) and Civaux power station in France (nuclear power plant with installed capacity of 3122 MW using recirculation (tower) cooling with water from the Vienne (Loire) River) (b).

Table 5.1: Reductions in usable capacity of power plants. Mean number of days per year that usable capacity (KW_{max}) is reduced by more than 25%, 50% and 90% for the control period (1971-2000) and for the 2040s (2031-2060) for the SRES B1 and A2 emissions scenario.

	n power plants	n days year ⁻¹ KW _{max} reduction > 25%			n days year ⁻¹ KW _{max} reduction > 50%			n days year ⁻¹ KW _{max} reduction > 90%		
		ctrl	B1	A2	Ctrl	B1	A2	ctrl	B1	A2
once-through or combination cooling										
Europe	8	64	84	90	31	44	50	0.5	1.4	1.5
U.S.	29	24	29	30	11	15	15	0.8	1.0	1.2
total	37	34	43	45	16	22	24	0.7	1.1	1.3
recirculation (tower) cooling										
Europe	27	14	18	19	9	10	11	0.02	0.09	0.08
U.S.	32	9	12	14	7	10	11	0.03	0.09	0.12
total	59	12	15	17	8	10	11	0.03	0.09	0.10

We conclude that climate change will impact thermoelectric power production in Europe and the U.S. through a combination of increased water temperatures and reduced river flow, especially during summer. In particular, thermoelectric power plants in southern and south-eastern Europe, and the south-eastern U.S. will be affected by climate change. Power plants with once-through cooling are most strongly impacted by future water temperature rises and reductions in summer flows, although also substantial decreases in usable capacity for power plants with recirculation (tower) cooling were found.

Owing to the smaller adaptive capacity of the thermoelectric sector for the SRES A2 scenario, the vulnerability to climate change will be substantially higher for the SRES A2 when compared with the B1 scenario. Although replacement of once-through by recirculation systems reduces freshwater withdrawal, water consumption increases (owing to evaporative losses) and could therefore contribute to higher water scarcity. Dry cooling systems or non-freshwater sources for cooling are possible alternatives but may be limited by locally available resources and have costs and performance disadvantages (Macknick et al., 2011). A switch to new gas-fired power plants with higher efficiencies (~58%) could also reduce the vulnerability because of smaller water demands when compared with coal- and nuclear-fuelled stations (with mean efficiencies of ~46% and ~34%)(Koch et al., 2012). Considering the projected decreases in cooling water availability during summer in combination with the long design life of power plant infrastructure, adaptation options should be included in today's planning and strategies to meet the growing electricity demand in the 21st century. In this respect, the electricity sector is on the receiving (impacts) as well as producing (emissions) side of the climate change equation.

Methods summary

We used a physically-based modelling framework to simulate daily river flows and water temperatures for the U.S. and Europe. This modelling framework consists of the Variable Infiltration Capacity (VIC) macro-scale hydrological model (Liang et al., 1994) and the one-dimensional stream temperature model RBM (Yearsley, 2009), which was modified to apply for the whole European and North American region (Supplementary Section B1).

The performance of the modelling framework was tested for the historical period 1971-2000. Observed daily series of river flow and water temperature for 1,267 river discharge stations and 240 water temperature monitoring stations were used to evaluate the quality of the simulations for Europe and North America (Supplementary Section B2, Figures B2- B5).

The modelling framework was forced with bias-corrected output (Hagemann et al., 2011) from three GCMs (ECHAM5/MPIOM, CNRM-CM3 and IPSL-CM4) for both the SRES A2 and B1 emissions scenarios (Nakicenovic, 2000) for the control period 1971-2000 and future periods 2031-2060 (2040s) and 2071-2100 (2080s) (Supplementary Section B3).

Daily water temperature projections were used to calculate the mean number of days per year that the 23°C (Europe) and 27°C (U.S.) limits were exceeded for the control and future periods for both the SRES A2 and B1 scenario. These river water temperature limits reflect the start of potential reductions in production capacity rather than full production stops (reflected by maximum allowed river water temperature thresholds). Selection of these water temperature limits is discussed in the Supplementary Section B4. In combination with areas for which a large decrease in low flows (>25%) is expected, we identified regions in Europe and the U.S. where cooling water problems are expected to increase.

In addition, we calculated the effects on the usable capacity of 35 existing thermoelectric power plants in Europe and 61 in the U.S. using the daily water temperature and river flow projections for the 2040s. A distinction was made between power plants using recirculation systems with cooling tower(s), once-through systems and combination cooling systems (once-through with supplementary tower). Data of the National Energy Technology Laboratory Coal Power Plant Database (NETL-CPPDB) database (NETL, 2007) were used for thermoelectric power plants in the U.S.. For power plants in Europe we used data of the selected nuclear power stations extracted from the power plant database at the Institute of Energy and Climate Research – Systems Analyses and Technology Evaluation (IEF-STE) of the Forschungszentrum in Jülich (Germany) in combination with published data of fossil-fuelled power plants (VGE, 2011). The equations used to calculate the required water withdrawal and usable capacity of the power plants are modified from Koch and Vögele (2009) and Rubbelke and Vögele (2011) and are described in the Supplementary Section B5, along with the criteria that were used to select the thermoelectric power plants.

Acknowledgements

This study was financially supported by the European Commission through the FP6 WATCH project and through the FP7 ECLISE project. We thank R. Leemans for helpful comments on a previous version of this manuscript. The Global Runoff Data Centre, 56068 Koblenz, Germany, and United Nations Global Environment Monitoring System are kindly acknowledged for supplying daily observed river flow and water temperature data for river stations in the U.S. and Europe.

Global Streamflow and Thermal Habitats of Freshwater Fishes under Climate Change

Abstract

Flow regimes and thermal regimes of rivers will be affected by climate change and other anthropogenic impacts during the 21st century. This will directly affect freshwater habitats and ecosystem health. In particular fish species, which are strongly adapted to a certain level of flow variability will be sensitive to future changes in flow regime. In addition, all freshwater fish species are exotherms, and increasing water temperatures will therefore directly affect fishes' biochemical reaction rates and physiology. Until now, very few studies assessed the combined impacts of changes in river flow and water temperatures on fish habitats. In addition, most previous studies focussed on local and regional scales. Here we assess the potential impacts of climate change on large-scale freshwater fish habitats by using global river flow and water temperature projections for the 21st century. These projections were produced with a physically-based hydrological and water temperature modelling framework forced with an ensemble of climate model output. Projections were used in combination with current spatial distributions of several fish species, thermal tolerance values and ecologically relevant flow indices to explore impacts on fish habitats in different regions worldwide. Our results show that climate change will have distinct impacts on flow and thermal characteristics of freshwater fish habitat. Climate change will affect seasonal flow amplitudes, magnitude and timing of high and low flow events for large fractions of the global land surface area. Also, significant increases in both the occurrence and magnitude of exceeding maximum temperature tolerance values of selected fish species were found. Although the adaptive capacity of fish species to changing hydrologic regimes and rising water temperatures could be variable, our global results show that fish habitats are likely to change in the near future, and this is expected to affect species distributions.

This chapter has been submitted as:

van Vliet, M.T.H., F. Ludwig and P. Kabat, Global streamflow and thermal habitats of freshwater fishes under climate change.

6.1 Introduction

Climate change and other anthropogenic impacts are likely to increase pressure on water for ecosystems and human uses globally. Freshwater ecosystems have of all ecosystems the highest proportion of species threatened with extinction due to climate change and increased human impacts (Kundzewicz et al., 2007; Millennium Ecosystem Assessment, 2005). Populations of freshwater species decreased by 50% during 1970-2000, which is greater than found for terrestrial and marine species included in the Living Planet Index (WWF, 2004). Main stresses on freshwater ecosystems are habitat degradation (e.g. driven by climate change and other human impacts), invasive species, overexploitation and water pollution (Dudgeon et al., 2006; Millennium Ecosystem Assessment, 2005). Vörösmarty et al. (2010) found that freshwater habitats supported by 65% of global river discharge are under moderate to high threat. Overall, stress on freshwater ecosystems that have already been (heavily) affected by human influences is expected to increase substantially due to climate change (Kundzewicz et al., 2007; Millennium Ecosystem Assessment, 2005).

Climate change mainly affects freshwater ecosystems by altered river flow regimes (which involves the timing of river flows of different magnitudes), changes in water levels, increases in water temperatures and changes in water quality (Ficke et al., 2007; Fischlin et al., 2007). Future river flow regimes will be affected by changes in precipitation and evapotranspiration patterns (Bates et al., 2008). Overall, mean river discharges in the tropical and high northern latitudes regions are likely to increase under climate change, while consistent decreases are projected for southern and central Europe, South Africa and South America (e.g. Arnell, 2004; Sperna Weiland et al., 2012). Flow seasonality is also expected to increase due to climate change, resulting in higher peak flows and reduced low flows for several regions worldwide (e.g. Bates et al., 2008). A global study of Döll and Zhang (2010) showed that climate change significantly affects river flow regimes for 90% of the global land surface area, compared to 25% of the land area where flow regime is affected by dams and human water withdrawals.

In addition to changes in river flow, global freshwater habitats will be directly affected by rising water temperatures under a warmer climate. River temperatures are expected to further increase due to atmospheric warming (e.g. Mantua et al., 2010; Mohseni et al., 1999; Stefan and Sinokrot, 1993), and for several rivers, also due to expected declines in summer river flows, which reduce the thermal capacity and increase the sensitivity to atmospheric warming (van Vliet et al., 2011). Worldwide, the highest water temperature increases under climate change are projected for rivers and streams in the United States, Europe, Southeast Asia, South Africa and Australia (van Vliet et al., in press). In most of these regions, water temperature rises are exacerbated due to projected decreases in summer river flows.

As fish species are commonly adapted to specific flow and thermal regimes, changes are likely to affect species distribution (e.g. Ficke et al., 2007; Mohseni et al., 2003; Poff and Allan, 1995) with potentially increased success of invasive fish species (Baltz and Moyle, 1993; Dudgeon et al., 2006). Flow regime characteristics, in particular flow seasonality, affect life-history

patterns like spawning and migration (Dudgeon et al., 2006). Increases in flow amplitude for tropical rivers, like the Mekong, with higher flow peaks and declines in low flow could negatively affect fish populations (Ficke et al., 2007; Welcomme, 1979). Increases in annual mean high flow could increase habitat availability (e.g. for spawning) on flood plains (Ficke et al., 2007), but increases in severity of flood peaks can displace adult or injure juveniles and larvae (Grossman et al., 1998; Harvey, 1987). Strong declines in low flow and more severe streamflow droughts can increase the severity of crowded, stressful conditions in refuge pools, causing population declines and changes in fish species compositions (Grossman et al., 1998; Matthews and Marsh-Matthews, 2003; Richter et al., 1997).

All freshwater fish species are exotherms, meaning that their body temperature is virtually identical to their environmental (water) temperatures. Fish species thermoregulate behaviourally by selecting (migrating to) more suitable thermal habitats, but they are constrained by the temperature range available within the water system (Ficke et al., 2007; Jeppesen et al., 2010). Biochemical reaction rates affecting fish physiology vary as a function of body temperature (Coutant, 1969; Poole and Berman, 2001), and aspects like growth, reproduction, activity and migration will therefore be directly impacted by water temperature increases (Ficke et al., 2007; Jeppesen et al., 2010). In addition, rising water temperatures also decrease oxygen solubility and increase organic matter decomposition, resulting in lower dissolved oxygen concentrations (e.g. Caruso, 2002; Kundzewicz and Krysanova, 2010; Murdoch et al., 2000). This increases oxygen stress for fish (e.g. Meyer et al., 1999; Mulholland et al., 1997). In addition, remobilisation and bioaccumulation of toxic substances (e.g. mercury, lead, polycyclic aromatic hydrocarbons (PAHs)) in fish also increase under higher water temperatures (Ficke et al., 2007; Whitehead et al., 2009). Water temperature rises could therefore also affect fish populations indirectly due to its impacts on other water quality parameters.

Improved understanding of climate change impacts on freshwater fishes is relevant, not only in terms of biodiversity and ecosystems health, but also for food production. Freshwater fisheries provide an important source of affordable protein for large communities around the globe (for example China, India, Brazil) (Ficke et al., 2007), and contribute to a significant amount of economy, for example Bangladesh (Hossain, 1994) and India (Chauhan, 1994). Although the vulnerability of freshwater fisheries to climate change has been widely recognized (e.g. Ficke et al., 2007) the knowledge is very scattered and only a few studies assessed the impacts on a large (continental/global) scale. Previous work mainly focussed on either the impacts of streamflow (e.g. Döll and Zhang, 2010; Xenopoulos et al., 2005) or water temperature changes (Eaton and Scheller, 1996; Mohseni et al., 2003). However, there is a strong need for assessments that integrate impacts of streamflow and water temperature on freshwater ecosystems and fish habitats (Olden and Naiman, 2010; Thompson et al., 2012; Wenger et al., 2011).

The objective of this study was to assess the combined impacts of both streamflow and water temperature changes on large-scale freshwater fish habitats under climate change. Global

streamflow and water temperature projections were produced with a physically-based hydrological and water temperature modelling framework (van Vliet et al., 2012a) forced with an ensemble of general circulation model (GCM) output (Section 6.2). These global projections were used in combination with a selection of ecologically relevant flow and water temperature indices, maximum temperature tolerance values and current spatial distributions of 34 fish species in different regions worldwide. Results of the impacts of streamflow and water temperature changes on freshwater fish habitats under climate change are first discussed in general terms on a global level (Section 6.3.1-6.3.2), followed by the potential impacts for specific fish species in different regions (Section 6.3.3). Potential consequences of projected changes in streamflow and thermal habitat for freshwater fishes are discussed in a broader context in Section 6.4.

6.2 Methods

The methodological framework of this study is summarized in Figure 6.1. The global hydrological - water temperature modelling framework was forced with bias-corrected output of three different GCMs for both the SRES A2 and B1 emissions scenario (Nakicenovic, 2000) for 2071-2100 and for a control period 1971-2000 (see Section 6.2.1). The streamflow and water temperature simulations were subsequently used in combination with ecologically relevant flow and water temperature indices and limits (see Section 6.2.2 and 6.2.3), and with maximum temperature tolerance values and spatial data of suitable habitat distributions of several fish species in different regions (Section 6.2.4).

6.2.1 Global modelling of streamflow and water temperature under climate change

A physically-based hydrological and water temperature modelling framework was used on a global scale and $0.5^\circ \times 0.5^\circ$ spatial resolution. The modelling framework consists of the Variable Infiltration Capacity (VIC) macro-scale hydrological model (Liang et al., 1994) and one-dimensional stream temperature River Basin Model (RBM) (Yearsley, 2009; Yearsley, 2012), which was adjusted for global-scale applications (van Vliet et al., 2012a). Reservoir impacts on streamflow were simulated by using the reservoir scheme of Haddeland et al. (2006), which is combined with the river routing model of Lohmann et al. (1998). The VIC hydrological model was applied using the elevation and land cover (vegetation, soil) classification as described in Nijssen et al. (2001b). The global DDM30 routing network (Döll and Lehner, 2002) was used for lateral streamflow routing. Information about dams from University of New Hampshire were used, updated according to the World Register of Dams (ICOLD, 2003), as described by Haddeland et al. (2006). Hydraulic characteristics were calculated based on power relations relating mean cross-sectional area and width to streamflow (Leopold and Maddock, 1953). For unregulated streams we used coefficients found by Allen et al. (1994). For river reaches controlled by reservoirs, we assumed water surface elevation, and depth and width to remain constant in time (for details see van Vliet et al. (2012a)). Head water temperatures were assessed using the nonlinear water temperature regression model of Mohseni et al. (1998). Impacts of thermal effluents on water temperature

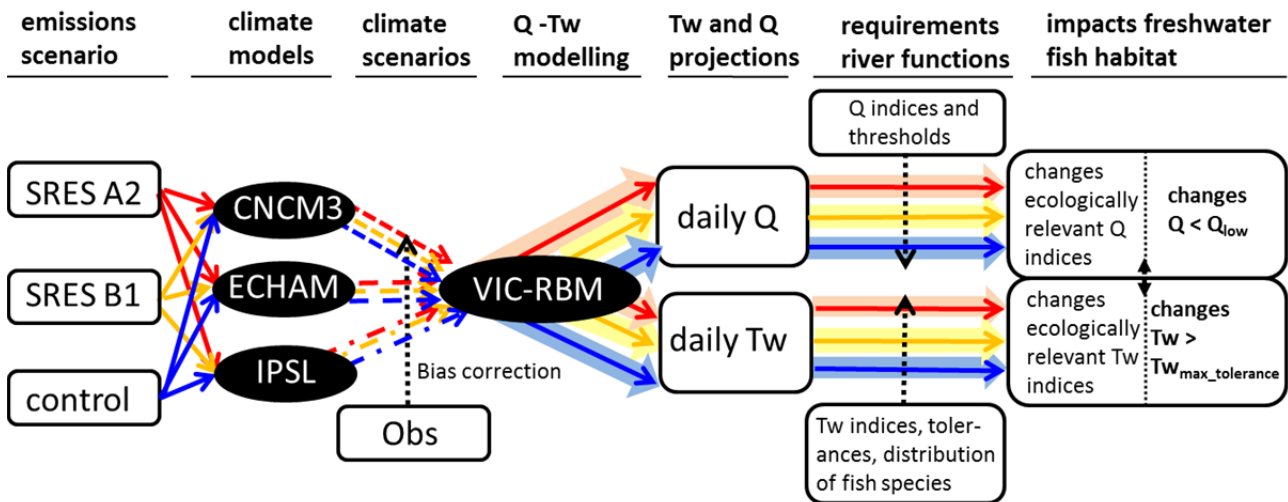


Figure 6.1: Schematic representation of methodological framework. Abbreviations are used for streamflow (Q) and water temperature (Tw).

were included by using global gridded ($0.5^\circ \times 0.5^\circ$) datasets of thermoelectric water consumption and withdrawal for 1971-2000 to calculate return flows (Flörke et al., 2011; Voß and Flörke, 2010). The assumption was made that the return flow water temperature was 3°C higher than inlet water temperature (for details see Supplementary Information B1).

The performance of the modelling framework was evaluated for large river basins (van Vliet et al., 2012a) and on a global scale (van Vliet et al., in press) using daily streamflow and water temperature series for a high number of monitoring stations. The simulations showed an overall realistic representation of the observed conditions, although streamflows in some river basins (e.g. Orange, Murray-Darling) were somewhat overestimated due to the neglect of human water withdrawals (van Vliet et al., 2012a). In this study, impacts of both reservoirs and human water uses were incorporated in the global modelling framework to improve streamflow estimates for ecological impact assessment. We used global gridded ($0.5^\circ \times 0.5^\circ$ spatial resolution) estimates of water consumption for agriculture (irrigation and livestock), energy, industry and domestic uses for 1971-2000 in the modelling framework. For irrigation water use, monthly mean estimates of actual irrigation water extraction were modelled with VIC and its irrigation scheme (Haddeland et al., 2006) using similar forcing (Haddeland, in prep.). Global gridded ($0.5^\circ \times 0.5^\circ$) estimates of industrial, thermoelectric power, livestock, and domestic uses on annual time step were modelled by the WaterGAP water use modules (Alcamo et al., 2003a) and were provided within the EU FP6 WATCH project (Flörke and Eisner, 2011 ; Voß and Flörke, 2010; Voß et al., 2009).

To produce projections of daily streamflow and water temperature under future climate, we forced the VIC-RBM modelling framework (including reservoir scheme) with bias-corrected output of three different GCMs: ECHAM5/MPIOM, CNCRM-CM3, IPSL-CM4 (which are denoted as ECHAM, CNCM3 and IPSL, henceforth) (Hagemann et al., 2011). Climate model output for both the SRES A2 (Figure 6.1; red) and B1 emissions scenario (orange) for 2071-2100 and for 1971-2000 (control; blue) were used. This resulted in global daily streamflow and water

temperature simulations for three control experiments and six future GCM experiments to account for some uncertainties in GCM output (van Vliet et al., in press). As the focus of this study is on climate change impacts on global freshwater fish habitats, impacts of human water uses on streamflow and effects of thermal effluents on water temperatures were assumed to remain constant after 2000.

6.2.2 Impacts of streamflow changes on freshwater habitats globally

Several previous studies that addressed impacts of streamflow changes on freshwater ecosystems used the concept of 'environmental flows' or 'environmental flow requirements', which commonly refer to the amount of flows that needs to be allocated for the maintenance of freshwater ecosystem health and services (Dyson et al., 2003; Tharme, 2003). In this respect, freshwater ecosystems are considered as a 'water use sector', similar to agriculture, power generation, domestic or industrial uses (Smakhtin, 2008). At least 200 environmental flow methods and approaches have been used to quantify the water requirements for freshwater ecosystems (Arthington et al., 2010; Richter et al., 2006; Smakhtin, 2007; Tharme, 2003). Many environmental flow assessment studies focussed on definition of a minimum flow requirement or threshold, like the widely applied Tennant-method (Tennant, 1976). However, these thresholds are often arbitrary defined (Smakhtin et al., 2006), because of limited availability of freshwater species response data in large parts of the world (Revenge et al., 2005). In addition to a minimum flow requirement, it has also been widely recognized that a dynamic river regime and flow variability is required to sustain ecosystem functioning (Arthington et al., 2010; Lytle and Poff, 2004; Poff et al., 1997). However, due to limited data availability of freshwater species responses it is often not possible to directly derive transferable quantitative relationships between ecological responses (e.g. species distribution) and streamflow changes. Therefore, ecologically relevant flow indices (e.g. Richter et al., 1996) and ecological limits (e.g. Poff et al., 2010) have been developed to assess ecological risks of altered flow regimes and variability (Gibson et al., 2005; Poff and Zimmerman, 2010).

Richter et al. (1996) defined 32 hydrological indicators for identifying ecologically relevant changes in mean and extreme flow conditions using a set of natural flow and a set of altered river flow time series. Döll and Zhang (2010) assessed the impacts of climate change and human flow alternations on a global scale by using five ecologically relevant parameters. The approach of our study extends the approach of Döll and Zhang (2010) by selecting more ecologically relevant flow indicators of Richter et al. (1996) that are related to changes in flow extremes, and by integrating the results of changes in different ecologically relevant flow indices with changes in thermal habitat conditions under future climate. In addition, we focus in more detail on changes in the probability and magnitude of low flow conditions (streamflow droughts), which are main critical aspect for fish habitats (Grossman et al., 1998; Matthews and Marsh-Matthews, 2003).

We calculated relative changes in mean flow, low flow (Q_{10} ; 10-percentile daily flow distributions), high flow (Q_{95} ; 95-percentile), annual 1-, 7- and 30-day minimum and maximum flow, and seasonal flow amplitude using future (2071-2000) and control (1971-2000) streamflow simulations (Table 6.1). Absolute changes (shifts) were calculated in timing of annual high and low flow peaks. We calculated GCM ensemble mean changes in flow indices for the SRES A2 and B1 scenario (for 2071-2100) and control period (1971-2000). Based on spatial patterns of changes in these ecologically relevant flow indices, we identified regions with strongest (>50%) increases or decreases in seasonal flow amplitude, declines in low flow (>25%) and shifts in timing of the annual maximum flow events (>30 days). These regions are considered to experience largest changes in fish habitats due to climate change induced streamflow changes.

We focussed in more detail on the potential impacts of climate change on available stream habitats for fishes by calculating changes in occurrence and magnitude of streamflows, which are below a threshold minimum flow under future compared to control climate. A fixed threshold level, which has been widely used to define streamflow droughts (Fleig et al., 2006; Hisdal et al., 2004), was selected to define a threshold minimum flow. Although variable threshold levels (on seasonal, monthly and daily basis) have also been widely used to identify streamflow droughts under current climate (e.g. Perez et al., 2011; van Huijgevoort et al., 2012), we used a fixed threshold, because shifts in timing of mean high and low flow events under climate change would make the use of a variable threshold level method (without corrections of future changes in timing of flow events) less suitable. As a fixed threshold level, we selected the 10th percentile of the simulated daily river discharge for the control period 1971-2000 (Q_{10} , also known as 90th exceedence percentile), which is a widely used ecologically relevant low flow threshold (Pyrce, 2004; Smakhtin, 2001; Tharme, 2003). The threshold minimum flow was quantified on grid cell level using the control simulations (1971-2000). Grid cells where the mean flow values were less than $1 \text{ m}^3\text{s}^{-1}$ were excluded from the analysis. We calculated GCM ensemble mean changes in occurrence (mean number of days per year) and mean magnitude that streamflows were below the threshold minimum flow for both the SRES A2 and B1 scenario for 2071-2100 relative to the control period 1971-2000. Regions with strongest increases in occurrence and magnitude of flow deficits are expected to experience the largest increase in the severity of crowded, stressful conditions for freshwater fish species (Grossman et al., 1998; Matthews and Marsh-Matthews, 2003; Richter et al., 1997).

6.2.3 Impacts of water temperature changes on freshwater habitats globally

Changes in thermal characteristics of rivers affect life-cycles of freshwater organisms and fishes (Coutant, 1987; Olden and Naiman, 2010). The thermal regime of rivers can be decomposed in components of magnitude, frequency, duration, and timing of high and low thermal events. The quantification of its characteristic properties can thus be described using similar indices as used for streamflow regime (Olden and Naiman, 2010). Therefore, changes

Table 6.1: Selected ecologically relevant flow (Q) and water temperature (Tw) indices and their definition and references to previous studies that used these indices.

ecologically relevant index	definition	reference flow/water temperature index	dimension
A) mean streamflow and water temperature:			
Q _{mean} , Tw _{mean}	annual mean flow, water temperature	(Döll et al., 2009; Döll and Zhang, 2010; Oberdorff et al., 1995; Xenopoulos et al., 2005)	magnitude
B) high flow and water temperature:			
Q ₉₅ , Tw ₉₅	95 th percentile daily flow, water temperature exceeded 5% of the time	(Eaton et al., 1995)	magnitude
1-, 7- and 30-day Q _{max} , 1-, 7- and 30-day Tw _{max}	annual 1-, 7- and 30-day average maximum flow, water temperature	(Gibson et al., 2005; Richter et al., 1996)	magnitude- duration
date 1-, 7- and 30-day Q _{max}	Julian date of annual 1-, 7-, 30-day average maximum flow	(Richter et al., 1996), but used 1-day Q _{max})	timing
C) low flow and water temperature:			
Q ₁₀ Tw ₁₀	10 th percentile daily flow, water temperature exceeded 90% of time	(Döll et al., 2009; Döll and Zhang, 2010), but used monthly 10 th percentile	magnitude
1-, 7- and 30-day Q _{min} , 1-, 7- and 30-day Tw _{min} ,	annual 1-, 7- and 30-day average minimum flow, water temperature	(Gibson et al., 2005; Richter et al., 1996)	magnitude- duration
date 1-, 7- and 30-day Q _{min}	Julian date of annual 1-, 7-, 30 day average minimum flow	(Richter et al., 1996)	timing
days Tw<=0.5	mean number of days per year with water temperatures reaching 0.5°C (minimum tolerance value for cold and cool water fishes)	(Mohseni et al., 2003), but used 0°C as minimum temperature tolerance value for cold water species	frequency
D) seasonal amplitude:			
30-dayQ _{max} – 30-dayQ _{min} , 30-dayTw _{max} – 30-dayTw _{min}	seasonal amplitude flow and water temperature using annual 30-day average minimum and maximum values	(Döll et al., 2009; Döll and Zhang, 2010)	magnitude

in similar ecologically relevant indices were calculated to assess ecological impacts of water temperature changes under climate change on a global scale. We calculated absolute changes in mean water temperature, low water temperature (Tw₁₀; 10-percentile daily temperature distributions), high water temperature (Tw₉₅; 95-percentile), annual 1-, 7- and 30-day minimum and maximum water temperature, and seasonal temperature amplitude using the daily water temperature simulations for the future (2071-2000) and control (1971-2000) periods (Table 6.1). Minimum temperature tolerance values for many cold water fishes are assumed to be 0°C (Mohseni et al., 2003). The minimum temperature value that RBM

simulates during (almost) freezing periods is 0.5°C. We therefore used 0.5°C as a minimum water temperature value to assess changes in the mean number of days per year that water temperatures are reaching this critical low value. As for streamflow, the GCM ensemble mean changes in water temperature indices were calculated for the SRES A2 and B1 (for 2071-2100) relative to the control period (1971-2000).

In addition, the physiological thermal tolerances are of importance by affecting the biogeographic of freshwater fish species distributions. Different fish species are commonly grouped based on climate zone, distinguishing (sub)arctic fishes, temperate fishes and (sub)tropical fishes (Ficke et al., 2007). Temperate fishes fall into three thermal classes – cold (e.g. *Salmonidae*), cool (e.g. *Percidae*) and warm (e.g. *Cyprinidae*) water fishes (Magnuson et al., 1979). Climate change is expected to affect distributions of freshwater fishes, as some species will colonize habitats at higher latitudes and/or disappear from the low latitude limits of their distribution (Carpenter et al., 1992; Johnson and Evans, 1990; Shuter and Post, 1990). It is therefore relevant for fish species to assess the distances over which water temperature (thermal habitat) zones will move under future climate. Using the gridded datasets of mean and high (95th percentile) water temperature values under control and future climate, we assessed latitude-average values of mean and high water temperatures, and calculated isolines (joining points (gridcells) of equal water temperatures above/below a given value) for both control and future climate. Based on the latitude-average values of water temperature statistics we calculated the mean polewards movement in water temperature (thermal habitat) zones under future (2071-2100) relative to control (1971-2000) climate.

6.2.4 Regional freshwater fish habitats under water temperature and streamflow changes

In addition to the global analyses, we assessed the impacts of water temperature increases on several fish species in different regions around the globe, combined with spatial patterns of large changes in streamflow habitat conditions. We used the global gridded water temperature simulations in combination with maximum temperature tolerance values ($T_{w_{max_tolerance}}$) and spatial data with current suitable habitats of selected cold (n=15), cool (n=8), warm water (n=7) and (sub)tropical (n=4) fish species in different regions (Americas, Europe, Africa and Southeast Asia). Fish species were selected based on their large spatial extent (geographic distribution), availability of information on $T_{w_{max_tolerance}}$ and relevance for fisheries. Although suitable thermal habitat is assumed to be constrained by both maximum temperature and minimum temperature tolerance, information of minimum temperature tolerances of freshwater fishes is sparser. This is mainly because observations of fishes are mainly during summer and therefore during periods with high water temperatures (Mohseni et al., 2003). This analysis therefore specifically focusses on changes in thermal habitat using maximum temperature tolerance values of fish species. Table 6.2 presents an overview of selected fish species included in this analysis, along with the region of occurrence and $T_{w_{max_tolerance}}$ value and purpose (fisheries, aquaculture and game fish).

Table 6.2: Selected fish species, $TW_{\max_tolerance}$ and purpose for fisheries (F), aquaculture (C) and game fish (G).

common name	scientific name	class	$TW_{\max_tolerance}$	source $TW_{\max_tolerance}$	purpose
North America					
Chum salmon	<i>Oncorhynchus keta</i>	cold	19.8	<i>Eaton and Scheller (1996)</i>	F, C, G
Pink salmon	<i>Oncorhynchus gorbuscha</i>	cold	21.0	<i>Eaton and Scheller (1996)</i>	F, C, G
Brook trout	<i>Salvelinus fontinalis</i>	cold	22.4	<i>Eaton and Scheller (1996)</i>	F, C, G
Mountain white fish	<i>Prosopium williamsoni</i>	cold	23.1	<i>Eaton and Scheller (1996)</i>	F, G
Coho salmon	<i>Oncorhynchus kisutch</i>	cold	23.4	<i>Eaton and Scheller (1996)</i>	F, C, G
Rainbow trout	<i>Oncorhynchus mykiss</i>	cold	24.0	<i>Eaton and Scheller (1996)</i>	F, C, G
Chinook salmon	<i>Oncorhynchus tshawytscha</i>	cold	24.0	<i>Eaton and Scheller (1996)</i>	F, C, G
Mottled sculpin	<i>Cottus bairdi</i>	cold	24.3	<i>Eaton and Scheller (1996)</i>	-
Blacknose dace	<i>Rhinichthys atratulus</i>	cool	27.2	<i>Eaton and Scheller (1996)</i>	-
White sucker	<i>Catostomus commersoni</i>	cool	27.4	<i>Eaton and Scheller (1996)</i>	F, C, G
Northern pike	<i>Esox lucius</i>	cool	28.0	<i>Eaton and Scheller (1996)</i>	F, C, G
North, Central and South America					
Longnose dace	<i>Rhinichthys cataractae</i>	cool	26.5	<i>Eaton and Scheller (1996)</i>	C
Johnny darter	<i>Etheostoma nigrum</i>	cool	26.5	<i>Eaton and Scheller (1996)</i>	-
Creek chub	<i>Semotilus atromaculatus</i>	cool	27.1	<i>Eaton and Scheller (1996)</i>	-
Bluntnose minnow	<i>Pimephales notatus</i>	warm	30.1	<i>Eaton and Scheller (1996)</i>	-
Black crappie	<i>Pomoxis nigromaculatus</i>	warm	30.5	<i>Eaton and Scheller (1996)</i>	F, G
Golden shiner	<i>Notemigonus crysoleucas</i>	warm	30.9	<i>Eaton and Scheller (1996)</i>	F, C
Emerald shiner	<i>Notropis atherinoides</i>	warm	31.8	<i>Eaton and Scheller (1996)</i>	F
Sand shiner	<i>Notropis stramineus</i>	warm	32.1	<i>Eaton and Scheller (1996)</i>	-
Black bullhead	<i>Amieurus melas</i>	warm	34.0	<i>Eaton and Scheller (1996)</i>	F, C, G
Flathead minnow	<i>Pimephales promelas</i>	warm	34.0	<i>Eaton and Scheller (1996)</i>	F
Europe					
Arctic char	<i>Salvelinus alpinus alpinus</i>	cold	16.0	<i>Baench and Riehl (1991)</i>	F, C, G
Spined loach	<i>Cobitis taenia</i>	cold	18.0	<i>Riehl and Baensch (1991)</i>	F
Burbot	<i>Lota lota</i>	cold	18.0	<i>Baench and Riehl (1991)</i>	F, C, G
Roach	<i>Rutilus rutilus</i>	cold	20.0	<i>Riehl and Baensch (1991)</i>	F, C, G
Wels catfish	<i>Silurus glanis</i>	cold	20.0	<i>Baench and Riehl (1991)</i>	F, C, G
Brown trout	<i>Salmo trutta</i>	cold	24.1	<i>Eaton and Scheller (1996)</i>	F, C, G
Freshwater bream	<i>Abramis brama</i>	cold	24.0	<i>Baench and Riehl (1991)</i>	F, C, G
Northern pike	<i>Esox Lucius</i>	cool	28.0	<i>Eaton and Scheller (1996)</i>	F, C, G
Africa					
Nile tilapia	<i>Oreochromis niloticus niloticus</i>	tropical	33.0	<i>Philippart and Ruwet (1982)</i>	F, C
North African catfish	<i>Clarias gariepinus</i>	tropical	35.0	<i>de Moor and Bruton (1988)</i>	F, C, G
Asia					
Mottled loach	<i>Acanthocobitis botia</i>	cool	26.0	<i>Baensch and Riehl (1985)</i>	-
Silver carp	<i>Hypophthalmichthys molitrix</i>	cool	28.0	<i>Li et al (1990)</i>	F, C
Grass carp	<i>Ctenopharyngodon idella</i>	tropical	35.0	<i>Laird and Page (1996)</i>	F, C
Black carp	<i>Mylopharyngodon piceus</i>	tropical	40.0	<i>Nico et al (2005)</i>	F, C

Global gridded datasets with mean distributions of fish species on 0.5° x 0.5° spatial resolution were downloaded from the Freshwater Biodiversity Maps of Aquamaps (http://www.aquamaps.org/main/home_fw.php) (Kaschner et al., 2010). These datasets represent species' distribution maps of the large-scale and current mean annual presence of a species in geographic space. The gridded maps are derived by combining numerical algorithms, that describe the relationships between known species' presence and selected environmental parameters (e.g. water depth, temperature, salinity), with expert knowledge and information on species habitat usage and occurrence. The datasets do not capture the effects of biological interactions (e.g. inter- or intraspecific competition, predation), which affect the actual presence or absence of species on smaller scales. For each fish species we selected all grid cells with current suitable habitats. Climate change impacts on thermal habitat conditions were subsequently assessed by calculating for each grid cell the occurrence and annual mean and maximum magnitude of exceeded $T_{W_{max_tolerance}}$ under both control and future climate. GCM ensemble mean changes in occurrence and magnitude of exceeded $T_{W_{max_tolerance}}$ were assessed for the SRES A2 and B1 scenario (2071-2100) relative to the control climate period (1971-2000). For each fish species, paired t-tests were applied to assess the significance of changes in occurrence and magnitude of exceeded $T_{W_{max_tolerance}}$ using the data for all gridcells with suitable habitat. While different fish species could have different responses to flow changes (Mims and Olden, 2012), limited information however exists regarding the magnitude to which species distributions are controlled by flow alterations. We defined uniform spatial patterns of large changes in streamflow habitat (i.e. more than 50% changes in seasonal flow amplitude, shifts in timing of high flow events of more than 30 days, or declines in low flow larger than 25%). For each fish species, the results of changes in exceeded $T_{W_{max_tolerance}}$ were combined with spatial patterns of large changes in streamflow habitat. Based on this, we identified for each fish species which parts of current suitable habitats are likely to be most strongly affected by climate change and related streamflow and water temperature changes.

6.3 Results

6.3.1 Impacts of streamflow changes on freshwater habitats globally

Global spatial patterns of changes in ecologically relevant flow indices, show increases in mean annual flow and associated streamflow habitat availability for the high northern latitude and parts of the tropical region (Figure 6.2a). Decreases are projected for the U.S., Central America, the central and southern Europe, Southeast Asia and southern parts of South America, Africa and Australia. Substantial increases (>25%) in mean flow (using the GCM ensemble mean changes) are projected for 28-42% and decreases for 6-10% of global surface area for 2071-2100 (SRES B1-A2) relative to 1971-2000. Spatial patterns of changes in high flow (Q_{95} , annual 1-, 7-, 30-day Q_{max}) strongly correspond with projected changes in mean flow (see Supplementary Figure C1 for changes in 30-day Q_{max}). Increases in annual mean high flow could increase habitat availability (e.g. for spawning) on flood plains, and could

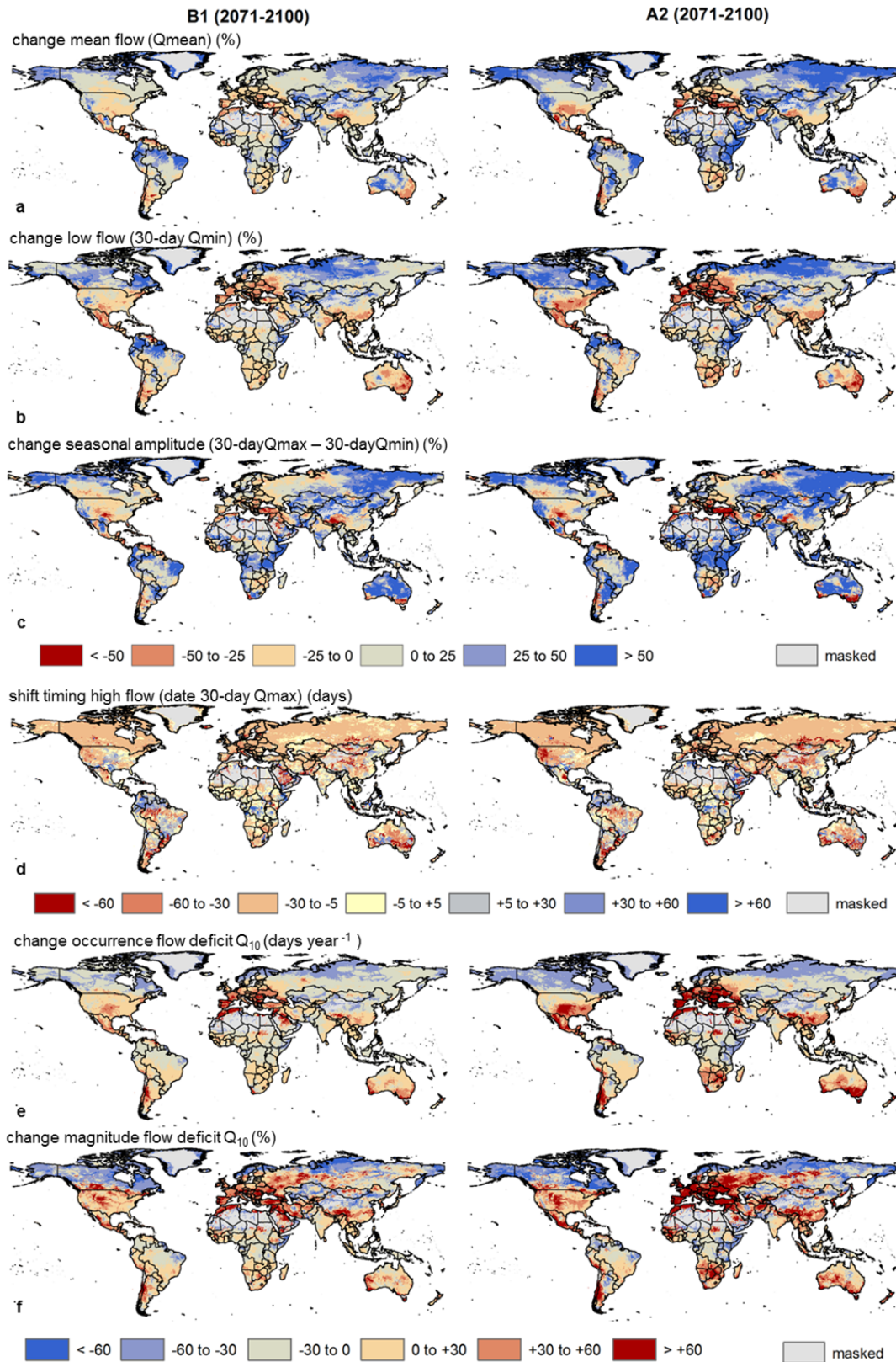


Figure 6.2: Global projected changes in annual mean flow (a), annual 30-day average minimum flow (b), seasonal flow amplitude (c), shift in 30-day average maximum flow (d) relative changes in occurrence (e) and magnitude (f) of flow deficits (with streamflow below threshold minimum flow) using fixed 10th percentile of river flow (under control climate) as threshold. The changes in flow indices are averaged for the three selected GCMs for both the SRES A2 and B1 scenario for 2071-2100 relative to 1971-2000. Regions with mean flow less than 1 m³ s⁻¹ are masked.

affect geomorphology of rivers (Ficke et al., 2007). Low flows (Q_{10} , annual 1-, 7-, 30-day Q_{min}) are likely to decline in the southern U.S., Central America, Europe (expect northern part), Southeast Asia, Australia, southern South America and southern Africa (Figure 6.2b for 30-day Q_{min}). In these regions, strong increases are also projected in the occurrence (mean number of days per year) and magnitude of streamflow deficits with streamflows below the threshold minimum flow values (Figure 6.2e-f). This could potentially deteriorate fish habitats in these regions, due to decreased habitat availability and connectivity of stream channels and deterioration of water quality (limited dilution capacity for pollutions) (Matthews and Marsh-Matthews, 2003). Substantial increases in seasonal flow amplitude are projected for 39-50%, while strong decreases (>25%) are expected for 9-11% (Figure 6.2c based 30-day Q_{min} and Q_{max}). Changes in seasonal flow amplitude could affect habitat characteristics and compatibility with life cycles of fish species (e.g. spawning). Overall, climate change will result in an earlier onset of the high flow (snowmelt) peak, especially in the high northern latitude zone (Figure 6.2d). For 10-12% of the global surface area this earlier onset is >30 days. A backward shift in high flow peak is mainly found for parts of the tropical regions (delay >30 days for 7-8% global surface area) and could be related to changes in onset of the monsoon period.

To identify regions with expected largest impacts of climate change on streamflow habitat characteristics, we combined areas with projected largest changes in seasonal flow amplitude, declines in low flow and shifts in timing of high flow for 2071-2100 relative to 1971-2000 (Figure 6.3). These integrated patterns of changes in streamflow habitat characteristics show strong (>50%) increases in seasonal flow amplitude for parts of the high northern latitude region and tropical region, substantial (>25%) declines in low flow for the southern U.S., Central and southern South America, Europe (except northern part), southern Africa, eastern China and parts of Australia. Largest shifts in the timing of high flow events (>30 days) are projected for central parts of Asia, South America and Africa, western part of North America and eastern Australia.

6.3.2 Impacts of water temperature changes on freshwater habitats globally

Global spatial patterns of changes in water temperature indices show largest increases in mean annual water temperature for the U.S., Europe, eastern China, and parts of southern Africa and Australia (Figure 6.4a). These regions are all characterized by strong declines in low flow (see Figure 6.2b), which are likely to exacerbate water temperature rises (van Vliet et al., in press). The combined effects of increased water temperatures and decreased streamflow during summer can be critical and will likely reduce the reproductive success for fish species populations with impacts varying for different watershed types (Mantua et al., 2010). Mean water temperatures are expected to increase by >1°C for 39-74% and >2°C for 10-33% of the global land surface area (for SRES B1-A2 for 2071-2100 relative to 1971-2000). Increases in high water temperatures are larger than in annual mean and low water temperatures. As a result, the seasonal thermal regime will increase with >1°C under future

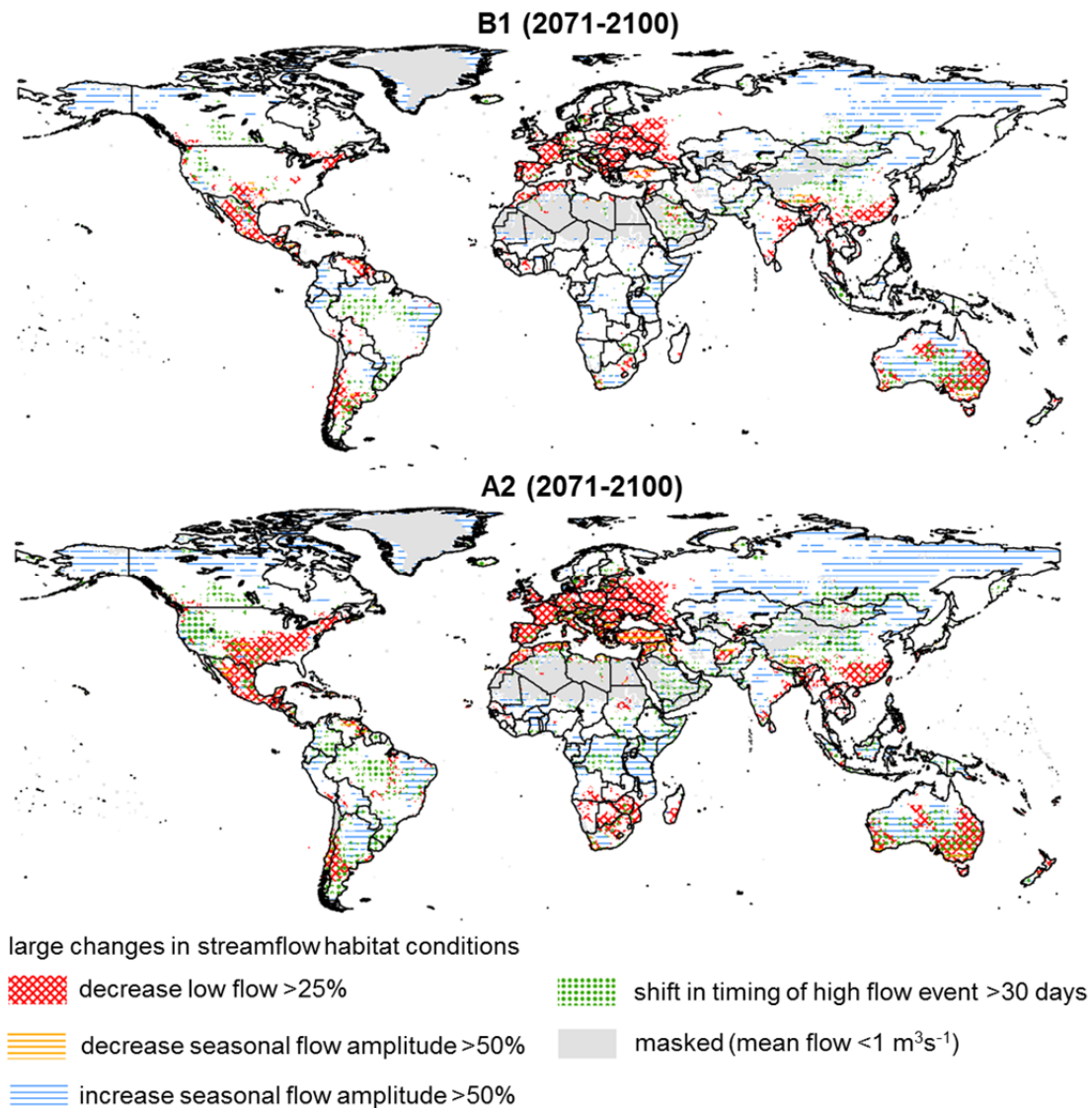


Figure 6.3: Regions with projected large changes in streamflow habitat characteristics. Regions are identified with large decreases in low flow (30-day Q_{min}), large decreases or increases in seasonal flow amplitude (based on 30-day Q_{min} and Q_{max}) and large shifts in timing of high flow (date 30-day Q_{max}) by more than 30 days.

climate for 65–66% (SRES B1-A2) of the global land surface area. The stronger increase in high water temperature is also relevant in terms of the probability of exceedance of maximum temperature tolerance values of fish species. High water temperatures are expected to increase on average by 1.0 – 2.2°C (1-day T_{wmax} and T_{w95} ; Figure 6.4b) and 1.0 – 1.9°C (annual 7- and 30-day T_{wmax}). Low water temperatures (T_{w10} , annual 1-, 7-, 30-day T_{wmin}) will increase on average with 0.4 – 0.9°C. In case regions with simulated water temperature of 0.5°C (indicating potential ice coverage on streams) are excluded, the global mean increase in low water temperature is 0.6 – 1.3°C. The mean number of days per year with critical low water temperatures of 0.5°C are expected to decrease with >15 days per year for 14-23% and >30 days per year for 1-10% of the global land surface area under future (SRES B1-A2 2071-2100) compared to control climate (1971-2000) (Figure 6.4c). Increases in low water

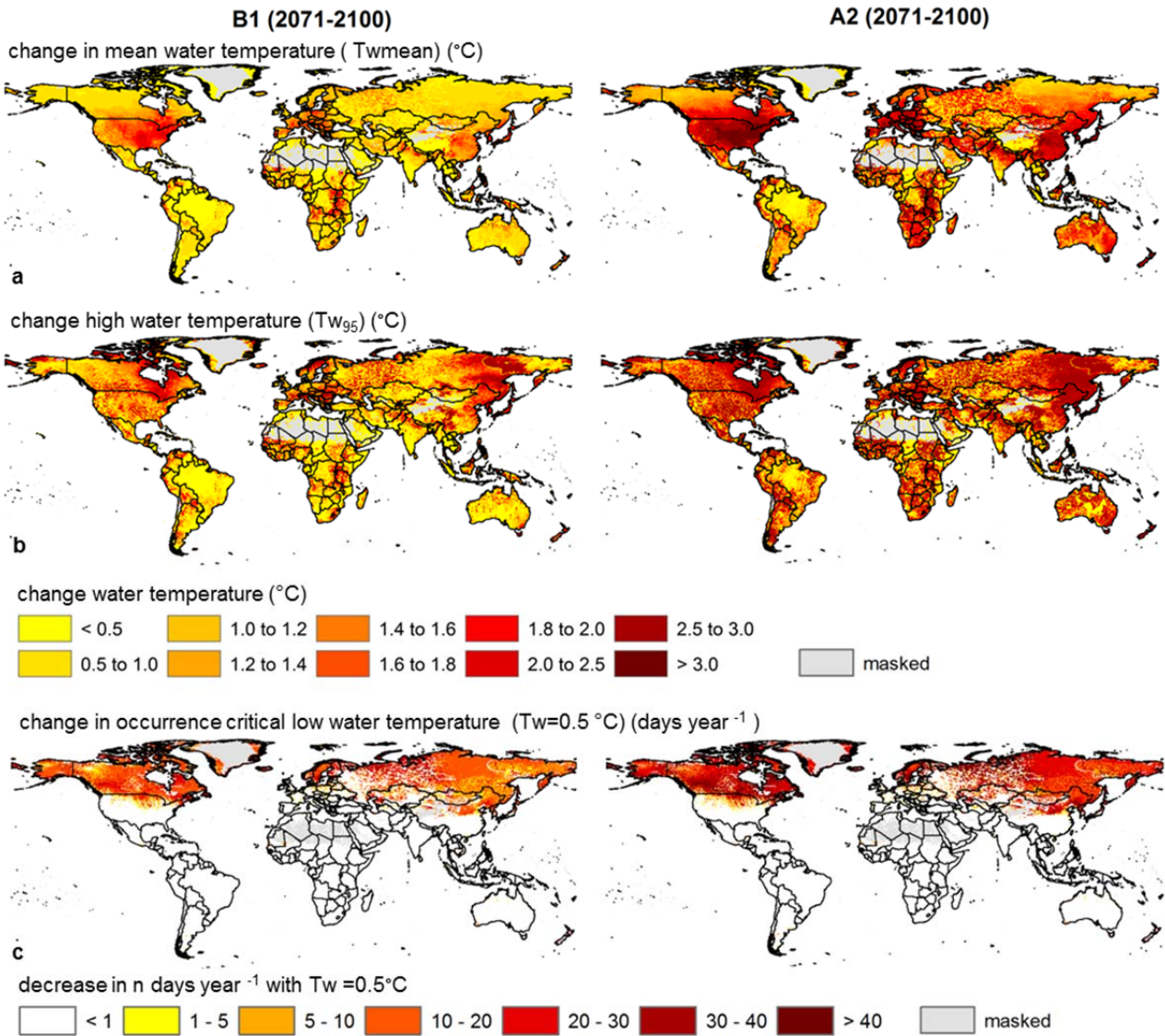


Figure 6.4: Global projected changes in mean water temperature (a), high (95-percentile) water temperature (b) and decrease in number of days per year with water temperatures of $0.5^{\circ}C$ (minimum temperature tolerance of cold water fishes) (c). The changes in water temperature indices are averaged for the three selected GCMs for both the SRES A2 and B1 scenario for 2071-2100 relative to 1971-2000. Regions with mean annual river flow less than $1\ m^3\ s^{-1}$ are masked.

temperatures and duration of ice-free periods under warmer climate could be beneficial by decreasing overwintering stress and extending the growing season (Coleman and Fausch, 2007). However, the reproductive success of temperate fishes can also be negatively affected by increases in low water temperatures (Ficke et al., 2007), because low overwinter temperatures (cold-tempering) are often essential for the spawning success of temperate fishes, such as salmonids (Gerdaux, 1998).

To assess the lateral distances over which thermal habitat zones are expected to move polewards under warmer climate, we show isolines and latitude-average values of mean

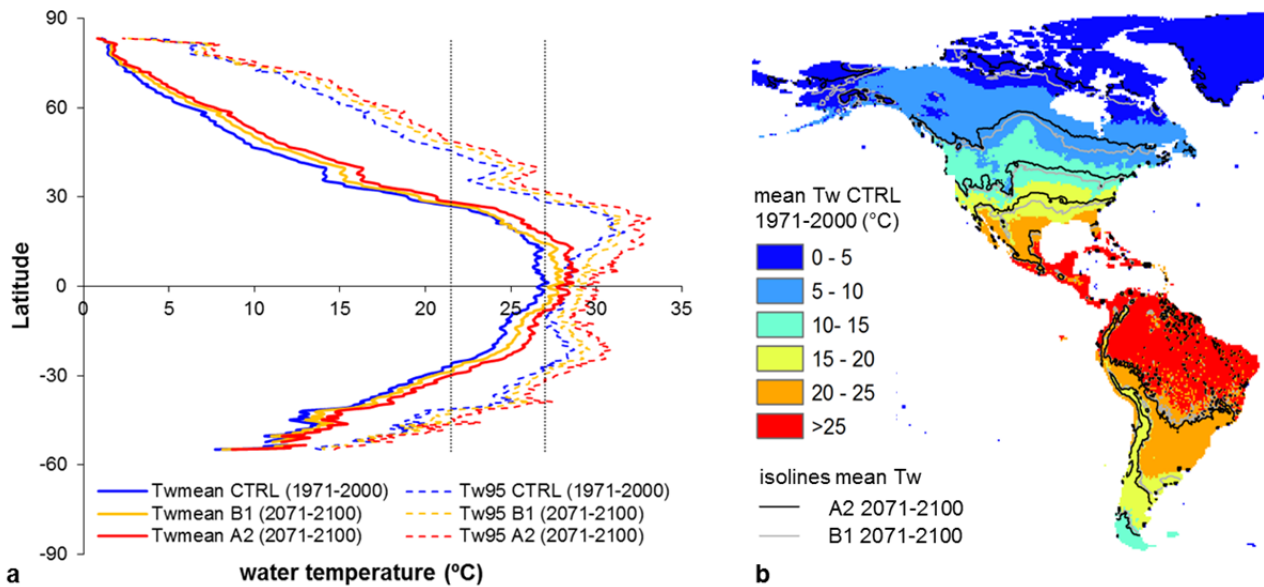


Figure 6.5: Global mean polewards movement of mean (T_{wmean}) and high (T_{w95}) water temperature (a) and movement of thermal zones in the Americas with mean annual water temperature classes for the control period 1971-2000 (colours) and isolines of mean water temperature for same classes for 2071-2100 under SRES A2 (black) and B1 (grey) scenario (b).

water temperatures for 2071-2100 relative to 1971-2000 (Figure 6.5). In addition, latitude-average values in 95th percentile values in water temperature (T_{w95}) are shown, because of the relevance of this water temperature statistic for testing exceedence of maximum temperature tolerance values for fish species (Eaton et al., 1995). The isoline (boundary) of $T_{w95} < 21.5^{\circ}\text{C}$ and $T_{w95} < 27.0^{\circ}\text{C}$ were selected, because these water temperature values indicate the average $T_{w_{max_tolerance}}$ for selected cold water and cool water fishes. The 21.5°C -isoline is expected to move northwards with approximately 190-400 km and southwards with 230-275 km (SRES B1-A2). The global land surface area with $T_{w95} < 21.5^{\circ}\text{C}$ is expected to decrease from 39% (1971-2000) to 32-35% for SRES A2-B1 (2071-2100). This reflects a potential decrease in suitable habitat for cold water fish species. For the 27°C -isoline, we found a movement of approximately 260-415 km (northern hemisphere) and 250-410 km (southern hemisphere). Overall, the global surface area with $T_{w95} > 30^{\circ}\text{C}$ is expected to increase from 14% (1971-2000) to 18-26% for SRES B1-A2 (2071-2100), which could reflect a potential decrease in suitable habitat for cold and cool water fishes, and increase for warm and tropical fish species.

6.3.3 Regional freshwater fish habitats under water temperature and streamflow changes

For each fish species, the magnitude and probability of exceeded $T_{w_{max_tolerance}}$ values under control (1971-2000) and future climate (2071-2000) were calculated for all grid cells with suitable habitat. For all selected fish species statistically significant ($p < 0.01$) increases in occurrence (mean number of days per year) and mean and maximum magnitude of exceeded $T_{w_{max_tolerance}}$ were found. Increases are highest for cold and cool water fish species in Europe,

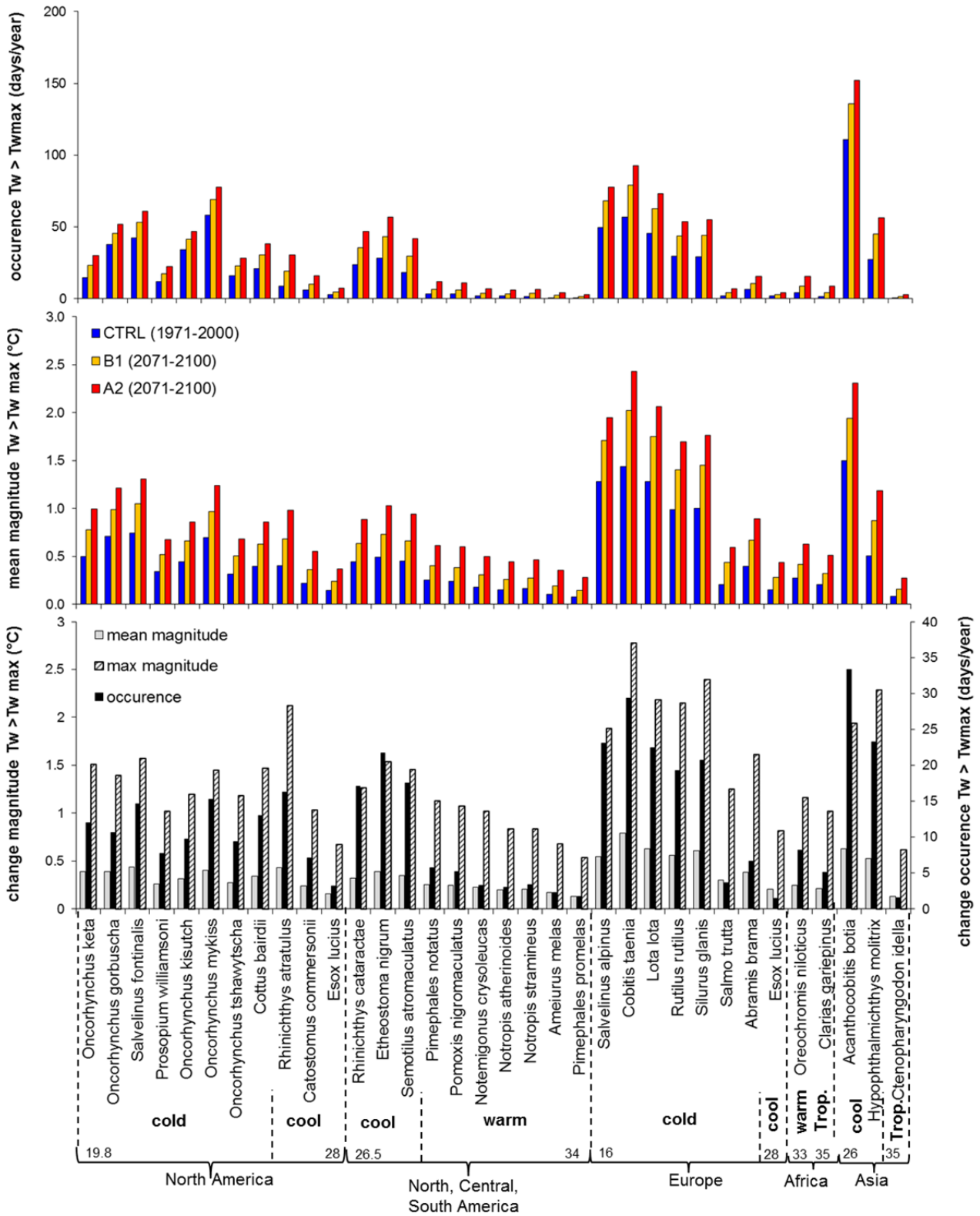


Figure 6.6: Mean number of days per year that maximum temperature tolerance values are exceeded (a), mean magnitude of exceeded water temperature limits (b) and relative change in number of days per year, and mean and maximum magnitude of exceeded water temperature limits (c) for control period (1971-2000) and SRES B1 and A2 scenario (2071-2100) using the ensemble mean changes for all six GCM experiments. The fish species are grouped per region and ordered from lowest to highest $T_{w,max_tolerance}$ with the values indicating the range for each geographic region.

North America and Southeast Asia (Figure 6.6). For most of these fish species $TW_{\max_tolerance}$ were already exceeded during 1971-2000. The highest increases in occurrence and magnitude of exceeding $TW_{\max_tolerance}$ correspond with projected highest increase in mean water temperature for these regions (Figure 6.4). The absolute increase in maximum magnitude of exceeded $TW_{\max_tolerance}$ is on average a factor of four higher than the increase in mean magnitude of exceeded $TW_{\max_tolerance}$.

Spatial patterns of changes in occurrence of exceeding $TW_{\max_tolerance}$, combined with regions of large changes in streamflow habitat characteristics are presented for seven fish species for control and future climate under SRES A2 in Figure 6.7. These fish species are situated in different regions and together cover a large range of $TW_{\max_tolerance}$ values (from 19.8°C for chum salmon (*Oncorhynchus keta*) in North America to 33.0°C for Nile tilapia (*Oreochromis niloticus niloticus*) in Africa). Curves combining the mean magnitude of exceeded $TW_{\max_tolerance}$, occurrence of exceedance (>5 and >20 days per year) and area (as fraction of current suitable habitat area) are shown for SRES B1 and A2 in Figure 6.8.

Overall, the number of days per year with exceeded $TW_{\max_tolerance}$ and magnitude of exceedance is expected to increase for considerable fractions of current suitable habitat areas under future climate (Figure 6.7 and 6.8). For chum salmon (*O. keta*) and chinook salmon (*O. tshawytscha*) in North America (Figure 6.7a-b), we found distinct increases in mean number of days per year with exceeded $TW_{\max_tolerance}$ for the central part of their spatial extents (i.e. region northern of Great Lakes). This was also found for pink salmon (*O. gorbuscha*) and coho salmon (*O. kisutch*) (see Supplementary Figure C2a-b). For black crappie (*Pomoxis nigromaculatus*) in the Americas (Figure 6.7c), overall highest increases in exceeded $TW_{\max_tolerance}$ are shown for the south-eastern United States. In this region, water temperature increases are high (Figure 6.4) and substantial (>25%) declines in low flow are projected. For wels catfish (*Silurus glanis*) and freshwater bream (*Abramis brama*) in Europe (Figure 6.7d-e) we found large increases in $TW_{\max_tolerance}$ exceedance combined with distinct declines in low flow for central and southern Europe. Relative increases in fraction area of suitable habitats with exceeded $TW_{\max_tolerance}$ are especially large for freshwater bream (Figure 6.8). For silver carp (*Hypophthalmichthys molitrix*) in Asia (Figure 6.7f), largest increases in exceeded $TW_{\max_tolerance}$ in combination with substantial declines in low flows are projected for the eastern part of China. Nile tilapia (*Oreochromis niloticus niloticus*) (Figure 6.7g) and North African catfish (*Clarias gariepinus*) (see Supplementary Figure C2c) in Africa has the highest $TW_{\max_tolerance}$ of the presented fish species. For both African fish species the occurrence and magnitude of exceeding $TW_{\max_tolerance}$ is low for the control period but increases considerably under future climate, as shown by the curves combining magnitude, occurrence and area of exceeded $TW_{\max_tolerance}$ for Nile tilapia (Figure 6.8). This could in combination with the projected large increases in seasonal flow amplitude (owing to large increases in high flow) affect habitat conditions for these tropical fish species.

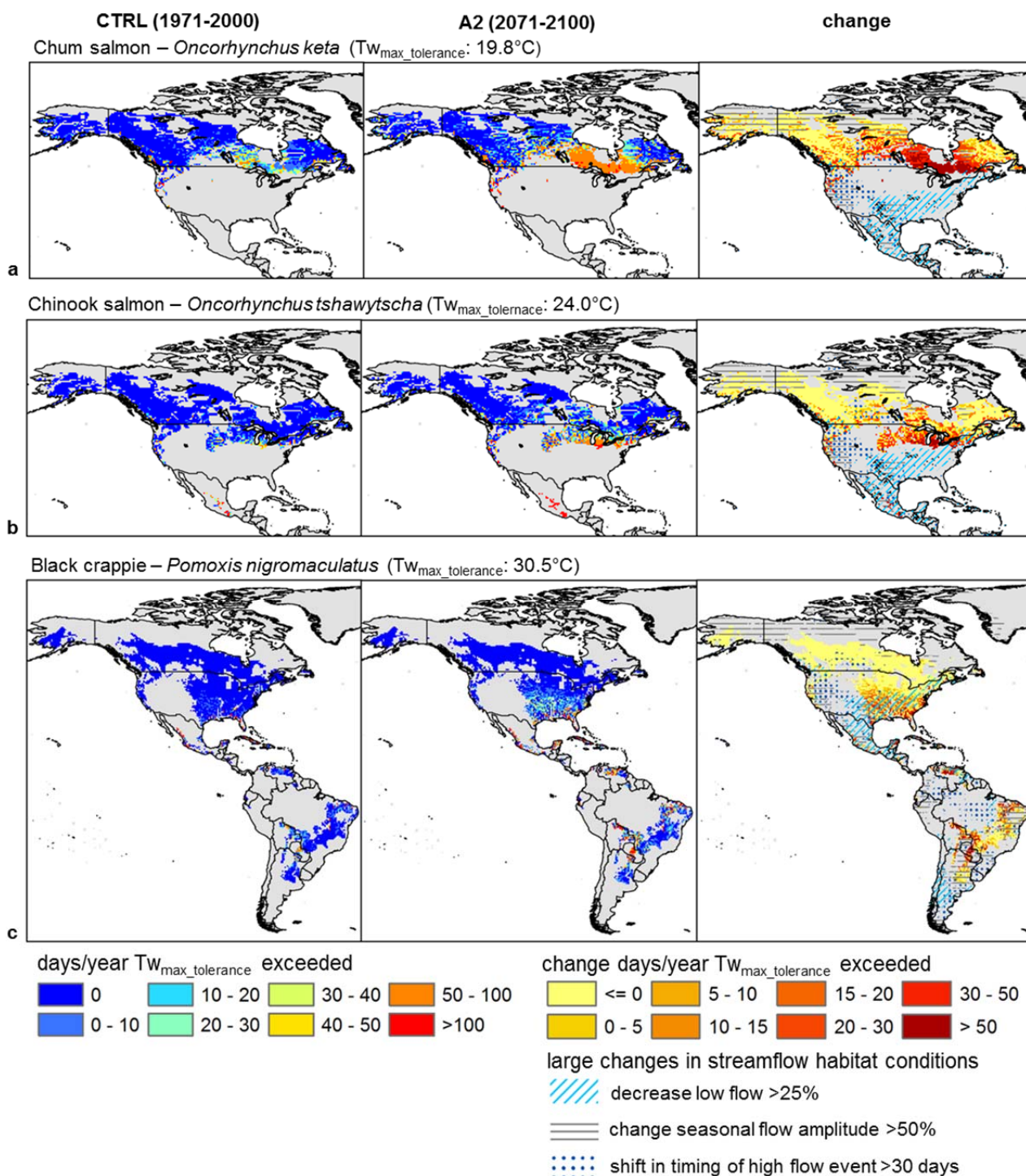


Figure 6.7a-c: Impact of water temperature increases on the occurrence (mean number of days per year) that $T_{w_{max_tolerance}}$ is exceeded of selected fish species in North America, Central and South America, combined with large changes in streamflow habitat conditions. Changes are presented for the period 2071-2100 for the SRES A2 scenario relative to 1971-2000 using the average of the three GCM experiments.

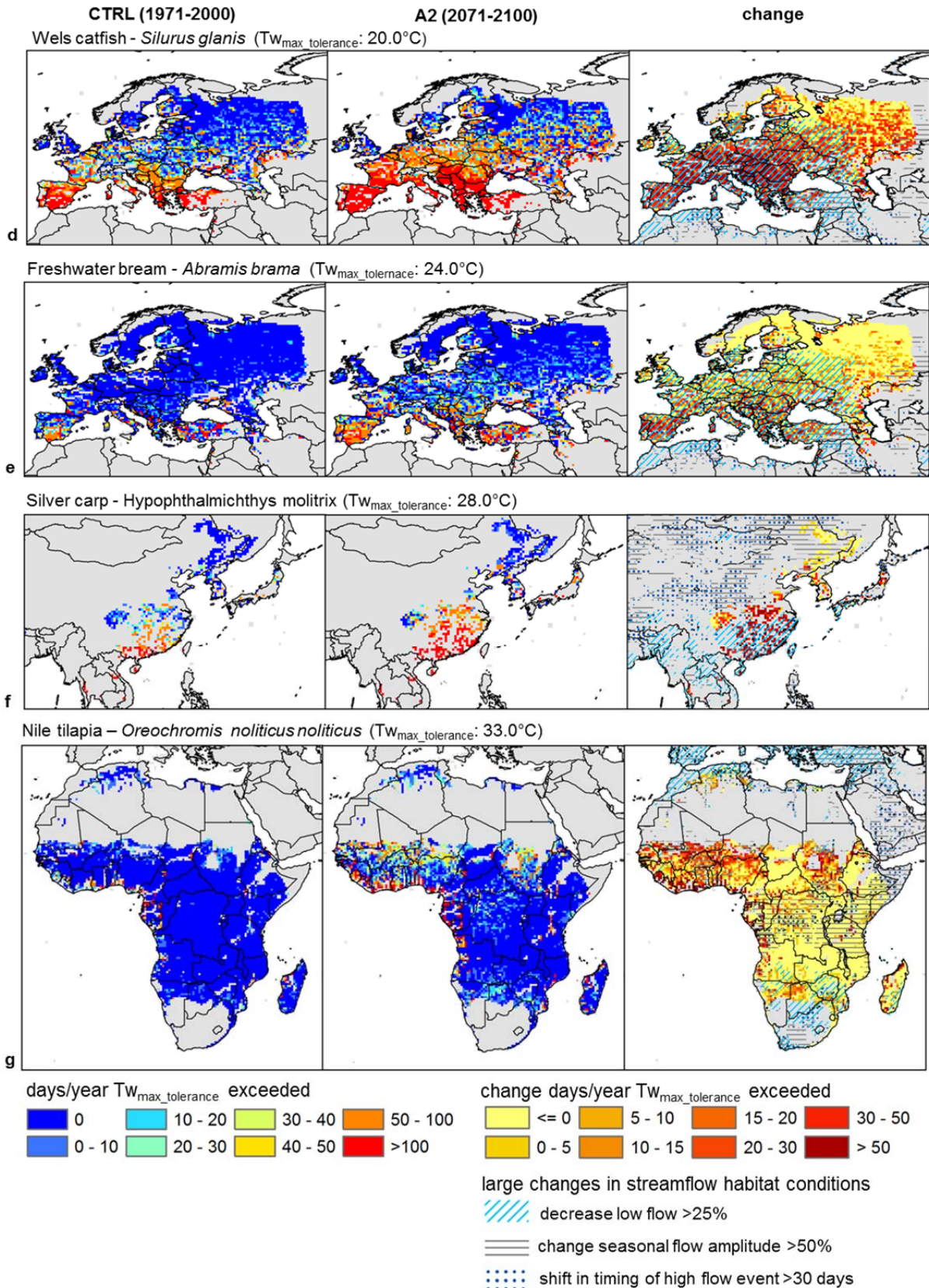


Figure 6.7d-g: Impact of water temperature increases on the occurrence (mean number of days per year) that $T_{w_{max_tolerance}}$ is exceeded of selected fish species in Europe, Asia and Africa, combined with large changes in streamflow habitat conditions. Changes are presented for the period 2071-2100 for the SRES A2 scenario relative to 1971-2000 using the average of the three GCM experiments.

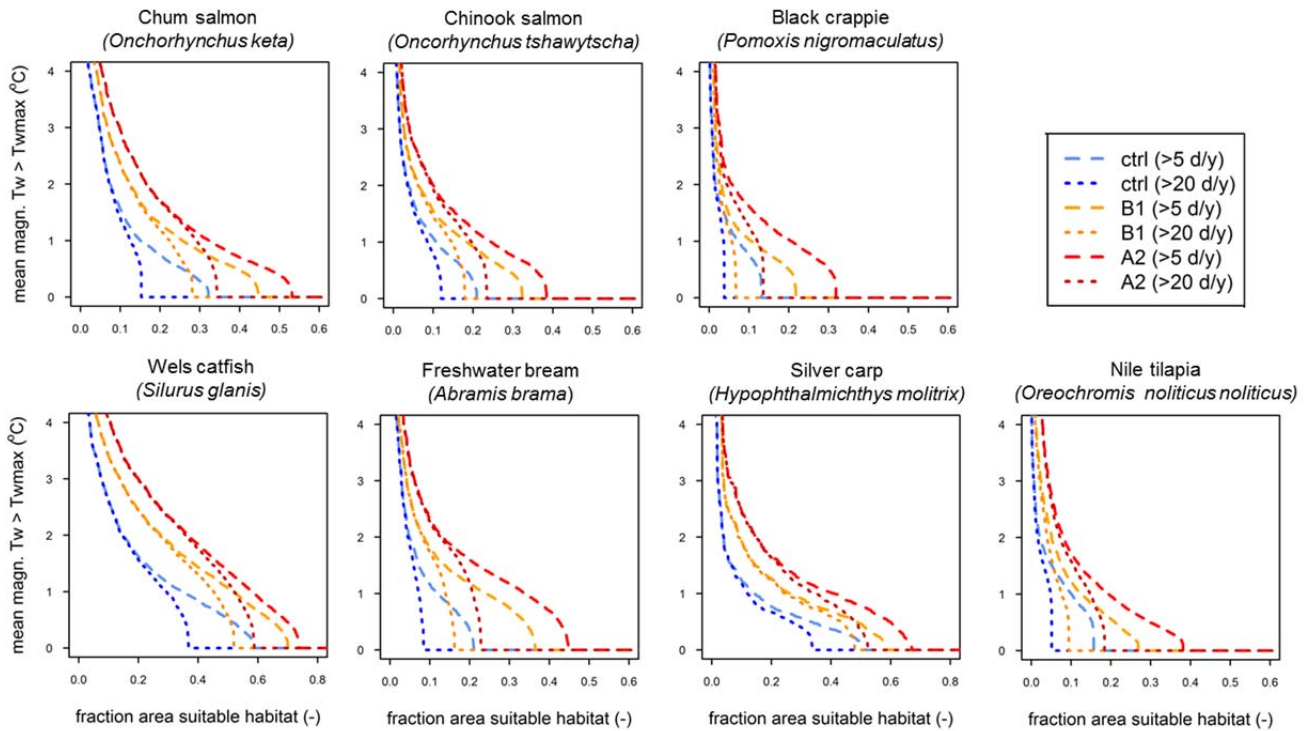


Figure 6.8: Curves combining mean magnitude, occurrence (>5 and >20 days per year) and fractional area of current suitable habitat with exceeded $T_{w_{max_tolerance}}$ for control (1971-2000) and future climate (2071-2100) for SRES B1 and A2 emissions scenario. The horizontal scale of the graphs for wels catfish and silver carp is different from the graphs for other species.

6.4 Discussion and conclusions

Our global results show that climate change will have distinct impacts on flow and thermal characteristics of freshwater fish habitat. Climate change will affect seasonal flow amplitudes, magnitude and timing of high and low flow events for large fractions of the global land surface area. Substantial decreases in mean streamflow are projected for the U.S., Central America, central and southern Europe, Southeast Asia and southern parts of South America, Africa and Australia. More importantly, relative decreases in low flows for most regions are larger than projected decrease in mean flows, and this is likely to reduce fish habitat availability. As expected, climate change will further increase water temperatures during the 21st century. Using a physically-based hydrological - water temperature modelling framework we were able to quantify the impacts of both atmospheric warming and changes in streamflow on water temperature (thermal habitat characteristics). Worldwide, largest mean water temperature increases are projected for the U.S., Europe, eastern China and parts of southern Africa and Australia. Most of these regions are also characterized by strong declines in low (summer) flow for the end of the 21st century, and this combination could in particular threaten fish populations (Connor et al., 2003). Overall, our results show that freshwater fish habitats and species distributions will not only be affected by climate change on a local level, as previously addressed for individual river systems (e.g. Mantua et al., 2010), but for large regions worldwide.

Many previous studies have indicated the impacts of uncertainty of climate change projections on simulated streamflow or river runoff changes (e.g. Chen et al., 2011; Haddeland et al., 2012; Sperna Weiland, 2011). Especially the impact of climate change on regional precipitation and river runoff can highly differ, depending on choice of climate model and/or emission scenario (e.g. Fowler et al., 2007a). To cover part of these uncertainties, the modelling framework was forced with an ensemble of bias-corrected GCM output to produce streamflow and water temperature projections for both a medium-high (SRES A2) and low (B1) emission scenario. A larger number of GCM outputs would better represent the structural uncertainty in climate models (Tebaldi and Knutti, 2007). However, the mean change in precipitation in the three climate models is similar as shown by all 21 models used in CMIP3 (Hagemann et al., in prep.). Also, the spatial patterns of changes in mean, annual high and low flow, and shifts in timing of high flow peaks generally correspond with results of other recent global hydrological model studies (Döll and Müller Schmied, 2012; Döll and Zhang, 2010; Sperna Weiland et al., 2012), despite different choices of climate models and hydrological impact models. Our global modelling projections under future climate change could therefore be considered as robust.

Global patterns of changes in streamflow and water temperature were used in combination with spatial extent of suitable habitats and maximum thermal tolerance values of fish species in different regions. We found significant increases in both the occurrence and magnitude of exceeding maximum temperature tolerance values of all selected fish species under future (2071-2100) compared to control (1971-2000) climate. Our results confirm outcomes of previous local and regional studies that showed reductions in suitable thermal habitats of cold water fishes (e.g. salmonides) for streams in North America under climate change (Mantua et al., 2010; Rahel et al., 1996). Chu et al. (2005) suggested that cold water fish species in Canada may be extirpated from a large part of their present range, while warm water species may expand northward. In our study, we quantified a northwards movement of the 21.5°C-isoline of approximately 190-400 km (northern hemisphere) and a reduction in global surface area with high water temperatures (T_{w95}) below 21.5°C (39% for 1971-2000 to 32-35% for 2071-2100). Hence, climate change is likely to reduce the spatial area of suitable habitats of cold water fishes, which could be invaded by cool or warm water species if other habitat requirements (e.g. food availability) are also fulfilled (Chu et al., 2005; Ficke et al., 2007; Mohseni et al., 2003).

Several previous studies focussed on either impacts of water temperature increases (e.g. Eaton and Scheller, 1996; Stefan et al., 2001) or streamflow changes (e.g. Xenopoulos et al., 2005). However, in particular the combination of alterations in water temperature and streamflow characteristics e.g. reduced low flows and higher water temperatures, could threaten fish populations. Prediction of future species distributions is, however, difficult due to uncertainties in the adaptive capacity of different fish populations to changes in streamflow and thermal habitat conditions. The duration over which water temperatures are below or above the minimum and maximum temperature tolerance values is also a relevant factor. However, for most fish species it is uncertain to what extent their distribution is affected by

the duration of water temperatures above or below the temperature tolerance values. Physiological adaptation to thermal habitat changes occurs at a local level, and depends on the population and genetic diversity, as shown for sockeye salmon in the Fraser River (Eliason et al., 2011). There is also a strong need for an improved understanding of adaptive response of freshwater (fish) species to streamflow changes (Arthington et al., 2010) and, in particular, to the combination of streamflow and thermal habitat changes.

Our results show a need for the development of adaptation strategies to minimize habitat loss. This is not only relevant in terms of biodiversity conservation, but also for future fisheries and food production (FAO, 2008). An obvious measure to reduce habitat loss is to minimize anthropogenic activities that affect the quality of the river systems habitats, such as limits on human water extractions during low flow periods. However, this could increase conflicts with human water use sectors (e.g. agriculture, energy and domestic uses) that commonly have highest water demands during warm, dry periods. Reductions in thermal pollution of rivers would be desirable to reduce water temperature increases, especially during periods with high water temperature and low flow (limited dilution capacity for thermal effluents). In the United States and Europe, strict regulations exist for the maximum temperatures of water discharged by thermoelectric power plants. However, in case these regulations are maintained, the thermoelectric power sector in the U.S. and Europe could be seriously hampered over the next 20-50 years (van Vliet et al., 2012b). To prevent strong reductions in electricity production potentials, the thermoelectric power sector would benefit by more flexible regulations (i.e. higher water temperature and extraction permits), but this could negatively affect freshwater (fish) habitats.

While changes in anthropogenic impacts (e.g. water use extractions, reservoir regulation and thermal pollution) will affect future streamflow and water temperature on a local (subbasin) level, climate change will inevitably impact streamflow and thermal habitats on a larger scale. River management and conservation strategies should therefore take into account that both streamflow and thermal characteristics of freshwater habitats are changing on a large scale due to climate change, and this is expected to affect species distributions.

Acknowledgements

This study was funded by the European Commission through the FP6 WATCH project and through the FP7 ECLISE project. Kathleen Reyes of the FishBase Information and Research Group, Inc. (FIN) is gratefully acknowledged for supplying data of suitable habitat distributions of selected fish species. We would like to thank Ingjerd Haddeland of the Norwegian Water Resources and Energy Directorate for supplying data of global irrigation water extractions. Martina Flörke and Frank Voß of University of Kassel are kindly acknowledged for supplying global datasets of other human water uses.

Synthesis

7.1 Introduction

Worldwide, the pressure on water between freshwater ecosystems and different water use sectors is expected to increase due to climate change and increasing water demands under a growing global population. Several macro-scale hydrological studies addressed the impacts of climate change on global water resources (e.g. Alcamo et al., 2007; Arnell, 1999a; Döll and Müller Schmied, 2012; Sperna Weiland et al., 2012), but with a clear focus on water quantity. However, climate change is also likely to increase river temperatures on a large scale, and combined with changes in river flow patterns this may have direct consequences for human water uses, like cooling use, and freshwater ecosystems.

This study therefore focussed on the effects of climate change on global river temperatures and river flows, and the potential consequences for cooling water use in the energy sector and freshwater ecosystems. Four research questions were defined (Chapter 1) and addressed (Chapter 2-6). For the first question, we evaluated the performance of both a statistical and physically-based water temperature model. Both models were further developed and used for the first time on a worldwide level. A global database with observed daily water temperature series (from different data sources) was developed and used to evaluate modelling performances. Both the statistical and physically-based modelling approach were used to obtain more robust estimates of the sensitivities of river temperature to river flow changes under current climate variability (Chapter 2 and 3). For the second question, this study quantified and combined the effects of climate change on both river flows and water temperatures globally, and showed which regions will experience largest river temperature and flow changes (Chapter 4). In a next step, a translation was made from hydrological and water temperature impacts to the consequences for electricity supply on a large scale. We quantified how electricity production in Europe and the United States could be affected by changes in cooling water availability and water temperatures under future climate (Chapter 5). In addition, we addressed the consequences of climate change on flow and thermal habitat characteristics of fish species in different regions worldwide (Chapter 6). Dependencies of both the energy sector and freshwater ecosystems on climate, water availability and water temperature have not previously been addressed on such a large scale. The main results of this study are summarized in Table 7.1. In the next section of this chapter the four research questions and results are discussed in a broader context. In addition, the contribution to science and water management, and an outlook for further research on this topic are given.

Table 7.1: Overview of research questions and main results and conclusions. Abbreviations are used for water temperature (Tw) and river flow (Q) (see Figure 1.7 for schematic representation of methodological framework used to address these research questions).

research question	main results and conclusions
<p>Q1: Performance of statistical and physical Tw modelling, and sensitivity Tw to Q changes? (Chapter 2 and 3)</p>	<ul style="list-style-type: none"> Realistic daily Tw estimates were obtained with both the statistical and physically-based Tw modelling approach. Although modelling errors for the physical model were slightly higher, better performances for locations with limited data availability were obtained. The physically-based Tw model is also more suitable for extrapolation (in space and time) and for scenario analyses (e.g. climate change impact). Both modelling approaches showed moderate impacts of Q on mean Tw values, but significant impacts on high Tw extremes. This shows the importance of incorporation of hydrological conditions in Tw modelling to obtain more realistic Tw estimates, especially during dry, warm spells.
<p>Q2: Effects of climate change on Q and Tw globally? (Chapter 4)</p>	<ul style="list-style-type: none"> Climate change is likely to increase Q seasonality for about one-third of the global land surface area. Consistent increases in mean Q are projected for the high northern latitudes and parts of the tropical region. Decreases in mean and low Q are projected for the U.S., Central America, Europe, Southeast Asia, and the southern parts of South America, Africa and Australia. Global mean Tw is projected to increase on average by 0.8–1.6°C for the SRES B1-A2 scenario for 2071-2100 relative to 1971-2000. Largest Tw increases are projected for the U.S., Europe, eastern China, and parts of southern Africa and Australia, where the sensitivities of Tw are exacerbated by decreases in low Q. These regions could potentially experience a deterioration of water quality, freshwater habitats and reduced potentials for human water uses under climate change.
<p>Q3: Impacts on cooling water use and thermoelectric power production? (Chapter 5)</p>	<ul style="list-style-type: none"> Lower summer Q combined with higher Tw under future climate will increase environmental restrictions on cooling water use in the U.S. and Europe. This could result in substantial reductions in thermoelectric power production, especially in the south-eastern U.S. and southern Europe. Considering expected increases in electricity and water demand, there is a need for improved climate adaptation strategies to ensure future water and energy security, without compromising environmental objectives.
<p>Q4: Impacts on freshwater (fish) habitats? (Chapter 6)</p>	<ul style="list-style-type: none"> Freshwater (fish) habitats are likely to change for large regions worldwide due to rising Tw combined with changes in Q characteristics (e.g. seasonal amplitude, timing and magnitude of low and high Q). Thermal habitat zones are expected to move pole wards. Significant increases in both the frequency and magnitude of exceeding maximum Tw tolerances of freshwater fish species in different regions were found. This could, in combination with changes in Q regime, affect species distributions, depending on the adaptive capacity of freshwater (fish) species.

7.2 Discussion of main results

7.2.1 Global hydrological - water temperature modelling under current climate variability and sensitivities (Q1)

Performance of statistical and physically-based water temperature model

Both a statistical (regression) and physically-based (heat transport) water temperature modelling approach were used to estimate river temperatures globally, and to quantify the sensitivities to river flow changes. The performances of both water temperature modelling approaches were evaluated using observed daily water temperature series for river stations on a global scale.

The nonlinear water temperature regression model of Mohseni et al. (1998) was modified to include river discharge as independent variable, in addition to air temperature, and to apply the regression model on a daily time step (Chapter 2). This resulted in a significant improvement in water temperature estimates, especially during warm and dry periods. Despite its simplicity, the modified regression model was able to estimate daily water temperatures for present-day climate (1980-1999) with a reasonable performance (Chapter 2, median RMSE of 1.8°C for global GEMS/Water stations). Differences in performances were mainly explained by the number of water temperature measurements to fit relations. As the regression model was fitted for point (station) locations and for a specific period, the approach is limited in application for extrapolation, such as spatially-variable water temperature projections under changing climate. However, the regression modelling approach was useful to explore sensitivities of daily water temperature distributions to changes in air temperature (reflecting atmospheric energy input) and river discharge (reflecting thermal capacity and dilution capacity for thermal effluents) under current climate variability. The results showed largest impacts of river flow on water temperatures during warm, dry spells. Hence, the results of the regression modelling provided the rationale for use of a coupled hydrological - water temperature modelling framework in this study.

The heat transport model RBM (Yearsley, 2009), linked to the VIC macro-scale hydrological model (Liang et al., 1994), was further developed to apply RBM on a global scale and to improve water temperature simulations for river basins which are strongly affected by reservoirs and heat effluents of thermoelectric power plants (Chapter 3). The performance of the VIC-RBM framework for daily river discharge and water temperature simulations was evaluated at river basin (Chapter 3), continental (Supplementary Information B) and global level (Supplementary Information A). Overall, simulated daily water temperatures generally correspond well with observations. Compared to the regression modelling approach, however, slightly higher values of RMSE (Chapter 3, Table 3.3; median of 2.8°C and range of 1.6 to 6.7°C for study basin stations) were obtained, although it should be kept in mind that RBM was not directly calibrated. In addition, an overall better performance with RBM was found for stations with limited availability of measurements (< 150) to fit the regression

model (Figure 7.1). This indicates the usefulness of this heat transport modelling approach for areas with limited or no availability of water temperature measurements.

Overall the best water temperature modelling estimates with RBM were found for river basins in the temperate climate zone, while water temperatures in the tropical region were on average slightly overestimated (see Table 3.3 (e.g. Mekong); Supplementary Figures A2–A3 (global validation)). This overestimation is likely due to overestimations in incoming shortwave radiation, partly related to the neglect of vegetation shading effects. Some underestimations were found in water temperatures during summer for high northern latitude rivers (see Table 3.3 (e.g. Ob, Yenisey, Lena); Figures A2–A3 (global validation)). This could be due to the neglect of impacts of complex snowmelt processes on the water temperature simulations.

Significant improvements in water temperature estimates with RBM were obtained in thermally polluted basins (Rhine, Meuse, Danube, Mississippi) by implementing heat discharges as advected heat sources in the heat transport equation. In addition, the use of a reservoir routing model and corrected geometry - streamflow relations significantly improved river discharge and water temperature modelling in highly regulated basins, like the Columbia. Incorporation of vertical stratification and mixing in reservoirs and lakes could further improve water temperature estimates downstream of reservoirs. The newest VIC version is able to simulate lake water temperatures (Bowling and Lettenmaier, 2010), and could be linked to the reservoir routing model and RBM. As this step requires detailed information of outlet depths of reservoirs, and vertical water temperature profiles, which are rather difficult to collect on macro-hydrological scale, a focus on selected regulated basins with sufficient data availability is recommended.

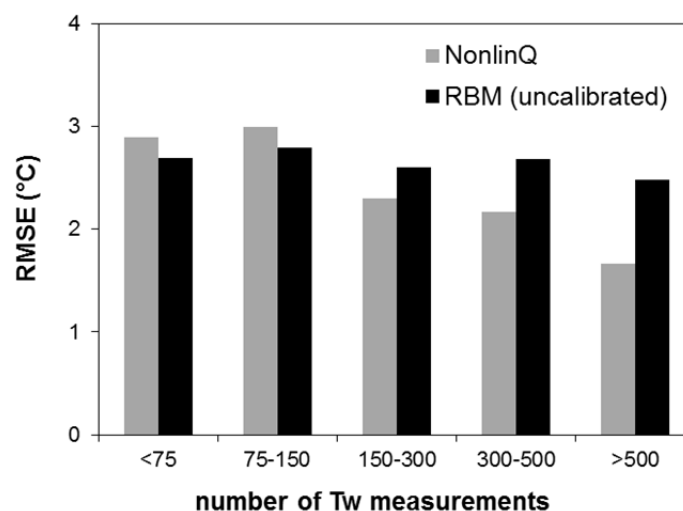


Figure 7.1: Comparison of median RMSE ($^{\circ}\text{C}$) for daily water temperature estimates using the nonlinear water temperature regression model NonlinQ (including river discharge as independent variable) and the heat transport model RBM. Median values of RMSE are based on water temperature simulations (1980-1999) with both modelling approaches for the same monitoring stations globally.

Further implementations to the VIC-RBM modelling framework (such as improved representation of frozen soils and snowmelt on water temperatures, vegetation shading and thermal stratification in reservoirs and lakes) and calibration are recommended to improve water temperature estimates. A relevant improvement of the VIC hydrological model for simulations of extreme low flow (streamflow droughts) would be to explicitly model the representation of groundwater. However, considering the general objective of this study, we believe the VIC-RBM framework produces spatially-variable daily river flow and water temperatures estimates with an acceptable performance for further sensitivity analyses and for climate change impact assessment on macro-hydrological (continental, global) scale.

Sensitivity of water temperatures to river flow changes

Both the regression and heat transport modelling approach were used to assess the sensitivity of water temperatures to changes in river flow. While contrasting conclusions of the magnitude of river discharge changes on water temperatures were reported by previous studies, showing limited effects (e.g. Crisp and Howson, 1982; Webb and Nobilis, 2007) or substantial effects of river flow changes (Sinokrot and Gulliver, 2000; Webb et al., 2003), consistent results were obtained for both modelling approaches used in this thesis. Overall, moderate effects of river flow on water temperatures in mean values were found, but significant impacts on the outer ranges, and especially high water temperature extremes (Chapter 2 and 3). Decreases in river flow reduce the thermal capacity, which increases the sensitivity to atmospheric warming and cooling, especially when river discharges (volumes and flow velocities) are low and atmospheric energy input is high. In addition, reductions in river flow also reduce the dilution capacity for thermal effluents, which contributes to nonlinear increases in water temperature in thermally polluted rivers. An increase in river flow has an opposite impact on water temperature and extremes.

The magnitude of sensitivities of water temperatures to streamflow changes were compared for both modelling approaches using simulations for river stations in 14 study basins globally (described in Chapter 3). Overall, the calculated sensitivities in mean and maximum water temperatures are comparable for both approaches. For minimum water temperatures, RBM, however, shows smaller sensitivities to river flow changes than the regression model (Table 7.2). Smaller impacts of river flow changes on minimum water temperatures are expected in high latitude regions, because water temperatures remain around freezing point during winter (see Section 3.3.5; Figure 3.9). In addition, the impact of changes in dilution capacity for thermal effluents, which is explicitly included in RBM, is opposite to (partly counterbalances) the effects of thermal capacity changes. This can result in smaller decreases (or even slight increases) in minimum water temperatures in thermally polluted basins under decreasing river flow and atmospheric cooling (see for example Figure 3.10, Danube station).

Table 7.2: Impacts of changes in river flow on minimum, mean and maximum water temperatures (°C). Mean absolute differences in water temperature statistics are calculated based on water temperature simulations under river flow changes of -50%, -25%, +25% and +50% and reference water temperature simulations for both the heat transport model RBM and regression model NonlinQ (including discharge). The differences are calculated with both modelling approaches for the same water temperature monitoring stations in different hydro-climatic zones and with different anthropogenic impacts (see river basins Chapter 3).

	-50%Q		-25%Q		+25%Q		+50%Q	
	RBM	NonlinQ	RBM	NonlinQ	RBM	NonlinQ	RBM	NonlinQ
minimum Tw	-0.3	-1.3	-0.2	-0.5	+0.1	+0.3	+0.2	+0.5
mean Tw	+0.4	+0.6	+0.1	+0.2	-0.0	-0.1	-0.1	-0.1
maximum Tw	+1.0	+1.2	+0.3	+0.4	-0.2	-0.2	-0.4	-0.3

To conclude, realistic water temperature estimates were obtained on daily time step with both the statistical (regression) and physically-based (heat transport) modelling approach. Although modelling errors for the physically-based RBM model were slightly higher, RBM is more suitable for extrapolation (in space and time) and for scenario analyses (e.g. climate change impact) than the regression model. Both modelling approaches were consistent in showing moderate impacts of river flow on mean water temperature values, but significant impacts on especially high water temperature extremes. This shows the importance of incorporation of hydrological conditions in water temperature modelling to obtain realistic water temperature estimates, especially during dry, warm spells.

7.2.2 Effects of climate change on global river flow and water temperatures (Q2)

The VIC-RBM modelling framework was forced with an ensemble of bias-corrected climate model output to assess global river flows and water temperatures under climate change, and to identify in which regions impacts will be largest. Prior to these results, we discuss the impacts of uncertainties in GCM output on simulated river flow and water temperature for historic (control) climate.

Impacts of uncertainties in GCM output

In this thesis, a chain of impact models (VIC hydrological model – routing model – RBM water temperature model – thermoelectric power production model) was forced with climate model output (Chapter 4-6). This results in a ‘cascade of uncertainty’ (Schneider, 1983) whereby uncertainty accumulates throughout the process of climate change projections and impact assessment. We used output of three GCMs for both the SRES A2 and B1 emissions scenario to reflect some uncertainties arising from different socio-economic storylines, climate model structures and parameterizations, notwithstanding that the use of a larger number of GCM outputs would better represent the structural uncertainty in climate models (Fowler et al., 2007a; Sperna Weiland, 2011; Tebaldi and Knutti, 2007).

The VIC-RBM modelling framework was forced with statistically bias-corrected GCM output of precipitation and air temperature. We used a minimum of forcing variables into VIC (bias-corrected precipitation, air temperature and uncorrected wind speed) to reduce impacts of uncorrected GCM output of radiation, humidity and wind speed data, which considerably affect evapotranspiration and runoff estimates (Haddeland et al., 2012). In this case, vapor pressure, incoming shortwave and net longwave radiation are calculated based on precipitation and minimum and maximum temperature, using algorithms developed by Kimball et al. (1997), Thornton and Running (1999) and Bras (1990), as described by Nijssen et al. (2001b). Although it should be kept in mind that uncertainties are also associated with estimating these variables internally within VIC, overall better results for the control simulation period were obtained when the forcing was restricted to bias-corrected precipitation, temperature and (uncorrected) wind speed. The statistics for simulated daily river discharge and water temperature for the control simulations of the GCMs correspond well with the simulations using the observed forcing dataset and observed values (Chapter 4, Figure 4.2). While river discharge simulations are used as input into the RBM water temperature model, we found an overall greater robustness (i.e. persistence of the system under uncertainties in input) for the water temperature predictions compared to the river discharge predictions. This is mainly because water temperature is, in contrast to river flow, less strongly affected by precipitation and its uncertainties, which potentially have a large impact on simulated river discharge on a global scale (Biemans et al., 2009; Fekete et al., 2004; Voisin et al., 2008). This shows that a larger cascade of impact models does not necessarily increase the uncertainties throughout the modelling chain.

Climate change impacts on river flows and water temperatures

Global projections of river flow and water temperatures under climate change were obtained by forcing the VIC-RBM modelling framework with bias-corrected GCM output for both the SRES A2 and B1 emissions scenario. Our results project an increase in the seasonality of river discharge (increase in high flow and decrease in low flow) for about one-third of the global land surface area for 2071-2100 relative to 1971-2000 (Chapter 4). Consistent increases in mean flow for the tropical region and the high northern latitudes (with an earlier start of the snowmelt peak) are projected for the different GCM experiments. Our results show consistent decreases in mean flow for the U.S., southern and central Europe, Southeast Asia and southern parts of South America, Africa and Australia. These results generally correspond with previous global hydrological model studies (Arnell, 2004; Döll and Zhang, 2010; Milly et al., 2005; Nijssen et al., 2001a; Sperna Weiland et al., 2012), despite different choices of emission scenarios and GCMs and different hydrological models that were used. Low (10th percentile) flows are projected to decrease, especially in the southern U.S., Central America, Europe (except northern part), Southeast Asia, Australia and southern parts of South America and Africa.

Global mean and high (95th percentile) water temperatures are projected to increase on average by 0.8–1.6 (1.0–2.2)°C for the SRES B1-A2 scenario for 2071-2100 relative to 1971-

2000. Moderate water temperature increases are projected for the tropical basins due to dominant impacts of increased evaporative cooling and back radiation under warmer conditions. Largest increases in mean water temperature are projected in the U.S., Europe, eastern China, and parts of southern Africa and Australia, where the sensitivities of river temperatures are exacerbated by projected declines in low flows.

Strong declines in low flow (>25%) combined with high water temperature increases (>2°C) are mainly projected for the south-eastern U.S., central and southern Europe and eastern China (see Figure 4.8). These regions could potentially experience an increased deterioration of water quality, freshwater habitats and reduced potentials for human water uses, such as thermoelectric power and drinking water, under future climate. Figure 7.2 shows these regions hatched (based on results for 2071-2100 SRES A2) combined with global gridded population counts (CIESIN, 2005) and gross domestic product (GDP) (IIASA, 2007) for the year 2000. Especially Europe and eastern China are regions with relatively high population densities and counts. In total 1.2 billion people currently live in regions that are expected to experience large declines in low flow combined with high water temperature increases. This number is expected to increase to 1.8 billion in 2070, using population scenarios for SRES A2 (IIASA, 2007). From economic perspective, the developed regions (U.S. and Europe) and the economically fast growing China, are expected to experience largest declines in (low) flow and strongest increases in water temperature, while the economic consequences, for instance, the costs of insufficient water availability and high water temperatures (e.g. for cooling water use in energy and industrial sector) are also highest in these parts of the world. Regions with projected large declines in low flow combined with high water temperatures currently represent 39% of global GDP. In this respect, the economic impacts of changes in river flows and water temperatures are expected to be largest for the developed regions of the world.

To conclude, climate change is expected to increase river discharge seasonality for one-third of the global land surface area. Largest water temperature increases are mainly projected for the U.S., Europe and eastern China, where sensitivities are exacerbated by declines in low flow. In these regions, the socio-economic impacts of large river temperature increases and declines in low (summer) flow could be potentially large (e.g. for beneficial uses like cooling water use in energy and industrial sector, and drinking water production).

7.2.3 Impact on cooling water use and thermoelectric power production (Q3)

For the third question, we quantified how river flow and water temperature changes under future climate can affect thermoelectric power production (Chapter 5). This part focussed on Europe and the U.S., where most electricity is currently produced by thermoelectric power plants that depend on water resources for cooling. In addition, both regions already experienced reductions in electricity production during recent warm, dry periods with low river flow and high water temperatures.

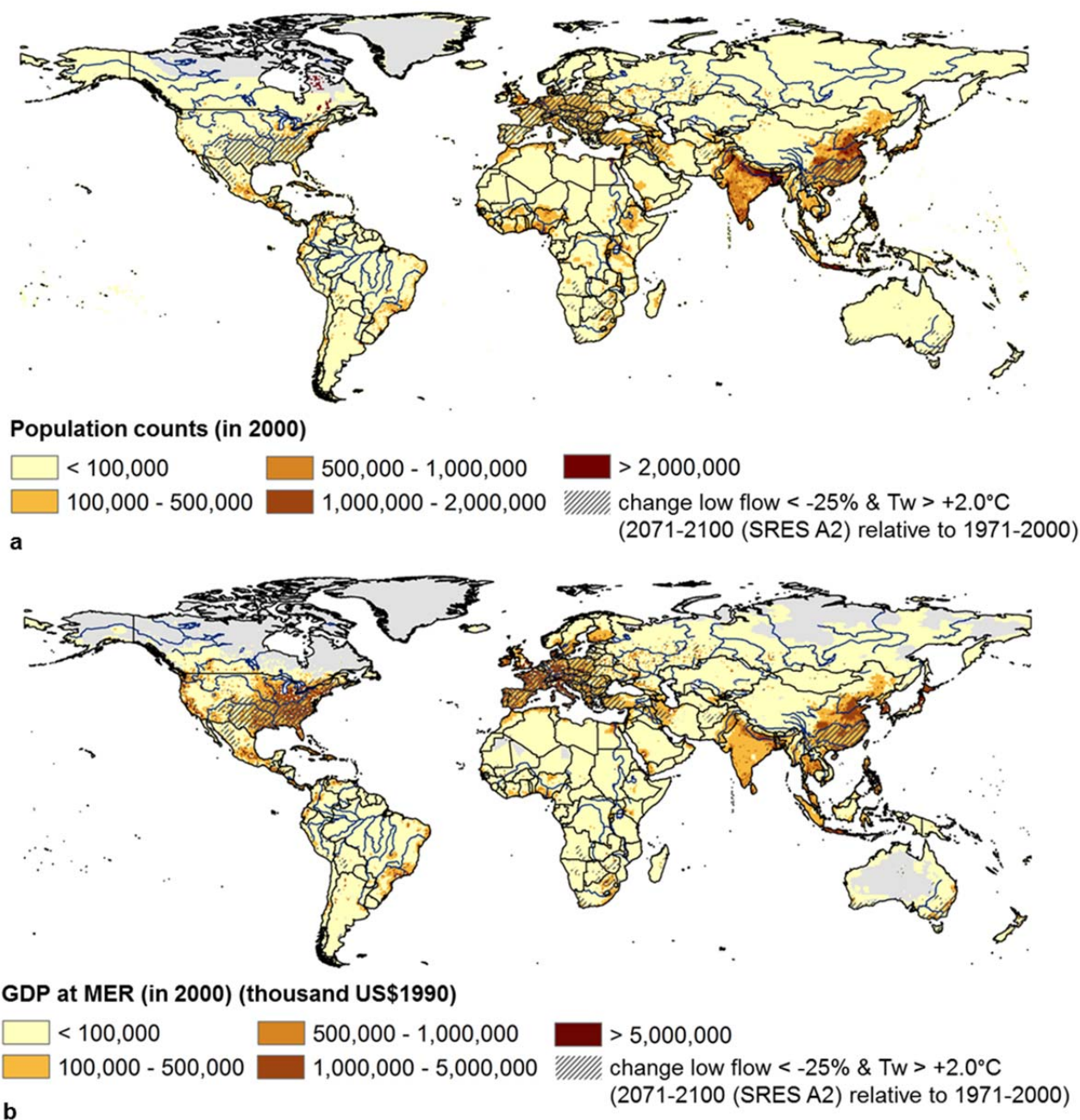


Fig 7.2: Regions with strong declines in low flow combined with high increases in water temperature for SRES A2 2071-2100 (relative to 1971-2000), and global gridded population counts (CIESIN, 2005) (a) and gross domestic product (GDP) at market exchange rates (MER) (IIASA, 2007) (b) in 2000.

Overall, the results show that projected water temperature increases and declines in low summer flows for both regions are likely to increase cooling water shortage and environmental restrictions on thermal discharges. This can result in substantial reductions in electricity production potentials of thermoelectric power plants in both the U.S. and Europe. For 76% of the power plants with once-through or combination cooling systems and 41% of the power plants with recirculation (tower) cooling systems electricity production potentials will be reduced significantly. The summer mean usable capacity of power plants with once-through or combination cooling systems is projected to decrease by 12-16% (U.S.) and 13-

19% (Europe) (B1-A2 SRES emissions scenario for 2031-2060). For recirculation (tower) cooling systems, the decrease in usable capacity during summer is much lower, but non-negligible (on average 6.3-8.0% for power plants in Europe and 4.4-5.9% in the U.S.). In particular, thermoelectric power plants in south and south-eastern U.S. and southern Europe could be affected by climate change. Considering the expected increase in electricity demand in both regions and globally (GEA, 2012), there is a need for improved climate adaptation strategies. Adaptation strategies could be defined for the thermoelectric power sector specifically (e.g. new cooling technologies and non-freshwater sources for cooling as alternatives). However, the vulnerability of the whole energy sector will be lower under a rapid transition to renewable energy resources than in future world with many (fossil-fuelled) power plants still in need of cooling water. Hence, an increase in diversity of energy resources is, therefore, recommended to decrease the vulnerability of the energy sector to climate change.

While this study focussed on thermoelectric power plants, the industrial sector could also be affected by changes in cooling water availability. Several industrial processes need cooling water to operate efficiently (e.g. refineries, paper mills, steel mills, petrochemical manufacturing). A cross-sectoral water use study that includes cooling water use for both thermoelectric power and manufacturing could be a next research step. In addition, integration with the potential impacts on hydropower would also provide a more complete 'picture' of how climate change could affect water for electricity production. In Europe and the U.S., 16% and 6% (EIA, accessed 2011) (data for 2008) of the total electricity is currently produced by hydropower. Lehner et al. (2005) provided a first assessment of the impacts of climate change on river discharge and hydropower potential of Europe. Their results show an average decrease in hydropower potential for Europe by 6% for the 2070s, with a projected increase for Scandinavia (with 15-30% and above) and decreases for southern Europe (with 20-50% and more). Given these results, both thermoelectric and hydroelectric power production potentials are projected to decline in the southern part of Europe. This urges a need for a transition to alternative energy resources (e.g. solar and wind energy) in this region, without compromising environmental objectives to compensate for reductions in summer flow and increasing water temperatures.

To conclude, lower summer flows combined with higher water temperature under future climate are expected to increase environmental restrictions on cooling water use, with substantial reductions in thermoelectric power production (especially in southern Europe and the south-eastern U.S.). Considering the increases in electricity demand, there is a strong need for improved climate adaptation strategies in the energy sector.

7.2.4 Impacts on freshwater (fish) habitats (Q4)

For the final research question, we addressed the consequences of climate induced streamflow and water temperature alterations for freshwater fish habitats in different regions worldwide. We focussed on fish habitats, because fish species are in particular strongly adapted to a certain level of flow variability, and all freshwater fish species are exotherms,

meaning that water temperature changes will directly affect fishes' biochemical reaction rates and physiology.

Global streamflow and water temperature projections under current and future climate were used in combination with ecologically relevant flow and water temperature indices to identify regions with largest changes in streamflow and thermal habitats (Chapter 6). For most regions with largest projected water temperature increases (e.g. U.S., Europe, eastern China, and parts of southern Africa and Australia) also strong declines in low flow are projected, and this could in particular threaten fish populations (Connor et al., 2003). Also large shifts in timing of low and high flow events (e.g. North America, central parts of Asia, South America and Africa, and eastern Australia) and strong changes in seasonal flow amplitude (e.g. high northern latitudes and tropical region) could affect habitat characteristics and compatibility with life cycles of fish species (e.g. spawning).

Increasing water temperatures under future climate are expected to result in a pole wards movement of thermal habitat zones in the order of 200-400 km (for cold and cool water fishes) for 2071-2100 relative to 1971-2000. As a result, the global surface area with suitable habitat for cold water fishes is expected to decrease (from 39% for 1971-2000 to 32-35% for 2071-2100), while habitats for warm and tropical fishes could increase (from 14% to 18-26%).

Streamflow and water temperatures projections were also combined with spatial distributions and thermal tolerances of fish species (with large geographic distributions) in the Americas, Europe, Africa and Southeast Asia. Overall, the results show significant increases in both the frequency and magnitude of exceeding maximum temperature tolerance values of all fish species. Combined with changes in streamflow characteristics (seasonal amplitude, timing and magnitude of high and low flow), this will affect the physical conditions of freshwater habitats. Although the adaptive capacity of fishes to changing hydrologic and thermal regimes could be highly variable (depending on the population and genetic diversity), our results show that fish habitats are likely to change for large regions. This could affect fish populations and species distributions, which is not only relevant in terms of biodiversity and conservation, but also for future food production and fisheries (FAO, 2008; Ficke et al., 2007; Williams, 1996). River basin management and conservation strategies should therefore focus on minimizing habitat loss, for example by reducing human pressure of large water withdrawals and thermal pollution as much as possible, especially during low flow conditions.

To conclude, increasing water temperatures combined with river flow changes under future climate will affect freshwater (fish) habitats for large regions worldwide. Thermal habitat zones are expected to move polewards. Increased exceedences of maximum temperature tolerance values of freshwater species combined with streamflow changes are likely to affect freshwater (fish) species distributions, depending on the adaptive capacity of species.

7.3 Scientific contribution

While integrated hydrological and water temperature modelling approaches have been successfully applied for small-scale catchments (e.g. Caissie et al., 2007; Haag and Luce, 2008; St-Hilaire et al., 2000), considerably less work was done at coarse (continental, global) scales. Although macro-scale hydrological models have been widely applied to simulate river discharge (commonly on monthly or annual basis), only one study is known to us that assessed water temperature on a macro-hydrological scale (van Beek et al., 2012). This thesis is the first study that quantifies and combines climate change impacts on both river temperatures and flows on a global scale. Robust estimates were obtained with both a statistical (regression) and physically-based water modelling approach under current climate variability, showing considerable impacts of river flow changes on water temperatures, especially during dry, warm conditions. This study therefore assessed the effects of climate variability and change on water temperatures by including both the direct effects of atmospheric warming and indirect effects of changes in river flow.

For the evaluation of the performances of water temperature models, a global database of observed daily water temperature series was created using observation records of water temperature of the United Nations GEMS/Water database and water temperature records provided by various sources (e.g. river basin management commissions, researchers, online databases). The database and the global simulations of water temperature and river flow produced in this study provide new opportunities for research, for example global assessment of water quality and ecosystem health in relation to climate change.

We have identified which regions are characterized by strong declines in low river flow combined with high increases in water temperatures under climate change. These areas could potentially experience an increased deterioration of water quality, freshwater habitats, and reduced potentials for beneficial uses, such as thermoelectric power production. This provides opportunities for case studies in these regions to address potential consequences for human water use sectors and freshwater ecosystems in more detail.

This study shows the vulnerability of the electricity sector in the U.S. and Europe to climate change. An integrated modelling approach of large-scale hydrological and water temperature models and a thermoelectric power production model was used for the first time, and was forced with different socio-economic and climate change scenarios. We show that especially the combination of lower summer flows and higher water temperatures under future climate will result in significantly high (and nonlinear) reductions in electricity production potential. To our knowledge, no previous studies have quantified the climate, water and energy dependencies on such a large scale. These results can be used by a broad scientific community involved in water, energy, climate and socio-economic research. The results could, for example provide a basis for economic assessments, such as impacts on electricity exchange prices or calculations of optimal adaptation within the thermoelectric power sector.

In addition, a translation was made from macro-hydrological impacts to the consequences for freshwater fish habitats on macro-ecological scale. While most previous studies focussed on individual river systems and on either impacts of streamflow or water temperature, our integrated results show that freshwater fish habitats and species distributions are likely to change for large regions worldwide. The results provide possibilities for ecological studies on large scales. Global water temperature and streamflow series could, for example, be used to derive quantitative relations between freshwater species assemblages, streamflow and water temperature. These relations could be useful to improve understanding of freshwater ecosystem responses in relation to alterations in hydrological and thermal regimes, and to define 'environmental flows' (flows to be allocated for the maintenance of freshwater ecosystem health and services (Dyson et al., 2003; Tharme, 2003)).

Overall, this is the first large-scale study that addresses the increasing pressure on water between freshwater ecosystems and cooling water use in the energy sector, considering both the changes in river flow and temperature under climate change. The results and modelling framework of this study could contribute to cross-sectoral studies addressing the linkages between human water uses (energy, industry, agriculture and domestic uses) and freshwater ecosystems for the next decades.

7.4 Contribution to water management

For effective management of water and freshwater ecosystems, high temporal resolution (e.g. daily) estimates of streamflow and water temperature are required, since water quality standards for protecting freshwater ecosystems are based on time periods of the order of days rather than months. The global modelling framework of this study was, for that reason, tested for daily time step simulations. Notwithstanding that a direct calibration of the VIC-RBM modelling framework and further implementations (e.g. improved representation of groundwater, soil heat and snowmelt) are recommended, the framework shows potential for providing useful information for large-scale water management. For instance, the modelling framework can be used for risk and scenario analyses, and has potential for operational use (now- and forecasting of streamflow and water temperature) on continental and global scale.

Recent warm, dry periods, raised concern of the consequences of higher water temperatures and lower summer flows on freshwater ecosystems and electricity supply in the U.S. and Europe. To anticipate and adapt to changes in cooling water availability, the projected changes in river flow, water temperature, and quantified impacts on power plant production capacity could be useful for climate services for the energy sector in the U.S. and Europe. While the simulations were performed on a coarse ($0.5^\circ \times 0.5^\circ$) spatial resolution, the results are consistent in showing that especially the combination of lower summer flows and higher water temperatures will result in significantly high reductions in thermoelectric production potential. In addition, this study shows that climate change is expected to exacerbate the pressure on the water in the energy sector. Considering the projected decreases in cooling

water availability during summer in combination with the long design life of power plant infrastructure, adaptation options should be included in today's planning and strategies to meet the growing electricity demand in the 21st century.

In addition, we addressed how climate change could affect large-scale fish habitats, due to changes in both river temperature and flow patterns. The results could be used to define future river basin management and conservation strategies, which should take into account that streamflow and thermal characteristics of freshwater habitat are likely to change on a large scale. Overall, conflicts between water for freshwater ecosystems and cooling water use in the energy sector are expected to increase under climate change. This urges the need for improved river basin conservation strategies and adaptation strategies in the energy sector to assure future water and energy security and ecosystem health.

7.5 Outlook and directions for further research

This thesis focussed on climate change impacts on river flow and water temperatures on a global scale, and addressed the potential consequences for cooling water use in the energy sector and freshwater habitats. Although the focus of this study has been limited to climate change impacts, the modelling framework of this study has the potential to address impacts of other aspects of global change (e.g. land use change) that are likely to affect freshwater resources and ecosystems during the 21st century. A next step would, for instance be to include also impacts of land use and water use changes (including reservoir construction, future water extractions and heat effluents of power plants and industries).

For further research on the combined impacts of climate change and land use changes on water resources, new climate and land use scenarios based on representative concentration pathways (RCPs) (Moss et al., 2010) (see Section 1.4) could be used. While it is not yet clear whether the new scenarios based on RCPs will show different impacts compared to the previous scenarios, an important advantage is that the new scenarios provide opportunities to study impacts of climate change and socio-economic changes separately. For instance, the vulnerability of the thermoelectric power sector to climate change could be assessed for climate scenarios based on one specific RCP (emission scenario), but using a set of different corresponding Shared Socioeconomic Pathways (SSPs; socio-economic scenarios with different focusses on mitigation versus adaptation) (IPCC, 2012).

In addition to new scenarios for climate research, alternative impact assessment approaches could be used for decision making and climate adaptation policies, such as the use of 'adaptation tipping points' (Kwadijk et al., 2010) or 'adaptation turning points' (Werners et al., 2012) (ATPs) in water management. ATPs are critical points where the magnitude of alterations due to climate change is such that current management practices and policies will no longer be able to meet the objectives. The ATP-approach starts at the opposite end of the impact chain. First, threshold values and the resilience of sectors of concern are defined. In a next step, projections of future climate (impacts) are used to assess the expected time left

when the critical points (thresholds) will be reached. An ATP-approach was used to study whether a reintroduction of Atlantic salmon in Rhine basin could be sustainable under projected water temperature rises during the 21st century (Bölcher et al., submitted). A comparable approach could be used to explore the expected time left until the production capacities of thermoelectric power plants are no longer able to meet the growing electricity demand.

Another logical next research step to be taken is testing of adaptation strategies. While not all adaptation strategies could be directly implemented in VIC-RBM, the modelling framework could provide a basis, for instance, for testing whether flow regulation (construction of reservoirs) could be used as an adaptive measure to regulate low flows and high water temperatures during warm, dry periods. In addition, the modelling framework could be optimized to explore new suitable production sites with sufficient cooling water availability for thermoelectric power under future climate.

The concept of 'water footprints' (total volume of freshwater used to produce goods and services) (e.g. Hoekstra and Mekonnen, 2012) could be useful in the decision making of which adaptation measures are suitable to reduce the pressure on water by the energy sector. Recently, water footprints of bioenergy (Gerbens-Leenes et al., 2009) and electricity from hydropower (Mekonnen and Hoekstra, 2012) have been quantified. Regarding thermoelectric power, it would, for instance, be interesting to assess how a switch in energy source (e.g. from coal- to nuclear- or gas-fuelled) or cooling system (e.g. from once-through to tower cooling) of power plants will affect water footprints.

Considering the growing recognition of the need for information about climate change impacts on water quality (Kundzewicz and Krysanova, 2010; Whitehead et al., 2009) and health issues, an extension of the modelling framework to other water quality parameters, which are affected by water temperature (e.g. dissolved oxygen), streamflow (e.g. chloride, fluoride) or both (nutrients, chlorophyll-a (algae), pathogens) could be a next step. The stream temperature model RBM used in this study has potential to include other water quality parameters, because of the strength of the semi-Lagrangian numerical scheme with regard to accuracy and computational efficiency (Yearsley, 2009).

Implementation of water quality in macro-scale hydrological models could also be an important step to obtain more realistic projections of large-scale water resources and competition between water use sectors in relation to climate change. Most water use sectors require not only sufficient water availability (quantity), but also suitable water quality. As pointed out in this study, water temperature is a critical parameter for cooling water use of thermoelectric power plants and industries, while salinity and nutrient concentrations are important for agricultural and domestic (drinking) water uses.

This study shows an increase in pressure on water between cooling water use in the energy sector and freshwater ecosystems under future climate. Overall, conflicts between water for human uses (agriculture, energy, industry and domestic uses) and ecosystems are expected to increase under climate change and a growing global population. We therefore need to better understand how water, food and energy security can be ensured in the future without compromising on the needs that ecosystems have on water. A cross-sectoral analysis of the competition for water between different water use sectors and freshwater ecosystems under future climate and land use changes will be a next step. This could provide improved understanding of how global change (climate change, land use changes) will affect the developments of the 'water-energy-food-ecosystem nexus' (i.e. complex linkages among water, energy and food security, and ecosystem health). Overall, improved understanding of the relations between water resources (water availability and quality) and cross-sectoral water uses, including water needs for ecosystems, will be an important step towards solutions for sustainable water, food and energy supply in the coming decades.

Global River Discharge and Water Temperature under Climate Change (Chapter 4)

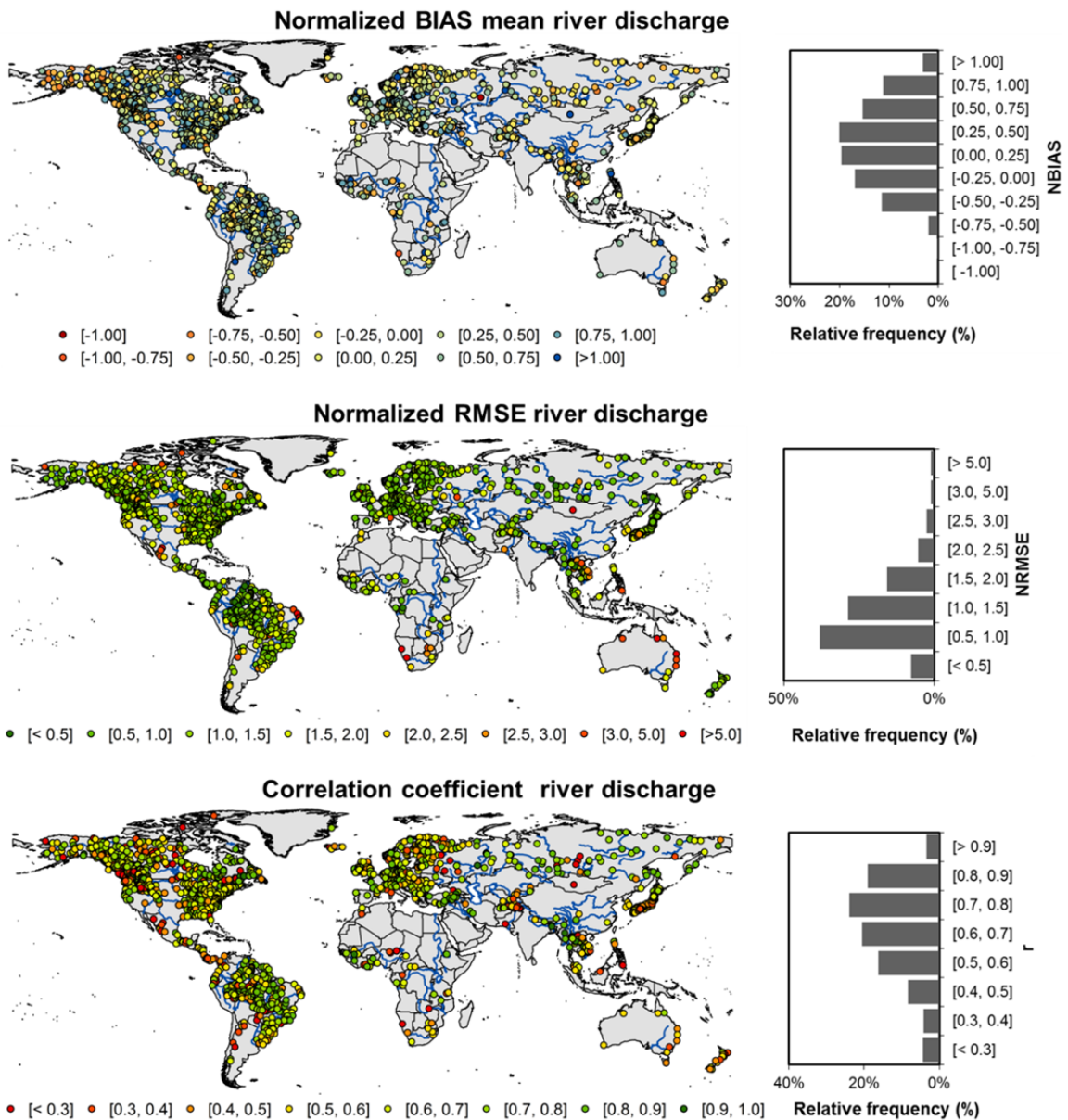


Figure A1: Performance of hydrological modelling for current climate. Global maps of normalized mean bias, normalized root mean squared error (RMSE) and Pearson correlation coefficient for simulated daily river discharge using the historical WATCH forcing data (WFD) as input to the VIC model and observed daily river discharge series of 1612 GRDC stations globally for 1971-2000.

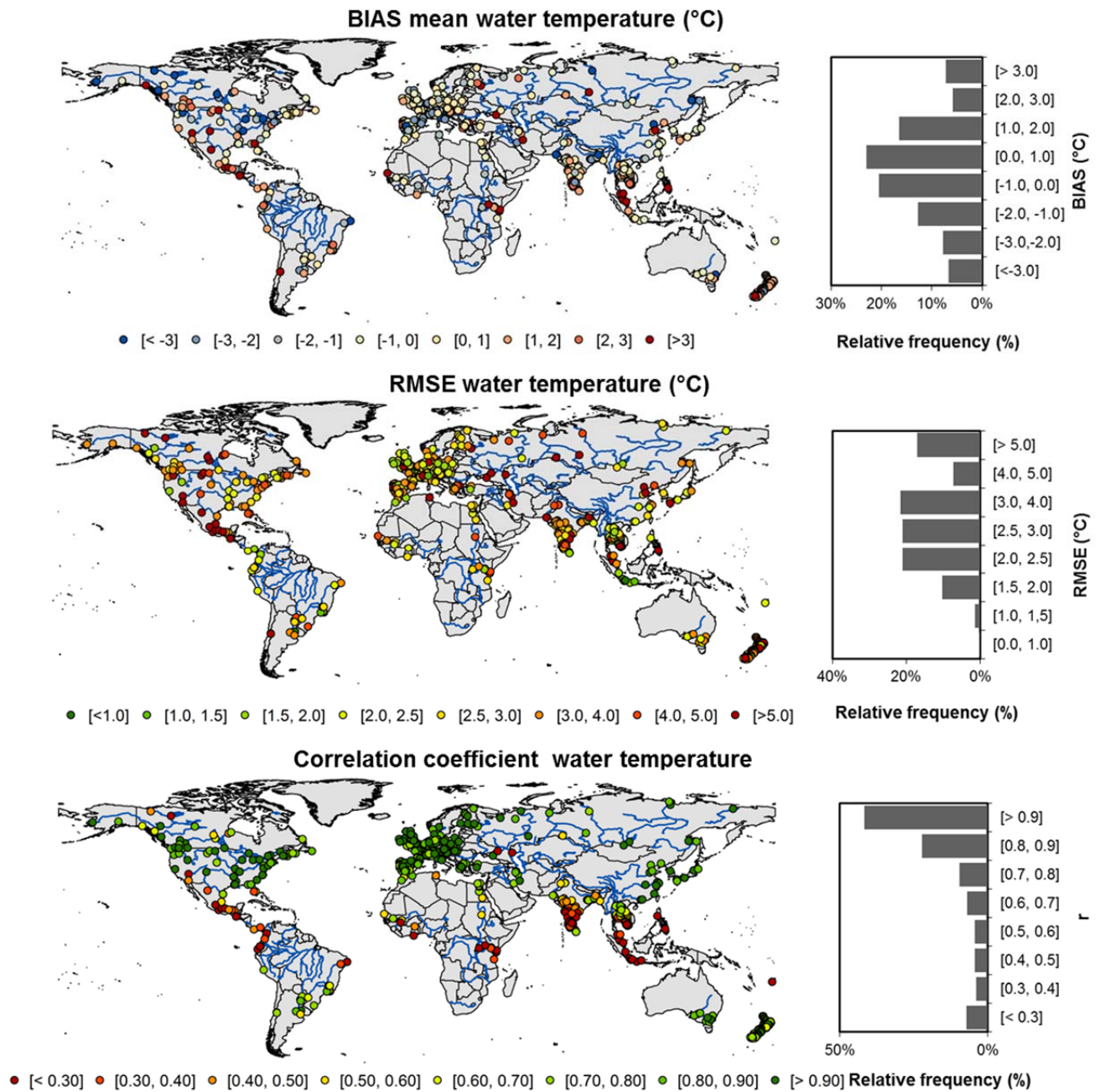


Figure A2: Performance of water temperature modelling for current climate. Global maps of mean bias (°C), root mean squared error (RMSE; °C) and Pearson correlation coefficient for simulated daily river temperature using the historical WATCH forcing data (WFD) as input into VIC-RBM and observed daily water temperature series of 347 GEMS/Water stations globally for 1980-2000. Correlation coefficients between simulated and observed daily water temperature for tropical basins are lower, because seasonal signal in water temperature is weaker, resulting in a lower signal-to-noise ratio and thus a lower explained variance.

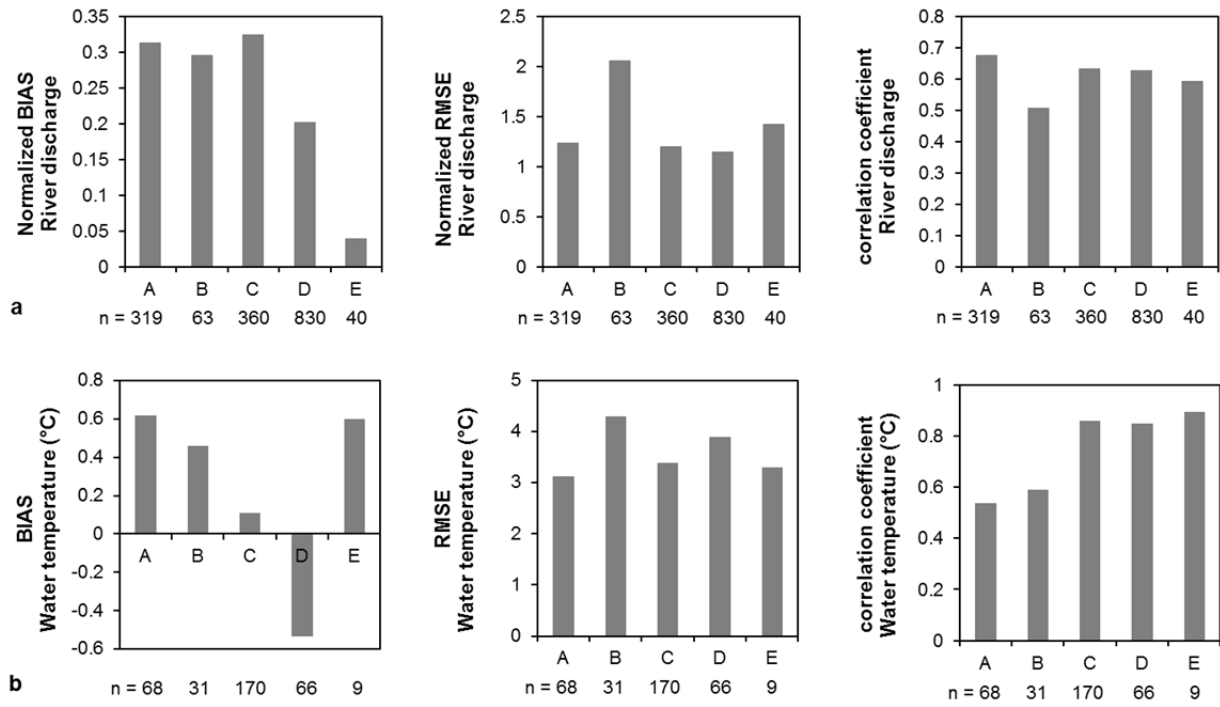


Figure A3: Performance coefficients of daily simulated river discharge (a) and water temperature (b) for selected river stations in the A (tropical; n=68), B (dry; n=31), C (temperate; n=170), D (continental; n=66) and E (polar; n=9) Köppen climate zones.

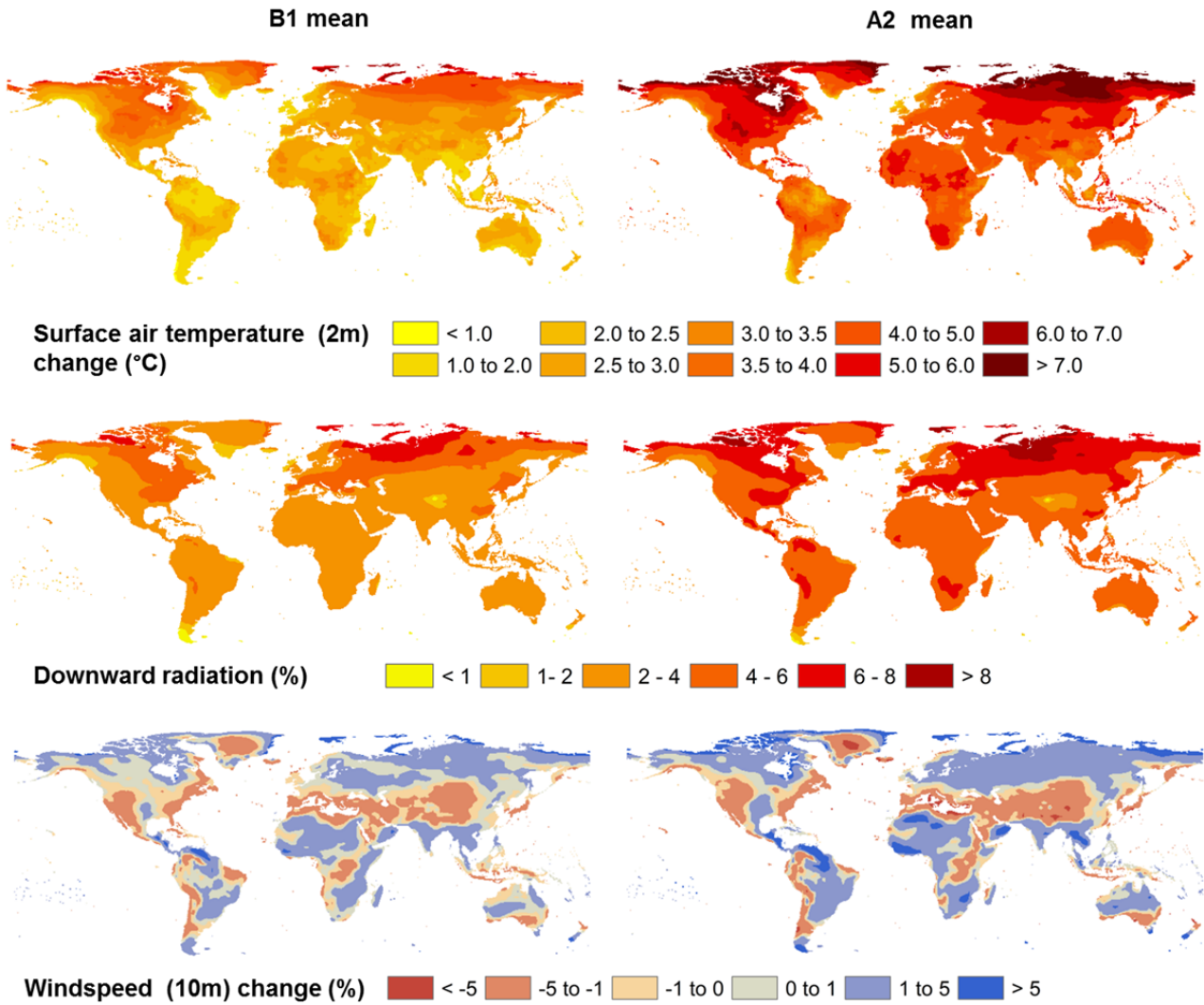


Figure A4: Global projected changes in mean climate forcing for 2071-2100 relative to 1971-2000 averaged for the three GCMs for both the SRES A2 and B1 scenario. Radiation is derived from the VIC hydrological model based on minimum and maximum air temperature and used as input into the RBM water temperature model.

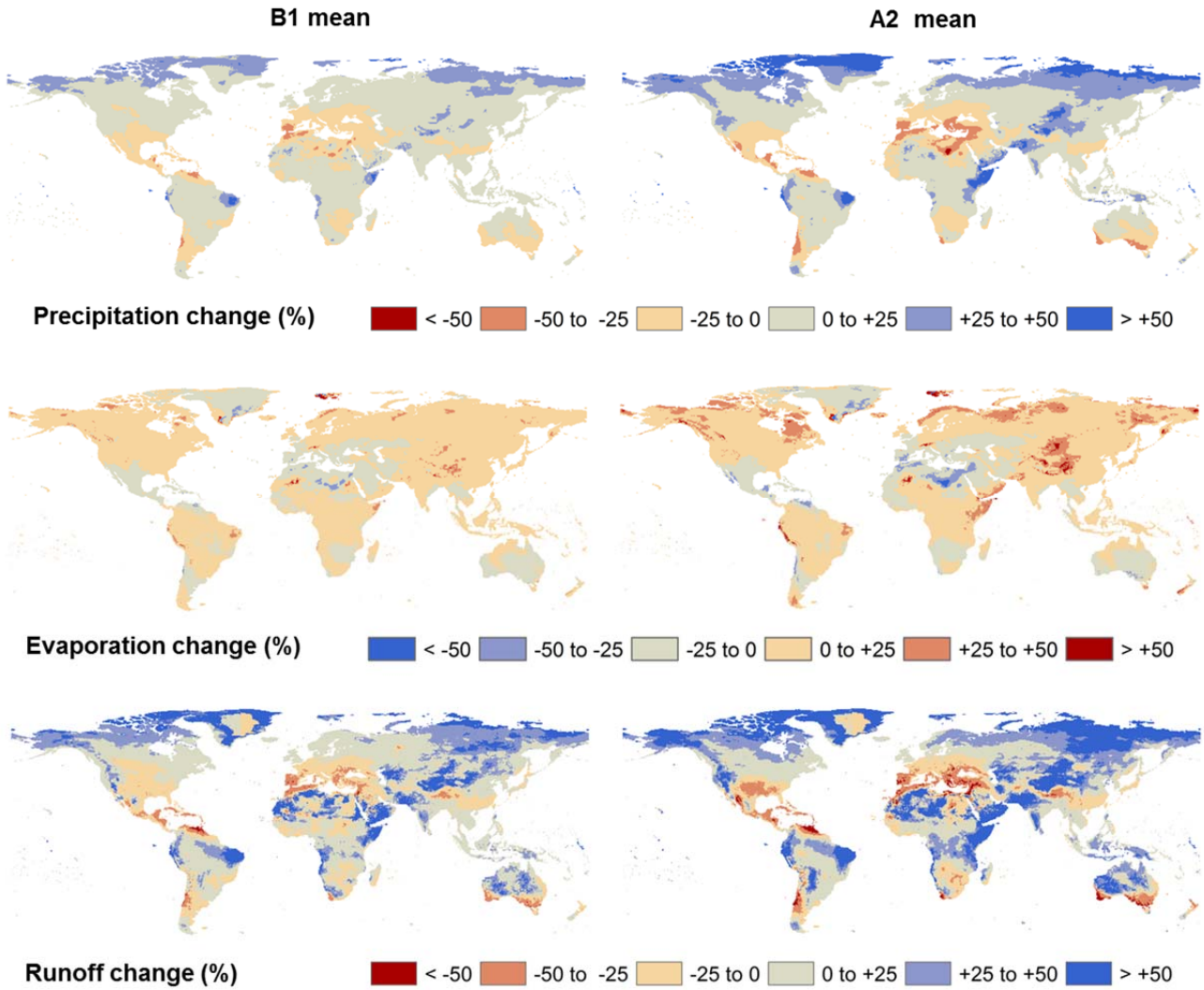


Figure A5: Global projected changes in mean precipitation and simulated evaporation and total runoff (sum of direct runoff and baseflow) for 2071-2100 relative to 1971-2000 for both the SRES A2 and B1 scenario.

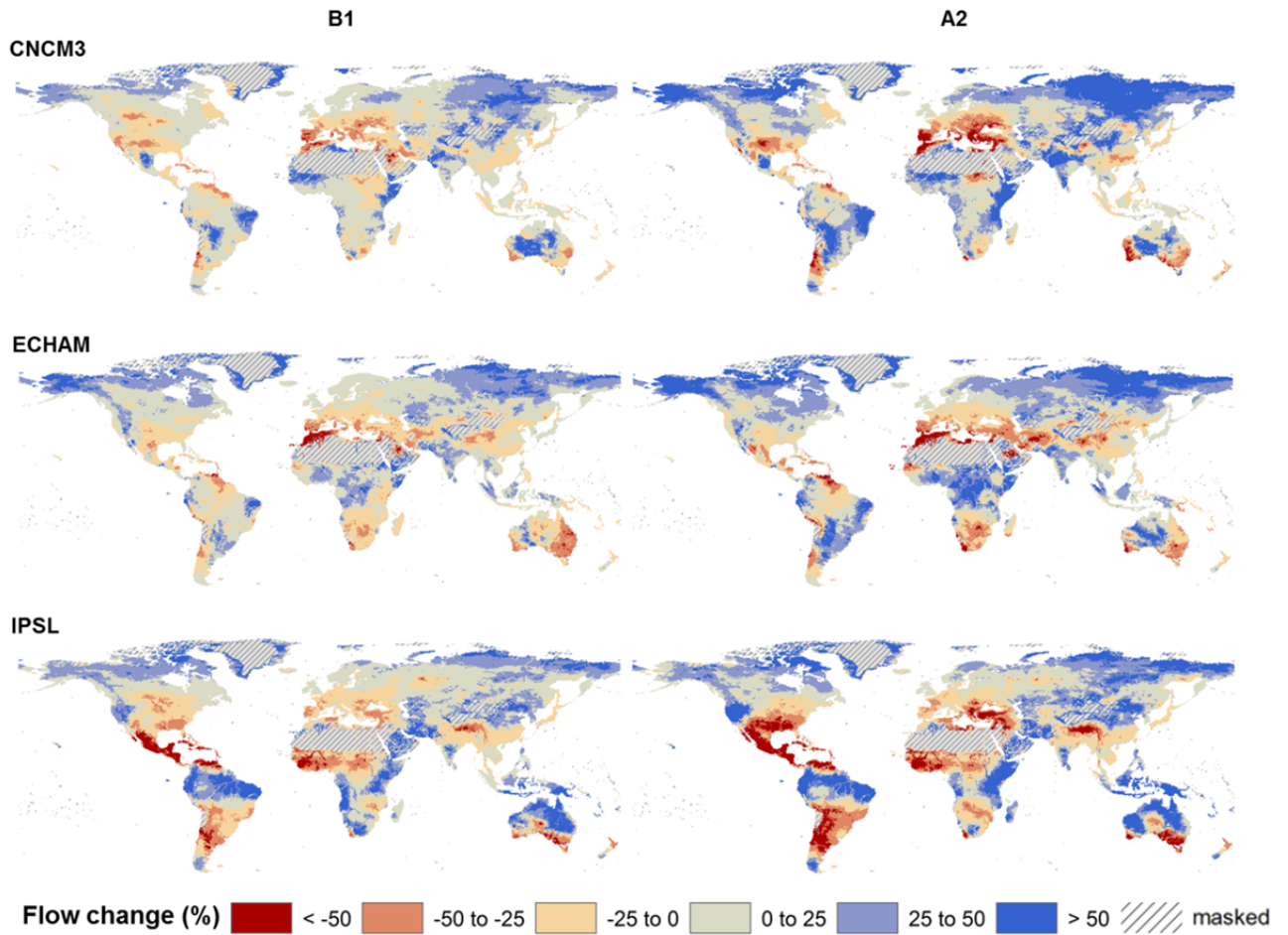


Figure A6: Global projected changes in mean flow for 2071-2100 relative to 1971-2000 for the three selected GCMs for both the SRES A2 and B1 scenario. Regions with mean flow less than $1 \text{ m}^3 \text{ s}^{-1}$ are masked.

Vulnerability of U.S. and European Electricity Supply to Climate Change (Chapter 5)

B1 Hydrological - water temperature modelling framework

We used a physically-based modelling framework to simulate river flow and water temperature for Europe and the U.S. at a daily time step and $0.5^\circ \times 0.5^\circ$ spatial resolution. This modelling framework consists of the Variable Infiltration Capacity (VIC) macro-scale hydrological model (Liang et al., 1994) and the one-dimensional stream temperature model RBM (Yearsley, 2009).

The VIC model and an offline routing model (Lohmann et al., 1998) were used to simulate daily river flow. The routing model was modified to include the calculation of the hydraulic characteristics based on power equations relating mean cross-sectional area and width to river discharge (Leopold and Maddock, 1953). The coefficients of these relations were obtained using the empirical relations with river discharge based on 674 river monitoring stations from watersheds across the U.S. found by Allen et al. (1994). The assumption was made that these fitted relations can be applied to estimate the hydraulic characteristic of rivers in other regions as well. The VIC hydrological model was applied using the elevation and land cover classification procedure (elevation, vegetation, and soil characteristics) as described in Nijssen et al. (2001c), which was later implemented at $0.5^\circ \times 0.5^\circ$. In their study, direct calibration on soil characteristics was performed for selected large river basins globally and the calibrated parameters values were subsequently transferred to other basins based on climate characteristics. The global DDM30 routing network (Döll and Lehner, 2002) was used for the lateral routing of streamflow.

Daily water temperature was simulated with the stream temperature River Basin Model (RBM)(Yearsley, 2009), which directly uses output from the VIC hydrological model. RBM is a process-based model that solves the 1D-heat advection equation using the semi-Lagrangian (mixed Eulerian-Lagrangian) approach. Water temperature in each stream segment is simulated based on the upstream water temperature and inflow into the stream segment, the dominant heat exchange at the air - water surface, and the inflow and temperature of water advected from tributaries and (anthropogenic) point sources of heat. RBM was developed for subbasins of the Columbia (Yearsley, 2009; Yearsley, 2012). For our study, modifications were made to apply RBM for the whole European and North American region. To make the model

also applicable in thermally polluted river basins, heat dumps of thermoelectric power plants were included as advected heat source resulting in the following heat advection equation.

$$\rho_w C_p \frac{\delta(T_w A_x)}{\delta t} = H_{air-water} w_x + \frac{\rho_w C_p Q_{trb} \Delta T_{trb}}{\delta x} + \frac{\rho_w C_p Q_{effl} \Delta T_{effl}}{\delta x} \quad (B1)$$

Where: ρ_w = density of water [kg m^{-3}]; C_p = specific heat capacity of water [$\text{J kg}^{-1} \text{°C}^{-1}$]; T_w = water temperature [°C]; A_x = cross-sectional area of river at distance x [m^2]; $H_{air-water}$ = heat flux at air - water interface [$\text{J m}^{-2} \text{s}^{-1}$]; w_x = stream width at distance x [m]; Q_{trb} = advected flow from tributaries or subsurface [$\text{m}^3 \text{s}^{-1}$]; ΔT_{trb} = the difference between advected temperature from tributaries or subsurface, T_{trb} , and T_w [°C]; Q_{effl} = advected flow from heat dumps of thermoelectric power plants [$\text{m}^3 \text{s}^{-1}$]; ΔT_{effl} = the difference between the advected temperature from heat dumps of thermoelectric power plants, T_{effl} , and T_w [°C]; x = longitudinal distance along the axis of the river [m]; t = time [s].

We used global gridded ($0.5^\circ \times 0.5^\circ$) estimates of thermoelectric water consumption and water withdrawal for the 20th century and 21st century for the SRES A2 and B1 scenario (Flörke et al., 2011) to calculate return flows of thermoelectric water use (Q_{effl}). For the difference between return flow temperatures and river temperatures we assumed that the temperature of return flow (ΔT_{effl}) is on average 3°C higher than the inlet river water temperature. This value was selected because standards for heat discharges in the U.S., which are written under the requirements of the Clean Water Act, limit the ΔT_{effl} to 3°C in most of the states in our study. In addition, the best overall results of daily simulated water temperature were obtained under a ΔT_{effl} of 3°C when we tested this for thermally polluted basins in the U.S. and Europe with values ranging from 2 to 10°C . Results of that sensitivity analysis show that the selected values of ΔT_{effl} (3 , 5 and 7°C) have relatively moderate impact on the simulated water temperature compared to the impact of thermal effluents on water temperatures in thermally polluted basins like the Rhine and the Danube in Europe (Figure B1). For the Mississippi we found larger differences in simulated water temperature, but overall best results were found under a ΔT_{effl} of 3°C . Based on dominant cooling type in each grid cell, Q_{effl} , and ΔT_{effl} , we calculated gridded ($0.5^\circ \times 0.5^\circ$) datasets of heat dumps for the control period 1971-2000 and for the future periods 2031-2060 and 2071-2100 according to equation B2. These datasets were subsequently used as input into RBM.

$$HD = \rho_w C_p Q_{effl} \Delta T_{effl} \quad (B2)$$

Where: HD = heat dump [MW]; Q_{effl} = discharge of cooling water [$\text{m}^3 \text{s}^{-1}$]; ΔT_{effl} = difference in temperature between heat effluents and river water [°C]; ρ_w = density fresh water [kg m^{-3}]; C_p = heat capacity of water [$\text{J kg}^{-1} \text{°C}^{-1}$].

The boundary conditions of RBM were estimated by fitting the water temperature regression model of Mohseni et al. (1998) for a selection of 333 GEMS/Water river stations globally for

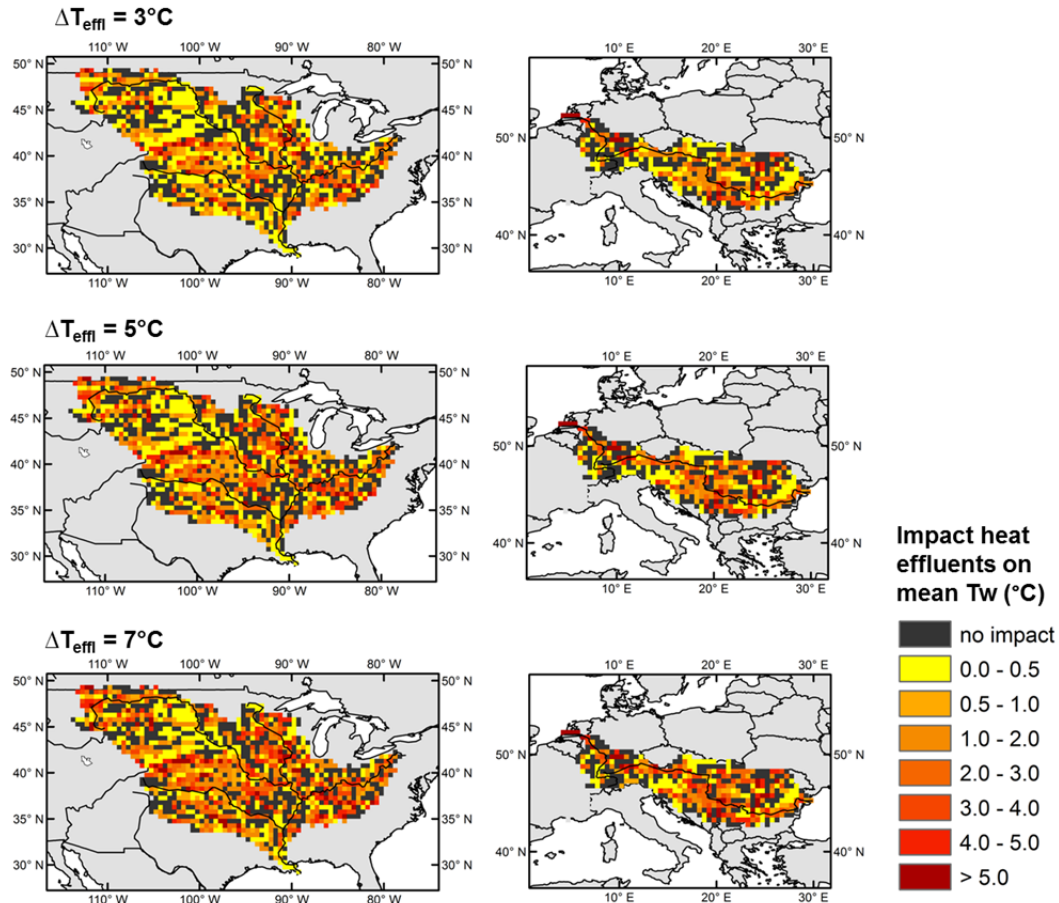


Figure B1: Sensitivity of simulated mean water temperatures to difference in temperature between heat effluents and river water (ΔT_{eff}). Spatial patterns of mean water temperature impact of heat effluents in the Mississippi, Rhine and Danube basins under ΔT_{eff} of 3, 5 and 7°C.

the period 1980-2000. The estimated parameter values were globally interpolated using ordinary kriging, resulting in $0.5^\circ \times 0.5^\circ$ interpolated grids of these parameter values. Water temperature for the headwater grid cells in RBM is estimated based on the daily air temperature series and the parameter values for these head water grid cells.

B2 Model validation

The performance of the hydrological - water temperature modelling framework was tested for large river basins for the historical period 1971-2000 using a global meteorological dataset on a $0.5^\circ \times 0.5^\circ$ spatial resolution (Weedon et al., 2011) produced by the EU FP6 Water and Global Change (WATCH) project.

Observed daily river discharge and water temperature records of selected monitoring stations were used to evaluate the performance of the hydrological - water temperature modelling framework. We used daily series of river discharge for 766 and 501 river discharge stations in North America and Europe, respectively, which were provided by the Global Runoff Data Centre (GRDC; <http://grdc.bafg.de/>) for the period 1971-2000. For water temperature, daily

records of 58 (North America) and 182 (Europe) river stations for the period 1980-2000 of the United Nations Environment Programme Global Environment Monitoring System (GEMS/Water; <http://www.gemswater.org>) were used to evaluate the model performance. We used all observed daily data available for the validation periods. The observed daily records for these long (>20 year) periods were used without interpolation for missing data values because interpolation could introduce uncertainties in the observed records, which is undesirable for evaluations of model performance.

To quantify the performance of VIC-RBM for daily river flow and water temperature simulations, the Pearson correlation coefficient was calculated to assess the linear dependence between the daily simulated and daily observed values. In addition, we used the root mean squared error (RMSE) and mean BIAS to assess the quality of the fit. For river discharge, normalized values of RMSE and BIAS were calculated (by dividing by the mean observed river discharge values). For stations in Europe, the river discharge is on average slightly overestimated (largest group of stations had positive NBIAS 0.25 - 0.50) while a normal distribution in NBIAS is found for the stations in the U.S. (see histograms Figure B2).

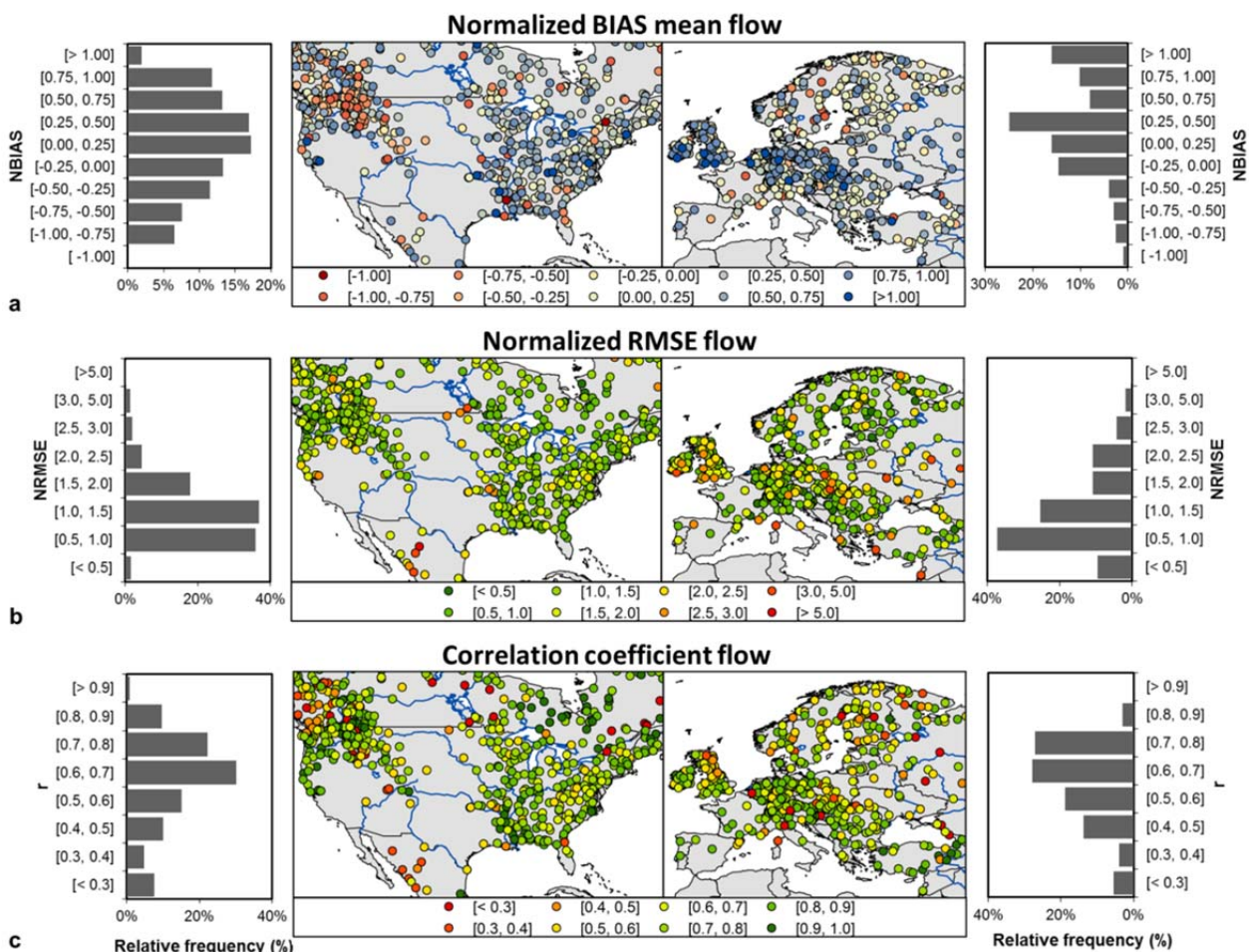


Figure B2: Performance of daily river flow modelling. Maps with the calculated normalized BIAS (a), normalized RMSE (b), and Pearson correlation coefficient (c) for the period 1971-2000 for river discharge monitoring stations in the U.S. and Europe. Histograms at the left and right present the relative frequency distribution of the performance coefficients for the stations in the U.S. and Europe, respectively.

For water temperature, the largest group of stations in Europe and the U.S. have a very small (negative) BIAS of -1.0 - 0.0°C and high correlation coefficient (>0.9) (Figure B3). In addition, scatter plots and histograms of daily simulated versus daily observed water temperature (Figure B4) and river discharge (Figure B5) for selected stations presented in the paper, show that simulated water temperature and river discharge values strongly relate to the observed values.

B3 Climate change scenarios

The hydrological - water temperature modelling framework was forced with daily bias-corrected output of three different coupled atmosphere/ocean general circulation models (GCMs) (ECHAM5/MPIOM, CNRM-CM3 and IPSL-CM4) for both the SRES A2 and B1 emissions scenario (Nakicenovic, 2000), resulting in six GCM experiments. The A2 scenario considers a

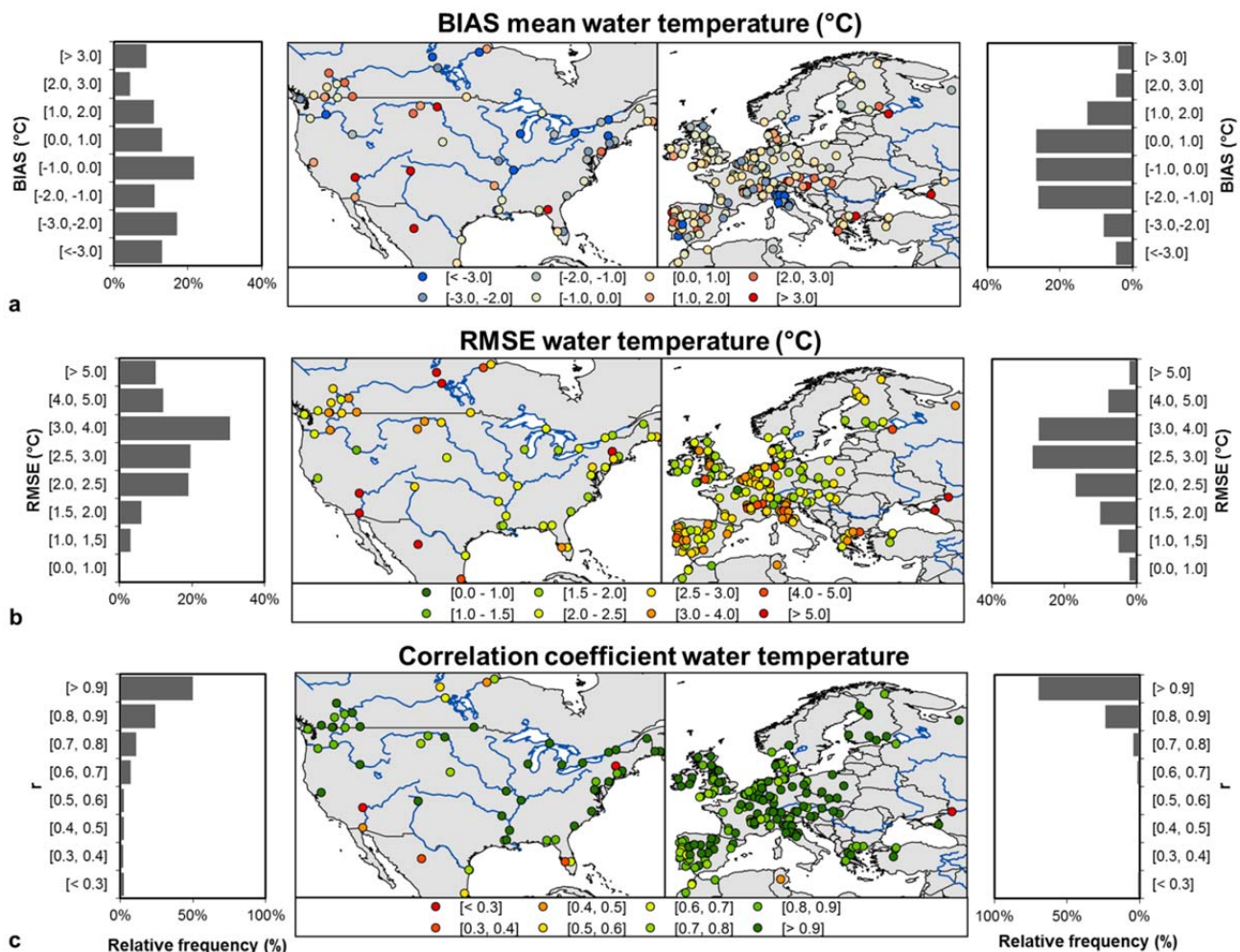


Figure B3: Performance of daily river water temperature modelling. Maps with the calculated mean BIAS (a), RMSE (b), and Pearson correlation coefficient (c) for the period 1980-2000 for water temperature monitoring stations in the U.S. and Europe. Histograms at the left and right present the relative frequency distribution of the performance coefficients for the stations in the U.S. and Europe, respectively.

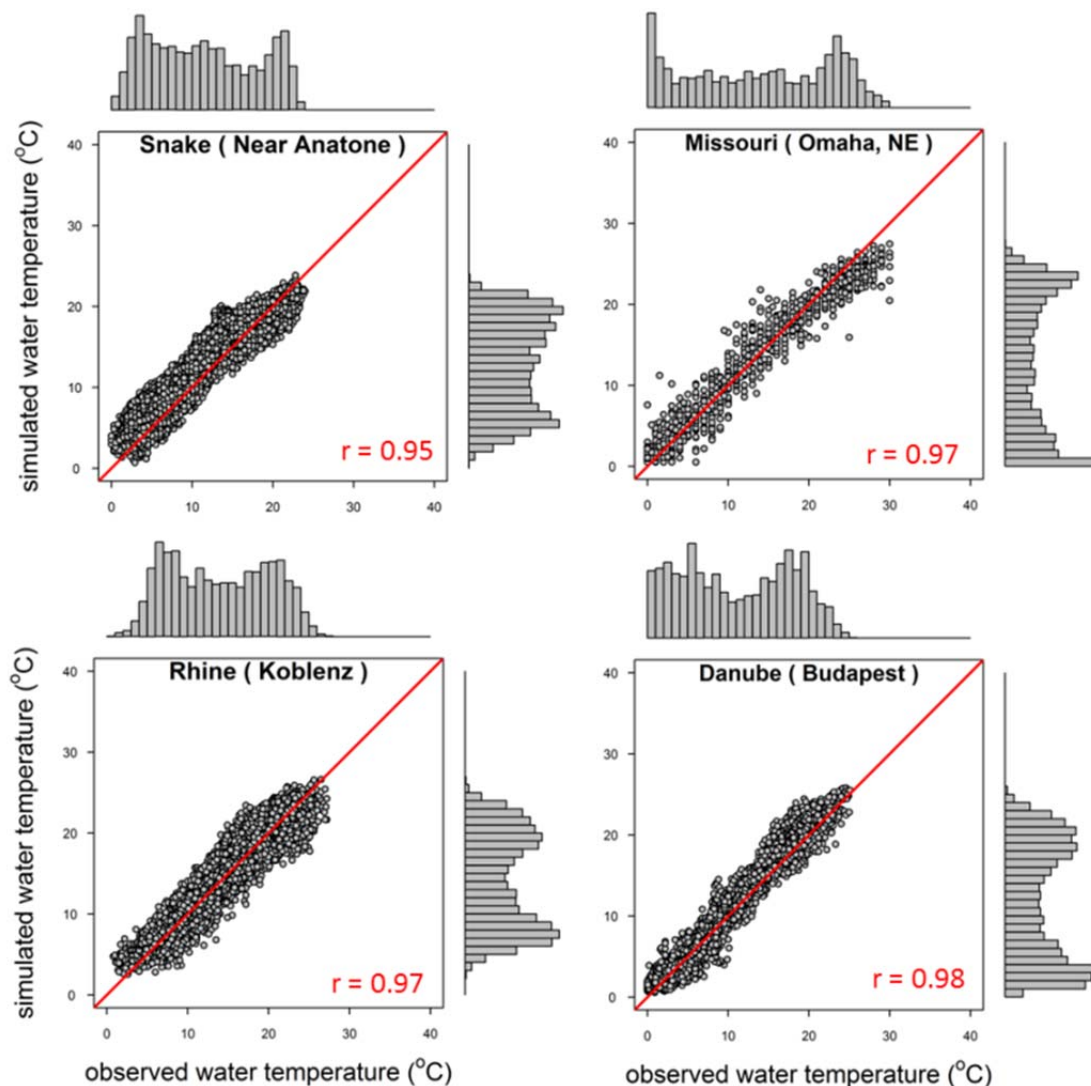


Figure B4: Scatter plots and histograms of daily simulated river temperature versus daily observed river temperature. Histograms on the vertical axis are for simulated values and histograms on horizontal axis for observed water temperature values for selected stations in the U.S. and Europe for 1980-2000.

world of fragmented and slow technological change, while the B1 scenario assumes environmental sustainability and a much more rapid introduction of renewables (Nakicenovic, 2000). Both SRES scenarios were selected, because they represent contrasting storylines and emissions scenarios, which results in the largest range from the four IPCC SRES main emissions scenarios. In addition, climate data were widely available for both SRES A2 and B1. The three GCMs were selected because output was available on a daily time step. A bias correction was performed on daily precipitation, mean, minimum and maximum surface air temperature for these six selected GCM experiments (Hagemann et al., 2011) based on transfer functions that describe the relation between the daily modelled (corrected) and daily observed time series (Piani et al., 2010).

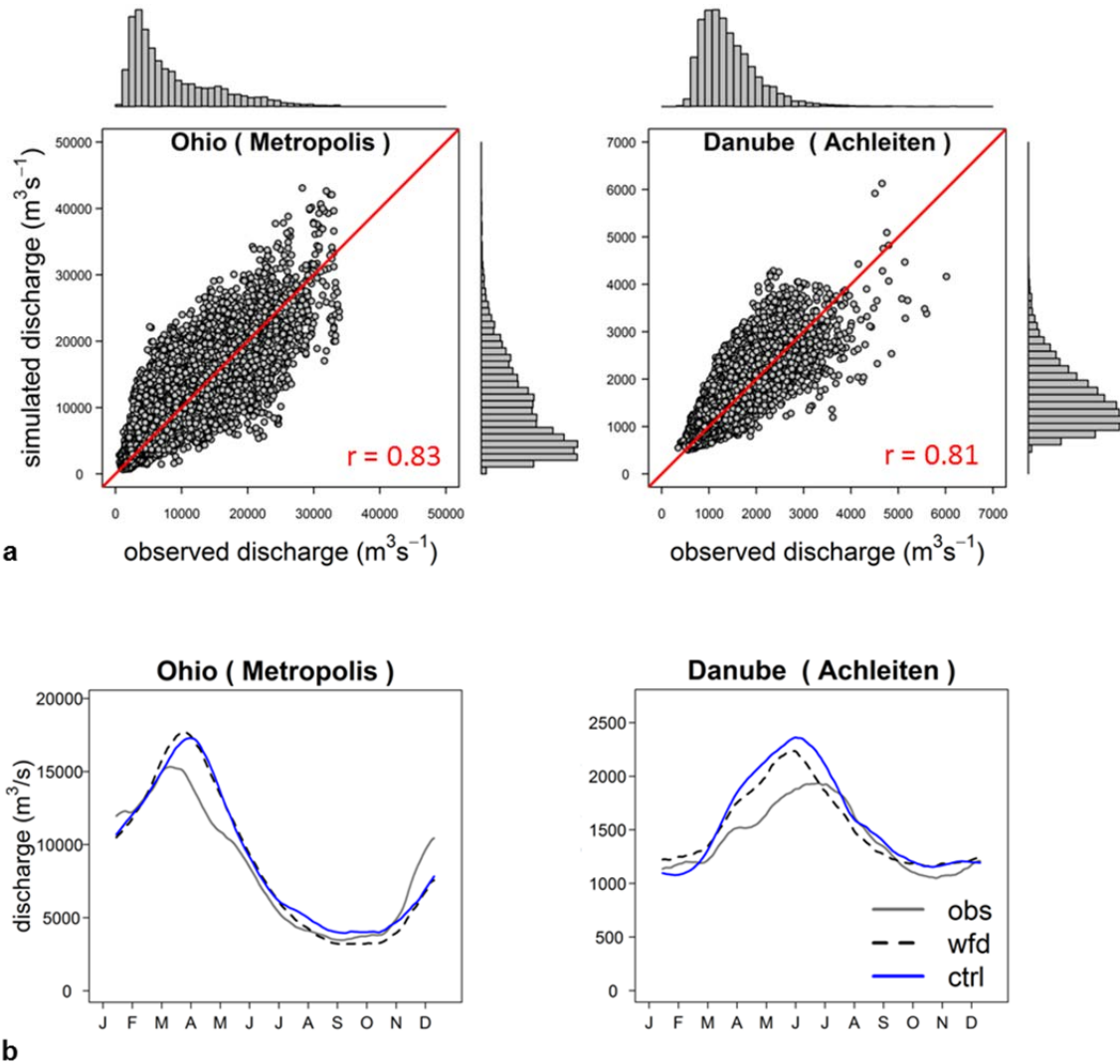


Figure B5: Scatter plots and histograms, and mean annual cycles of daily observed and simulated river discharge. Histograms on the vertical axis are for simulated values and histograms on horizontal axis for observed river discharge values for selected stations in the U.S. and Europe for the 1971-2000 period. For these simulations we used the global historical WATCH forcing data set (wfd) as input (a). Lower panel shows mean annual cycles for observed discharge and simulated river discharge based on wfd and based on the control runs of the three selected GCMs presented as ensemble mean (ctrl) for 1971-2000 (b).

B4 Cooling water shortage regions

Daily water temperature projections were used to calculate the mean number of days per year (probability) that river water temperature thresholds for cooling water use were exceeded in the U.S. and Europe. For cooling water use in Europe, the Water Framework Directive (Directive 2000/60/EC) and the Freshwater Fish Directive (Directive 2006/44/EC) are of importance. The highest maximum allowed river water temperature for cooling water use in the EU countries is 28°C (EU Freshwater Fish Directive 2006/44/EC). This value is defined for cyprinid waters and a large part of thermoelectric power plants in Europe are extracting water from such river bodies. Water temperature standards for the U.S. are defined on state level and vary throughout the year (EPA, 1988). The highest maximum allowed river

temperatures during summer are, however, quite consistent between different states, with a median value for all states of 89°F (~32°C). As indicator of changes in the number of days with cooling water problems and potential reductions in thermoelectric power capacity, we selected a water temperature limit which reflects the start of potential reductions in production capacity rather than a full production stop (which would be reflected by the use of maximum river water temperature limits). According to EEA (2008a), the 23°C water temperature value can be considered as a critical limit for the inlet of river water for cooling water use in Europe, which is 5°C lower than the maximum river water temperature limit of 28°C. We used the 23°C threshold as river water temperature limit for which potential cooling water problems start. Under these conditions the maximum allowed temperature difference between inlet river water temperature and discharge temperature is reduced and water demands of thermoelectric power need to be increased to continue production at maximum capacity. Similar as for Europe, we selected a river water temperature threshold that reflects a potential start in cooling water problems for the U.S., which is ~5°C lower than the median value in maximum allowed water temperature of 89°F. This resulted in a river water temperature threshold of 27°C for the U.S..

Using the daily water temperature simulations for the control and future periods for both the SRES A2 and B1 scenario, we calculated the mean number of days per year that the 23°C (Europe) and 27°C (U.S.) thresholds were exceeded. In combination with areas for which large decreases in low flows (>25%) are expected, we identified regions in Europe and the U.S. where cooling water problems are expected to increase due to reduced water availability and exceeded water temperature limits.

To evaluate the impact of biases in simulated water temperature, we compared the mean number of days per year that water temperature limits are exceeded based on the control period simulations with values based on observed daily water temperature for all monitoring stations for 1980-2000 (Figure B6a). Overall, the mean number of days per year with exceeded water temperature limits corresponds with values based on observed water temperature series, although there is an overestimation (positive biases) of ~10–50 days per year with an exceeded 23°C and 27°C limit for some stations in southern Europe and southern U.S.. An underestimation (negative bias) in the same order of magnitude is found for several stations in Central Europe (Figure B6b), resulting in an average negative bias in number of days with exceeded water temperature limits for Europe (Figure B6c). However, the bias in days with exceeded water temperature thresholds is small for Europe and negligible for the U.S. for the largest group of river stations.

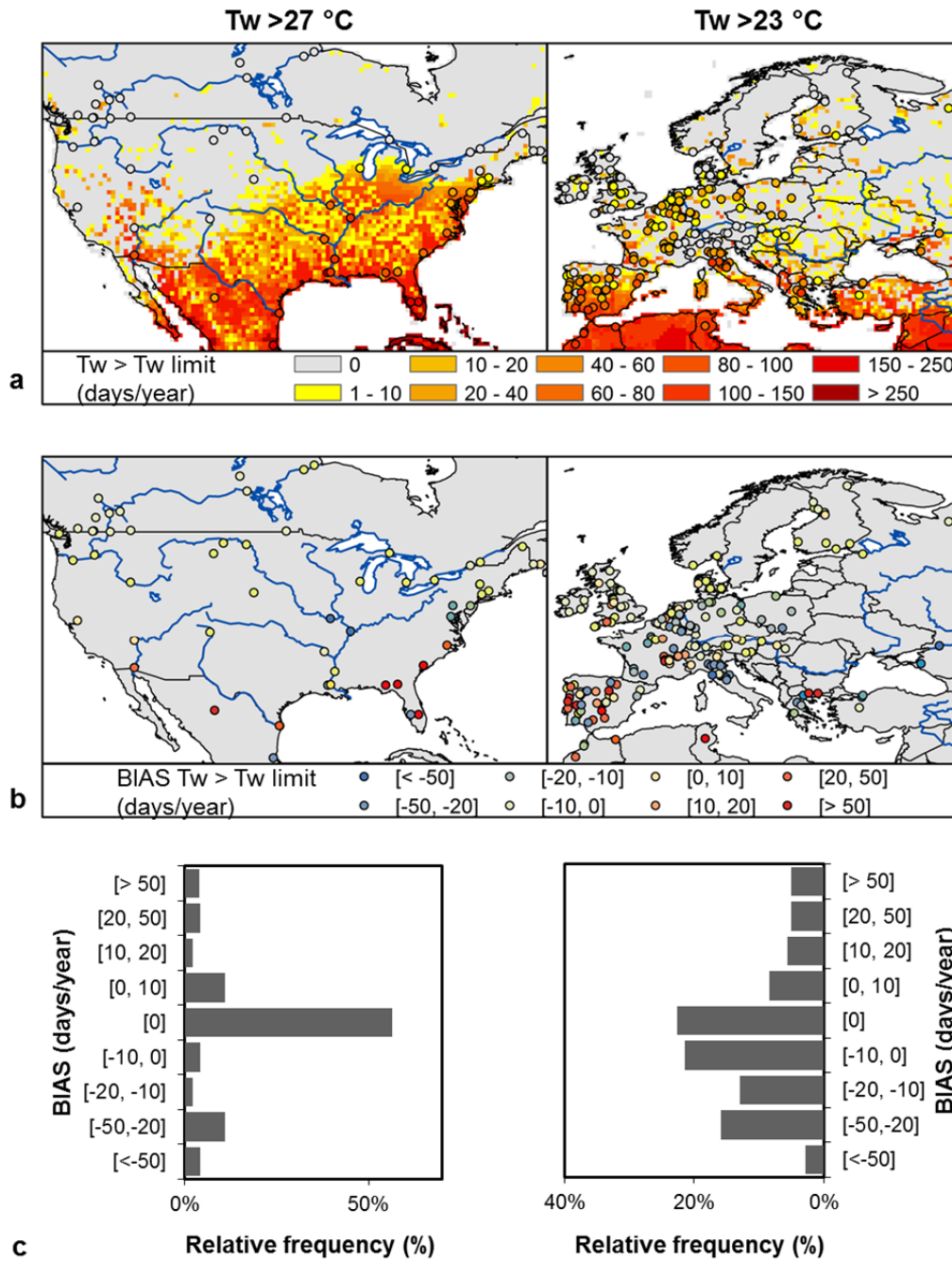


Figure B6: Impact of biases in daily water temperature simulations on exceeded water temperature limits. Mean number of days per year that the water temperature limit of 27°C (in the U.S.) and 23°C (in Europe) is exceeded using the mean of the control water temperature simulations for the three GCMs and the daily observed water temperature records at the monitoring stations for 1980-2000 (circles) (a). The absolute bias in mean number of days per year with exceeded water temperature limits for the mean of the control water simulations and observed water temperature is calculated at each monitoring station (b). Histograms present the relative frequency distribution of the bias in number of days per year that the water temperature limit is exceeded for the river stations in the U.S. (left) and Europe (right)(c).

B5 Usable capacity of thermoelectric power plants

In addition to the analyses of cooling water scarcity regions, we calculated the potential effects of climate change on the usable capacity of 61 existing thermoelectric power plants in the U.S. and 35 power plants in Europe. We focus on power plants located in the central and eastern part of the U.S., for which most data was available. A distinction was made between power plants using once-through systems, recirculation (closed-loop) systems with cooling tower(s) and combination cooling systems (once-through with supplementary tower). Once-through systems withdrawn relatively large quantities of surface water, and subsequently discharge high heat loads to the same water body after leaving the condenser. These cooling systems are commonly used when sufficient surface water is available for cooling of the power plant. Recirculation systems use cooling towers to cool the water via contact with air before the water is discharged back to the surface water body. These systems require smaller amounts of surface water withdrawal, but water consumption is higher (due to evaporative losses) compared to once-through systems (Koch and Vögele, 2009).

Both nuclear- and fossil-fuelled power plants were selected. We used data of the National Energy Technology Laboratory Coal Power Plant Database (NETL-CPPDB) database (NETL, 2007) for thermoelectric power plants in the U.S.. For power plants in Europe we used data of the selected nuclear power stations extracted from the power plant database at the Institute of Energy and Climate Research – Systems Analyses and Technology Evaluation (IEF-STE) of the Forschungszentrum in Jülich (Germany) in combination with published data of fossil-fuelled power plants (VGE, 2011).

We selected power plants according to the following criteria: 1) availability of detailed location (latitude-longitude) information of power plant; 2) use of river water as source of cooling; 3) availability of information on the type of cooling; 4) availability of water temperature limitations (maximum intake and discharge temperature during summer and winter) at power plant location; and 5) installed capacity of power plants > 370 MW. Plants with cooling ponds or reservoirs were excluded since these systems have different performance and contribute to only a small percentage of the total number of thermoelectric power plants (EPA, 2011).

The location, cooling type and installed capacity of the power plants included in the analyses are presented in Figure B7. For a high number of power plants in Europe the installed capacity is >2500 MW. For power plants in the U.S., a large part has a capacity <1000 MW, although several power plants were also included with installed capacities of >2500 MW.

The methodology used to assess the impact of climate change induced daily water temperature and river flow changes on the usable capacity of thermoelectric power plants was based on Koch and Vögele (2009) and Rubbelke and Vögele (2011). However, we slightly modified the equations for use on a daily time step (with daily estimates of water temperature and river discharge) and to include limitations in withdrawal of river water for thermoelectric cooling.

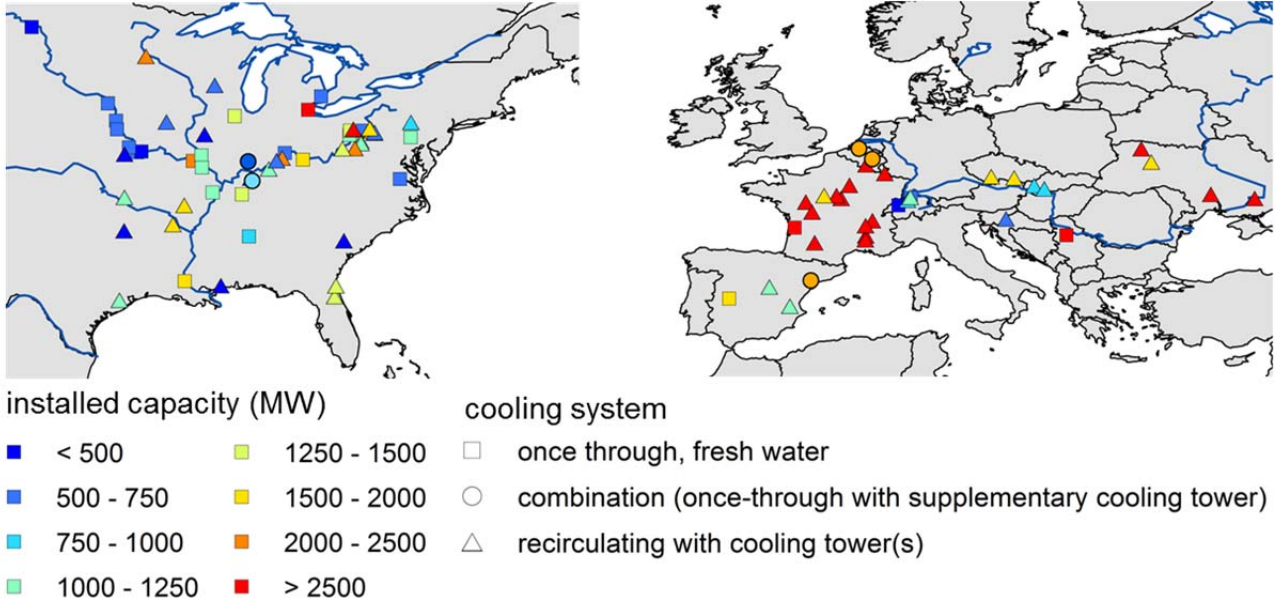


Figure B7: Location, cooling system (symbols) and installed capacity (colours) of the thermoelectric power plants in the U.S. and Europe included in the analyses.

In this approach, a distinction is made between power plants with once-through cooling systems and power plants with recirculation systems (tower) cooling. In a first step, the required water withdrawal (q) of the power plant is calculated based on the installed capacity (KW), efficiency (η_{total} , η_{elec}) and parameters related to the cooling system (once-through cooling: α ; tower cooling: α , β , ω , EZ) of the power plant in combination with water temperature limitations (Tl_{max} , ΔTl_{max}) and simulated daily water temperature (Tw) at the power plant location. In the second equation, the maximum usable capacity is calculated based on the daily required water withdrawal (q), river discharge (Q) and water temperature (Tw), in combination with parameters describing the maximum fraction of river discharge withdrawn for cooling (γ), water temperature limitations (Tl_{max} , ΔTl_{max}) and parameters related to the cooling system (α , β , ω , EZ).

Once-through cooling systems:

$$q = KW \cdot \frac{1 - \eta_{total}}{\eta_{elec}} \cdot \frac{(1 - \alpha)}{\rho_w \cdot C_p \cdot \max(\min((Tl_{max} - Tw), \Delta Tl_{max}), 0)} \quad (B3a)$$

$$KW_{max} = \frac{\min((\gamma \cdot Q), q) \cdot \rho_w \cdot C_p \cdot \max(\min((Tl_{max} - Tw), \Delta Tl_{max}), 0)}{\frac{1 - \eta_{total}}{\eta_{elec}} \cdot \lambda \cdot (1 - \alpha)} \quad (B3b)$$

Recirculation (tower) cooling systems:

$$q = KW \cdot \frac{1 - \eta_{total}}{\eta_{elec}} \cdot \frac{(1 - \alpha) \cdot (1 - \beta) \cdot \omega \cdot EZ}{\rho_w \cdot C_p \cdot \max(\min((Tl_{max} - Tw), \Delta Tl_{max}), 0)} \quad (B4a)$$

$$KW_{max} = \frac{\min((\gamma \cdot Q), q) \cdot \rho_w \cdot C_p \cdot \max(\min((Tl_{max} - Tw), \Delta Tl_{max}), 0)}{\frac{1 - \eta_{total}}{\eta_{elec}} \cdot \lambda \cdot (1 - \alpha) \cdot (1 - \beta) \cdot \omega \cdot EZ} \quad (B4b)$$

Where: KW = installed capacity [MW]; η_{total} = total efficiency [%]; η_{elec} = electric efficiency [%]; α = share of waste heat not discharged by cooling water [%]; β = share of waste heat released into the air; ω : correction factor accounting for effects of changes in air temperature and humidity within a year; EZ = densification factor; λ = correction factor accounting for the effects of changes in efficiencies; ρ_w = density fresh water [kg m^{-3}]; C_p = heat capacity of water [$\text{J kg}^{-1} \text{ }^\circ\text{C}^{-1}$]; Tl_{max} = maximum permissible temperature of the cooling water [$^\circ\text{C}$]; ΔTl_{max} = maximum permissible temperature increase of the cooling water [$^\circ\text{C}$]; γ = maximum fraction of river discharge to be withdrawn for cooling of thermoelectric power plants [%]; q = daily cooling water demand [m^3s^{-1}]; Tw = daily mean river temperature [$^\circ\text{C}$]; Q = daily river discharge [m^3s^{-1}]; KW_{max} = usable capacity of power plant [MW].

The equations show that during warm periods, when water temperature (Tw) increases to a level that the permitted temperature difference between river water (inlet) temperature and discharge temperature is reduced ($(Tl_{max} - Tw) < \Delta Tl_{max}$), water withdrawal q needs to be amplified in order to discharge the same waste heat load. The power plant can continue operation at maximum capacity ($KW_{max} = KW$) if the required water withdrawal is smaller or equal than the availability of river water for thermoelectric water extraction ($q \leq \gamma Q$). However, when required water withdrawal further increases and/or river water availability decreases and becomes inadequate to fulfil the thermoelectric water requirements ($q > \gamma Q$), the usable capacity needs to be reduced ($KW_{max} < KW$). This decrease in KW_{max} is gradual. However, in case river temperatures reach the maximum discharge water temperature ($(Tw - Tl_{max}) \approx 0$) the usable capacity of the power plant needs to be drastically reduced or operation must be curtailed.

For power plants with combination cooling systems, we used the equations for recirculation systems with parameter values representing the combined conditions of once-through and tower cooling. For each power plant, we calculated daily q and KW_{max} using the daily river discharge and water temperature simulations for the grid cell where the power plant is located. In case that several power plants units are located in the same grid cell we calculated, comparable with the studies of Flörke et al. (2011) and Vassolo and Döll (2005), the total daily water withdrawals of all power plants within the cell. In our study, we used the sum of installed capacity of all power plant units and calculated weighted mean values of the other parameters of equation B3-B4 to estimate daily water withdrawal and usable capacity. Weights were defined based on the ratio of the installed capacities of each power plant unit to the sum of the installed capacity of all power plant units in that cell. This resulted in daily estimates of the total water withdrawal and total usable capacity for all power plant units in that cell. Daily river discharge and water temperature simulations were used for the control period 1971-2000 and future period 2031-2060 for all six climate change scenarios.

The impact of biases in daily river discharge and water temperature simulations on the usable capacity was addressed for three power plants in Europe and two power plants in the U.S.. These power plants were selected because of the availability of daily observed river discharge and water temperature records of a nearby monitoring station. We compared values of summer mean usable capacity for the control simulations of water temperature and river discharge with values based on observed daily river discharge and water temperature for the period 1980-2000. Summer period was defined as 21 June-20 September, which is generally also the period when decreases in usable capacity are highest. Overall, the impact of biases in simulated water temperature and river discharge on the summer mean values in usable capacity is moderate. For the power plants Cattenom-4 (Moselle), mean summer usable capacity for the control simulations is slightly overestimated (relative bias of +1.4%), while a relative negative bias in summer mean usable capacity of -0.1% for Nogent (Seine), -4.2% for New Madrid (Mississippi) and -2.6% for White Bluff (Arkansas) was found (Table B1). For the analysis of the number of days with production limitations, impacts of biases in simulated daily river discharge and water temperature are larger, although the strength in climate signal is on average a factor 3 higher than the range in bias for these power plants.

Table B1: Impact of biases in daily river flow and water temperature simulations on usable capacity of power plants. Summer mean usable capacity using observed daily water temperature and river discharge of nearby monitoring station for 1980-2000 (obs) and using control simulations of daily water temperature and river discharge for 1980-2000 (ctrl). The five power plants were selected based on the availability of daily observed river discharge and water temperature records of a nearby monitoring station.

plant name	river	plant type	cooling type	KW _{installed} (MW)	summer mean KW _{max}		
					obs (MW)	ctrl (MW)	relative bias(%)
Cattenom-4	Moselle (France)	N	CT	5200	5125	5177	+1.4
Nogent	Seine (France)	N	CT	2620	2619	2617	-0.1
Beznau	Aare (Switzerland)	N	OT	730	730	730	0
New Madrid	Mississippi	C	OT	1200	896	858	-4.2
White Bluff	Arkansas	C	CT	1700	1685	1656	-2.6

N = nuclear; C = coal; CT = cooling tower(s); OT = once-through, freshwater

Global Streamflow and Thermal Habitats of Freshwater Fishes under Climate Change (Chapter 6)

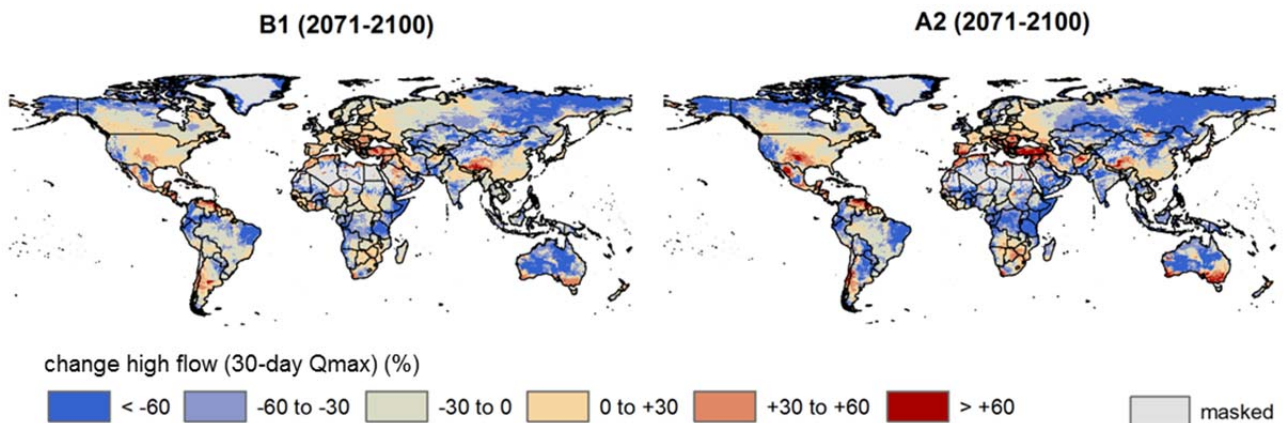


Figure C1: Global projected changes in annual 30-day average maximum flow. The changes are averaged for the three selected GCMs for both the SRES A2 and B1 scenario for 2071-2100 relative to 1971-2000. Regions with mean annual river flow less than $1 \text{ m}^3 \text{ s}^{-1}$ are masked.

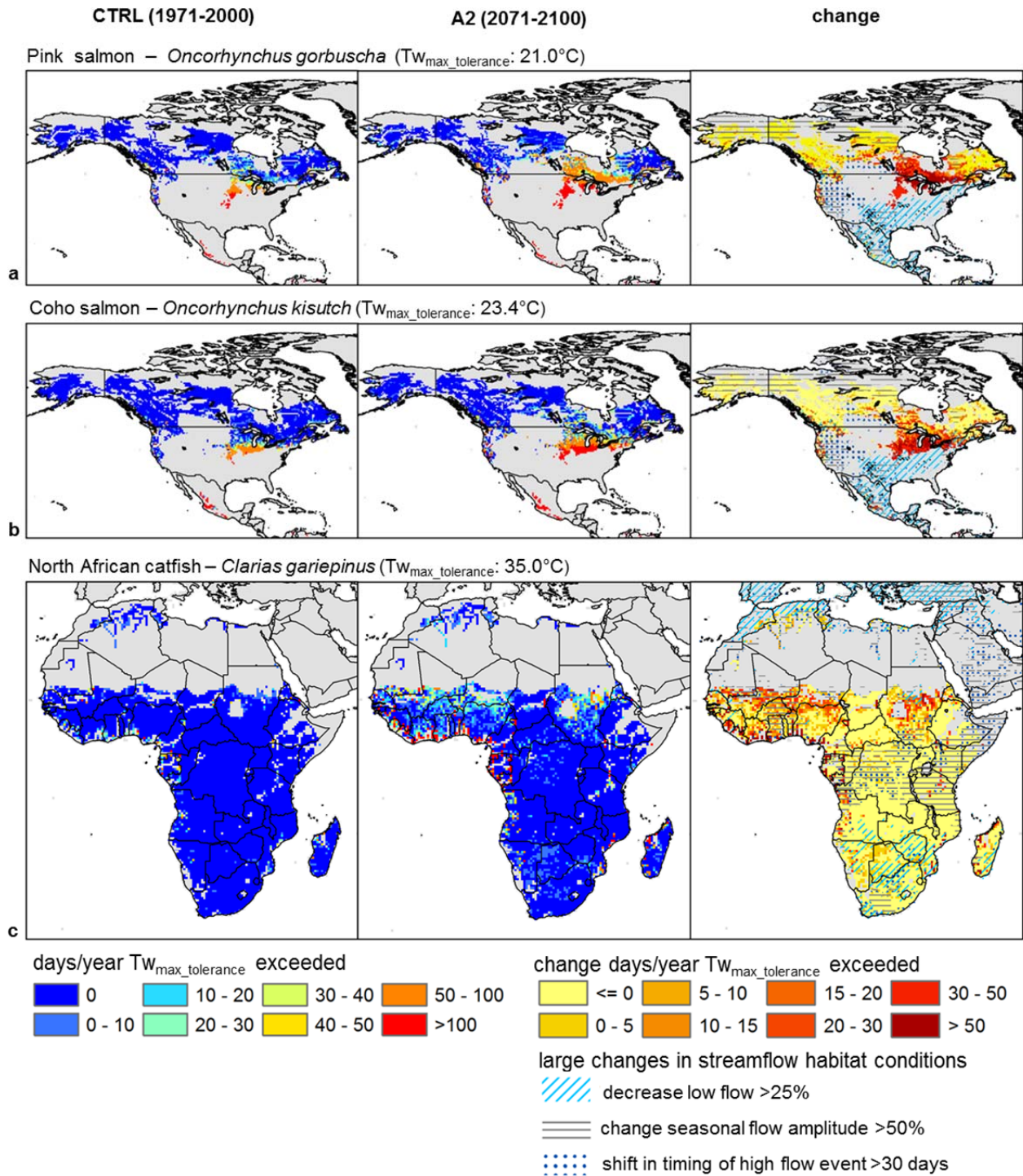


Figure C2: Impact of water temperature increases on the occurrence (mean number of days per year) that $T_{w_{max_tolerance}}$ is exceeded of selected fish species in North America and Africa, combined with large changes in streamflow habitat conditions. Changes are presented for the period 2071-2100 for the SRES A2 scenario relative to 1971-2000 using the average of the three GCM experiments.

References

- Ahmadi-Nedushan, B. et al., 2007. Predicting river water temperatures using stochastic models: case study of the Moisie River (Quebec, Canada). *Hydrological Processes*, 21(1): 21-34.
- Alcamo, J. et al., 2003a. Development and testing of the WaterGAP 2 global model of water use and availability. *Hydrological Sciences Journal-Journal Des Sciences Hydrologiques*, 48(3): 317-337.
- Alcamo, J. et al., 2003b. Global estimates of water withdrawals and availability under current and future "business-as-usual" conditions. *Hydrological Sciences Journal-Journal Des Sciences Hydrologiques*, 48(3): 339-348.
- Alcamo, J., Flörke, M., Marker, M., 2007. Future long-term changes in global water resources driven by socio-economic and climatic changes. *Hydrological Sciences Journal-Journal Des Sciences Hydrologiques*, 52(2): 247-275.
- Allen, P.M., Arnold, J.G., Bruce, W.B., 1994. Downstream channel geometry for use in planning-level models. *Water resources bulletin*, 30(4): 663-671.
- Andrews, T., Gregory, J.M., Webb, M.J., Taylor, K.E., 2012. Forcing, feedbacks and climate sensitivity in CMIP5 coupled atmosphere-ocean climate models. *Geophys. Res. Lett.*, 39 (L09712).
- Arnell, N.W., 1999a. Climate change and global water resources. *Global Environmental Change-Human and Policy Dimensions*, 9: S31-S49.
- Arnell, N.W., 1999b. The effect of climate change on hydrological regimes in Europe: a continental perspective. *Global Environmental Change-Human and Policy Dimensions*, 9(1): 5-23.
- Arnell, N.W., 1999c. A simple water balance model for the simulation of streamflow over a large geographic domain. *Journal of Hydrology*, 217(3-4): 314-335.
- Arnell, N.W., 2003a. Effects of IPCC SRES emissions scenarios on river runoff: a global perspective. *Hydrology and Earth System Sciences*, 7(5): 619-641.
- Arnell, N.W., 2003b. Relative effects of multi-decadal climatic variability and changes in the mean and variability of climate due to global warming: future streamflows in Britain. *Journal of Hydrology*, 270(3-4): 195-213.
- Arnell, N.W., 2004. Climate change and global water resources: SRES emissions and socio-economic scenarios. *Global Environmental Change-Human and Policy Dimensions*, 14(1): 31-52.
- Arthington, A.H., Naiman, R.J., McClain, M.E., Nilsson, C., 2010. Preserving the biodiversity and ecological services of rivers: new challenges and research opportunities. *Freshwater Biology*, 55(1): 1-16.
- Augustin, N.H., Beevers, L., Sloan, W.T., 2008. Predicting river flows for future climates using an autoregressive multinomial logit model. *Water Resources Research*, 44(W07403).
- Balsamo, G. et al., 2009. A Revised Hydrology for the ECMWF Model: Verification from Field Site to Terrestrial Water Storage and Impact in the Integrated Forecast System. *Journal of Hydrometeorology*, 10(3): 623-643.
- Baltz, D.M., Moyle, P.B., 1993. Invasion resistance to introduced species by a native assemblage of California stream fishes. *Ecological Applications*, 3(2): 246-255.
- Barnett, T.P., Adam, J.C., Lettenmaier, D.P., 2005. Potential impacts of a warming climate on water availability in snow-dominated regions. *Nature*, 438(7066): 303-309.
- Bartholow, J.M., 1991. A Modeling Assessment of the Thermal Regime for an Urban Sport Fishery. *Environmental Management*, 15(6): 833-845.

References

- Bartholow, J.M., 2005. Recent water temperature trends in the lower Klamath River, California. *North American Journal of Fisheries Management*, 25(1): 152-162.
- Bates, B.C., Kundzewicz, Z.W., Wu, S., Palutikof, J.P. (Eds.), 2008. *Climate Change and Water*. Technical Paper of the Intergovernmental Panel on Climate Change. IPCC Secretariat, Geneva, 210 pp.
- Beven, K., 2011. I believe in climate change but how precautionary do we need to be in planning for the future? *Hydrological Processes*, 25(9): 1517-1520.
- Biemans, H. et al., 2009. Effects of Precipitation Uncertainty on Discharge Calculations for Main River Basins. *Journal of Hydrometeorology*, 10(4): 1011-1025.
- Boer, G.J., Yu, B., 2003. Climate sensitivity and climate state. *Climate Dynamics*, 21(2): 167-176.
- Bogan, T., Mohseni, O., Stefan, H.G., 2003. Stream temperature-equilibrium temperature relationship. *Water Resources Research*, 39(9): 1245.
- Bogan, T., Othmer, J., Mohseni, O., Stefan, H., 2006. Estimating extreme stream temperatures by the standard deviate method. *Journal of Hydrology*, 317(3-4): 173-189.
- Bölcher, T., van Slobbe, E., van Vliet, M.T.H., Werners, S., submitted. Adaptive turning points in river restoration? The Rhine salmon case.
- Boogert, A., Dupont, D., 2005. The nature of supply side effects on electricity prices: The impact of water temperature. *Economics Letters*, 88(1): 121-125.
- Bowling, L.C., Lettenmaier, D.P., 2010. Modeling the Effects of Lakes and Wetlands on the Water Balance of Arctic Environments. *Journal of Hydrometeorology*, 11(2): 276-295.
- Bras, R.A., 1990. *Hydrology, an Introduction to Hydrologic Science*. Addison Wesley, 643 pp.
- Brown, G.W., 1969. Predicting temperatures of small streams. *Water Resources Research* 5: 68- 75.
- Burlando, P., Rosso, R., 2002. Effects of transient climate change on basin hydrology. 2. Impacts on runoff variability in the Arno River, central Italy. *Hydrological Processes*, 16(6): 1177-1199.
- Caissie, D., 2006. The thermal regime of rivers: a review. *Freshwater Biology*, 51(8): 1389-1406.
- Caissie, D., El-Jabi, N., St-Hilaire, A., 1998. Stochastic modelling of water temperatures in a small stream using air to water relations. *Canadian Journal of Civil Engineering*, 25(2): 250-260.
- Caissie, D., Satish, M.G., El-Jabi, N., 2005. Predicting river water temperatures using the equilibrium temperature concept with application on Miramichi River catchments (New Brunswick, Canada). *Hydrological Processes*, 19(11): 2137-2159.
- Caissie, D., Satish, M.G., El-Jabi, N., 2007. Predicting water temperatures using a deterministic model: Application on Miramichi River catchments (New Brunswick, Canada). *Journal of Hydrology*, 336(3-4): 303-315.
- Carpenter, S.R., Fisher, S.G., Grimm, N.B., Kitchell, J.F., 1992. Global Change and Fresh-water Ecosystems. *Annual Review of Ecology and Systematics*, 23: 119-139.
- Caruso, B.S., 2002. Temporal and spatial patterns of extreme low flows and effects on stream ecosystems in Otago, New Zealand. *Journal of Hydrology*, 257(1-4): 115-133.
- Chauhan, D.P.S., 1994. India I. In: *Fishery cooperatives in Asia*, Asian Productivity Organization, Tokyo, Japan.
- Chen, C. et al., 2011. Projected hydrological changes in the 21st century and related uncertainties obtained from a multi-model ensemble. *WATCH Technical Report No. 45*, 28 pp.
- Chenard, J.F., Caissie, D., 2008. Stream temperature modelling using artificial neural networks: application on Catamaran Brook, New Brunswick, Canada. *Hydrological Processes*, 22(17): 3361-3372.
- Cherkauer, K.A., Bowling, L.C., Lettenmaier, D.P., 2003. Variable infiltration capacity cold land process model updates. *Global and Planetary Change*, 38(1-2): 151-159.
- Chu, C., Mandrak, N.E., Minns, C.K., 2005. Potential impacts of climate change on the distributions of several common and rare freshwater fishes in Canada. *Diversity and Distributions*, 11(4): 299-310.
- CIESIN, 2005. *Gridded Population of the World Version 3 (GPWv3): Population Grids*. In: International Earth Science Information Network (CIESIN), C.U., USA.
- Coleman, M.A., Fausch, K.D., 2007. Cold summer temperature regimes cause a recruitment bottleneck in age-0 Colorado River cutthroat trout reared in laboratory streams. *Transactions of the American Fisheries Society*, 136(3): 639-654.

- Connor, W.P., Burge, H.L., Yearsley, J.R., Bjornn, T.C., 2003. Influence of flow and temperature on survival of wild subyearling fall chinook salmon in the Snake River. *North American Journal of Fisheries Management*, 23(2): 362-375.
- Coutant, C.C., 1969. Temperature, Reproduction and Behavior. *Chesapeake Science*, 10(3-4): 261-274
- Coutant, C.C., 1987. Thermal preference - when does an asset become a liability. *Environmental Biology of Fishes*, 18(3): 161-172.
- Cox, P.M. et al., 1999. The impact of new land surface physics on the GCM simulation of climate and climate sensitivity. *Climate Dynamics*, 15(3): 183-203.
- Crisp, D.T., Howson, G., 1982. Effect of air-temperature upon mean water temperature in streams in the north Pennines and English lake district. *Freshwater Biology*, 12(4): 359-367.
- Cristea, N.C., Burges, S.J., 2009. An assessment of the current and future thermal regimes of three streams located in the Wenatchee River basin, Washington State: some implications for regional river basin systems. *Climatic Change*, 102(3-4): 493-520
- Dai, A., Qian, T.T., Trenberth, K.E., Milliman, J.D., 2009. Changes in Continental Freshwater Discharge from 1948 to 2004. *Journal of Climate*, 22(10): 2773-2792.
- Dallas, H., 2008. Water temperature and riverine ecosystems: An overview of knowledge and approaches for assessing biotic responses, with special reference to South Africa. *Water SA*, 34(3): 393-404.
- de Rosnay, P., Polcher, J., 1998. Modelling root water uptake in a complex land surface scheme coupled to a GCM. *Hydrology and Earth System Sciences*, 2(2-3): 239-255.
- Del Genio, A.D., Lacis, A.A., Ruedy, R.A., 1991. Simulations of the Effect of a Warmer Climate on Atmospheric Humidity. *Nature* 351(6325): 382-385.
- Delpla, I., Jung, A.-V., Baures, E., Clement, M., Thomas, O., 2009. Impacts of climate change on surface water quality in relation to drinking water production. *Environment International* 35(8): 1225-1233.
- Déqué, M., Dreveton, C., Braun, A., Cariolle, D., 1994. The ARPEGE/IFS atmosphere model : A contribution to the French community climate modelling. *Climate Dyn.*, 10: 249-266.
- Diaz-Nieto, J., Wilby, R.L., 2005. A comparison of statistical downscaling and climate change factor methods: Impacts on low flows in the River Thames, United Kingdom. *Climatic Change*, 69(2-3): 245-268.
- Döll, P., Fiedler, K., Zhang, J., 2009. Global-scale analysis of river flow alterations due to water withdrawals and reservoirs. *Hydrology and Earth System Sciences*, 13(12): 2413-2432.
- Döll, P., Lehner, B., 2002. Validation of a new global 30-min drainage direction map. *Journal of Hydrology*, 258(1-4): 214-231.
- Döll, P., Müller Schmied, H., 2012. How is the impact of climate change on river flow regimes related to the impact on mean annual runoff? A global-scale analysis. *Environ. Res. Lett.* , 7(1): 014037.
- Döll, P., Zhang, J., 2010. Impact of climate change on freshwater ecosystems: a global-scale analysis of ecologically relevant river flow alterations. *Hydrology and Earth System Sciences*, 14(5): 783-799.
- Ducharne, A., 2008. Importance of stream temperature to climate change impact on water quality. *Hydrol. Earth Syst. Sci.* , 12: 797-810.
- Dudgeon, D. et al., 2006. Freshwater biodiversity: importance, threats, status and conservation challenges. *Biological Reviews*, 81(2): 163-182.
- Durack, P.J., Wijffels, S.E., Matear, R.J., 2012. Ocean Salinities Reveal Strong Global Water Cycle Intensification During 1950 to 2000. *Science*, 336(6080): 455-458.
- Dyson, M., Bergkamp, M., Scanlon, J., 2003. *Flow: The Essentials of Environmental Flows*, IUCN, Gland, Switzerland and Cambridge, U.K..
- Easterling, D.R. et al., 2000. Climate extremes: Observations, modeling, and impacts. *Science*, 289(5487): 2068-2074.
- Eaton, J.G. et al., 1995. A Field Information-based System for Estimating Fish Temperature Tolerances. *Fisheries*, 20(4): 10-18.
- Eaton, J.G., Scheller, R.M., 1996. Effects of climate warming on fish thermal habitat in streams of the United States. *Limnol. Oceanogr.*, 41(5): 1109-1115.

References

- Ebersole, J.L., Liss, W.J., Frissell, C.A., 2001. Relationship between stream temperature, thermal refugia and rainbow trout *Oncorhynchus mykiss* abundance in arid-land streams in the northwestern United States. *Ecology of Freshwater Fish*, 10: 1-10.
- Edinger, J.E., Brady, D.K., Graves, W.L., 1968a. Variation of Water Temperatures due to Steam Electric Cooling Operations. *Journal Water Pollution Control Federation*, 40(9): 1632-1639.
- Edinger, J.E., Duttweil, D.W., Geyer, J.C., 1968b. Response of water temperatures to meteorological conditions. *Water Resources Research*, 4(5): 1137-1143.
- EEA, 2008a. Energy and environment report 2008, Copenhagen, EEA Report No 6/2008, 100 pp.
- EEA, 2008b. Impacts of Europe's changing climate - indicator-based assessment Copenhagen, EEA Report No 4/2008, 242 pp.
- EIA, accessed 2011. U.S. Energy Information Administration, Independent Statistics & Analysis, International Energy Statistics.
- Eliason, E.J. et al., 2011. Differences in Thermal Tolerance Among Sockeye Salmon Populations. *Science*, 332(6025): 109-112.
- Elsner, M.M. et al., 2010. Implications of 21st century climate change for the hydrology of Washington State. *Climatic Change*, 102(1-2): 225-260.
- EPA, 1988. Temperature, Water Quality Standards Criteria Summaries: A Compilation of State/Federal Criteria. EPA/440/5-88-023, United States Environmental Protection Agency, Office of Water Washington, DC 20460, 84 pp.
- EPA, 2011. Technical Development Document for the Proposed Section 316(b) Phase II Existing Facilities Rule, U.S. Environmental Protection Agency Washington, DC 20460, 428 pp.
- Erickson, T.R., Stefan, H.G., ASCE, M., 2000. Linear air/water temperature correlations for streams during open water periods. *Journal of Hydrologic Engineering*, 5(3): 317-322.
- FAO, 2008. Climate change implications for fisheries and aquaculture. FAO, Rome, Italy, pp. 41.
- Fekete, B.M., Vörösmarty, C.J., Roads, J.O., Willmott, C.J., 2004. Uncertainties in precipitation and their impacts on runoff estimates. *Journal of Climate*, 17(2): 294-304.
- Ferrari, M.R., Miller, J.R., Russell, G.L., 2007. Modeling changes in summer temperature of the Fraser River during the next century. *Journal of Hydrology*, 342(3-4): 336-346.
- Feyen, L., Dankers, R., 2009. Impact of global warming on streamflow drought in Europe. *Journal of Geophysical Research-Atmospheres*, 114.
- Fichefet, T., Morales Maqueda, M.A., 1997. Sensitivity of a global sea ice model to the treatment of ice thermodynamics and dynamics. *J. Geophys. Res.*, 102: 12609-12646.
- Ficke, A.D., Myrick, C.A., Hansen, L.J., 2007. Potential impacts of global climate change on freshwater fisheries. *Reviews in Fish Biology and Fisheries*, 17(4): 581-613.
- Fischlin, A. et al., 2007. Ecosystems, their properties, goods, and services. In: Parry, M.L., Canziani, O.F., Palutikof, J.P., van der Linden, P.J., Hanson, C.E. (Eds.), *Climate Change 2007: Impacts, Adaptation and Vulnerability. Contribution of Working Group II to the Fourth Assessment Report of the Intergovernmental Panel on Climate Change*. Cambridge University Press, Cambridge pp. 211-272.
- Fleig, A.K., Tallaksen, L.M., Hisdal, H., Demuth, S., 2006. A global evaluation of streamflow drought characteristics. *Hydrology and Earth System Sciences*, 10(4): 535-552.
- Flörke, M., Barlund, I., Kynast, E., 2012. Will climate change affect the electricity production sector? A European study. *Journal of Water and Climate Change*, 3(1): 44-54.
- Flörke, M., Eisner, S., 2011. The development of global spatially detailed estimates of sectoral water requirements, past, present and future, including discussion of the main uncertainties, risks and vulnerabilities of human water demand. *WATCH Technical Report No. 46*, 25 pp.
- Flörke, M., Teichert, E., Bärlund, I., 2011. Future changes of freshwater needs in European power plants. *Management of Environmental Quality: An International Journal*, 22(1): 89 - 104.
- Foreman, M.G. et al., 2001. Simulations and retrospective analyses of Fraser watershed flows and temperatures. *Atmos. Ocean*, 39(2): 89- 105.
- Forster, H., Lilliestam, J., 2011. Modeling Thermoelectric Power Generation in View of Climate Change. *Regional Environmental Change*, 4(4): 327-338.

- Fowler, H., Blenkinsop, S., Tebaldi, C., 2007a. Linking climate change modelling to impacts studies: recent advances in downscaling techniques for hydrological modelling. *International Journal of Climatology*, 27: 1547-1578.
- Fowler, H.J., Blenkinsop, S., Tebaldi, C., 2007b. Linking climate change modelling to impacts studies: recent advances in downscaling techniques for hydrological modelling. *International Journal of Climatology*, 27(12): 1547-1578.
- GEA, 2012. *Global Energy Assessment – Toward a Sustainable Future*, International Institute for Applied Systems Analysis, Laxenburg, Austria, Cambridge UK and New York, NY, USA.
- Gerbens-Leenes, W., Hoekstra, A.Y., van der Meer, T.H., 2009. The water footprint of bioenergy. *Proceedings of the National Academy of Sciences of the United States of America*, 106(25): 10219-10223.
- Gerdaux, D., 1998. *Fluctuations in lake fisheries and global warming. Mangement of lakes and reservoirs during global climate change*. Kluwer Publishers, Dordrecht, The Netherlands.
- Gibson, C.A., Meyer, J.L., Poff, N.L., Hay, L.E., Georgakakos, A., 2005. Flow regime alterations under changing climate in two river basins: Implications for freshwater ecosystems. *River Research and Applications*, 21(8): 849-864.
- Gooseff, M.N., Strzepek, K., Chapra, S.C., 2005. Modeling the potential effects of climate change on water temperature downstream of a shallow reservoir, Lower Madison River, MT. *Climatic Change*, 68(3): 331-353.
- Goose, H., Fichefet, T., 1999. Importance of ice-ocean interactions for the global ocean circulation: A model study. *J. Geophys. Res.*, 104: 23337-23355.
- Graham, L.P., Hagemann, S., Jaun, S., Beniston, M., 2007. On interpreting hydrological change from regional climate models. *Climatic Change*, 81: 97-122.
- Grossman, G.D., Ratajczak, R.E., Crawford, M., Freeman, M.C., 1998. Assemblage organization in stream fishes: Effects of environmental variation and interspecific interactions. *Ecological Monographs*, 68(3): 395-420.
- Haag, I., Luce, A., 2008. The integrated water balance and water temperature model LARSIM-WT. *Hydrological Processes*, 22(7): 1046-1056.
- Haag, I., Westrich, B., 2002. Processes governing river water quality identified by principal component analysis. *Hydrological Processes*, 16(16): 3113-3130.
- Haddeland, I., in prep. *Global water availability and demand: What might the future bring?* (in prep).
- Haddeland, I., D.B. Clark, W. Franssen, F. Ludwig, F. Voß, N.W. Arnell, N. Bertrand, M. Best, S. Folwell, D. Gerten, S. Gomes, S.N. Gosling, S. Hagemann, N. Hanasaki, R. Harding, J. Heinke, P. Kabat, S. Koirala, T. Oki, J. Polcher, T. Stacke, P. Viterbo, G.P. Weedon, and P. Yeh, 2011. Multimodel Estimate of the Terrestrial Global Water Balance: Setup and First Results. *J. Hydrometeor.*, 12: 869–884.
- Haddeland, I. et al., 2012. Effects of climate model radiation, humidity and wind estimates on hydrological simulations. *Hydrol. Earth Syst. Sci.*, 16: 305-318.
- Haddeland, I., Skaugen, T., Lettenmaier, D.P., 2006. Anthropogenic impacts on continental surface water fluxes. *Geophysical Research Letters*, 33(8): L08406.
- Hagemann, S. et al., in prep. *Climate change impact on available water resources obtained using multiple GCMs and GHMs*.
- Hagemann, S. et al., 2011. Impact of a Statistical Bias Correction on the Projected Hydrological Changes Obtained from Three GCMs and Two Hydrology Models. *Journal of Hydrometeorology*, 12(4): 556-578.
- Hagemann, S., Dumenil, L., 1998. A parametrization of the lateral waterflow for the global scale. *Climate Dynamics*, 14(1): 17-31.
- Hamlet, A.F., Lettenmaier, D.P., 1999. Effects of climate change on hydrology and water resources in the Columbia River basin. *Journal of the American Water Resources Association*, 35(6): 1597-1623.
- Hanasaki, N. et al., 2008. An integrated model for the assessment of global water resources Part 1: Model description and input meteorological forcing. *Hydrology and Earth System Sciences*, 12(4): 1007-1025.

References

- Harvey, B.C., 1987. Susceptibility of young-of-the-year fishes to downstream displacement by flooding. *Transactions of the American Fisheries Society*, 116(6): 851-855.
- Hay, L.E., Wilby, R.J.L., Leavesley, G.H., 2000. A comparison of delta change and downscaled GCM scenarios for three mountainous basins in the United States. *Journal of the American Water Resources Association*, 36(2): 387-397.
- Held, I.M., Soden, B.J., 2006. Robust Responses of the Hydrological Cycle to Global Warming. *Journal of Climate* 19: 5686-99.
- Hisdal, H., Clausen, B., Gustard, A., Peters, E., Tallaksen, L.M., 2004. Event Definitions and Indices, In: Tallaksen, L. M. and van Lanen, H. A. J.(Eds.), *Hydrological Drought – Processes and Estimation Methods for Streamflow and Groundwater*, Developments in Water Science, 48, Elsevier Science B.V., Amsterdam, pp. 139–198.
- Hisdal, H., Stahl, K., Tallaksen, L.M., Demuth, S., 2001. Have streamflow droughts in Europe become more severe or frequent? *International Journal of Climatology*, 21(3): 317-333.
- Hockey, J.B., Owens, I.F., Tapper, N.J., 1982. Empirical and theoretical models to isolate the effect of discharge on summer water temperatures in the Hurunui River. *J. Hydrol.*, 21: 1-12.
- Hodgkins, G.A., Dudley, R.W., Huntington, T.G., 2003. Changes in the timing of high river flows in New England over the 20th Century. *Journal of Hydrology*, 278(1-4): 244-252.
- Hoekstra, A.Y., Mekonnen, M.M., 2012. The water footprint of humanity. *Proceedings of the National Academy of Sciences of the United States of America*, 109(9): 3232-3237.
- Hossain, D., 1994. Bangladesh. In: *Fishery cooperatives in Asia*, Asian Productivity Organization, Tokyo, Japan.
- Hourdin, F. et al., 2006. The LMDZ4 general circulation model: climate performance and sensitivity to parametrized physics with emphasis on tropical convection. *Climate Dyn.*, 27: 787-813.
- Huntington, T.G., 2006. Evidence for Intensification of the Global Water Cycle: Review and Synthesis. *Journal of Hydrology*, 319: 83-95.
- Hurkmans, R., De Moel, H., Aerts, J., Troch, P.A., 2008. Water balance versus land surface model in the simulation of Rhine river discharges. *Water Resources Research*, 44(1).
- Hurkmans, R. et al., 2010. Changes in Streamflow Dynamics in the Rhine Basin under Three High-Resolution Regional Climate Scenarios. *Journal of Climate*, 23(3): 679-699.
- Hurkmans, R.T.W.L. et al., 2009. Effects of land use changes on streamflow generation in the Rhine basin. *Water Resour. Res.*, 45(W06405).
- Icke, J., Penailillo, R., Rutten, M., 2006. De invloed van warmtelozingen op de watertemperatuur van de Rijn, WL Delft Hydraulics (Deltares), Delft, The Netherlands.
- ICOLD, 2003. *World Register of Dams 2003*. International Commission on Large Dams, Paris, France, 340 pp.
- IEA-NEA, 2010. *Projected Costs of Generating Electricity*, International Energy Agency and Nuclear Energy Agency, 218 pp.
- IIASA, 2007. *GGI Scenario Database*. Institute for Applied System Analysis, <http://www.iiasa.ac.at/Research/GGI/DB/>
- Ines, A.V.M., Hansen, J.W., 2006. Bias correction of daily GCM rainfall for crop simulation studies. *Agricultural and Forest Meteorology*, 138(1-4): 44-53.
- IPCC, 2007. *Summary for Policymakers*. In: Solomon, S., D. Qin, M. Manning, Z. Chen, M. Marquis, K.B. Averyt, M. Tignor and H.L. Miller (Ed.), *Climate Change 2007: The Physical Science Basis*. Contribution of Working Group I to the Fourth Assessment Report of the Intergovernmental Panel on Climate Change Cambridge University Press, Cambridge, United Kingdom and New York, NY, USA. 21 pp.
- IPCC, 2012. *Workshop Report of the Intergovernmental Panel on Climate Change, Workshop on Socio-Economic Scenarios*, Potsdam Institute for Climate Impact Research, Potsdam, Germany. 61 pp.
- IPCC, 2001. *Reference Document on the application of Best Available Techniques to Industrial Cooling Systems, Integrated Pollution Prevention and Control*. 335 pp.
- Isaak, D.J., Wollrab, S., Horan, D., Chandler, G., 2012. Climate change effects on stream and river temperatures across the northwest U.S. from 1980–2009 and implications for salmonid fishes. *Climatic Change*, 113 (2): 499-524.

- Jacob, D. et al., 2007. An inter-comparison of regional climate models for Europe: model performance in present-day climate. *Climatic Change*, 81: 31-52.
- Janssen, P.H.M., Heuberger, P.S.C., 1995. Calibration of process-oriented models. *Ecological Modelling*, 83(1-2): 55-66.
- Jeppesen, E., Iversen, T.M., 1987. Two simple-models for estimating daily mean water temperatures and diel variations in a Danish low gradient stream. *Oikos*, 49(2): 149-155.
- Jeppesen, E. et al., 2010. Impacts of climate warming on lake fish community structure and potential effects on ecosystem function. *Hydrobiologia*, 646(1): 73-90.
- Johnson, T.B., Evans, D.O., 1990. Size-dependent winter mortality of young-of-the-year white perch - Climate warming and invasion of the Laurentian Great-Lakes. *Transactions of the American Fisheries Society*, 119(2): 301-313.
- Jones, R.N., 2000. Managing uncertainty in climate change projections - Issues for impact assessment - An editorial comment. *Climatic Change*, 45(3-4): 403-419.
- Jungclaus, J.H. et al., 2006. Ocean circulation and tropical variability in the coupled model ECHAM5/MPI-OM. *J Climate*, 19: 3952-3972.
- Kaschner, K. et al., 2010. AquaMaps: Predicted range maps for aquatic species, www.aquamaps.org, Version 08/2010.
- Kaushal, S.S. et al., 2010. Rising stream and river temperatures in the United States. *Front Ecol Environ*, 8(9): 461-466.
- Kimball, J.S., Running, S.W., Nemani, R., 1997. An improved method for estimating surface humidity from daily minimum temperature. *Agricultural and Forest Meteorology*, 85(1-2): 87-98.
- King, C.W., Holman, A.S., Webber, M.E., 2008. Thirst for energy. *Nature Geoscience*, 1(5): 283-286.
- Klein Tank, A.M.G. et al., 2002. Daily dataset of 20th-century surface air temperature and precipitation series for the European Climate Assessment. *International Journal of Climatology*, 22(12): 1441-1453.
- Koch, H., Vögele, S., 2009. Dynamic modelling of water demand, water availability and adaptation strategies for power plants to global change. *Ecological Economics*, 68: 2031-2039.
- Koch, H., Vögele, S., Kaltofen, M., Grünewald, U., 2012. Trends in water demand and water availability for power plants - scenario analyses for the German capital Berlin. *Climatic Change* 110: 879-899.
- Köppen, W., 1923. *Die Klimate der Erde*. Walter de Gruyter, Berlin.
- Kundzewicz, Z.W. et al., 2005. Trend detection in river flow series: 1. Annual maximum flow. *Hydrological Sciences Journal-Journal Des Sciences Hydrologiques*, 50(5): 797-810.
- Kundzewicz, Z.W., Krysanova, V., 2010. Climate change and stream water quality in the multi-factor context. *Climatic Change*, 103(3-4): 353-362.
- Kundzewicz, Z.W. et al., 2007. Freshwater resources and their management. . In: Parry, M.L., Canziani, O.F., Palutikof, J.P., van der Linden, P.J., Hanson, C.E. (Eds.), *Climate Change 2007: Impacts, Adaptation and Vulnerability. Contribution of Working Group II to the Fourth Assessment Report of the Intergovernmental Panel on Climate Change*. Cambridge University Press, Cambridge, UK, pp. 173-210.
- Kwadijk, J.C.J. et al., 2010. Using adaptation tipping points to prepare for climate change and sea level rise: a case study in the Netherlands. *Wiley Interdisciplinary Reviews-Climate Change*, 1(5): 729-740.
- Lammers, R.B., Pundsack, J.W., Shiklomanov, A.I., 2007. Variability in river temperature, discharge, and energy flux from the Russian pan-Arctic landmass. *Journal of Geophysical Research-Biogeosciences*, 112(G04S59).
- Lehner, B., Czisch, G., Vassolo, S., 2005. The impact of global change on the hydropower potential of Europe: a model-based analysis. *Energy Policy*, 33(7): 839-855.
- Lehner, B., Döll, P., Alcamo, J., Henrichs, T., Kaspar, F., 2006. Estimating the impact of global change on flood and drought risks in Europe: A continental, integrated analysis. *Climatic Change*, 75(3): 273-299.
- Leopold, L.B., Maddock, T., 1953. The hydraulic geometry of stream channels and some physiographic implications. U.S. Geological Survey Professional Paper, U.S. Geological Survey, 252 pp.

References

- Li, H.B., Sheffield, J., Wood, E.F., 2010. Bias correction of monthly precipitation and temperature fields from Intergovernmental Panel on Climate Change AR4 models using equidistant quantile matching. *Journal of Geophysical Research-Atmospheres*, 115, D10101.
- Liang, X., Guo, J.Z., Leung, L.R., 2004. Assessment of the effects of spatial resolutions on daily water flux simulations. *Journal of Hydrology*, 298(1-4): 287-310.
- Liang, X., Lettenmaier, D.P., Wood, E.F., Burges, S.J., 1994. A Simple Hydrologically Based Model of Land-Surface Water and Energy Fluxes for General-Circulation Models. *Journal of Geophysical Research-Atmospheres*, 99(D7): 14415-14428.
- Liu, B.Z., Yang, D.Q., Ye, B.S., Berezovskaya, S., 2005. Long-term open-water season stream temperature variations and changes over Lena River Basin in Siberia. *Global and Planetary Change*, 48(1-3): 96-111.
- Lobmeyr, M., Lohmann, D., Ruhe, C., 1999. An application of a large scale conceptual hydrological model over the Elbe region. *Hydrology and Earth System Sciences*, 3(3): 363-374.
- Lohmann, D., Raschke, E., Nijssen, B., Lettenmaier, D.P., 1998. Regional scale hydrology: I. Formulation of the VIC-2L model coupled to a routing model. *Hydrological Sciences Journal-Journal Des Sciences Hydrologiques*, 43(1): 131-141.
- Lowney, C.L., 2000. Stream temperature variation in regulated rivers: Evidence for a spatial pattern in daily minimum and maximum magnitudes. *Water Resources Research*, 36(10): 2947-2955.
- Lytle, D.A., Poff, N.L., 2004. Adaptation to natural flow regimes. *Trends in Ecology & Evolution*, 19(2): 94-100.
- Mackay, J.R., Mackay, D.K., 1975. Heat energy of the Mackenzie River. Further hydrologic studies in the Mackenzie Valley, Canada, Environmental-Social Committee Northern Pipelines. Task Force on Northern Oil Development report, Ottawa, 110 pp.
- Macknick, J., Newmark, R., Heath, G., Hallett, K.C., 2011. A Review of Operational Water Consumption and Withdrawal Factors for Electricity Generating Technologies, National Renewable Energy Laboratory, Colorado, 29 pp.
- Madec, G., Delecluse, P., Imbard, M., Lévy, C., 1998. OPA version 8.1 Ocean General Circulation Model Reference Manual, Notes du Pôle de Modélisation, Institut Pierre-Simon Laplace, n°11. Available from Laboratoire d'Océanographie Dynamique et de Climatologie, Université Paris VI, Paris 75252, France, pp. 91.
- Magnuson, J.J., Crowder, L.B., Medvick, P.A., 1979. Temperature as an ecological resource. *American Zoologist*, 19(1): 331-343.
- Manoha, B., Hendrickx, F., Dupeyrat, A., Bertier, C., Parey, S., 2008. Climate change impact on the activities of Electricite de France. *Houille Blanche-Revue Internationale De L Eau*(2): 55-60.
- Mantua, N., Tohver, I., Hamlet, A., 2010. Climate change impacts on streamflow extremes and summertime stream temperature and their possible consequences for freshwater salmon habitat in Washington State. *Climatic Change* 102(1-2): 187-223.
- Matthews, W.J., Marsh-Matthews, E., 2003. Effects of drought on fish across axes of space, time and ecological complexity. *Freshwater Biology*, 48(7): 1232-1253.
- McDermott, G.R., Nilsen, Ø.A., 2011. Electricity Prices, River Temperatures and Cooling Water Scarcity. Discussion Paper Series in Economics 18/2011, Department of Economics, Norwegian School of Economics.
- Meehl, G.A. et al., 2007. Global Climate Projections. In: Solomon, S., D. Qin, M. Manning, Z. Chen, M. Marquis, K.B. Averyt, M. Tignor and H.L. Miller (Ed.), *Climate Change 2007: The Physical Science Basis. Contribution of Working Group I to the Fourth Assessment Report of the Intergovernmental Panel on Climate Change* Cambridge University Press, Cambridge, United Kingdom and New York, NY, USA. pp. 747-846.
- Meigh, J.R., McKenzie, A.A., Sene, K.J., 1999. A grid-based approach to water scarcity estimates for eastern and southern Africa. *Water Resources Management*, 13(2): 85-115.
- Mekonnen, M.M., Hoekstra, A.Y., 2012. The blue water footprint of electricity from hydropower. *Hydrol. Earth Syst. Sci.*, 16 179-187.
- Menzel, L., Burger, G., 2002. Climate change scenarios and runoff response in the Mulde catchment (Southern Elbe, Germany). *Journal of Hydrology*, 267(1-2): 53-64.

- Meyer, J.L., Sale, M.J., Mulholland, P.J., Poff, N.L., 1999. Impacts of climate change on aquatic ecosystem functioning and health. *Journal of the American Water Resources Association*, 35(6): 1373-1386.
- Millennium Ecosystem Assessment, 2005. *Ecosystems and Human Well-being: Biodiversity Synthesis*, World Resources Institute, Washington, DC, 100 pp.
- Milly, P.C.D., Dunne, K.A., Vecchia, A.V., 2005. Global pattern of trends in streamflow and water availability in a changing climate. *Nature*, 438(7066): 347-350.
- Mims, M.C., Olden, J.D., 2012. Life history theory predicts fish assemblage response to hydrologic regimes. *Ecology*, 93(1): 35-45.
- Moatar, F., Gailhard, J., 2006. Water temperature behaviour in the River Loire since 1976 and 1881. *Comptes Rendus Geoscience*, 338(5): 319-328.
- Mohseni, O., Erickson, T.R., Stefan, H.G., 1999. Sensitivity of stream temperatures in the United States to air temperatures projected under a global warming scenario. *Water Resources Research*, 35(12): 3723-3733.
- Mohseni, O., Erickson, T.R., Stefan, H.G., 2002. Upper bounds for stream temperatures in the contiguous United States. *Journal of Environmental Engineering-Asce*, 128(1): 4-11.
- Mohseni, O., Stefan, H.G., 1999. Stream temperature air temperature relationship: a physical interpretation. *Journal of Hydrology*, 218(3-4): 128-141.
- Mohseni, O., Stefan, H.G., Eaton, J.G., 2003. Global warming and potential changes in fish habitat in US streams. *Climatic Change*, 59(3): 389-409.
- Mohseni, O., Stefan, H.G., Erickson, T.R., 1998. A nonlinear regression model for weekly stream temperatures. *Water Resources Research*, 34(10): 2685-2692.
- Monteith, J.L., 1965. Evaporation and environment. *Proceedings of the 19th symposium of the Society for Experimental Biology*: 205-233.
- Moore, M.V. et al., 1997. Potential effects of climate change on freshwater ecosystems of the New England/Mid-Atlantic Region. *Hydrological Processes*, 11(8): 925-947.
- Morrison, J., Quick, M.C., Foreman, M.G.G., 2002. Climate change in the Fraser River watershed: flow and temperature projections. *Journal of Hydrology*, 263(1-4): 230-244.
- Moss, R.H. et al., 2010. The next generation of scenarios for climate change research and assessment. *Nature*, 463(7282): 747-756.
- Mulholland, P.J. et al., 1997. Effects of climate change on freshwater ecosystems of the south-eastern United States and the Gulf Coast of Mexico. *Hydrological Processes*, 11(8): 949-970.
- Murdoch, P.S., Baron, J.S., Miller, T.L., 2000. Potential effects of climate change on surface-water quality in North America. *Journal of the American Water Resources Association*, 36(2): 347-366.
- Muttiah, R.S., Srinivasan, R., Allen, P.M., 1997. Prediction of two-year peak stream discharges using neural networks. *Journal of the American Water Resources Association*, 33(3): 625-630.
- Nakicenovic, N., J. Alcamo, G. Davis, H.J.M. de Vries, J. Fenhann, S. Gaffin, K. Gregory, A. Grubler, T.Y. Jung, T. Kram, E.L. La Rovere, L. Michaelis, S. Mori, T. Morita, W. Papper, H. Pitcher, L. Price, K. Riahi, A. Roehrl, H-H. Rogner, A. Sankovski, M. Schlesinger, P. Shukla, S. Smith, R. Swart, S. van Rooijen, N. Victor, Z. Dadi, 2000. *Emissions Scenarios. A Special Report of Working Group III of the Intergovernmental Panel on Climate Change*, Cambridge University Press, Cambridge, 27 pp.
- Nash, J.E., Sutcliffe, J.V., 1970. River flow forecasting through conceptual models, part 1 - a discussion of principles. *Journal of Hydrology*, 10: 282-290.
- Nelson, K.C., Palmer, M.A., 2007. Stream temperature surges under urbanization and climate change: Data, models, and responses. *Journal of the American Water Resources Association*, 43(2): 440-452.
- NETL, 2007. *National Energy Technology Laboratory Coal Power Plant Database (NETL-CPPDB)* In: Laboratory, U.S. Department of Energy National Energy Technology Laboratory, <http://www.netl.doe.gov/about/index.html>.
- NETL, 2009. *Impact of Drought on U.S. Steam Electric Power Plant Cooling Water Intakes and Related Water Resource Management Issues*, National Energy Technology Laboratory, Pittsburgh, DOE/NETL-2009/1364, 58 pp.

References

- Nijssen, B., O'Donnell, G.M., Hamlet, A.F., Lettenmaier, D.P., 2001a. Hydrologic sensitivity of global rivers to climate change. *Climatic Change*, 50(1-2): 143-175.
- Nijssen, B., O'Donnell, G.M., Lettenmaier, D.P., Lohmann, D., Wood, E.F., 2001b. Predicting the discharge of global rivers. *Journal of Climate*, 14(15): 3307-3323.
- Nijssen, B., Schnur, R., Lettenmaier, D.P., 2001c. Global retrospective estimation of soil moisture using the variable infiltration capacity land surface model, 1980-93. *Journal of Climate*, 14(8): 1790-1808.
- Oberdorff, T., Guegan, J.F., Hugueny, B., 1995. Global scale patterns of fish species richness in rivers. *Ecography*, 18(4): 345-352.
- Oki, T. et al., 2001. Global assessment of current water resources using total runoff integrating pathways. *Hydrological Sciences Journal-Journal Des Sciences Hydrologiques*, 46(6): 983-995.
- Oki, T., Kanae, S., 2006. Global hydrological cycles and world water resources. *Science*, 313(5790): 1068-1072.
- Olden, J.D., Naiman, R.J., 2010. Incorporating thermal regimes into environmental flows assessments: modifying dam operations to restore freshwater ecosystem integrity. *Freshwater Biology*, 55(1): 86-107.
- Ozaki, N. et al., 2003. Statistical analyses on the effects of air temperature fluctuations on river water qualities. *Hydrological Processes*, 17(14): 2837-2853.
- Palmer, M.A. et al., 2008. Climate change and the world's river basins: anticipating management options. *Frontiers in Ecology and the Environment*, 6(2): 81-89.
- Pan, M. et al., 2012. Multisource Estimation of Long-Term Terrestrial Water Budget for Major Global River Basins. *Journal of Climate*, 25(9): 3191-3206.
- Parry, S., Prudhomme, C., Hannaford, J., Lloyd-Hughes, B., 2010. Examining the spatio-temporal evolution and characteristics of large-scale European droughts, In: Kirby, Celia, (Ed.) *Role of Hydrology in Managing Consequences of a Changing Global Environment*. British Hydrological Society Third International Symposium, Newcastle, British Hydrological Society, pp. 135-142
- Pekarova, P. et al., 2008a. Is the Water Temperature of the Danube River at Bratislava, Slovakia, Rising? *Journal of Hydrometeorology*, 9: 1115-1122.
- Pekarova, P. et al., 2011. Long-term trend and multi-annual variability of water temperature in the pristine Bela River basin (Slovakia). *Journal of Hydrology* 400: 333-340.
- Pekarova, P. et al., 2008b. *Hydrologic Scenarios for the Danube River at Bratislava*, Ostrava KEY Publishing, 159 pp.
- Penman, H.L., 1948. Natural evaporation from open water, bare soil and grass. *Proceedings of the Royal Society A193*: 120-146.
- Perez, G.A.C., van Huijgevoort, M.H.J., Voss, F., van Lanen, H.A.J., 2011. On the spatio-temporal analysis of hydrological droughts from global hydrological models. *Hydrology and Earth System Sciences*, 15(9): 2963-2978.
- Piani, C. et al., 2010. Statistical bias correction of global simulated daily precipitation and temperature for the application of hydrological models. *Journal of Hydrology* 395: 199-215.
- Pilgrim, J.M., Fang, X., Stefan, H.G., 1998. Stream temperature correlations with air temperatures in Minnesota: Implications for climate warming. *Journal of the American Water Resources Association*, 34(5): 1109-1121.
- Poff, N.L., Allan, J.D., 1995. Functional-organization of stream fish assemblages in relation to hydrological variability. *Ecology*, 76(2): 606-627.
- Poff, N.L. et al., 1997. The natural flow regime. *Bioscience*, 47(11): 769-784.
- Poff, N.L. et al., 2010. The ecological limits of hydrologic alteration (ELOHA): a new framework for developing regional environmental flow standards. *Freshwater Biology*, 55(1): 147-170.
- Poff, N.L., Zimmerman, J.K.H., 2010. Ecological responses to altered flow regimes: a literature review to inform the science and management of environmental flows. *Freshwater Biology*, 55(1): 194-205.
- Poole, G.C., Berman, C.H., 2001. An ecological perspective on in-stream temperature: Natural heat dynamics and mechanisms of human-caused thermal degradation. *Environmental Management*, 27(6): 787-802.

- Preudhomme, E.B., Stefan, H.G., 1992. Errors Related to Random Stream Temperature Data-Collection in Upper Mississippi River Watershed. *Water Resources Bulletin*, 28(6): 1077-1082.
- Pyrce, R., 2004. Hydrological Low Flow Indices and their Uses, Watershed Science Centre. Trent University. Symons Campus, Peterborough WSC Report No. 04-2004, 37 pp.
- Rahel, F.J., Keleher, C.J., Anderson, J.L., 1996. Potential habitat loss and population fragmentation for cold water fish in the north platte river drainage of the rocky mountains: Response to climate warming. *Limnology and Oceanography*, 41(5): 1116-1123.
- Ramaker, T.A.B., Meuleman, A.F.M., Bernhardt, L., Cirkel, G., 2005. Climate change and drinking water production in The Netherlands: a flexible approach. *Water Science and Technology*, 51(5): 37-44.
- Randall, D.A. et al., 2007. Climate Models and Their Evaluation. In: *Climate Change 2007: The Physical Science Basis. Contribution of Working Group I to the Fourth Assessment Report of the Intergovernmental Panel on Climate Change* Cambridge, United Kingdom and New York, NY, USA.
- Revenga, C., Campbell, I., Abell, R., de Villiers, P., Bryer, M., 2005. Prospects for monitoring freshwater ecosystems towards the 2010 targets, pp. 397-413.
- Richter, B.D., Baumgartner, J.V., Powell, J., Braun, D.P., 1996. A method for assessing hydrologic alteration within ecosystems. *Conservation Biology*, 10(4): 1163-1174.
- Richter, B.D., Baumgartner, J.V., Wigington, R., Braun, D.P., 1997. How much water does a river need? *Freshwater Biology*, 37(1): 231-249.
- Richter, B.D., Warner, A.T., Meyer, J.L., Lutz, K., 2006. A collaborative and adaptive process for developing environmental flow recommendations. *River Research and Applications*, 22(3): 297-318.
- Risley, J.C., Constantz, J., Essaid, H., Rounds, S., 2010. Effects of upstream dams versus groundwater pumping on stream temperature under varying climate conditions. *Water Resour. Res.*, 46(W06517).
- Rivers-Moore, N.A., Jewitt, G.P.W., 2007. Adaptive management and water temperature variability within a South African river system: What are the management options? *Journal of Environmental Management*, 82(1): 39-50.
- Roeckner, E., Coauthors, 2003. The atmospheric general circulation model ECHAM5. Part I: Model description. Max Planck Institute for Meteorology, Hamburg, Germany, 349, 127 pp.
- Rost, S. et al., 2008. Agricultural green and blue water consumption and its influence on the global water system. *Water Resources Research*, 44(9): W09405.
- Rubbelke, D., Vögele, S., 2011. Impacts of climate change on European critical infrastructures: The case of the power sector. *Environmental Science & Policy* 14: 53-63.
- Ruddiman, W.F., 2001. *Earth's climate, Past and future*. W.H. Freeman and Company, New York, 465 pp.
- Rundquist, L.A., Baldrige, J.E., 1990. *Fish Habitat Considerations in Cold Region Hydrology and Hydraulics*. ASCE, New York, NY.
- Rutten, M., van de Giesen, N., Baptist, M., Icke, J., Uijttewaal, W., 2008. Seasonal forecast of cooling water problems in the River Rhine. *Hydrol. Process.*, 22: 1037-1045
- Sabo, J.L., Post, D.M., 2008. Quantifying periodic, stochastic, and catastrophic environmental variation. *Ecological Monographs*, 78(1): 19-40.
- Sahoo, G.B., Schladow, S.G., Reuter, J.E., 2009. Forecasting stream water temperature using regression analysis, artificial neural network, and chaotic non-linear dynamic models. *Journal of Hydrology* 378: 325-342.
- Salas-Méla, D., 2002. A global coupled sea ice-ocean model. *Ocean Modelling*, 4: 137-172.
- Schar, C. et al., 2004. The role of increasing temperature variability in European summer heatwaves. *Nature*, 427(6972): 332-336.
- Schindler, D.W., 2001. The cumulative effects of climate warming and other human stresses on Canadian freshwaters in the new millennium. *Canadian Journal of Fisheries and Aquatic Sciences*, 58(1): 18-29.

References

- Schneider, S., 1983. CO₂, climate and society: a brief overview. In: Chen, R., Boulding, E., Schneider, S. (Eds.), *Social science research and climate change: in interdisciplinary appraisal*, D Reidel, Boston, MA, USA, pp. 9–15.
- Segrave, A.J., 2009. SCENES: Briefing Paper River water temperature for industrial cooling, KWR Watercycle Research Institute, 93 pp.
- Seneviratne, S.I., Nicholls, D., Easterling, C.M., Goodess, S. Kanae, J. Kossin, Y. Luo, J. Marengo, K. McInnes, M. Rahimi, M. Reichstein, A. Sorteberg, C. Vera, and X. Zhang, 2012. Changes in climate extremes and their impacts on the natural physical environment. In: Field, C.B., V. Barros, T.F. Stocker, D. Qin, D.J. Dokken, K.L. Ebi, M.D. Mastrandrea, K.J. Mach, G.-K. Plattner, S.K. Allen, M. Tignor, and P.M. Midgley (Ed.), *Managing the Risks of Extreme Events and Disasters to Advance Climate Change Adaptation, A Special Report of Working Groups I and II of the Intergovernmental Panel on Climate Change (IPCC)*. Cambridge University Press Cambridge, UK, and New York, NY, USA,, pp. 109-230.
- Senhorst, H.A.J., Zwolsman, J.J.G., 2005. Climate change and effects on water quality: a first impression. *Water Science and Technology*, 51(5): 53-59.
- Sheffield, J., Andreadis, K.M., Wood, E.F., Lettenmaier, D.P., 2009. Global and Continental Drought in the Second Half of the Twentieth Century: Severity-Area-Duration Analysis and Temporal Variability of Large-Scale Events. *Journal of Climate*, 22(8): 1962-1981.
- Sheffield, J., Wood, E.F., 2008. Projected changes in drought occurrence under future global warming from multi-model, multi-scenario, IPCC AR4 simulations. *Climate Dynamics*, 31(1): 79-105.
- Shuter, B.J., Post, J.R., 1990. Climate, Population Viability, and the Zoogeography of Temperate Fishes. *Transactions of the American Fisheries Society*, 119(2): 314-336.
- Sinokrot, B.A., Gulliver, J.S., 2000. In-stream flow impact on river water temperatures *Journal of Hydraulic Research*, 38(5): 339-349.
- Sinokrot, B.A., Stefan, H.G., 1993. Stream Temperature Dynamics - Measurements and Modeling. *Water Resources Research*, 29(7): 2299-2312.
- Sinokrot, B.A., Stefan, H.G., 1994. Stream Water-Temperature Sensitivity to Weather and Bed Parameters. *Journal of Hydraulic Engineering-Asce*, 120(6): 722-736.
- Sinokrot, B.A., Stefan, H.G., McCormick, J.H., Eaton, J.G., 1995. Modeling of Climate-Change Effects on Stream Temperatures and Fish Habitats Below Dams and near Groundwater Inputs. *Climatic Change*, 30(2): 181-200.
- Smakhtin, V., 2007. Environmental flows: a call for hydrology. *Hydrological Processes*, 21(5): 701-703.
- Smakhtin, V., 2008. Basin Closure and Environmental Flow Requirements. *International Journal of Water Resources Development*, 24(2): 227-233.
- Smakhtin, V.U., 2001. Low flow hydrology: a review. *Journal of Hydrology*, 240(3-4): 147-186.
- Smakhtin, V.U., Shilpakar, R.L., Hughes, D.A., 2006. Hydrology-based assessment of environmental flows: an example from Nepal. *Hydrological Sciences Journal-Journal Des Sciences Hydrologiques*, 51(2): 207-222.
- Sperna Weiland, F.C., 2011. Hydrological impacts of climate change: Interpretation of uncertainties introduced by global models of climate and hydrology. PhD thesis Utrecht University, Utrecht Studies in Earth Sciences 006, 235 pp.
- Sperna Weiland, F.C., van Beek, L.P.H., Kwadijk, J.C.J., Bierkens, M.F.P., 2012. Global patterns of change in discharge regimes for 2100. *Hydrol. Earth Syst. Sci.*, 16: 1047–1062
- Sridhar, V., Sansone, A.L., LaMarche, J., Dubin, T., Lettenmaier, D.P., 2004. Prediction of stream temperature in forested watersheds. *Journal of the American Water Resources Association*, 40(1): 197-213.
- St-Hilaire, A., El-Jabi, N., Caissie, D., Morin, G., 2003. Sensitivity analysis of a deterministic water temperature model to forest canopy and soil temperature in Catamaran Brook (New Brunswick, Canada). *Hydrological Processes*, 17(10): 2033-2047.
- St-Hilaire, A., Morin, G., El-Jabi, N., Caissie, D., 2000. Water temperature modelling in a small forested stream: implication of forest canopy and soil temperature. *Canadian Journal of Civil Engineering*, 27(6): 1095-1108.

- Stahl, K. et al., 2010. Streamflow trends in Europe: evidence from a dataset of near-natural catchments. *Hydrology and Earth System Sciences*, 14(12): 2367-2382.
- Stefan, H.G., Fang, X., Eaton, J.G., 2001. Simulated fish habitat changes in North American lakes in response to projected climate warming. *Transactions of the American Fisheries Society*, 130(3): 459-477.
- Stefan, H.G., Preudhomme, E.B., 1993. Stream Temperature Estimation from Air-Temperature. *Water Resources Bulletin*, 29(1): 27-45.
- Stefan, H.G., Sinokrot, B.A., 1993. Projected Global Climate-Change Impact on Water Temperatures in 5 North Central United-States Streams. *Climatic Change*, 24(4): 353-381.
- Stott, P.A., Stone, D.A., Allen, M.R., 2004. Human contribution to the European heatwave of 2003. *Nature*, 432(7017): 610-614.
- Stucki, V., Sojamo, S., 2012. Nouns and Numbers of the Water–Energy–Security Nexus in Central Asia. *International Journal of Water Resources Development*, 28(3): 399-418.
- Svensson, C., Kundzewicz, Z.W., Maurer, T., 2005. Trend detection in river flow series: 2. Flood and low-flow index series. *Hydrological Sciences Journal-Journal Des Sciences Hydrologiques*, 50(5): 811-824.
- Takata, K., Emori, S., Watanabe, T., 2003. Development of the minimal advanced treatments of surface interaction and runoff. *Global and Planetary Change*, 38(1-2): 209-222.
- Tan, A., Adam, J.C., Lettenmaier, D.P., 2011. Change in spring snowmelt timing in Eurasian Arctic rivers. *Journal of Geophysical Research-Atmospheres*, 116.
- Tebaldi, C., Knutti, R., 2007. The use of the multi-model ensemble in probabilistic climate projections. *Philosophical Transactions of the Royal Society a-Mathematical Physical and Engineering Sciences*, 365(1857): 2053-2075.
- Tennant, D.L., 1976. Instream flow regimens for fish, wildlife, recreation and related environmental resources. *Fisheries*, 1(4): 6–10.
- Tharme, R.E., 2003. A global perspective on environmental flow assessment: Emerging trends in the development and application of environmental flow methodologies for rivers. *River Research and Applications*, 19(5-6): 397-441.
- Thompson, L.C. et al., 2012. Water management adaptations to prevent loss of spring-run Chinook salmon in California under climate change. *Journal of Water Resources Planning and Management*, 138: 465-478
- Thornton, P.E., Running, S.W., 1999. An improved algorithm for estimating incident daily solar radiation from measurements of temperature, humidity, and precipitation. *Agricultural and Forest Meteorology*, 93(4): 211-228.
- Todini, E., 1996. The ARNO rainfall-runoff model. *Journal of Hydrology*, 175(1-4): 339-382.
- Toprak, Z.F., Savci, M.E., 2007. Longitudinal dispersion coefficient modeling in natural channels using fuzzy logic. *Clean-Soil Air Water*, 35(6): 626-637.
- van Beek, L.P.H., Eikelboom, T., van Vliet, M.T.H., Bierkens, M.F.P., 2012. A physically-based model of global freshwater surface temperature. *Water Resour. Res.*, 48: W09530.
- van Beek, L.P.H., Wada, Y., Bierkens, M.F.P., 2011. Global monthly water stress: 1. Water balance and water availability. *Water Resour. Res.*, 47: W07517.
- van Huijgevoort, M.H.J., Hazenberg, P., van Lanen, H.A.J., Uijlenhoet, R., 2012. A generic method for hydrological drought identification across different climate regions. *Hydrol. Earth Syst. Sci. Discuss.*, 9: 2033–2070.
- van Vliet, M.T.H. et al., in press. Global River Discharge and Water Temperature under Climate Change. *Global Environmental Change-Human and Policy Dimensions*.
- van Vliet, M.T.H., Ludwig, F., Zwolsman, J.J.G., Weedon, G.P., Kabat, P., 2011. Global river temperatures and sensitivity to atmospheric warming and changes in river flow. *Water Resour. Res.*, 47: W02544.
- van Vliet, M.T.H. et al., 2012a. Coupled Daily Streamflow and Water Temperature Modelling in Large River Basins. *Hydrology and Earth System Sciences Discussions*, 9: 8335-8374.
- van Vliet, M.T.H. et al., 2012b. Vulnerability of US and European electricity supply to climate change. *Nature Climate Change*, 2: 676–681

References

- van Vliet, M.T.H., Zwolsman, J.J.G., 2008. Impact of summer droughts on the water quality of the Meuse river. *Journal of Hydrology*, 353(1-2): 1-17.
- van Vuuren, D.P. et al., 2011. The representative concentration pathways: an overview. *Climatic Change*, 109(1-2): 5-31.
- Vassolo, S., Döll, P., 2005. Global-scale gridded estimates of thermoelectric power and manufacturing water use. *Water Resources Research*, 41(4): W04010.
- VGE, 2011. *Jahrbuch der europäischen Energie- und Rohstoffwirtschaft*, 118. VGE Verlag GmbH, Essen, 952 pp.
- Voisin, N., Wood, A.W., Lettenmaier, D.P., 2008. Evaluation of precipitation products for global hydrological prediction. *Journal of Hydrometeorology*, 9(3): 388-407.
- Vörösmarty, C.J., Federer, C.A., Schloss, A.L., 1998. Evaporation functions compared on US watersheds: Possible implications for global-scale water balance and terrestrial ecosystem modeling. *Journal of Hydrology*, 207(3-4): 147-169.
- Vörösmarty, C.J., Green, P., Salisbury, J., Lammers, R.B., 2000. Global water resources: Vulnerability from climate change acid population growth. *Science*, 289(5477): 284-288.
- Vörösmarty, C.J. et al., 2010. Global threats to human water security and river biodiversity. *Nature*, 468(7321): 334-334.
- Voß, F., Flörke, M., 2010. Spatially explicit estimates of past and present manufacturing and energy water use, WATCH Technical Report No. 23, 17 pp.
- Voß, F., Flörke, M., Alcamo, J., 2009. Preliminary spatially explicit estimates of past and present domestic water use, WATCH Technical Report No. 17, 16 pp.
- Webb, B.W., 1996. Trends in stream and river temperature. *Hydrological Processes*, 10(2): 205-226.
- Webb, B.W., Clack, P.D., Walling, D.E., 2003. Water-air temperature relationships in a Devon river system and the role of flow. *Hydrological Processes*, 17(15): 3069-3084.
- Webb, B.W., Hannah, D.M., Moore, R.D., Brown, L.E., Nobilis, F., 2008. Recent advances in stream and river temperature research. *Hydrological Processes*, 22(7): 902-918.
- Webb, B.W., Nobilis, F., 1994. Water Temperature Behavior in the River Danube During the 20th-Century. *Hydrobiologia*, 291(2): 105-113.
- Webb, B.W., Nobilis, F., 1997. Long-term perspective on the nature of the air-water temperature relationship: A case study. *Hydrological Processes*, 11(2): 137-147.
- Webb, B.W., Nobilis, F., 2007. Long-term changes in river temperature and the influence of climatic and hydrological factors. *Hydrological Sciences Journal-Journal Des Sciences Hydrologiques*, 52(1): 74-85.
- Webb, B.W., Walling, D.E., 1993. Temporal Variability in the Impact of River Regulation on Thermal Regime and some Biological Implications. *Freshwater Biology*, 29(1): 167-182.
- Weedon, G.P. et al., 2010. The Watch Forcing Data 1958-2001: A meteorological forcing dataset for land surface and hydrological models, WATCH Technical report No. 22, 41 pp.
- Weedon, G.P. et al., 2011. Creation of the WATCH Forcing Data and Its Use to Assess Global and Regional Reference Crop Evaporation over Land during the Twentieth Century. *J. Hydrometeor.*, 12(5): 823-848.
- Welcomme, R., 1979. *Fisheries ecology of floodplain rivers* Prentice Hall Press, New York, 240 pp.
- Wenger, S.J. et al., 2011. Flow regime, temperature, and biotic interactions drive differential declines of trout species under climate change. *Proceedings of the National Academy of Sciences of the United States of America*, 108(34): 14175-14180.
- Werners, S. et al., 2012. *Turning Points in Climate Change Adaptation*, submitted to *The Governance of Adaptation*. <http://www.adaptgov.com/>
- Wetherald, R.T., Manabe, S., 1999. Detectability of summer dryness caused by greenhouse warming. *Climatic Change*, 43(3): 495-511.
- Whitehead, P.G., Wilby, R.L., Battarbee, R.W., Kernan, M., Wade, A.J., 2009. A review of the potential impacts of climate change on surface water quality. *Hydrological Sciences Journal-Journal Des Sciences Hydrologiques*, 54(1): 101-123.
- WHO, 2011. *Guidelines for Drinking-water Quality*, Fourth Edition, World Health Organization, Geneva, Switzerland, 564 pp.

- Wigmosta, M.S., Vail, L.W., Lettenmaier, D.P., 1994. A distributed hydrology-vegetation model for complex terrain. *Water Resources Research*, 30(6): 1665-1679.
- Williams, K.D., Ringer, M.A., Senior, C.A., 2003. Evaluating the cloud response to climate change and current climate variability. *Climate Dynamics*, 20(7-8): 705-721.
- Williams, M., 1996. *The Transition in the Contribution of Living Aquatic Resources to Food Security*, International Food Policy Research Institute, Washington D.C., No. 13, pp. 27-28
- Wood, A.W., Leung, L.R., Sridhar, V., Lettenmaier, D.P., 2004. Hydrologic implications of dynamical and statistical approaches to downscaling climate model outputs. *Climatic Change*, 62(1-3): 189-216.
- Wu, H., Kimball, J.S., Mantua, N., Stanford, J., 2011. Automated upscaling of river networks for macroscale hydrological modeling. *Water Resour. Res.*, 47: W03517.
- Wunderlich, W.O., Gras, R., 1967. *Heat and mass transfer between a water surface and the atmosphere*, Tenn. Valley Authority, Norris.
- WWAP, 2009. *World Water Assessment Programme The United Nations World Water Development Report 3: Water in a Changing World.* , UNESCO, Paris and London, 429 pp.
- WWF, 2004. *Living Planet Report*, World Wildlife Fund , 44 pp.
- Xenopoulos, M.A. et al., 2005. Scenarios of freshwater fish extinctions from climate change and water withdrawal. *Global Change Biology*, 11(10): 1557-1564.
- Yearsley, J.R., 2009. A semi-Lagrangian water temperature model for advection-dominated river systems. *Water Resources Research*, 45: W12405.
- Yearsley, J.R., 2012. A grid-based approach for simulating stream temperature. *Water Resources Research*, 48: W03506.
- Zhao, R.J., Zhang, Y.L., Fang, L.R., Zhang, Q.S., 1980. The Xinanjiang model, *Hydrological Forecasting*, Proc. Oxford Symp. on Hydrological Forecasting, IAHS. Oxford, United Kingdom, pp. 351-356.

References

Summary

Climate change will affect flow and thermal regimes of rivers worldwide. This will have a direct impact on freshwater ecosystems and human water uses during the 21st century. Up to present, limited knowledge exists of the magnitude of both streamflow and water temperature changes under future climate, especially for large rivers worldwide. Recent warm, dry summers showed adverse impacts of high river temperatures and low flows on freshwater ecosystems and human water uses, like cooling of thermoelectric power plants, for large regions. Therefore, we need to better understand to what extent large-scale changes in river flow and water temperature under climate change could affect freshwater ecosystems and cooling water use. This thesis addresses the impacts of climate change on river flows and water temperatures globally, along with the potential consequences for freshwater ecosystems and cooling water use in the energy sector.

It first shows the sensitivity of river temperatures to atmospheric warming (air temperature rises) and changes in river flow (thermal capacity) using a water temperature regression model (**Chapter 2**). The regression model was fitted based on historical air temperature, river discharge and water temperature series for river stations worldwide. The performance of the regression model improved for 87% of the global river stations by including river discharge as input variable. Significant impacts of river flow changes on water temperatures were found, especially during warm, dry periods. Hence, river flow impacts on water temperature should be incorporated to provide more accurate water temperature estimates during historical and future projected dry and warm periods.

A coupled hydrological - water temperature modelling approach was used, including the physically-based RBM stream temperature model linked to the macro-scale VIC hydrological model (**Chapter 3**). RBM was further developed for application to large river basins worldwide, including anthropogenic impacts of heat effluents and reservoirs. Model performance was tested for large basins in different hydro-climatic zones and with different anthropogenic impacts at 1/2° spatial resolution and on a daily time step. Significant increases in model performances were obtained for strongly regulated and thermally polluted basins. Overall, realistic daily estimates were obtained for both river flow and water temperature for the validation period 1971-2000, with similar performances during warm, dry periods.

In a next step, we assessed the impacts of climate change on both river flows and water temperatures globally (**Chapter 4**). The global VIC-RBM modelling framework was forced

with bias-corrected output of three general circulation models (GCMs) for both the SRES A2 and B1 emissions scenario. Our results show a decline in low flow combined with an increase in high (peak) flow for about one-third of the global land surface area for the period 2071-2100 relative to 1971-2000. Consistent increases in mean flow are projected for the high northern latitudes and parts of the tropical region, and consistent decreases for the U.S., central and southern Europe, Southeast Asia and southern parts of South America, Africa and Australia. Global mean water temperatures are expected to increase on average by 0.8–1.6°C. The largest water temperature increases are projected for the U.S., Europe, eastern China and parts of southern Africa and southern Australia. In most of these regions, water temperature rises are exacerbated by declines in low flows, resulting in reductions in thermal capacity and dilution capacity for thermal effluents. Under changing climate, these regions could therefore be affected by increased deterioration of water quality and freshwater habitats, and reduced water available for human uses (e.g. cooling water use for thermoelectric power production).

For Europe and the U.S., where most electricity is produced by power plants depending on cooling water, we quantified how climate change could affect cooling water availability and thermoelectric power production over the next 20-50 years (**Chapter 5**). VIC-RBM and an electricity production model were forced with the ensemble of bias-corrected GCM output. Impacts on production capacities were quantified for 96 existing nuclear- and fossil-fuelled power plants (with different cooling systems) in the U.S. and Europe. Results show that higher water temperatures and lower summer flow under climate change are likely to increase environmental restrictions on cooling water use. This could result in substantial reductions in summer mean usable capacity of 6–19% for Europe and 4–16% for the U.S. (depending on cooling system type and climate scenario for 2031-2060 relative to 1971-2000). Considering the long design life of power plant infrastructure, adaptation options should be included in today's planning and strategies to meet the growing electricity demand in the 21st century.

In addition, we focussed on the potential consequences of climate change for global freshwater fish habitats (**Chapter 6**). Global projections of daily streamflow and water temperature under future climate were used with spatial distributions and thermal tolerance values of several fish species in different regions worldwide, and ecologically relevant flow indices. The results show significant increases in both the frequency and magnitude of exceeding maximum temperature tolerance values of all fish species for 2071-2100 relative to 1971-2000. This could, in combination with alterations in river flow regime, affect freshwater fish habitats and possibly species distributions on a large scale.

This thesis shows that climate change will affect river temperatures directly by atmospheric warming and indirectly by changes in river flow. High water temperature increases combined with large declines in low flows are projected for the U.S., Europe and eastern China, where socio-economic consequences of these changes can potentially be large. In addition, it shows that climate change is likely to increase pressure on water between cooling water use in the energy sector (electricity supply) and freshwater ecosystems on a large scale. This study shows the need for improved adaptation strategies to ensure future water and energy security, without compromising water needs for ecosystems.

Samenvatting

Klimaatverandering zal afvoerregimes en watertemperatuur van rivieren wereldwijd beïnvloeden. Dit zal directe gevolgen hebben voor ecosystemen en watergebruik door mensen tijdens de 21^{ste} eeuw. Tot op heden was er echter weinig kennis over de mate waarin zowel watertemperaturen als afvoeren van grote riviersystemen wereldwijd kunnen veranderen. Recente warme, droge zomers lieten in grote regio's zien dat rivierecosystemen en menselijke gebruiksfuncties, zoals koeling van elektriciteitscentrales, negatieve gevolgen kunnen ondervinden tijdens perioden met lage rivierafvoer en hoge watertemperatuur. Het is daarom van groot belang om beter inzicht te verkrijgen in de mate waarin rivierafvoer en watertemperatuur op grote schaal kunnen veranderen. Dit proefschrift beschrijft de effecten van klimaatverandering op zowel rivierafvoer als watertemperatuur wereldwijd, samen met de mogelijke consequenties voor rivierecosystemen en koelwatergebruik in de energiesector.

Eerst is gekeken naar de effecten van atmosferische opwarming (luchttemperatuur stijgingen) en veranderingen in rivierafvoer (thermische capaciteit) op riviertemperaturen wereldwijd, gebruikmakend van een watertemperatuur regressiemodel (**Hoofdstuk 2**). Het regressiemodel was toegepast met meetreeksen van lucht- en watertemperatuur en rivierafvoer voor rivierstations wereldwijd. De kwaliteit van het regressiemodel werd significant verbeterd voor 87% van de rivierstations door naast luchttemperatuur, rivierafvoer als onafhankelijke variabele toe te voegen. De effecten van veranderingen in rivierafvoer op watertemperatuur zijn het sterkst tijdens warme, droge perioden. Het is daarom van groot belang om de invloed van rivierafvoer in beschouwing te nemen om meer betrouwbare simulaties te verkrijgen van riviertemperatuur tijdens warme, droge situaties.

Een gekoppeld hydrologisch - water temperatuur modelsysteem, bestaande uit het fysisch gebaseerde RBM riviertemperatuur model gekoppeld aan het macro-schaal VIC hydrologisch model, was gebruikt voor verdere analyses. RBM was verder ontwikkeld voor toepassing wereldwijd en voor stroomgebieden die sterk beïnvloed worden door stuwmeren (reservoirs) en warmtelozingen van elektriciteitscentrales (**Hoofdstuk 3**). De kwaliteit van het modelsysteem werd geëvalueerd op $1/2^\circ$ ruimtelijke resolutie en een dagelijkse tijdstap voor grote stroomgebieden in verschillende klimaatzones en met verschillende menselijke invloeden. De aanpassingen resulteerden in een significante verbetering in de modelkwaliteit. Realistische simulaties van dagelijkse rivierafvoer en watertemperatuur werden verkregen voor de gehele validatieperiode 1971-2000, ook tijdens warme, droge perioden.

Het VIC-RBM modelsysteem werd in een volgende stap gebruikt om de effecten van klimaatverandering op rivierafvoer en watertemperatuur wereldwijd door te rekenen (**Hoofdstuk 4**). Klimaatscenario's van drie mondiale klimaatmodellen (GCMs) en voor het SRES A2 en B1 emissiescenario werden als invoer datasets in VIC-RBM gebruikt. De modelprojecties tonen voor ongeveer één derde van het mondiale landoppervlak een daling in lage rivierafvoer gecombineerd met een toename in hoge (piek)afvoer voor de periode 2071-2100 ten opzichte van 1971-2000. Consistente toenames in jaargemiddelde afvoer zijn te verwachten voor de hoge noordelijke breedtegraden en delen van de tropische zone; consistente afnamen voor de VS, centraal en zuidelijk Europa, Zuidoost Azië en de zuidelijke delen van Zuid-Amerika, Afrika en Australië. Riviertemperaturen zullen naar verwachting stijgen met een mondiaal gemiddelde van 0.8–1.6°C voor deze periode. De sterkste stijgingen zijn geprojecteerd voor de VS, Europa, oostelijk China en zuidelijke delen van Afrika en Australië. In deze regio's zijn de stijgingen in riviertemperatuur sterker door dalingen in lage afvoer wat leidt tot afnamen in thermische capaciteit en verdunningscapaciteit voor warmtelozingen. Door klimaatverandering kunnen deze regio's te maken krijgen met een verslechtering van waterkwaliteit en zoetwater-habitats en verminderde mogelijkheden voor menselijk gebruik (b.v. koelwatergebruik voor de energiesector).

Voor Europa en de VS, waar het grootste deel van de elektriciteit wordt opgewekt door centrales die koelwater vereisen, is nader onderzocht hoe klimaatverandering de waterbeschikbaarheid voor koeling en potentiële elektriciteitsproductie kan beïnvloeden in de komende 20-50 jaar (**Hoofdstuk 5**). Een ensemble van klimaatscenario's werd als invoer in VIC-RBM en een elektriciteitsproductiemodel gebracht om de potentiële elektriciteitsproductie door te rekenen. Deze analyse richt zich op 96 bestaande (kern- en fossiele brandstof) centrales met verschillende koelsystemen verspreid over Europa en de VS. Resultaten laten zien dat beperkingen in koelwatergebruik (door overschrijding van ecologische normen) naar verwachting zullen toenemen door hogere watertemperaturen en lagere zomerafvoeren onder een veranderend klimaat. Dit kan leiden tot substantiële afnamen in de productiecapaciteit van centrales tijdens zomer met gemiddeld 6–19% voor Europa en 4–16% voor de VS (afhankelijk van koelsysteemtype en klimaatscenario voor 2031-2060 ten opzichte van 1971-2000). Gezien de lange levensduur van centrales is het van groot belang dat adaptatiemaatregelen nu al getroffen worden om te kunnen blijven voldoen aan de groeiende vraag naar elektriciteit in de 21^{ste} eeuw.

Verder is ook gekeken naar de mogelijke consequenties van klimaatverandering voor habitatcondities van verschillende vissoorten wereldwijd (**Hoofdstuk 6**). Mondiale projecties van dagelijkse rivierafvoer en watertemperatuur werden gecombineerd met datasets van de ruimtelijke verspreiding en thermische tolerantiewaarden van verschillende vissoorten en ecologisch relevante indexen voor rivierafvoer. De resultaten tonen een significante toename in zowel de frequentie als mate waarin maximale temperatuur-tolerantiewaarden van verschillende vissoorten overschreden worden voor 2071-2100 ten opzichte van 1971-2000. In combinatie met veranderingen in afvoerregime van rivieren kan dit leiden tot grootschalige veranderingen in habitatcondities en verspreiding van vissoorten.

Dit proefschrift laat zien dat klimaatverandering riviertemperatuur zal beïnvloeden door zowel de directe effecten van atmosferische opwarming en indirecte effecten van veranderingen in rivierafvoer. Sterke stijgingen in watertemperatuur gecombineerd met sterke dalingen in rivierafvoer worden verwacht voor de VS, Europa en oostelijk deel van China, waar de maatschappelijk-economische consequenties van deze veranderingen mogelijk groot kunnen zijn. Daarnaast toont dit proefschrift aan dat klimaatverandering de druk op water voor behoud van huidige rivierecosystemen enerzijds en koelwatergebruik binnen de energiesector anderzijds zal doen toenemen. De studie indiceert het belang van verbeterde aanpassingsstrategieën om de water- en energiezekerheid in de toekomst te kunnen garanderen, zonder daarbij te schikken op waterbehoeften voor het behoud van ecosystemen.

In the media ...

Scientific American made a 60-second podcast based on the article in Nature Climate Change (Chapter 5) published on 3rd of June 2012. The text of the podcast is given below (with permission from the author David Biello).

How Climate Change May Impact Electricity Supplies

Fossil fuel burning power plants aren't only causing climate change, they're likely to suffer from such global warming. David Biello reports

Ironic twist alert: most electricity production requires vast amounts of water.

Cold water. Which means that climate change is going to be bad for electricity supplies. Why's that ironic? Here's how we make electricity. In the U.S., we burn coal or natural gas, which produces massive quantities of the greenhouse gases causing climate change, or we fission uranium. The heat from those processes boils water that makes steam that spins a turbine. And those turbines produce more than 90 percent of our electricity. Massive cooling towers then help chill the power plant back down using river water, for example. Only river water isn't quite as cold as it used to be, or as available. As a result, in recent years, such thermal power plants in the southeastern U.S. have had to decrease power production because river temperatures were too high or water levels were too low.

That problem is only going to get worse, according to an analysis in the journal Nature Climate Change (Scientific American is part of Nature Publishing Group). By the 2040s, available electricity could be down by 16 percent in the summertime.

When you'd most like electricity. To run your air conditioner. To beat the heat.

Told you it was ironic.

—David Biello

The New York Times blog, 4 June 2012, USA:

'Climate Change Threatens Power Output, Study Says'

The Washington Post blog, 4 June 2012, USA:

'Even coal and nuclear plants are vulnerable to climate change'

USA Today, 4 June 2012, USA

'Climate change causes nuclear, coal power plant shutdowns'

Spiegel Online, 4 June 2012, Germany:

'Wassermangel könnte Stromproduktion gefährden'

National Geographic, Aktuelles, 4 June 2012, Germany:

'Klimawandel könnte Stromproduktion gefährden'

Berliner Morgen Post, 4 June 2012, Germany:

'Warme Flüsse und Trockenheit gefährden Krafwerke'

Kleine Zeitung, 4 June 2012, Austria:

'Stromversorgung gerät in Gefahr'

NU.nl, 4 June 2012, The Netherlands:

'Kolencentrales hebben last van warmer klimaat'

NRC Handelsblad, 9 June 2012, The Netherlands:

'Warmer water, minder elektriciteit'

Actualit News, 4 June 2012, France:

'Les centrales électriques nucléaires et au charbon manqueront bientôt d'eau'

Acknowledgements

This PhD study had many nice aspects, like trips to conferences and meetings around the world, pleasant collaborations with good researchers, and overall much freedom to perform this study. Although there were also days of lonely writing and fixing modelling errors and issues, I enjoyed it a lot! Many people directly (or indirectly) supported me during the four years I worked on this PhD project, and I am very grateful to all those people, but there are some people I would like to thank in particular.

First of all, my promotor Pavel Kabat and co-promotor Fulco Ludwig, I am very grateful that you created the possibilities for me to write my research proposal within the WATCH project and set up this PhD study on global river temperatures. We had very good discussions and you both supported me from the start. Pavel, you encouraged me to think in ambitious terms and not to doubt about taking big steps and submitting papers to higher impact journals. Thanks for your belief and your inspiring ideas! Fulco, I highly appreciate that you have given me much space to develop my own ideas, while at the same time your door was open when I had questions. Thanks for all your good suggestions and input, and your pragmatic views! I am also grateful that you, Eddy, Pavel and Rik created the possibilities to continue my work in new projects.

In addition to my supervisors in Wageningen, I would like to thank Dennis Lettenmaier and John Yearsley (University of Washington) that were willing to step on board of my PhD project during the second year. John, it was a pleasure to work together with you and to collaborate on your water temperature model. Thank you for sharing your model and for all your help, especially during the starting phase. Dennis, discussing my work with you was very helpful for my study, and I enjoyed the visits to your group a lot. While the geographical distance between Seattle and Wageningen is large, I am very grateful that you and John were closely involved in my work. Your comments and feedback on my papers were very valuable.

Eric Wood and Justin Sheffield (Princeton University), I also would like to thank you for your hospitality during my short visit to your group and for your useful feedback on my study. Another strong delegation of the VIC community (although only one person) is at the Norwegian Water Resources and Energy Directorate. Ingjerd, you provided me with very helpful and constructive feedback on the VIC-RBM modelling papers and my PhD study in general. Thanks for our good discussions (not only about VIC!) when you were in Wageningen. Wietse, you introduced me in the world of Linux and high performance

computing. I really learned a lot from you. Many thanks for all your technical support (and also funny stories)! I also would like to thank other co-authors of the papers in my thesis, Gertjan Zwolsman (KWR Watercycle Research Institute), Graham Weedon (UK Met Office Hadley Centre) and Stefan Vögele (Institute of Energy and Climate Research, Forschungszentrum Jülich). The work of the thesis committee is at the end of this PhD project. Eric Wood, Martina Flörke, Marc Bierkens, and Remko Uijlenhoet, thank you very much for your willingness to be committee member.

In Wageningen, I am pleased to have many nice colleagues around. Enjoyable discussions nearby the big machine which is supposed to produce coffee, and nice chats during lunch walks make me feel comfortable in Wageningen. I would like to thank in particular my office mates in Lumen (Saskia, Marleen, Robbert, Obbe, Olaf) and previously in Aqua (all PhD students) and Atlas (Olaf, Wietse and Herbert, I won't forget your passionate discussions about the newest gadgets! ;-). Hester and Obbe, thanks for the nice carpool rides on the A12 during the first years. Marjolein, I am very happy with the cover that you designed for my thesis, thank you so much.

In Utrecht where I live, dinners with friends at home and drinks in town were good to relax after long working days. There are a few friends I would like to mention in particular. Lisette, Thomas, you both provided me with very good (and convincing!) advices when I decided to start this PhD study. Eva, thanks for your useful editorial advice during the final stage and for all nice dinners and drinks with you and Maartje. Els, good to share with you the experiences of our PhD lives. Laura and Ake, thanks a lot for being my paranymphs during the defence. Ake, we became friends during our studies in Utrecht, but I am very pleased that we are also "colleagues" now in Wageningen. Laura, while distances got longer and lives got busier during the last fourteen years, I am happy that good friendship with you maintains.

I also would like to thank my family who have always given me warm support: Trees, Gerard, Liesbeth, Rex, Linda, Frank, Susanne, Annemieke, Kenneth, "grandpa" Sicherer and Mick. In particular my parents Gerard & Trees, sister Linda and brother Frank, thank you so much for your continuous support, your belief in me and all your advices during my whole life. Lin, I am looking forward to break new shopping records with you during our next city trip!

Bob, this acknowledgement will end with you. My PhD project, and of course life in general, would have been much less enjoyable without you. Thanks for your support, love and humoristic (and sometimes critical) views. You convinced me to not only *model* the rivers of the world, but also to *see* something of the world. Together we have made great holiday trips during the last four years. Our backpack adventure in Thailand/Laos, overland trip in eastern Africa, and road trips through the great landscapes of the U.S., and recently Iceland, were great experiences which I won't forget. Thanks for being together with you and sharing all the beautiful and challenging things in life!

Michelle

Curriculum Vitae

Michelle van Vliet was born on the 24th of December 1982 in Honselersdijk, The Netherlands. After finishing secondary school in 2001 she studied physical geography at Utrecht University. During her studies, she developed interest in hydrology and climate change. A part of her MSc research was performed in Abisko, northern Sweden, studying climate change impacts on sub-arctic hydrology. During her internship at KWR Watercycle Research Institute, she investigated the effects of climate change on water quality and the drinking water function of the Meuse River. Michelle worked as teaching assistant at Utrecht University (courses Statistics, Global Change and field survey in the Rhine-Meuse delta) during the period 2002-2006.

She graduated with distinction ('cum laude') in 2006 and started working as hydrologist at Deltares, Utrecht, and participated in both consultancy and research projects. In July 2008, she started her PhD study at the Earth System Science - Climate Change and Adaptive Land and Water Management Group of Wageningen University within the EU FP6 WATCH project and FP7 ECLISE project. During her PhD she visited the Land Surface Hydrology Research Group of University of Washington (summer 2009 and autumn 2010) and collaborated with Prof. Dennis Lettenmaier and his group on the VIC-RBM hydrological and water temperature modelling. Michelle previously received presentation awards at the conference of the Netherlands Centre for River studies in Enschede (in 2006) and at the conference 'Deltas in Times of Climate Change' in Rotterdam (in 2010).

Peer-Reviewed Publications

- van Vliet, M.T.H.**, J.R. Yearsley, F. Ludwig, S. Vögele, D. P. Lettenmaier, and P. Kabat (2012) Vulnerability of U.S. and European electricity supply to climate change, *Nature Climate Change*, 2(9), 676–681, doi:10.1038/nclimate1546
- van Vliet, M.T.H.**, W.H.P. Franssen, J.R. Yearsley, F. Ludwig, I. Haddeland, D.P. Lettenmaier, and P. Kabat (in press) Global river discharge and water temperature under climate change, *Global Environmental Change*, doi:10.1016/j.gloenvcha.2012.11.002
- van Vliet, M.T.H.**, J.R. Yearsley, W.H.P. Franssen, F. Ludwig, I. Haddeland, D.P. Lettenmaier, and P. Kabat (2012) Coupled daily streamflow and water temperature modelling in large river basins, *Hydrology and Earth System Sciences*, 16, 4303–4321, doi:10.5194/hess-16-4303-2012
- van Vliet, M.T.H.**, F. Ludwig, J.J.G. Zwolsman, G.P. Weedon, and P. Kabat (2011) Global river temperatures and sensitivity to atmospheric warming and changes in river flow, *Water Resources Research*, 47, W02544, doi:10.1029/2010WR009198
- van Beek, L.P.H., T. Eikelboom, **M.T.H. van Vliet**, and M.F.P. Bierkens (2012) A physically based model of global freshwater surface temperature, *Water Resources Research*, 48, W09530, doi:10.1029/2012WR011819
- van Vliet, M.T.H.**, S. Blenkinsop, A. Burton, C. Harpham, H.P. Broers, and H.J. Fowler (2011) A multi-model ensemble of downscaled spatial climate change scenarios for the Dommel catchment, western Europe, *Climatic Change*, 111(2), 249-277, doi:10.1007/s10584-011-0131-8
- Visser, A., J. Kroes, **M.T.H. van Vliet**, S. Blenkinsop, H.J. Fowler, and H.P. Broers (2011) Climate change impacts on the leaching of a heavy metal contamination in a small lowland catchment, *Journal of Contaminant Hydrology*, 127(1-4), 47-64, doi:10.1016/j.jconhyd.2011.04.007
- Brolsma, R.J., **M.T.H. van Vliet**, and M.F.P. Bierkens (2010) Climate change impact on a groundwater-influenced hillslope ecosystem, *Water Resources Research*, 46, W11503, doi:10.1029/2009WR008782
- van Vliet, M.T.H.** and J.J.G. Zwolsman (2008) Impact of summer droughts on the water quality of the Meuse River, *Journal of Hydrology*, 353(1-2), 1-17, doi: 10.1016/j.jhydrol.2008.01.001



Netherlands Research School for the
Socio-Economic and Natural Sciences of the Environment

C E R T I F I C A T E

The Netherlands Research School for the
Socio-Economic and Natural Sciences of the Environment
(SENSE), declares that

Michelle T.H. van Vliet

born on 24 December 1982 in Honselersdijk, the Netherlands

has successfully fulfilled all requirements of the
Educational Programme of SENSE.

Wageningen, 19 December 2012

the Chairman of the SENSE board

Prof. dr. Rik Leemans

the SENSE Director of Education

Dr. Ad van Dommelen

The SENSE Research School has been accredited by the Royal Netherlands Academy of Arts and Sciences (KNAW)



K O N I N K L I J K E N E D E R L A N D S E
A K A D E M I E V A N W E T E N S C H A P P E N



The SENSE Research School declares that **Ms. Michelle T.H. van Vliet** has successfully fulfilled all requirements of the Educational PhD Programme of SENSE with a work load of 56 ECTS, including the following activities:

SENSE PhD Courses

- o Environmental Research in Context
- o Research Context Activity: Co-organizing Writing Week (Oct 2010) and monthly PhD meetings (Apr 2011-Jul 2012) for ESS-CALM group and Media exposure Nature Climate Change publication (Jun-Aug 2012)
- o Understanding Global Environmental Change: Processes, Compartments and Interactions
- o Uncertainty Modelling and Analysis

Other PhD Courses

- o Project and Time Management
- o C-Programming

Management and Didactic Skills Training

- o Practical supervision, MSc course System Earth: Analysis at Regional and Global Scales
- o Supervision and co-supervision of four MSc theses

External training at a foreign research institute

- o Visiting scholar at the Land Surface Hydrology Research Group of Prof. Dennis Lettenmaier, University of Washington, Seattle, USA in 2009 and 2010

Oral Presentations

- o *The large-scale impact of climate change on river flow and water temperatures.* WATCH-GWSP Global Hydrological Modelling Intercomparison Workshop, 15-18 June 2010, Wageningen
- o *Large-scale Impact of Climate Change on River Temperatures.* World Water Week, 5-10 September 2010, Stockholm
- o *Global Rivers Heating Up: Climate Change Impacts on River Temperatures.* WATCH General Assembly 2010, 31 October – 4 November 2010, Amsterdam, and WIMEK-SENSE symposium, 22 February 2011, Wageningen
- o *Daily Water Temperature and River Discharge Modelling for Climate Change Impact Assessment in Large River Basins Globally.* American Geophysical Union (AGU) Fall meeting, 13-17 December 2010, San Francisco
- o *Impact of Climate Change on Thermoelectric Power in Europe and U.S.* ECLISE General Assembly 2012, 6-7 March 2012, Norrköping

SENSE Coordinator PhD Education and Research

Mr. Johan Feenstra

The research described in this thesis was financially supported by the European Commission through the FP6 WATCH (Water and Global Change) project and through the FP7 ECLISE (Enabling Climate Information Services for Europe) project.

Cover design Marjolein Pijnappels, Studio Lakmoes

Printing GVO drukkers & vormgevers B.V. | Ponsen & Looijen